THE UNIVERSITY
of EDINBURGH

A study of odontoclast dysregulation in feline tooth resorption

Seungmee Lee

A thesis submitted for the degree of Doctor of Philosophy

University of Edinburgh

2019

To my family for all their support

Abstract

Feline tooth resorption (TR) is a common and painful disease characterised by loss of mineralised tissues of the tooth. Due to the progressive nature of the disease the only available treatment is to extract affected teeth. Odontoclasts are specialised cells that resorb teeth and they share many similarities with osteoclasts, the bone resorbing cells. The main physiological role of these cells is to resorb deciduous teeth to allow for the permanent tooth replacement. In some cats these cells become dysregulated and attack the permanent teeth later in life. However, the aetiology of tooth resorption is still unclear.

The aim of this PhD project was to identify transcriptomic changes between TR negative and TR positive teeth, set up a TR model to study odontoclast dysregulation *in vitro* and to use this system to test a novel therapeutic target for the treatment of TR. In this study, a successful RNA isolation procedure for feline teeth collected in a clinical setting and at post-mortem was developed. To elucidate the role of inflammation and vitamin D involvement in TR, quantitative PCR was performed but there was no statistically significant difference in the expression of any inflammatory cytokines, vitamin D receptor or receptor activator of nuclear factor kappa-B ligand (RANKL) between TR negative and TR positive teeth. Feline osteoclasts were successfully generated from feline bone marrow *in vitro*. I also found that primary feline periodontal ligament cells could induce osteoclast formation. Osteoclast precursors from TR positive cats formed higher numbers of osteoclasts when co-cultured with periodontal ligament cells compared to TR negative cats. Transcriptome analysis by RNA sequencing identified many differentially expressed genes between TR negative and TR positive teeth from the same cat. I also found that up-regulated genes in TR positive teeth, from the literature, are known to be associated with osteoclast differentiation and calcium signalling pathways. Apart from the genes related to osteoclast biology, I also identified up-regulated genes involved in muscle and tooth development, which

suggests TR positive teeth undergo repair or bone formation in response to tooth resorption.

Based on RNA sequencing data and quantitative PCR, I was able to identify a list of genes which may be involved in odontoclast dysregulation in TR. Among those, matrix metalloproteinase 9 (MMP9) was of great interest due to its potential role in osteoclast biology. High MMP9 expressing odontoclasts were found in tooth sections undergoing tooth resorption by immunohistochemistry. In functional studies, MMP9 inhibitor reduced both osteoclast formation and resorption activity *in vitro*. Furthermore, feline *MMP9* siRNA inhibited osteoclast differentiation but showed little effect on dentine resorption activity.

These results confirm the hypothesis that the transcriptome of TR positive teeth was locally different from TR negative teeth. The results revealed an up-regulation of genes in pathways associated with osteoclast formation in TR positive teeth. Further testing of candidate genes as potential therapeutic targets in feline TR could be performed using the feline tooth resorption model system developed in this study.

Lay summary

Tooth resorption is an oral problem that causes tooth loss. Although tooth resorption affecting several teeth is rare in humans, it is very common in cats. Odontoclasts are specialised cells that resorb the milk teeth during tooth shedding in the young. This is their normal function, but sometimes these cells start to attack teeth when they are not supposed to, for example when they start attacking the permanent dentition later in life. This unregulated cell activity invades into teeth, and causes pain and loss of the tooth. The only available treatment is to remove the affected tooth. We do not know why this is happening. The aim of this research was firstly to detect the genetic changes of feline teeth, try to find out which genes promote odontoclast activity and test the role of target genes by blocking their function. It was hoped that this approach will provide a better understanding of the aetiology of this disease. In this study, there was no change in the expression levels of inflammation and vitamin D related genes with tooth resorption. More odontoclasts were formed in tooth resorption affected cats than tooth resorption unaffected cats, and a number of genes showed a different level of expression in cats with the disease when they were compared to cats free of the disease. Some of these genes with altered expression are known to be involved in odontoclast activation. One gene that makes a specific protein, matrix metalloproteinase 9 (*MMP9*), was chosen for further study. Its function in cat odontoclasts was tested using a drug that blocks MMP9 activity, and this approach resulted in fewer odontoclasts and it reduced their ability to break-down tooth tissue. Lastly, microscopic observation of thin teeth slices with tooth resorption showed that tooth odontoclasts expressed a lot of MMP9. In summary, this study was the first to report whole genome expression changes associated with tooth resorption in cats. Their changes revealed that the expression of genes associated with odontoclast formation pathways were increased in tooth resorption affected teeth. More of the differentially expressed genes identified in this study could potentially become drug targets to prevent tooth

resorption and towards this goal the cat tooth resorption model system developed in this study will help in their functional characterisation.

Declaration

I hereby declare that the work presented in this thesis has been composed and originated by myself, except where specifically acknowledged, and that it has not been presented for a degree at any other university.

Seungmee Lee

January 2019

Acknowledgements

Firstly I would like to give my sincere thanks to my supervisor Dr. Gurå Therese Bergkvist. Her enthusiasm for science and this project has encouraged me towards an academic career and finish this project. Her academic advice and personal insights have been an inspiration to me. I will miss her help and our daily chats. I would also like to extend my gratitude and appreciation to my co-supervisor Prof. Colin Farquharson for his invaluable support and profound scientific insights. Without their support, this thesis could never have been completed. Our meetings were rewarding with a lots of fun.

I owe lots of thanks to many people that have helped me in many ways. I would like to thank to Dr Norman Johnston and Dr Susan Thorne for diagnosis of TR. In addition thanks go to Dr Urmi Trivedi for help with RNA-seq. A special thanks to Dr Stephen Bush for invaluable bioinformatic support. I would like to thank to Miss Nicola Mawson for her input. I am grateful to all members of the Argyle Group and Farquharson Group for their help and support, in particularly Mrs Rhona Muirhead, Ms Elaine Seawright, Dr Lisa Pang, Dr Craig Johnson, Dr Katherine Staines, Dr Breno Beirao and Dr Karen Tan. Special thanks must go to Dr Erika Abbondati for her help with the histology as well as heartfelt friendship. Thank you to all my friends whom I met over the years of the PhD for cheering me up.

Finally I would like to thank my family and most importantly of all, my husband, Dr Sung-Dong Lee, without him I could never have achieved anything. A special thanks to my mother, Jung Suk Kwon and father in law, Seung Han Lee for all their supports and wamhearted words. I feel blessed and much grateful to the God, Almighty, for giving me the strength and opportunity to achieve my dream.

This work was supported by the University of Edinburgh via Edinburgh Global Research Scholarship, The Sym Charitable Trust, BBSRC and Fiona and Ian Russell Seed Corn Grant.

Table of Contents

List of figures

List of tables

Publications from thesis

Papers

Lee, S., Trivedi, U., Johnson, C., Farquharson, C., Bergkvist, G.T.

Optimised isolation method for RNA extraction suitable for RNA sequencing from feline teeth collected in a clinical setting and at post mortem

(Submitted and published on 6/Nov/2018 in Veterinary Research Communications)

Lee, S., Bush, S., Mawson, N. Abbondati, E., Farquharson, C., Bergkvist, G.T.

Feline tooth transcriptome changes and a potential role of MMP9 involvement in feline tooth resorption (TR)

(In preparation)

Abstracts, Oral Presentations

26th European Veterinary Dental Forum Malaga 2017

Oral presentation

Comprehensive transcriptional profiling of feline tooth resorption using next generation sequencing **Lee, S**. et al Congress proceedings, Page 85

Bone Research Society Annual Meeting 2015 Edinburgh 2015

Poster presentation

Identification of genetic mutations responsible for odontoclast dysregulation in feline tooth resorption **Lee, S**. et al Bone research society abstracts, Page 69

Abbreviations

$1,25(OH)_2D_3$	1,25-dihydroxyvitamin D_3
25(OH)D	25-hydroxyvitamin
AP-1	activator protein-1
ATP	adenosine triphosphate
Atp6v0d2	d2 isoform of vacuolar ATPase
BAP	bone alkaline phosphatase
BMP	bone morphogenetic protein
CALCR	calcitonin receptor
cDNA	complementary DNA
CEJ	cementoenamel junction
CSF-1	colony stimulating factor-1
CTSK	cathepsin K
CTx	carboxy terminal telopeptide
DC-STAMP	dendritic-cell-specific transmembrane protein
DMSO	dimethyl sulfoxide
DNA	deoxyribonucleic acid
DPD	deoxypyridinoline
DTT	dithiothreitol
EARR	external apical root resorption
ECM	extracellular matrix
EDTA	ethylenediaminetetraacetic acid
ELISA	enzyme-linked immunosorbent assay
EMAP	endothelial monocyte-activating polypeptide
ERK	extracellular signal-regulated kinase
ERM	epithelial rests of Malassez
FBS	foetal bovine serum
FDR	false discovery rate
FGF	fibroblast growth factor

GM-CSF	granulocyte macrophage-colony stimulating factor
GMP	granulocyte macrophage progenitors
H&E	haematoxylin and esoin
HERS	Hertwig epithelial root sheath
HPLC	high-performance liquid chromatography
IFNG	interferon gamma
IKK	inhibitory κB protein kinase
IκB	inhibitory κB protein
KEGG	Kyoto Encyclopaedia of Genes and Genomes metabolic pathways
MAPK	mitogen-activated protein kinase
MCP	monocyte chemotactic protein
M-CSF	macrophage colonystimulating factor
MEK	MAPK/ERK kinase
MITF	microphthalmia associated transcription factor
MKK	ERK mediating MAPK kinase
MMP	matrix metalloproteinase
NFATc1	NF κB activates nuclear factor of activated T-Cells 1
NF-κB	activator of nuclear factor-kappaB
NGS	next generation sequencing
NIK	NF-κB inducing kinase
NTC	no template control
OC-STAMP	osteoclast stimulatory transmembrane protein
OPG	osteoprotegerin
OSCAR	osteoclast-associated receptor
P2X receptor	purinergic-receptor-P2X, ligand-gated ion channel
PBMC	peripheral blood mononuclear cell
PBS	phosphate buffered saline
PBST	PBS containing Tween 20

PEGFP	plasmid enhanced green fluorescent protein
PGE2	prostaglandin E2
PI3K	phosphoinositide 3 kinase
PKB or Akt	protein kinase B
PTH	parathyroid hormone
PTHrP	PTH-related peptides
RANK	receptor activator of nuclear factor κ-B
RANKL	receptor activator of nuclear factor κ-B ligand
RIN^e	RNA Integrity Number equivalent
RNA	ribonucleic acid
RNase	ribonuclease
RNA-seq	RNA-sequencing
SDS-PAGE	sodium dodecyl sulfate–polyacrylamide gel electrophoresis
SHH	sonic hedgehog
SNP	single nucleotide polymorphism
TAB2	transforming growth factor β-activated protein kinase 1
TAK1	transforming growth factor β-activated protein kinase 1
TGF-β	transforming growth factor β
TR	tooth resorption
TR +ve	TR positive
TR –ve	TR negative
TRAFs	tumour necrosis factor receptor associated factors
TRAP	tartrate-resistant acid phosphatase
VCFs	variant call format files
VDR	vitamin D receptor
α-MEM	Alpha-Minimum Essential Medium

Chapter 1 Introduction

1.1 Tooth Biology

1.1.1 Tooth structure and its supporting apparatus

Teeth constitute approximately 20% of the surface of the mouth and serve several functions including mastication, a tool of attack and defence, protection of the oral cavity, and one of the speech organs especially in humans (1). The basic mammalian tooth consists of four major tissues: enamel, dentine, cementum and dental pulp (1, 2). The most common type is a brachyodont tooth that has a short crown and root ratio which is illustrated in Figure 1.1. Teeth are attached to the bones of the jaw by the periodontium consisting of cementum, periodontal ligament, the alveolar bone forming the tooth socket, and gingiva (gums). The crown of the tooth is the visible part exposed above the gingiva where a thick layer of dentine with the pulp chamber inside is covered by enamel. The neck of the tooth is the area between the crown and the root, also referred to as the cementoenamel junction (CEJ). The anatomical root is the part that extends into the tooth socket below the CEJ. It is composed of the pulp canals and dentine covered with cementum.

Enamel extends just beneath the soft gingival tissues and is the hardest tissue in the body consisting of more than 96% of inorganic material by volume and weight. The thickness enamel was found to be various from 0.1 mm to 1 mm in cats and dogs, which is thinner than that of human teeth (up to 2.5 mm)(3).

Dentine occupies the crown part of the tooth (coronal dentine), and extends into the tooth socket (radicular dentine). It is less mineralised than enamel consisting of approximately 70% mineral with an organic component made up of mainly collagen fibres. It possesses closely packed tubules traversing its entire bulk, and the inner edge of the dentine forms the peripheral boundary of the dental pulp cavity.

The dental pulp is the soft connective tissue which occupies the pulp cavity, the central part of the tooth. The pulp cavity is divided into the pulp chamber of the crown and the root canals (Figure 1.1). The volume of the pulp cavity gradually decreases with age due to deposition of the secondary dentin deposition in the pulp cavity (1, 4). Dentine and pulp comprise endodontium, the dentine-pulp complex. Both tissues develop from the same origin, the dental papilla and they maintain an intimate structural and functional relationship. The root canal terminates at the apical foramen where the nerve and blood vessels that supply the dental pulp enter the tooth. Immature apical foramen (open apex of tooth) becomes a closed apex around the time of completion of root development followed by tooth eruption (5). A tooth can have a single root or multiple roots depending on the type of the tooth. The nerve fibres extend into the dentine of the tooth allowing for transmission of stimuli including pain, heat, cold and pressure from the oral environment to the pulp when the dentine loses its protective enamel covering (6).

Cementum is a bone like avascular connective tissue with approximately 50% mineral (1). The cementum covering the upper portion of the root is acellular and the lower portion of cementum (apical third) is cellular rendering its self-repair to a limited degree (Figure 1.1). Dentine and cementum have limited capability for repair and regeneration, whereas enamel has no capacity for repair because the enamel producing cells are lost upon tooth eruption (1, 6).

Periodontal ligament is a fibrous connective tissue with neural and vascular components. The roles of the periodontal ligament are a supportive function through the principal fibres attaching the tooth to the surrounding alveolar bone proper, a remodelling function by providing stem cells, and a sensory and a nutritive function (1, 7).

The alveolar bone or process is the thickened ridge of bone that contains the tooth sockets. It comprises fibres, a variety of cells, intercellular substances, nerves, blood vessels, and lymphatics (1, 8).

Although basic histological features of the feline dentition have not been

widely studied, the tooth structure and its composition are generally similar to brachyodont teeth of other mammals based on limited studies (6, 9). There are some structures highlighted in cats including deficient mineralisation and well developed vascular networks between gingiva and periodontal ligament, thin layer and low microhardness of enamel, vasodentine-like structures in circumpulpal dentine and osteodentine-like structures in root dentine and gingival plexus (3, 9, 10). A detailed description of these features will be discussed in section 1.4 and 1.5.

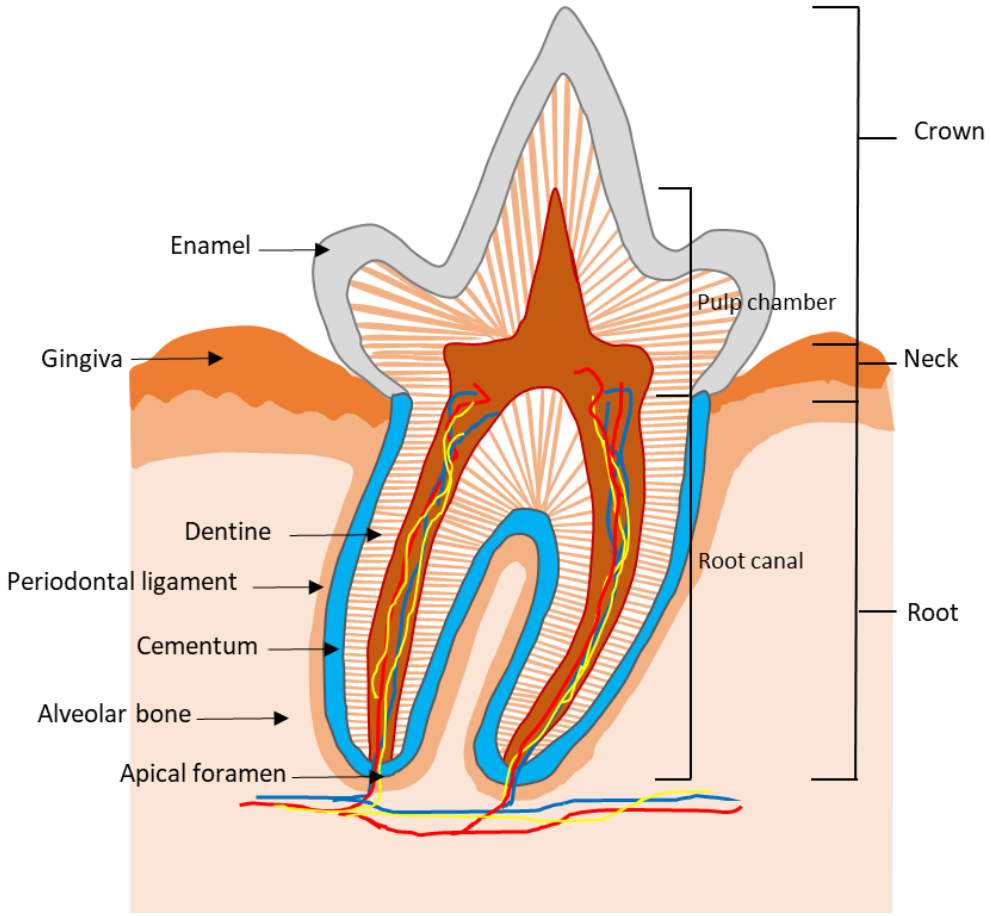

Figure 1.1 A diagram to show the structure of a mammalian (feline) brachyodont tooth. The tooth can be divided into the externally visible part (crown) over the gingiva, the extended part into the bone of the jaw (root), and the junction between the crown and root (neck). The crown is covered by enamel, the hardest tissue in the body. Dentine located beneath the enamel and cementum makes up the bulk of the tooth. Dentine possesses over 40,000/mm^2 dentinal tubules and form a dental-pulp complex which lines the pulp cavity. Pulp is a soft connective tissue and possesses nerves, lymphatics and blood vessels which enter via a passage at the root apex (apical foramen). The tooth is tightly anchored to the alveolar bone via the fibres of the periodontal ligament.

1.1.2 **Diversity and dentition of the mammalian tooth**

Most mammals are diphyodonts which have two sets of teeth, the deciduous teeth (commonly known as baby teeth or milk teeth) and permanent teeth. The deciduous teeth are gradually replaced by a new set of permanent teeth. In contrast to diphyodonts, polyphyodonts have their teeth replaced throughout life. Polyphyodonts include the toothed fishes and many reptiles but also rarely mammals (*e.g.* elephants and manatees). Mammalian teeth are typically heterodont possessing a variety of tooth shapes including incisors, canines, premolars, and molars while non-mammalian vertebrates (*e.g.* sharks and crocodiles) have only one tooth shape in their dental arcades referred to as a homodont dentition. The dolphin is the best example of a homodont mammal (2). In horses, premolars and molars are collectively termed cheek teeth as premolars have evolved to become morphologically identical to the molars to adapt to grinding (11). Another feature is that horses have hypsodont (long crowned) teeth that slowly erupt throughout life (11). The slow eruption of permanent teeth compensates physical wear (attrition) of the occlusal surface of the tooth during grinding of coarse foods (11).

There are considerable variations in the numbers of tooth types between species and this is described in Table 1.1 (11-14). The dentition of mammals is described by dental formulae which describe the number of each of the tooth types from one side of the upper and lower jaw.

In veterinary dentistry, the modified Triadan System is widely used across different animals for dental nomenclature. The modified Triadan system allocates a three digit number to each tooth. The oral cavity is divided into four quadrants 1-4, indicated by the first digit, then the next two digits indicate the tooth in each quadrant (01-03, 04, 05-08, 09-11 for incisors, canine, premolars and molars respectively) (Figure 1.2) (15).

1.1.3 **Cells of the tooth**

1.1.3.1 Ameloblasts

Ameloblasts are derived from the inner dental epithelium of the enamel organ. The ameloblasts cover the entire surface of the crown and are responsible for enamel formation during tooth development. These cells are lost when the tooth emerges into the oral cavity. The loss of these cells makes enamel non-vital and insensitive so that enamel cannot be replaced or regenerated when it is damaged or worn away (1, 2).

Species	Dental formula by number I.C.P.M I.C.P.M	Total teeth number
Human (deciduous)	2.1.0.2 2.1.0.2	20
Human (permanent)	2.1.2.3 2.1.2.3	32
Cat (deciduous)	3.1.3.0 3.1.2.0	26
Cat (permanent)	3.1.3.1 3.1.2.1	30
Dog (deciduous)	3.1.3.0 3.1.3.0	28
Dog (permanent)	3.1.4.2 3.1.4.3	42
Horse (deciduous)	3.0.3.0 3.1.3.0	24
Horse (permanent)	3.1.3-4.3 3.1.3.3	40 - 42
Rabbit (deciduous)	2.0.3.0 1.0.2.0	16
Rabbit (permanent)	2.0.3.3 1.0.2.3	28
Pig (deciduous)	3.1.3.0 3.1.3.0	28
Pig (permanent)	3.1.4.3. 3.1.4.3.	44

Table 1.1 Dental formulae and total number of teeth in mammals. Typical mammalian teeth are heterodont possessing a variety of tooth shapes: incisors, canines, premolars, and molars. The number of each type of tooth and total number vary depending on the species. I: incisor, C: canine, P: premolar, M: molar incisor, C: canine, P: premolar, M: molar.

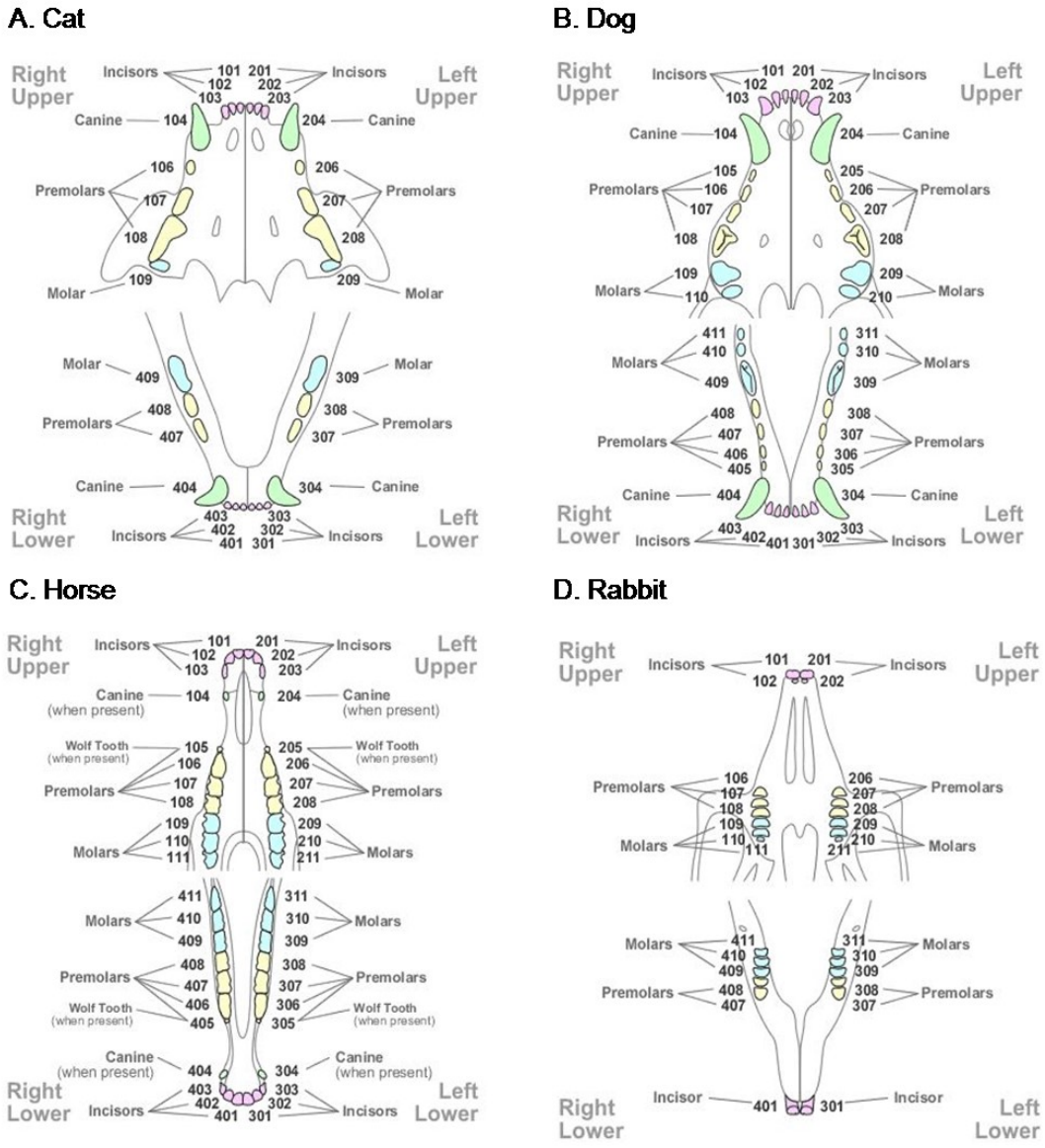

Figure 1.2 The Modified Triadan System for dental nomenclature in veterinary dentistry. Images available at https://www.rvc.ac.uk/review/dentistry/basics/triadan/dog.html

1.1.3.2 Odontoblasts

Odontoblasts are differentiated from ectomesenchymal cells of the dental papilla during foetal development and are present throughout life. Undifferentiated preodontoblasts are small and have central nuclei with few organelles. The inner dental epithelial cells produce signalling molecules and growth factors to induce differentiation of odontoblast precursors. The precursors enlarge and elongate in response to these signals to become preodontoblasts and further differentiated

odontoblasts. Odontoblasts form a single layer at the external boundary of the dental pulp and extend their cytoplasmic processes into canals in the dentine, called dentinal tubules (Figure 1.3). The tubules extend through the entire dentine from the dentinoenamel junction to the pulp (1, 11).

Odontoblasts are responsible for the deposition of dentine and this process is called dentinogenesis (1). Odontoblasts continue to produce dentine throughout life although their secretory activities are largely reduced following tooth eruption. The morphology of odontoblasts reflects their functional activities. During the active phase, cells are polarised and elongated possessing basal nuclei, prominent Golgi complex and increased cytoplasm containing protein synthesising organelles. By contrast, during their resting phase odontoblasts are smaller and stubby with scant cytoplasm.

During the first step of dentinogenesis odontoblasts secrete a layer of unmineralised matrix, predentine, consisting of collagen and non-collagenous components. The predentine is similar to osteoid in bone and it is further transformed into mineralised dentine (Figure 1.3). Primary dentine is formed before the root formation is completed. The mantle dentine is the first deposited dentine at the outer layer close to enamel. It is less mineralised than the majority inner layer of primary dentine (circumpulpal dentine). The circumpulpal dentine is secreted after the mantle dentin by the odontoblasts. Secondary dentine forms after completion of root formation by slow deposition (Figure 1.3). Tertiary dentine, also referred to as reactive or reparative dentine, is produced in response to various stimuli such as caries or tooth wear. The structure and the quantity of the tertiary dentine depend upon the intensity and duration of the stimuli. While primary or secondary dentine is formed along the dentine-pulp border, tertiary dentine is formed at specific sites where stimuli induce the activity of pre-existing odontoblasts or newly differentiated odontoblasts from pulp (16). Within the dentinal tubules, there are terminal branches of neural fibres that form an extensive plexus of nerves, called the plexus of Raschkow, just below the odontoblastic cell bodies. This plexus renders

the dentine and pulp sensitive to certain stimuli. Due to this anatomically close relationship, the odontoblast was considered as a receptor cell that mediates changes via synaptic junctions with nerves. However, the direct innervation theory or odontoblast receptor theory has not been proven experimentally (17). The most widely accepted theory to explain mechanism of dental sensitivity (intense and transitory pain or discomfort) is the hydrodynamic theory (17, 18). This proposes that stimuli abrupt dentinal fluid movements within the dentinal tubules, which distorts mechanical deformation of the local pulpal environment and activates nerve endings. Although clinical evidence-based research has been performed to investigate dentine hypersensitivity, the pain mechanism responsible is not fully understood. Dentine is sensitive to not only pain but also mechanical, thermal and tactile stimuli (1).

1.1.3.3 Osteoclasts/Odontoclasts/Cementoclasts

Odontoclasts and cementoclasts are multinucleated cells responsible for the resorption of hard tissues of teeth. These cells share similar characteristics with osteoclasts in bone. Bone constantly undergoes remodelling by a balance of bone formation and resorption by osteoblasts and osteoclasts respectively throughout life (19). Unlike bone, teeth do not remodel and have limited repair capacity. However, teeth can be degraded during normal physiological or as a consequence of pathological conditions. During tooth development, osteoclasts resorb the alveolar bone to aid tooth eruption, whereas odontoclasts and cementoclasts resorb and exfoliate primary teeth during tooth shedding (20-23). Researchers have reported some differences of odontoclasts *in vivo* (e.g. smaller cell size and smaller lacunae formation) compared to osteoclasts (21, 24). However, there is no clear evidence to prove that odontoclasts are morphologically and functionally different from osteoclasts (14, 21, 23, 25, 26). Thus, *in vitro* bone and tooth resorbing clastic cells can be referred to as osteoclasts in general, and current knowledge of odontoclasts is based on osteoclast biology (Figure 1.4 and Figure 1.5). Both cells are derived from osteoclast precursors, myeloid/monocyte lineage progenitors, present in bone

marrow, spleen, and circulating blood (Figure 1.4). These progenitors migrate through blood vessels and undergo similar differentiation pathways at their respective resorption sites, in bone at the trabecular and endosteal cortical bone surfaces and in dental hard tissues at the edge of the cementum, dentine and pulp cavity (20, 23) (Figure 1.5).

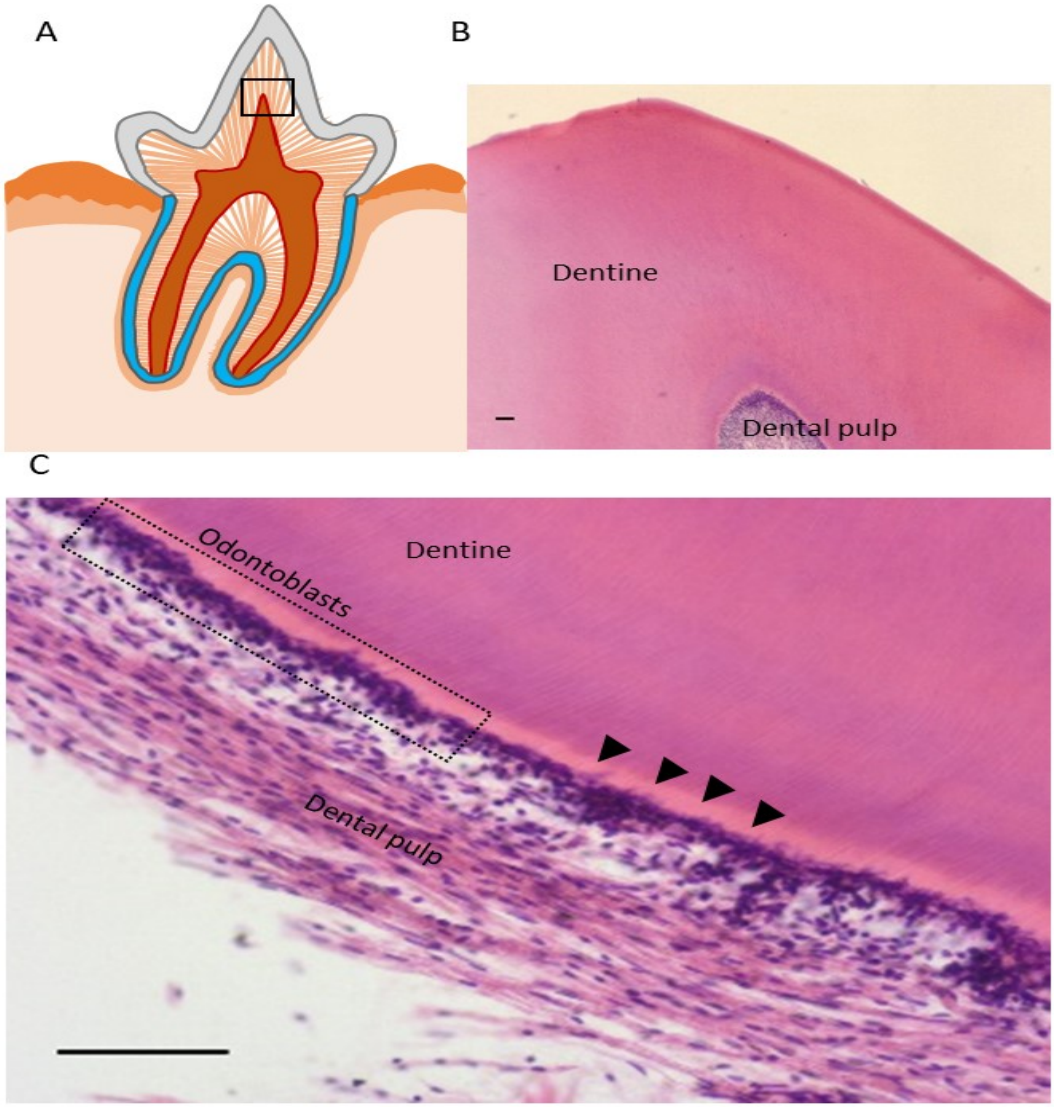

Figure 1.3 Histology of dentine-pulp complex of the feline tooth. (A) A diagram of observed area. (B) Dentine-pulp complex in boxed area (H&E). (C) Dental-pulp border contains a layer of odontoblasts (dotted box) and predentine (arrowheads). Secondary regular dentine occupies majority of dentine forming dentinal tubules. Dental pulp contains many cells (fibroblasts, undifferentiated mesenchymal stem cells and immune cells) in sub-odontoblastic layer (H&E). Scale bars = 100 µm.

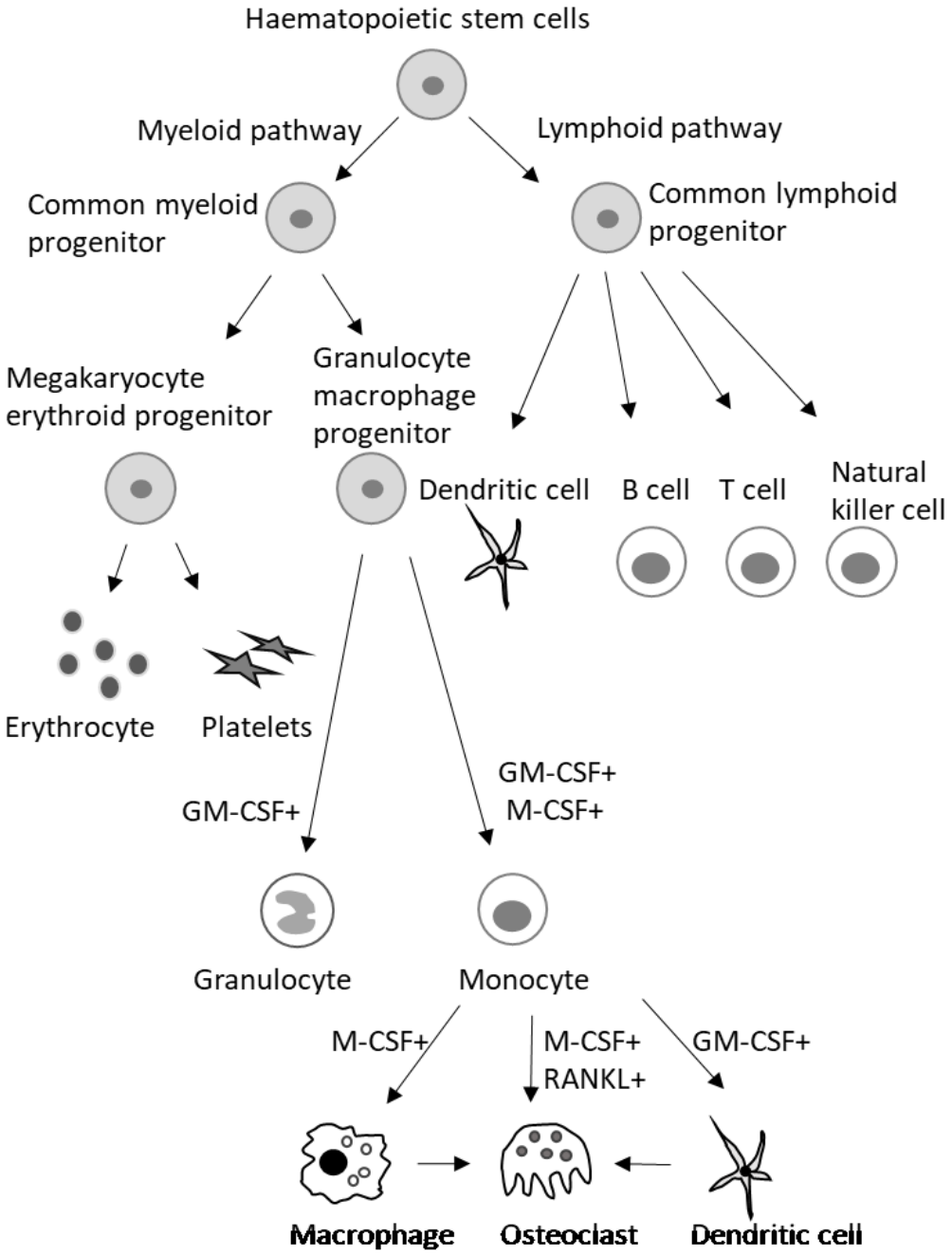

Figure 1.4 A schematic diagram showing the differentiation of the osteoclast lineage from haematopoietic stem cells. Haematopoietic stem cells give rise to common lymphoid and myeloid progenitors. Myeloid progenitors further generate megakaryocyte erythroid progenitors and granulocyte macrophage progenitors. Granulocyte macrophage progenitors give rise to granulocytes and monocytes then monocytes further differentiate into macrophages, dendritic cells and osteoclasts. Differentiation of macrophages, osteoclasts and dendritic cells is stimulated by GM-CSF and M-CSF. Additional RANKL is required for osteoclast commitment. GM-CSF: granulocyte macrophage-CSF, M-CSF: macrophage-CSF.

Osteoclasts are terminally differentiated cells which usually form as multinucleated giant cells that are incapable of self-renewing. Osteoclastogenesis is induced by a number of cytokines and transcription factors which starts to commit myeloid lineage cells to an osteoclast lineage. Osteoclast precursors are induced to express various receptors and undergo cellular changes and cytoplasmic fusion of cells via multiple differentiation steps (Figure 1.5). It has not been fully understood which specific sub-populations in bone marrow or circulating blood are committed to become osteoclast precursors and what attracts osteoclast precursors to the resorption sites (27-29).

However, it has been well documented that there are two essential key molecules that control osteoclast differentiation: colony stimulating factor-1 (CSF-1) also called macrophage colony-stimulating factor (M-CSF) and receptor activator of nuclear factor κ-B ligand (RANKL) (Figure 1.5) (30, 31).The discovery of three molecules, receptor activator of nuclear factor κ-B (RANK), RANKL and osteoprotegerin (OPG) and its RANK/RANKL/OPG axis pathway contributed a major advance in osteoclast biology especially the mid-to-later stages of osteoclastogenesis (Figure 1.5) (23, 32). It has been reported that many cell types are capable of RANKL expression including osteoblasts, osteocytes, chondrocytes, stromal cells, T and B lymphocytes in bone and cells of the dental follicle in developing teeth and periodontal ligament cells in adult teeth (33, 34). In this respect, osteoclast formation is regulated by the bone and tooth microenvironments. There are also co-stimulatory molecules that mediate osteoclastogenesis. The earliest required molecules to promote a myeloid lineage are the transcription factors PU.1 encoded by SPI1 and the microphthalmia associated transcription factor (MITF) (35-37). PU.1 and MITF regulate expression of the CSF-1 receptor called c-Fms on the early stage pre-osteoclasts (Figure 1.5). CSF-1 mediates the survival and proliferation of osteoclast precursors and osteoclasts. Since osteoclast precursors share a common monocyte/macrophage lineage with phagocytic immune cells, CSF-1 also induces differentiation of macrophages and dendritic cells (38, 39). The

important role of CSF-1 in osteoclastogenesis is to promote the expression of RANK on osteoclast progenitors. When RANKL binds to its receptor, RANK, it can fully induce osteoclastogenesis (Figure 1.5 and Figure 1.6).

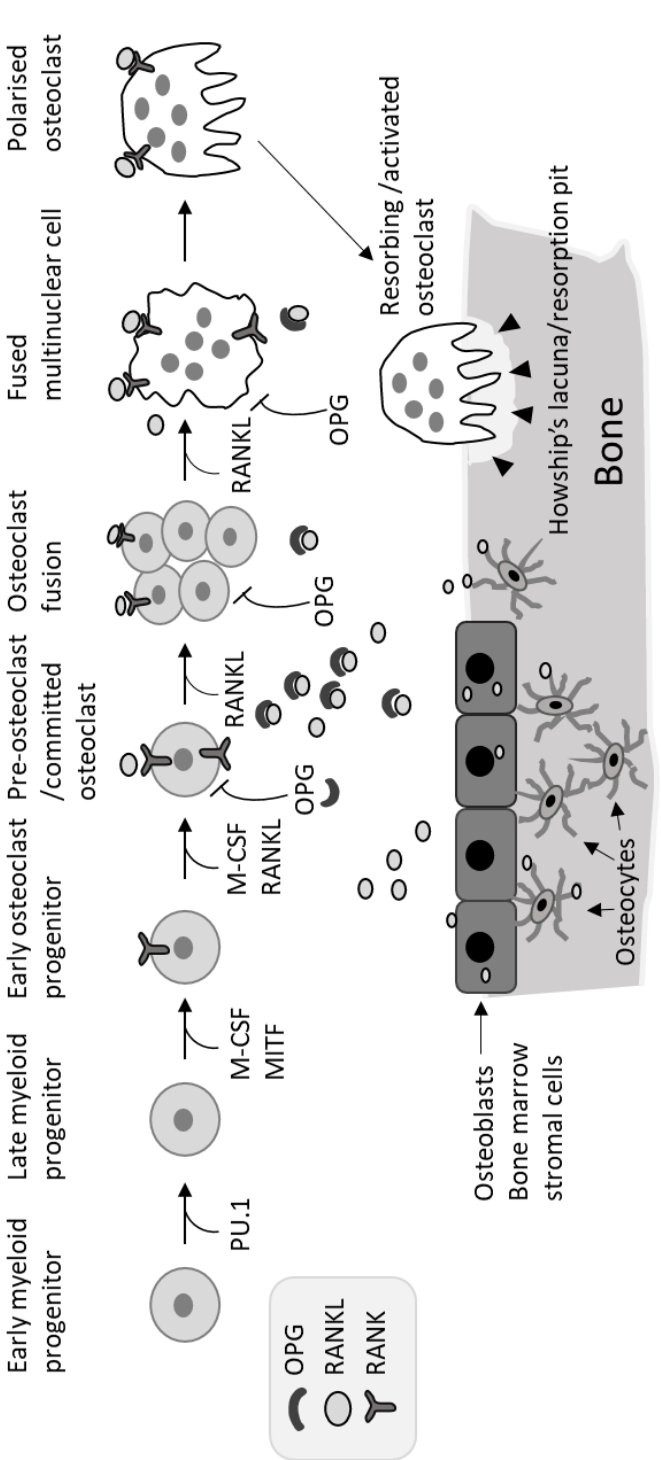

Figure 1.5 Osteoclast differentiation schema from osteoclast precursors into mature osteoclasts. The early commitment of myeloid lineage is stimulated by transcription factors including PU.1 and MITF. The committed osteoclast progenitors differentiate into pre-osteoclasts and they fuse together to form multinuclear osteoclast under the influence of M-CSF and RANKL. RANKL is expressed in many cells types including osteoblasts and osteocytes in bone. RANKL expressing cells also produce a decoy receptor, OPG that negatively regulate osteoclastogenesis. Osteoclasts adhere to bone at the resorption site and undergo cytodifferentiation into a mature osteoclast. Activated osteoclasts dissolve minerals and organic matrix components by secreting acid and proteolytic enzymes, respectively. See text for more details.

Negative regulation of osteoclastogenesis occurs via OPG, a glyco-protein that acts as a decoy receptor for RANKL. When OPG binds to RANKL, it prevents RANKL from interacting with RANK expressed on osteoclast precursors which results in reduction of the number of osteoclasts. Osteoclast formation is largely influenced by the ratio of RANKL to OPG present in the bone microenvironment (Figure 1.5) (40). RANK signalling mediates further downstream signalling pathways in the osteoclast precursors (Figure 1.6). As RANK lacks intrinsic kinase activity to phosphorylate and activate downstream pathways, it recruits tumour necrosis factor receptor associated factors (TRAFs) 1, 2, 3, 5 and 6. TRAFs are adaptor proteins that recruit protein kinases (35, 36). Of these, TRAF6 is the most powerful molecule for osteoclast formation and bone resorption whereas other TRAFs have a complementary role since only deletion of TRAF6 resulted in severe osteopetrosis due to impairment of osteoclast formation (41, 42). At least four TRAF-mediated protein kinase signalling cascades have been identified: including the activator of nuclear factor (NF)-kappaB (NF-κB) signalling as the main pathway, mitogen-activated protein kinase (MAPK) signalling, phosphoinositide 3 kinase (PI3K) signalling via Src, and calcium signalling (Figure 1.6) (36, 37, 43-46). Formation of a signalling complex containing RANK, TRAF6 and transforming growth factor β-activated protein kinase 1 binding protein-2 (TAB2) results in transforming growth factor β-activated protein kinase 1 (TAK1), which is essential for NF-κB and MAPK pathways (47). Under non-stimulated conditions, NF-κB exists as a complex with inhibitory κB protein (IκB) in the cytoplasm and it is released by IκB kinase (IKK) (48). In a canonical NF-κB signalling pathway, the TRAF/TAK1/TAB2 complex leads to trigger IKKα, β and γ to phosphorylate IκB (36, 47). A non-canonical pathway involves NF-κB inducing kinase (NIK) and mediates through IKKα (36, 49). IκB is then degraded by the proteasome, which allows to release and activate NF-κB to translocate to the nucleus where it stimulates transcription of osteoclastogenic genes (35, 37). There are 5 main NF-κB subunit proteins including RelA (p65), p50 (NF-κB1), RelB, p52 (NF-κB2), and c-Rel. RelA/p50 heterodimers are involved in the

canonical signalling and RelB/p52 heterodimers are recruited in the non-canonical signalling (36, 48). NF-κB activates nuclear factor of activated T-Cells 1 (NFATc1), a key transcription factor of osteoclast differentiation. The activation of NFATc1 is also regulated by the activator protein-1 (AP-1), c-Fos and calcineurin (50). In MAPK signalling, the RANK/TRAFs complex activates c-Jun N-terminal kinase (JNK), p38 and extracellular signal-regulated kinase (ERK) mediating MAPK kinase (MKK)7, MKK6 and MAPK/ERK kinase (MEK) to induce activation of their downstream targets such as AP-1, Mitf and c-Fos, respectively (Figure 1.6) (22, 46, 47). Downstream signal of TRAF6 also activates Src kinase dependent PI3K/Protein kinase B (PKB also known as Akt) pathway. The PI3K/Akt and MEK/ERK pathway mediates proliferation, survival and cytoskeleton arrangement of osteoclast (46, 51). Taken together, not only RANKL mediated signalling but costimulatory signalling pathways mediated by hormones and inflammatory cytokines (*e.g.* IL-1, TNF. CSF-1) also induce osteoclast differentiation (20, 37, 43, 52). Terminal differentiation of osteoclasts and further osteoclastogenesis occur via regulating expression of osteoclast-specific genes including tartrate-resistant acid phosphatase (TRAP), cathepsin K (CTSK), calcitonin receptor (CALCR), osteoclast-associated receptor (OSCAR), dendritic-cell-specific transmembrane protein (DC-STAMP), d2 isoform of vacuolar ATPase (Atp6v0d2, V-ATPase D2) and integrin $\alpha_v\beta_3$ (vitronectin receptor) in cooperation with other transcription factors (Figure 1.6) (20, 37). Osteoclasts are highly motile and capable of formation of integrin complexes. The integrin $\alpha_v\beta_3$ forms a complex with actin, known as the podosome which is responsible for the formation of the sealing zone between the osteoclasts and the bone/dentin matrix. Following osteoclast attachment to the bone surface, osteoclasts fuse intracellular vesicles with the cell membrane and consequently release hydrogen ions and proteolytic enzymes within a lacunae called Howship's lacunae, at the resorption site (Figure 1.5). This highly acidic environment results in dissolution of inorganic mineral while the proteolytic enzymes such as matrix metalloproteinases breakdown the organic collagenous material (22). Fully

differentiated osteoclasts possess numerous lysosomal and membranous enzymes for excavation and active motility (23).

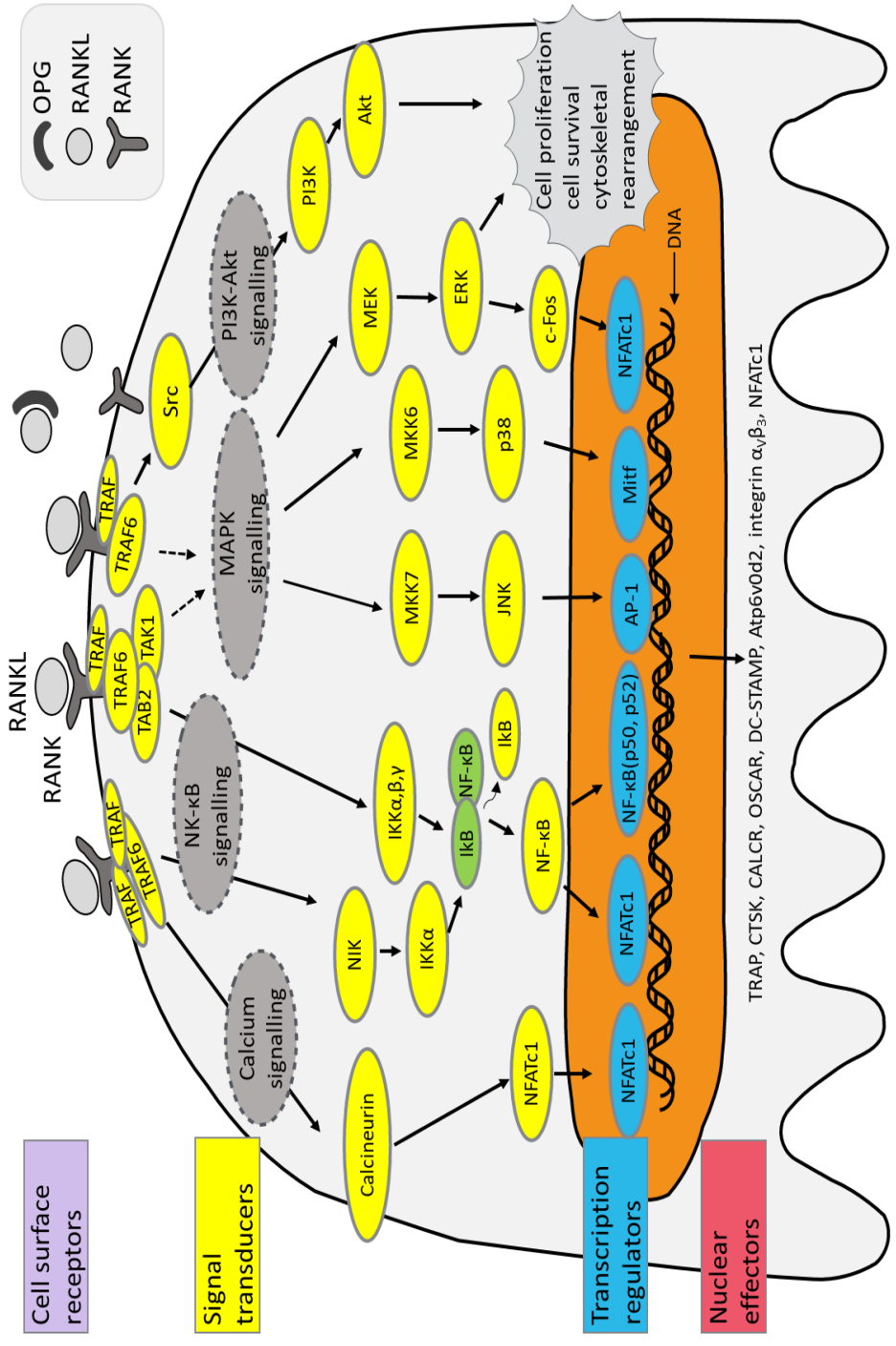

Figure 1.6 RANK/RANKL/OPG axis and downstream pathways in osteoclastogenesis. See text for more details.

1.1.3.4 Cellular components of periodontal ligament

The predominant cells of the periodontal ligament are fibroblast-like cells which are capable of production of collagen, mainly type I. The collagen fibres consist of larger extrinsic fibres, some of which form tight bundles of Sharpey's fibres that cross the periodontal space to become anchored in the alveolar bone. The periodontal ligament also possesses a variety of cells including epithelial cell rests of Malassez (ERM) which are clusters of residual cells from proliferating epithelial cells in developing teeth, vascular cells, sensory nerve cells, and stem cells that can differentiate into osteoblasts and cementoblasts (Figure 1.7) (2, 53). From the blood vessels, osteoclast/odontoclast precursors can be recruited into cementum and alveolar bone surfaces of the periodontal ligament.

1.1.3.5 Cementoblasts and cementocytes

Cementoblasts are derived from dental follicle/dental sac during tooth development. Their characteristics are similar to osteoblasts. Cementoblasts differentiate to cementocytes which deposit the organic matrix of cementum (cementoid) that becomes secondarily mineralised (Figure 1.7). Cementum is deposited in increments similar to bone and dentine (53).

1.1.3.6 Mesenchymal stem cells in the tooth

The dental tissues have been considered a rich source of mesenchymal stem cells that have the potential to differentiate into several cell types. Mesenchymal stem cells were demonstrated in dental tissues including in the dental papilla and dental follicle in developing teeth as well as in the dental pulp and in the periodontal ligament in adult teeth (Figure 1.3 and Figure 1.7) (1, 54).

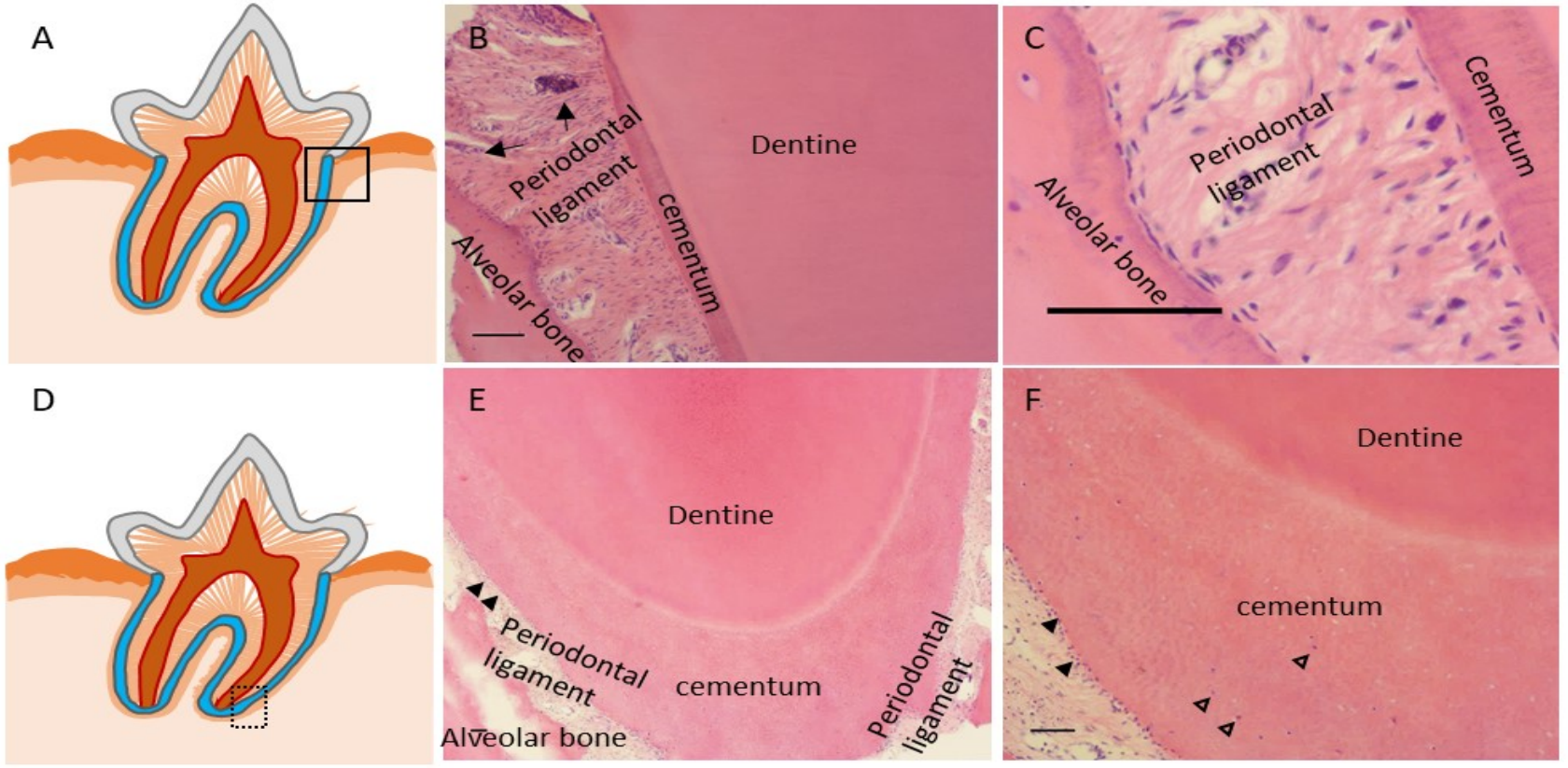

Figure 1.7 Histology of periodontium of the feline tooth. (A) A diagram of observed area (B) and (C). (B) Periodontium of upper root consists of acellular cementum, periodontal ligament and alveolar bone. Periodontal ligament possesses fibroblasts, mesenchymal stem cells and epithelial rests of Malassez (ERM) (arrows) (H&E). (C) The fibres in the periodontal ligament fill the periodontal space and they are aligned horizontally and obliquely (H&E). (D) A diagram of observed area (E) and (F). (E) Apical root contains cellular cementum (H&E). (E) High magnification shows cementoblasts (arrowheads) and cementocytes in lacunae (hollow arrowheads). Scale bars = 100 µm.

1.1.4 Organic and inorganic components of tooth

Hard tissues of the body including bone, cementum, and dentine have many similarities in their formation and structure. They are all specialised connective tissues that undergo biomineralisation where specialised cells secrete proteins to form an extracellular matrix (ECM) consisting of mainly collagen fibres that attract and organise calcium and phosphate ions in composition to calcium hydroxyapatite [$Ca_{10}(PO_4)_6(OH)_2$] (1, 8, 53). Although enamel has no collagen, its hard tissue formation follows a similar principle (53). Amelogenin as the most abundant ECM protein in enamel is believed to play an important role to organise a basic unit of enamel crystals during enamel formation (55). During crown formation, ameloblasts become polarised in the pre-secretory phase and then secret organic matrix proteins including amelogenin and non-amelogenins (ameloblastin, enamelin, tuftelin and amelotin). As the majority of the ECM proteins are proteolytically removed prior to maturation of enamel, fully formed enamel contains only 4% organic material (amelogenin and non-amelogenins and matrix proteinases), water and hydroxyapatite (96%).

Dentine is less mineralised than enamel and harder than bone. It is made up of 70% inorganic minerals (mainly hydroxyapatite), 20% organic materials including collagen, non-collagenous proteins and matrix proteinases, and 10% water. The organic materials constitute approximately 30% collagen (type I with small proportions of type III, V and VI), lipids and various non-collagenous proteins. The composition of non-collagenous matrix proteins in dentine are similar to bone, including dentine phosphoprotein, dentine sialoprotein, dentine phosphoprotein, dentine matrix protein-1, bone sialoprotein, osteopontin, osteocalcin, osteonectin, proteoglycans and matrix extracellular phosphoglycoprotein, all of which are also found in bone (1).

Cementum is similar to bone in terms of degree of mineralisation and constituents containing 45 to 50% of hydroxyapatite and 50% collagen and non-collagenous matrix proteins. Type I is the prominent collagen occupying 90% of the

organic matrix. Other types of collagen including type III, XII and XIV are also found in cementum. Non-collagenous proteins identified in cementum are bone sialoprotein, proteoglycan, osteocalcin, osteonectin, osteopontin, proteoglycan and vitronectin (1). Phosphatases known to be required for matrix mineralisation such as alkaline phosphatase and phosphoethanolamine/phosphocholine phosphatase encoded by Phospho1 have been localised to various cell types within the tooth (56, 57).

Enamel is the first line of defence due to its hardness and high mineral content. It plays the role of a physical resistance and barrier against the masticatory forces (*e.g.* tooth wear and tear, dental attrition). However, enamel is also brittle. Therefore it requires a more resilient structure in combination with it. Dentine is less mineralised compared to enamel, and this reduced hardness of dentine compensates for enamel as a supportive structure of the tooth.

1.1.5 Tooth development and physiological tooth resorption

1.1.5.1 Tooth formation

Although teeth share their mineralised nature with bone, tooth formation is markedly different from bone (8, 58). Tooth formation largely relies on odontogenic epithelial-mesenchymal interactions and integration of the root with the jaw bone, blood supply and nerve innervations. The importance of epithelial-mesenchyme interactions has been well denoted by Lumsden's mammalian tooth formation study (59). It demonstrated that tooth formation was only elicited when neural crest cells interacted with mandibular epithelium. If limb epithelium was used or just neural crest cells or mandibular epithelium on their own, no tooth formation occurred (59). Tooth formation starts with the thickening of the ectodermal epithelium in the position of the future upper and lower jaws during gestation. Neural crest cells migrate to under the oral epithelium and become ectomesenchyme. The thickened band of epithelium gives rise to two subdivisions: the vestibular lamina and the dental lamina. The cells in vestibule lamina proliferate rapidly and become the vestibule which is the space between the cheeks and the

gingiva. The dental lamina continues to produce epithelial outgrowths to form placode underlying the ectomesenchyme at regular intervals along the dental lamina at the sites of the future deciduous teeth (Figure 1.8, A). From this stage, tooth development proceeds in three stages: the bud, cap and bell stage (11, 53, 58).

In the bud stage, proliferative epithelial cells invaginate into the underlying ectomesenchyme and then the ectomesenchymal cells condense (Figure 1.8, B). In the following cap stage, the epithelial bud enlarges by cell division shaping a convex cap-like surface (Figure 1.8, C). The epithelial cells undergo differentiation into several cell layers to form the enamel organ including the outer enamel epithelium, the inner epithelium lining the concavity, and the stellate reticulum formed within the cap. Enamel knots are clusters of non-dividing epithelial cells that express many genes for signalling molecules to proliferate surrounding cells. As the ectomesenchyme becomes further condensed, the ball shaped dental papilla is formed below the enamel organ and surrounded by the condensed dental follicle (Figure 1.8, D). The enamel organ, dental papilla, and dental follicle together compose the tooth germ. The dental papilla contains cells that develop into odontoblasts responsible for formation of dentine as well as the mesenchymal cells developing into the pulpal cells. The dental follicle is a loose connective tissue that gives rise to three important entities: cementoblasts, osteoblasts and fibroblasts which all together form the future periodontium. The tooth crown shape is determined during the bell stage, and the terminally differentiated dental secretory cells start to deposit the hard substrates of the crown, dentine and enamel (Figure 1.8, D). The bell shape is established by folding of the inner enamel epithelium while dentine and enamel begin to form at the crest of the inner enamel epithelium. Crown formation continues until it reaches its complete size and is followed by root formation (Figure 1.8, E). One important event during the bell stage is that the dental lamina is separated from the primary tooth germ to initiate the permanent tooth bud. The permanent teeth are also formed by the proliferative activity of the tooth germs within the dental lamina (11, 53, 60, 61).

After crown formation, root formation is initiated by proliferation of epithelial cells from the cervical loop where the inner and outer epithelial cells join at the edge of the enamel organ (Figure 1.8, E). This double layer of cells further proliferate and form the Hertwig epithelial root sheath (HERS). It has been widely accepted that the role of HERS is related to induce root formation by regulating the size, shape and number of the roots even though the precise mechanism of these cells remains unclear (62, 63). HERS extends around the dental pulp until it encloses the basal portion of the pulp and the rim of this sheath surrounds the primary apical foramen. The inner epithelial cells of HERS give an inductive message to differentiate radicular dental papilla cells into odontoblasts that lay down the dentine of the root. While the crown of the tooth rapidly grow away from the bony socket of the jaw, the root sheath does not grow at the same speed so it rather stretches and eventually fragments to form a number of clusters of epithelial cells. Then HERS is separated from the root allowing the newly formed predentine to come in contact with dental follicle cells. Some cells in the outer layer of HERS in the coronal root region induce to differentiate dental follicle cells into cementoblasts that lead to cementum formation. HERS eventually undergoes apoptosis and the remnants of HERS form discrete masses surrounded by a basement membrane. These clustered cells are known as the epithelial cell rests of Malassez (ERM) which remain within the mature periodontal ligament along the cementum as previously discussed in section 1.1.3.4 and Figure 1.7. While cementogenesis initiates, fibroblast precursors from dental follicle make contact with predentine matrix and deposit bundles of collagen fibres to form extrinsic Sharpey's fibres. During the late stage of cementogenesis, cementoblasts and cementocytes are involved in the secretion of intrinsic fibres. In addition to collagen, non-collagenous proteins are secreted to maintain the space of periodontal ligament. Alveolar bone develops during the eruption of teeth to provide the osseous attachment to the developing periodontal ligament (2, 53, 58). The developmental biology of tooth root and periodontium formation is probably the least known aspect of tooth development and this

requires further studies (53).

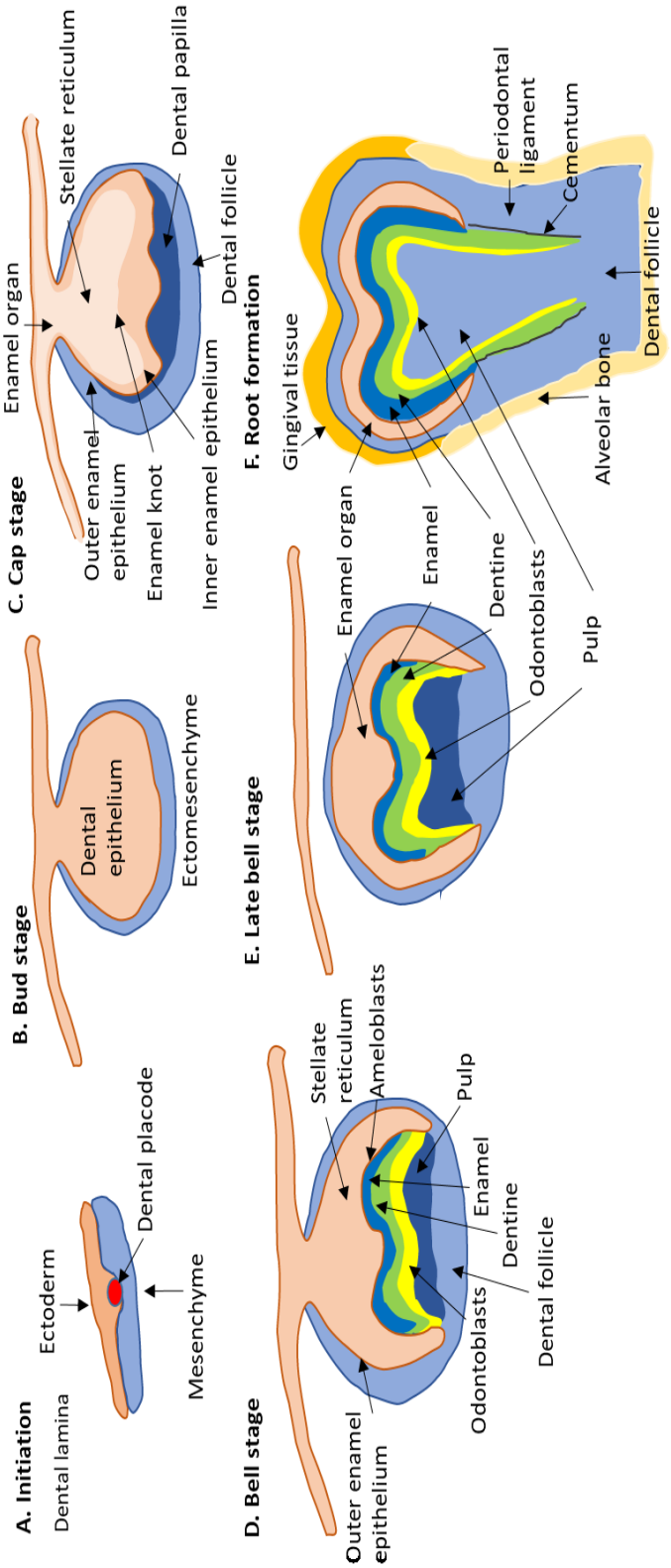

Figure 1.8 Schematic diagram of tooth formation. (A) Tooth formation starts with the thickening of the ectodermal epithelium that gives rise to dental lamina. The thickened ectoderm forms a dental placode. (B) The dental placode buds to the underlying neural crest derived ectomesenchyme. The underlying ectomesenchyme condenses and proliferates. (C) In the cap stage, the epithelial bud enlarges to a convex cap-like shape and undergoes differentiation into several cell layers to form the enamel organ including the inner and outer enamel epithelium, the stellate reticulum, and the enamel knot, a signalling centre. The dental papilla is formed below the enamel organ and it is surrounded by the condensed dental follicle. (D) In the bell stage, the shape of the crown is formed and differentiation of dental secretory cells is achieved. (E) The terminally differentiated ameloblasts and odontoblasts start to deposit the hard substrates of the crown, dentine and enamel in late bell stage. (F) After crown formation, root formation continues to elongate and tooth supporting tissues including cementum, periodontal ligament, and alveolar bone develop. See the text for more details.

1.1.5.2 Signalling pathways during tooth development

To understand tooth formation, the genes and molecular signals that control cell proliferation, migration and differentiation also need to be considered. Like other organ development (*e.g.* limb, kidney and bone), the molecular signals and gene expression cascades in the developing tooth are unique and very complex. Hundreds of genes have been identified for each development stage. The most conserved signalling pathways involved are the bone morphogenetic proteins (BMPs) belonging to the TGF-β superfamily, fibroblast growth factor (FGF), sonic hedgehog (SHH) and WNT ligands and their receptors. These are all involved during tooth development and in epithelial–mesenchymal interactions (53, 61, 64).

1.1.5.3 Tooth eruption, shedding and the role of osteoclast/odontoclast

After root formation is initiated, the tooth begins to erupt moving in an axial direction (14). Physiologically, osteoclasts are essential for eruption of the developing tooth in this critical embryonic period (23). The congenital osteoclast deficient osteopetrotic (op/op) mutant mice suffer from osteopetrosis due to the lack of functional CSF-1 and display a complete failure of tooth eruption (65). Similarly, reducing the number of odontoclasts by injecting CSF-1 receptor antagonists during tooth eruption resulted in a complete or partial failure of tooth eruption (66). Mononuclear osteoclast precursor cells are recruited into the dental follicle prior to the onset of eruption. When eruptive movement begins, the enamel of the crown is still covered by ameloblasts and the three layers of the enamel organ. The ameloblasts and the adjacent cells of the enamel organ together form the reduced dental epithelium. The reduced dental epithelium and dental follicle produce signals to recruit osteoclasts. While the connective tissue of the mucosa breaks down and the oral epithelium and the reduced dental epithelium fuse, the alveolar bone covering the erupting tooth is resorbed by osteoclasts so that the crown passes through the bone and overlying epithelium. During eruption, the central cells of the fused epithelium lose their nutritive supply and degenerate for formation of the epithelial canal. As the permanent teeth increase in size, the primary teeth need to

be resorbed and exfoliated. This is known as deciduous tooth shedding or colloquially as shedding of the milk teeth. The resorption process is achieved by odontoclasts. While resorption starts at the root and coronal pulp leaving the odontoblast layer within the pulp chamber intact until completion of root resorption at which point the odontoblasts degenerate and odontoclasts actively engage in the resorption of dentine. The internal resorption by odontoclasts in the pulp initiates at the predentine surface and proceeds to the dentine. An intriguing question is how permanent teeth are protected from osteoclastic/odontoclastic resorption and how these cells recognise and resorb only the deciduous cells.

1.1.5.4 Signalling pathways during tooth eruption and shedding

The clear pathways of tooth eruption and shedding have not been well defined. However, tooth eruption and shedding are recognised to be localised events and the patterns of differential gene expression involved in physiological tooth resorption are both chronological and spatial (14, 67, 68).

Extensive studies have shown that the dental follicle is required for tooth eruption (14, 23, 26, 69). The dental follicle that surrounds the un-erupted tooth has a dual role of alveolar bone resorption and bone formation. The major key for this process is how the molecular pathways are processed in a distinct temporal and spatial manner.

The coronal region of the dental follicle induces osteoclast mediated alveolar bone resorption whereas the basal dental follicle promotes the alveolar bone formation at the base of the crypt for tooth eruption (67). These spatial effects of the dental follicle are the result of regional differences in gene expression (67). The expression of RANKL was greater in the coronal part than the basal part whereas the expression of bone morphogenetic protein-2 (BMP-2), the bone formation marker was greater in the basal region than in the coronal half (67, 69). Dental follicle also gave signals to recruit osteoclast precursors via expression of chemokines including CSF-1, monocyte chemotactic protein-1 (MCP-1) and endothelial monocyte-activating polypeptide (EMAP-II). In addition to the role of a

chemokine, EMAP-II induced to upregulate the gene expression of both CSF1 and MCP-1, which indirectly promoted mononuclear cell recruitment *in vitro* (70). RANKL expression of the alveolar bone stromal cells adjacent to the dental follicle is considered to stimulate the fusion of the osteoclast precursors in the follicle (71).

The chronological changes of gene expression in the dental follicle largely controls osteoclastogenesis for alveolar bone resorption (67, 72). In rat and mouse studies, it has been shown that a major and minor influx of osteoclast precursors into the dental follicle exist at a specific time prior to the onset of eruption which is subsequently followed by a burst of osteoclastogenesis on alveolar bone (71). The maximal expression of CSF-1, EMAP-II and MCP-1 in the dental follicle corresponded to the time of the major burst of osteoclastogenesis (70, 73, 74). The period of major osteoclast formation was influenced by the down-regulation of OPG in the dental follicle rather than the upregulation of RANKL (67, 71). Although RANKL was also expressed in the dental follicle at this time, its gene expression was not upregulated (72). The difference in gene expression is the result of an increase in the RANKL/OPG ratio that supports osteoclastogenesis (67). This chronological and spatial process is believed to be a programmed event and this concept has been applied to primary tooth shedding (26). For root resorption of primary teeth, the dental follicle of permanent teeth is involved and the pressure of the erupting permanent teeth play a contributory role (75). RANK and RANKL are both expressed predominantly in the periodontal ligament from actively resorbing primary teeth, whereas OPG expression is decreased compared to non-resorbing deciduous teeth and permanent teeth. In contrast, OPG is highly abundant in non-resorbing deciduous teeth and permanent teeth (33, 76). Expression of RANKL in many other cells including pulpal fibroblasts, odontoblasts, cementoblasts, and ameloblasts in deciduous teeth may support the osteoclast resorption of primary teeth (23, 77-79).

In summary, physiological tooth resorption during tooth eruption including resorption of the alveolar bone and the deciduous tooth are regulated by the local

microenvironment of the tooth. Furthermore, the RANK/RANKL/OPG axis plays an important role during this process together with many co-stimulating factors.

1.2 Tooth resorption in cats

1.2.1 Definition and classification

Feline tooth resorption (TR), previously referred to as feline odontoclastic resorptive lesions (FORL) or neck lesions, is a common and painful oral pathologic condition in domestic cats. A similar problem has been reported in a wide range of mammals including humans, dogs and horses as well as wild cats (80-85). TR in other animals will be discussed in section 1.3. Since caries also destroy dental hard tissues, the early studies focused on distinguishing TR from caries. Hopewell-Smith was the first to report the histopathological differences between feline TR and caries in 1930 (86). TR lesions lack the typical histological features of caries (*e.g.* presence of bacteria in the dentinal tubules, liquefaction foci and pipe stem appearances in the dentine) as demineralisation, as a result of caries, is due to toxins produced by carbohydrate-fermenting bacteria. Dental caries are common in humans, however, they are rare in cats and dogs, and only a few studies have explored why cats and dogs are protected (87-89). The reasons proposed include (1) pH of saliva in cats and dogs is higher than that of humans so that it is able to buffer acids produced by bacteria causing caries, (2) carnivore's teeth have less pits and fissures with a conical shape of crown, (3) their diets are low in fermentable carbohydrates and (4) differences in oral flora may contain less bacteria responsible for caries (89, 90).

TR was not actually recognised as a separate condition until the 1970's following a microscopic study that conclusively differentiated TR from dental caries (91, 92). According to a thorough review of Hopewell-Smith's early report by Reiter (93), Hopewell-Smith used the terms osteolysis and odontolysis of the tooth which is now referred to as tooth resorption in both physiological deciduous tooth resorption and pathological permanent tooth resorption. It was noted that permanent teeth undergoing different stages of tooth resorption showed variable

degrees of dentine or pulp loss and the defects were often replaced with granulation tissues. However, Hopewell-Smith failed to identify the cells responsible for the odontolytic process and this according to Reiter was due to a lack of knowledge of the osteoclast/odontoclast in the early 1900's. More recent investigation of seven feline mandibles and one skull from an archaeological excavation revealed domestic cats living in the 13th to 14th centuries possessed lesions characteristic of TR suggesting that TR is not a recent disease (94).

According to the accumulated knowledge over the last several decades, TR is defined as loss of dental hard tissues (92) and this progressive condition is caused by dysregulation of odontoclasts. The destructive lesion initiates on the external surface of the tooth root and extends into enamel, dentine and pulp in the advanced stage (9). The lesions are seen most often at the gingival margin of the tooth and they are commonly covered by granulation tissue or plaque (Figure 1.4, E). At advanced stages of the disease, inflammation is frequently involved and the tooth structure is significantly resorbed leading to crown fractures and loss of dentition (9, 93, 95). It is noteworthy, however, that some lesions are not accompanied by inflammation which is similar to idiopathic root resorption in humans (96).

The diagnosis of TR is made by clinical oral examination including visual inspection and tactile exploration, often combined with radiography (97). Teeth undergoing early TR lesions can be difficult to diagnose. The current gold standard for diagnosis is a combination of oral examination and full mouth radiography where each tooth is properly represented in at least one view using a series of dental films (98).

Current TR classification follows the criteria suggested by the Nomenclature Committee of the American Veterinary Dental College (AVDC) based on the severity of the resorption (Stages 1-5) (Figure 1.9, Table 1.2) and on the location of the resorption sites by radiographic appearance (Types 1-3) (99, 100). Depending on the progression of TR, affected cats show varying clinical signs including anorexia, excessive salivation, swelling, bleeding, pain and reluctance to drink or eat (101).

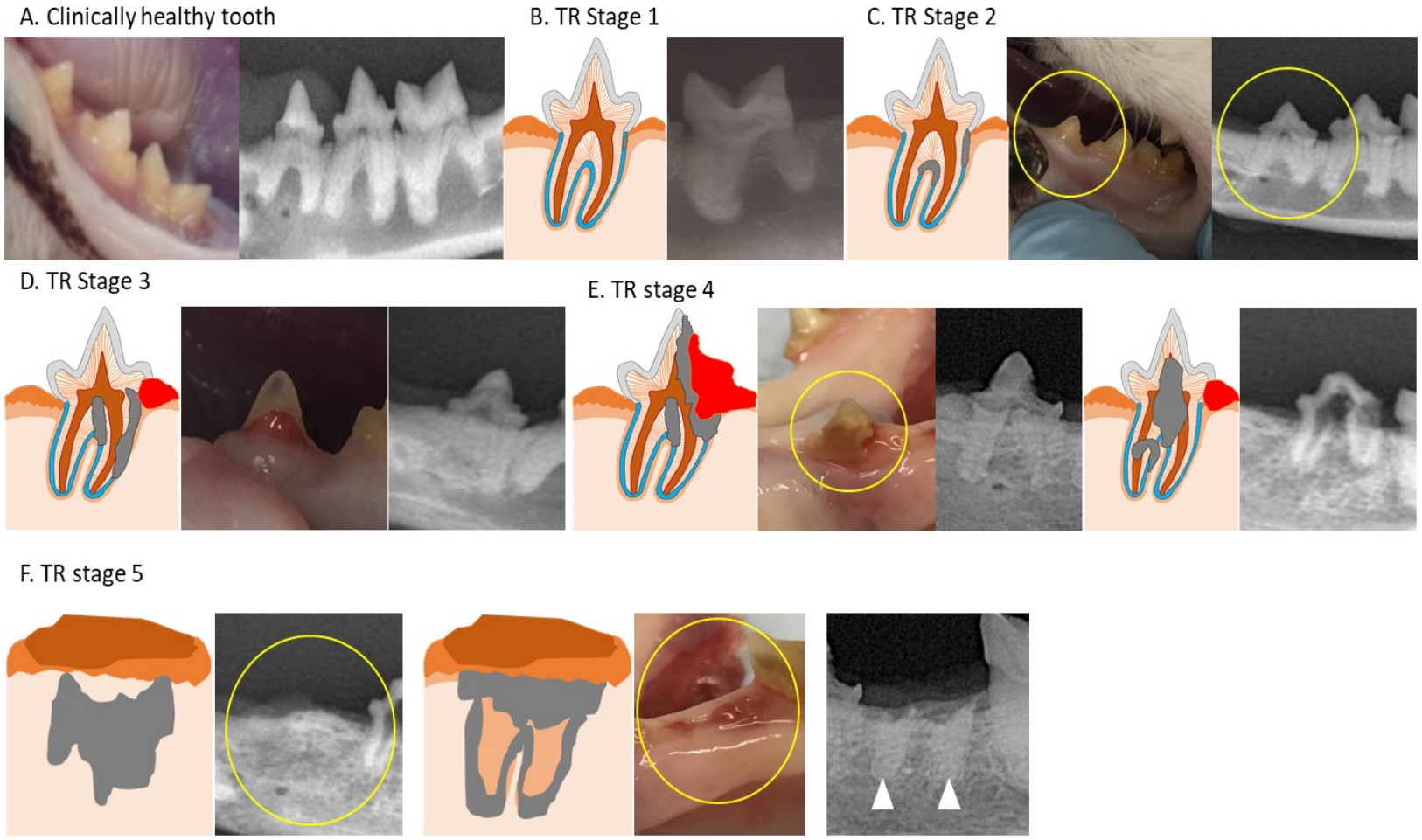

Figure 1.9 Schema and dental radiographs to show the AVDC classification of the clinical stages of feline TR. Please refer to Table 1.2 for detail of each stage.

Stage	Radiographic characteristics
1	Mild loss of dental hard tissue (cementum and enamel)
2	Moderate loss of dental hard tissue (cementum, enamel and dentin)
3	Deep loss of dental hard tissue (cementum, enamel, dentin and pulp cavity)
4	Extensive loss of dental hard tissue (cementum, enamel, dentin and pulp cavity)
4a	Crown and root are equally affected
4b	Crown is more severely affected than the root
4c	Root is more severely affected than the crown
5	Remnants of dental hard tissue are visible only as irregular opacities on radiographs, and gingiva completely covers the remnant of the resorbing root

Table 1.2 Descriptions of the severity of tooth resorption observed by dental radiographs based on a classification method described by the AVDC.

1.2.2 **Prevalence of TR and other oral diseases**

Although TR in cats was first reported in 1930, TR received little attention in veterinary dentistry until feline tooth surveys from the 1980's onwards reported increasing incidence and high prevalence. The sudden rise of TR in cats was likely due to several factors including the lengthened lifespan and rise population of aging cats, development of small animal practice and, increase of awareness and detection of this condition by systematic clinical examination and increased accessibility of dental radiology for diagnosis. During the last few decades, several epidemiological reports have been performed (Table 1.3). Reported prevalence varied depending on the sample population: 29 to 58% (average 43%) in the general population of cats (102-105) and 49 to 67% (average 56%) in cat populations with dental problems (98, 106-109). One survey of the general cat population revealed a difference of prevalence between breeds. In mixed breed cats, reported prevalence was 38% but it increased 70% in purebred cats (103, 106). The mandibular third premolars are the most commonly affected teeth and are thought be sentinel for a rapid screening for

TR since 90 % of TR cats were diagnosed by only assessing these two premolars (97). However, TR can affect any tooth (*e.g.* incisors, canines, other premolars, and molars) (103, 110). Prevalence and number of affected teeth increase with age (103, 108, 111).

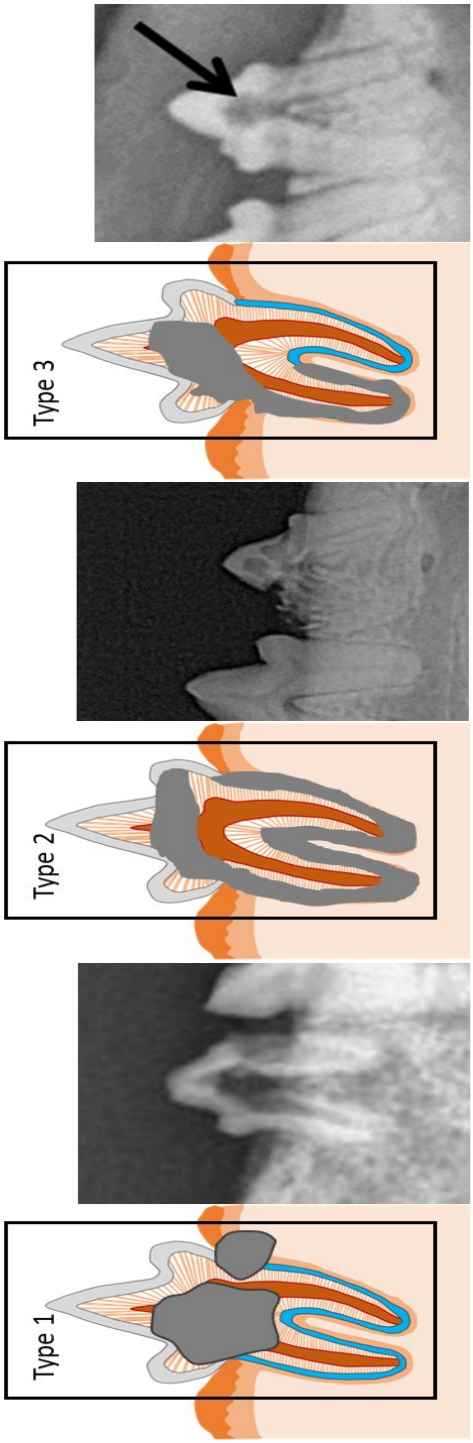

Figure 1.10 Type of feline TR based on radiographic appearance. In Type 1, focal or multifocal radiolucency lesions in feline teeth are present and unaffected lesions represent normal radiopacity with normal periodontal ligament space. Type 2 possesses narrowing or disappearance of the periodontal ligament space in at least some areas with decreased radiopacity of part of the tooth. In Type 3, there are features of both Type 1 and Type 2 present in the same tooth. A tooth with this appearance has areas of normal and narrow or lost periodontal ligament space, and there is focal or multifocal radiolucency in the tooth and decreased radiopacity in other areas of the tooth.

TR lesions are often diagnosed at the same time as other dental problems when cats are presented for dental treatment. The most common dental problems in cats are gingivitis, gingivo-stomatitis and periodontitis (108, 112). These three diseases are all inflammatory lesions at the corresponding anatomical sites. Periodontitis includes inflammation of the gingiva, periodontal ligament, cementum and alveolar bone. This causes gingival inflammation, recess of gingiva and periodontal ligament inflammation. In the advanced stage, inflammatory induced tooth resorption can lead to alveolar bone loss and this loss of bone is observed as a radiolucency feature in radiograph (99). The oral cavity is a moist environment and contains a reservoir of nutrition suitable for bacterial colonisation which eventually can result in dental inflammation. When inflammation progresses, cytokines are released locally which may attract osteoclast progenitors and progress TR. Therefore, TR sometimes presents with other inflammatory diseases and TR lesions are frequently observed with localised gingival inflammation. However, TR is a distinct condition from other oral inflammatory diseases in terms of non-inflammatory features. Some TR lesions are not associated with inflammation and this has been reported more in the early stage or in Type 2 TR (113). For this reason, whether TR is an inflammatory disease has not been conclusively determined yet, and TR is considered in the literature to be either an inflammatory or a non-inflammatory disease.

Study	Prevalence	Mean or median[#] age (years)	Population studied
Lund et al. 1998 (104)	48% (66/145)	-	General population
Ingham et al. 2001 (103)	29% (66/228)	4.9	General population
Girard 2008 (102)	38% (15/40)	6.2	General population (mixed breeds)
	70% (48/69)	3.6	General population (pure breeds)
Mestrinho et al. 2013 (105)	58% (41/71)	6.5[#]	General population
van Wessum 1992 (107)	62% (268/432)	-	Dental patients
Lommer and Verstraete 2000 (106)	60.8%(161/265)	-	Dental patients
Lommer and Verstraete 2001 (109)	67% (98/147)	-	Dental patients
Harvey et al 2004 **(110)**	49.3%(107/217)	9[#]	Dental patients
Farcas et al 2014 (108)	49%(49/101)	6[#]	Dental patients with chronic gingivostomatitis

Table 1.3 Reported prevalence in the veterinary literature.

1.2.3 **Treatment**

There is no known treatment that prevents the development of TR due to its progressive nature and the lack of knowledge of the cause of this condition (114). Therefore, the aim of current TR treatment is to relieve pain and prevent TR related infection. The suggested treatments are conservative management, total tooth extraction or coronal amputation depending on the presence of clinical symptoms and the type of TR. Conservative management includes monitoring the lesions clinically and radiographically. It is usually applicable for the early lesion whose resorption is confined to the root but has not progressed into the oral cavity with no evidence on clinical examination. Repair or restoration of the tooth surface can occur for the accessible lesions that extend only into the dentine by formation of mineralised tissue especially bone like tissues (114). This management requires further monitoring on a regular basis (every six to twelve months) to decide a surgical intervention (114, 115). However, several studies have shown that tooth resorption continues and the restorations or repairs are lost (9, 116). Consequently,

the use of restoration cannot be recommended as a major treatment technique for feline tooth resorption. In the general practice situation, extraction of entire tooth or crown coronal amputation is suggested. Restoration of the defects (*e.g.* removal of resorption and dental filling) is not indicated in cats. Total tooth extraction is the gold standard treatment to ensure removal of all resorbed and infected substance. However, teeth, especially those possessing Type 2 lesions, are notoriously difficult to extract since roots are extensively resorbed and replaced by bone tissue resulting in ankylosis between alveolar bone and tooth. In this case, crown amputation is often indicated. Crown amputation involves raising a gingival flap to expose and remove crown and upper part of root (1-2 mm below bone level) just enough to ensure retained root. The gingival flap is then replaced and sutured in place. In Type 3 TR, Type 1 root is extracted while Type 2 root can be amputated.

A pilot study attempted to use alendronate, a class of bisphosphonates (BPs) to prevent development of TR in cats (117). BPs are used to treat osteoporosis in humans and act via binding to hydroxyapatite in bone to inhibit osteoclast recruitment and resorptive activity, ultimately inducing osteoclast apoptosis (118). Alendronate predominantly accumulates on subgingival surfaces and adjacent alveolar bone around tooth roots where TR arises most commonly (117). At a dose of 9 mg/kg twice weekly for 27-weeks, alendronate-treated cats showed slowed or arrested the progression of tooth resorption with decreased radiographic area of resorption (22 % average change) during the post alendronate treatment period from 4 to 11-months compared to vehicle-treated cats (117).

Another study showed that topical application of BPs reduced root resorption and odontoclast formation in a rat model for orthodontic related tooth disease where the resorption was mediated by interleukine-1β (IL-1β) and tumour necrosis factor-α (TNF-α) (119). These findings may suggest that BPs may be a potential anti-resorptive drugs for the treatment of tooth resorption in the future (119). However, BPs have been associated with bisphosphonate-related osteonecrosis of the jaws which maybe a significant off target complication related

to long term use of these medications (120). Further studies are required for the local application of BPs to target odontoclasts and prevent TR.

These studies on the effect of BPs on TR have however demonstrated a couple of important things about TR. The high deposition of BPs in calcified tissues, especially in tooth resorption areas after intravenous or local injection, and their anti-resorptive efficacy via a reduction of odontoclast formation, support the hypothesis that dysregulated odontoclasts are responsible for TR (117).

1.3 Tooth resorption in animals other than cats

1.3.1 Humans

TR, or more specifically root resorption, has been reported in humans. Although TR has been more recognised in the last few decades, the first report of TR-like lesions date-back to 1859 where Tomes called the process absorption (83, 121). He described that the crown of the tooth was relatively intact but the root was absorbed. Resorption can occur both internally and externally. However, the phenomenon of multiple teeth being affected is rare in humans. Therefore multiple external resorption can be considered as the corresponding condition to feline TR (96, 122). Andreasen's classification is the widely accepted description that resorptions are classified into seven types based on their radiographic appearance: external surface resorption, external replacement resorption, external inflammatory resorption, external cervical root surface resorption, internal surface resorption, internal replacement resorption, and internal inflammatory resorption (Table 1.4) (83, 123). The initiation and progression of TR is related to many factors including pulpal necrosis, trauma, periodontal treatment, orthodontic treatment and tooth whitening agents (83). Regardless of the cause of TR, the process is largely related to inflammation in terms of odontoclast involvement and cellular mediators (83, 124). If caries or mechanical trauma are present within the pulpal tissue, they elicit an inflammatory process resulting in the production of nonspecific inflammatory mediators leading to internal resorption (125). As internal resorption (*e.g.* root

resorption by pulpal infection) progresses, treatment requires removal of resorbed substance and damaged pulp followed by preservation of vital pulp if possible and dental fillings with various mineral materials (125, 126). External resorption can be triggered by mechanical injury, local inflammatory or unknown causes. Depending on the duration and degree of stimuli TR lesions present various features. If stimuli are temporary and no further odontoclasts are involved, resorption is limited to a focal area and self-limiting root repair occurs within 2 to 3 weeks as a result of deposition of cementum-like tissue and reattachment to periodontal ligament (*e.g* external surface resorption) (126). If stimuli are prolonged, and a large area is resorbed including alveolar bone as well as dentine and pulp (*e.g*. external cervical root or inflammatory resorption), bone cells start to make new bone to cover the defect between root and alveolar bone forming ankylosis (*e.g* replacement resorption) (126, 127).

Tooth movement by orthodontic treatment is characterised by a remodelling process in both dental and paradental tissues. Orthodontic forces cause stress and pressure on the periodontal ligament in a certain direction and this leads to cellular responses that leads to osteoclast mediated alveolar bone resorption, tooth movement and complimentary bone formation to fill the bone defect and finally periodontal ligament rearrangement (128). This alveolar bone remodelling is the key to the success of orthodontic treatment. However, orthodontic treatment can cause off target effects such as massive alveolar bone or root resorption of the teeth. External apical root resorption (EARR) refers to a specific type of external inflammatory resorption characterised by a shortening of the apical third of the root (81, 129). EARR is believed to be related to various factors including orthodontic treatment methods, environmental factors or individual susceptibility to the disease.

Stage	Radiographic characteristics
External surface resorption	Shallow resorption lacunae (cementum and dentin)
External replacement resorption	Gradual disappearance of the periodontal ligament space with progressive replacement of root tissues
External inflammatory resorption	Loss of dental tissues adjacent to areas of loss of alveolar bone secondary to inflammatory conditions or prolonged stimuli
External cervical root resorption	Invasive resorption process that starts at the cervical area of the tooth and invades in both the coronal and apical directions
Internal surface resorption	Oval-shaped enlargement located in the apical third of the root canal, related to traumatic injuries
Internal replacement resorption	Irregular enlargement with a tunnel-like appearance adjacent to the root canal
Internal inflammatory resorption	Oval-shaped enlargement typically found in the cervical third of the root, inflammatory conditions of the pulp

Table 1.4 Descriptions of the types of TR reported in humans based on the Andreasen's classification method (123, 125).

1.3.2 **Dogs**

Only a few reports of canine TR have been documented, and they are mainly epidemiological reports or case reports (130-134). This might be because TR in dogs is relatively subclinical, usually found by chance. According to the reported prevalence, it could be called a clinically neglected condition, in comparison to cats (130, 135), but it might also be a reflection of the level of severity between the conditions with it rarely progressing beyond the subclinical stage in dogs. Hence canine TR has been poorly evaluated, despite reported prevalence ranging from 17.9% up to 56%. One epidemiological study reported 18% (6/33) dogs (> 10 years old) without clinical dental signs had one or more TR lesions identified on radiographs (130). Another study reported that 17.9% (29/162) of randomly selected dogs revealed TR lesions at post mortem (131). In a hospital cohort of 224 dogs undergoing dental treatments, the prevalence of TR was as high as 56% (80). This

study used human TR classification criteria described in Table 1.4 for evaluation of TR in dogs (80). The human TR classification criteria was applicable in 96.3% of TR teeth in dogs. Unclassified TR lesions (3.7%) were caused by mixed types of TR. The most common two types of TR were external replacement resorption (34.4%) and external inflammatory resorption (25.9%) followed by external cervical root resorption (5.8%), external surface resorption (4.5%), internal replacement resorption (4%) and internal surface resorption (0.4%) (80). External replacement resorption is a less common type in humans but it is known to be common in cats (83, 99). Although the aetiology of external replacement resorption has been poorly understood, several factors have been suggested including damage of root surface and periodontal ligament, and homeostatic process of periodontium which is bony remodelling following union of bone and dentine known to as ankylosis (83, 126). Except for external replacement resorption, frequency of other types of TR can be correlated to common dental diseases such as periodontal or endodontic disease given that the two diseases cause inflammatory TR involving cementum, dentine, pulp as well as alveolar bone. Inflammatory resorption and its clinical correlation is a similar finding in humans (80, 126). The authors of this study performed a parallel study using the same radiographs to apply veterinary TR classification criteria which is discussed in section 1.2.1 (136). They re-classified previously typed canine TR into the 5 stages of TR (1-5) and 90.2% of TR was applicable in this system. Although the major type, external replacement resorption was totally applicable in this classification, half of external inflammatory resorption and internal resorption failed to match this classification method. The majority of TR lesions in dogs was stage 2 (90.2%) followed by stage 4 (6.4%), stage 5 (2%) and stage 3 (1.4%) (136). This implies that TR in dogs is relatively less severe, that the progression is slow, and that only rare cases of TR will result in total loss of dentition. Based on these studies therefore it might be suggested that human TR criteria might be more suitable for canine TR classification. It also implies that the characteristics and aetiology of TR in dogs might be more similar to those of humans than cats (80). There are also

similarities to the scenario found in cats; dogs diagnosed with other dental problems also had more TR lesions than a random population of dogs, and the percentage of TR increased significantly with age (103, 108). One important note is that although most cases of TR in dogs are subclinical and they rarely develop to progress it is increasingly noted in radiographic and epidemiological reports which might require further investigations.

1.3.3 **Horses**

In horses, an equivalent disorder to feline TR has been reported named equine odontoclastic tooth resorption and hypercementosis. Equine odontoclastic tooth resorption and hypercementosis shares similar features with TR in humans and cats representing multiple resorptive lesions extending into the cementum, enamel, dentine or pulp cavity in severe cases (85). However, gross and histological observations identified some different pathological changes with distinct periodontal inflammation and predominant deposition of cementum by a highly reparative reaction (85). The basic anatomy of the equine dentition helps us get a better understanding of equine odontoclastic tooth resorption and hypercementosis. As mentioned earlier in section 1.1.2, horses have evolved to have hypsodont teeth that possess high crowns that erupt slowly to adapt to a rough diet (*e.g.* high fibre grass). To endure attrition on the occlusal surface of hypsodont teeth, there is an extensive distribution of calcified dental tissues on the occlusal surface. Unlike the single layer of enamel on the surface of brachyodont teeth, the crown of equine teeth is made up of enamel surrounded by softer dentine and cementum. As the softer tissues wears away quicker, the enamel forms sharp ridges on the surface, ideal for grinding down the horse's rough diet. The surface area of enamel is further increased by extensive enamel infolding and the presence of one (incisors) or two (maxillary cheek teeth) infundibula (11). As cementum is the most adaptable calcified tissues in teeth due to the presence of cementoblasts and a rich blood supply, this can be deposited quickly in response to stimuli (*e.g.* infection or trauma) (11). Due to the continual eruptive nature of the hypsodont tooth, the eruptive

crown is entirely covered in a layer of cementum. These anatomical features of equine teeth make them prone to hypercementosis in response to TR.

Incisor teeth are most frequently affected followed by canine teeth and reported cases are mainly in old horses (> 15 years old) (85). Mechanical stresses on the periodontal ligament factor has been suggested by Staszyk and colleagues (85), as an initiation however, the aetiology of equine odontoclastic tooth resorption and hypercementosis remains unclear (84, 85).

1.3.4 Wild cats

TR has been also reported in wild cats (82, 137). Macroscopic and radiological investigations revealed TR lesions in the dentition of one captive and one wild leopard, and two wild lions (82). Microscopic investigations were performed on two canine teeth and one molar collected from three animals. Although the sample size was small, it was possible to distinguish TR lesions from dental caries. At the ultrastructural level differences in the staining pattern of Rhodamin B, a caries detecting dye, and the width of the dentinal tubules was observed to identify typical features of caries. In terms of dentine hardness, the measured values were low in teeth with caries but remained normal in TR affected teeth. Finally, a larger study investigated dental disorders in 73 skulls from wild cats (8 caracals, 39 cheetahs, 14 leopards, 11 African wildcats, and 1 lion) and reported a 16% prevalence rate in wild cat species with varying stages of TR. This implies TR is not only confined to domestic cats, although the frequency was lower than those reported in the domestic cat populations (137). The authors could not make any conclusions on what the relevant factors causing TR were in wild cats.

1.4 Pathogenesis of tooth resorption

1.4.1 Histological manifestations of tooth resorption

Primary tooth resorption is the normal physiological process responsible for tooth eruption and shedding. The process is aided by osteoclasts/odontoclasts and the dental follicle as described in section 1.1.5.3. However, resorption of the

permanent dentition is largely pathological (83). In pathological TR there is no dental follicle involved as the entire follicle is shed during tooth eruption. Factors responsible for pathological TR may differ from those of physiological resorption. One important fact to note is that TR develops anywhere on the root surface and not only at CEJ (110). Although some authors have reported internal TR to be initiated within the pulp space (98, 138), TR usually occurs externally in cats (6, 106, 108). Internal resorption lesions including apical and coronal dentine/pulp are usually due to the inwards progression of external TR.

Early stage 1 lesions are barely detected clinically and radiographically because the size of the lesion is small and confined to cementum and enamel that are too thin to be observed radiographically (97, 106). A study revealed that clinically and radiographically TR unaffected teeth can possess early stages of TR (stage 1 TR) whose histological features include degeneration of periodontal ligament, a narrow periodontal ligament space and a localised resorption lesion such as surface root resorption with cementum resorption or replacement resorption (root resorption with ankylosing fusion between the tooth and alveolar bone) (113). This study also reported no inflammation adjacent to these early TR lesions. Stage 2 TR can be radiographically detected but it frequently does not accompany clinical signs and its histological features are similar to early stage of TR.

The histological features of active and advanced TR representing clinical signs detectable by oral examination (stages 3 to 5) have been described as two phases: resorptive phase and reparative phase. It is difficult to obtain histological sections from each stage due to the limited life time of the odontoclasts and their rapid resorbing process (9, 92, 122). The morphology of the resorptive phase (seen as numerous resorption pits), is similar to that of shedding deciduous teeth displaying multinucleated odontoclasts lining the lacunae of dentine and/or cementum (9) (Figure 1.11, E). Inflammatory lesions frequently accompanies TR involving the surrounding tissues, but there is no conclusive evidence to date to determine whether they are there as a consequence of the TR lesions, or whether they are part

of the aetiology of TR. (9, 86). Hyperplastic gingiva and vascular granulation tissue fill the resorptive defects. The TR lesions are surrounded by infiltrated inflammatory cells including neutrophils, plasma cells, macrophages and fibroblasts. In the following reparative phase the actions of osteoblasts and cementoblasts are coordinated; rounded cementoblasts or osteoblasts produce new hard tissues including cementum and osteodentine to replace the defect (Figure 1.11, E). In a prolonged stage which is the odontoclast quiescent stage, most dental tissues are replaced by bone-like tissue appearing as dental-alveolar ankylosis (Figure 1.11, F). The resorptive and reparative phases can occur simultaneously (Figure 1.11 E and F). The morphology of the periodontal ligament is also altered or destroyed by the involvement of bone resorption at the alveolar crest (Figure 1.11, E and F) compared to healthy periodontal ligament at the CEJ, the gingival sulcus (Figure 1.11, B) or at the root furcation (Figure 1.11, C). These histological findings highlight the importance of the dynamic property of the periodontium in the development of TR (9, 92, 98, 122, 139).

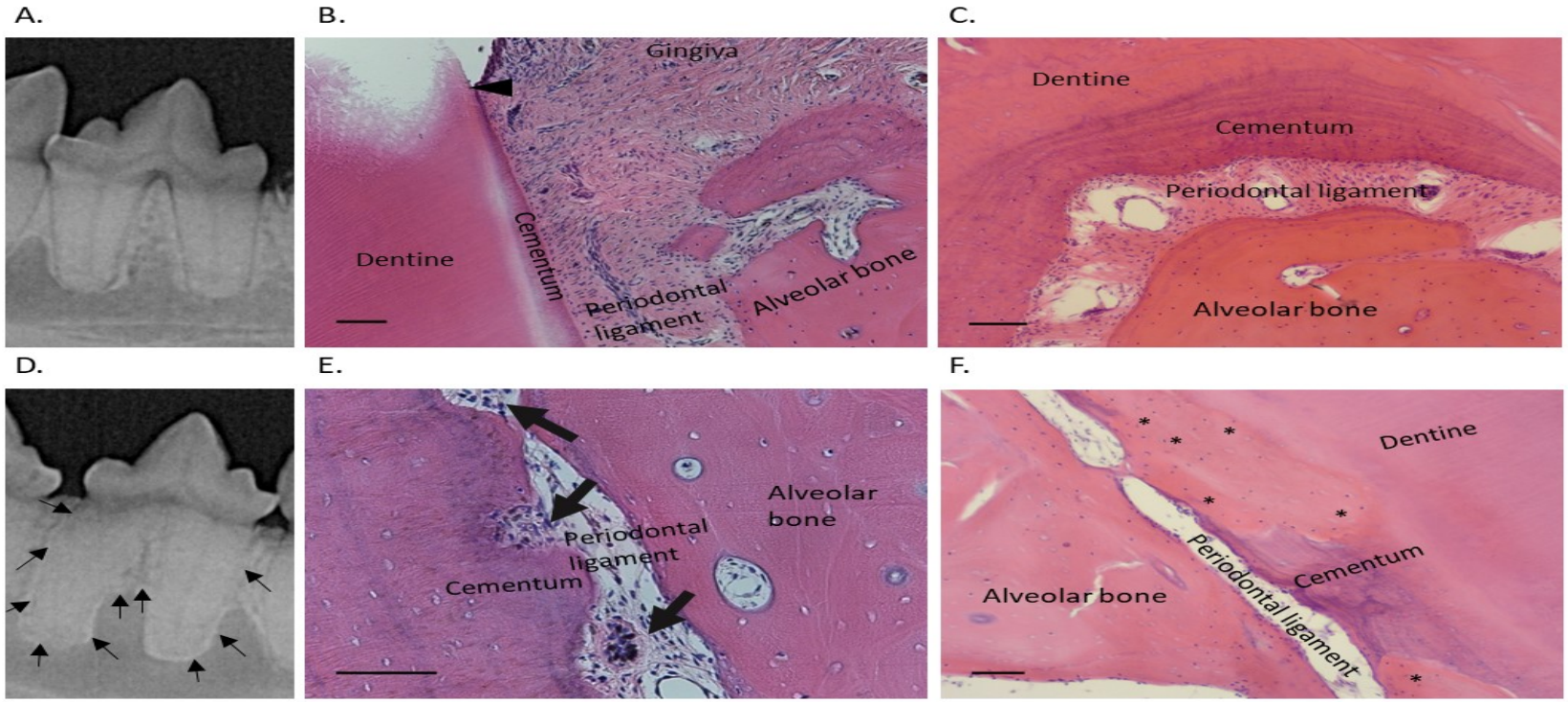

Figure 1.11 Histological features of feline healthy and TR affected teeth. Healthy feline tooth in (A) dental radiograph and (B) and (C) H&E sections. (A) and (B): Intact periodontal ligament is tightly attached to periodontium in the gingival sulcus (arrow head). (C): Normal furcation of root area showing an intact periodontal ligament and secondary cement deposition with incremental lines. Tooth affected by TR in (D) radiograph (Stage 3, Type 2) and (E) and (F) H&E sections. (D): TR affected tooth shows disappearance of the periodontal ligament space and replacement of bone-like material in both roots but TR has not yet extended into the coronal dentine. Arrows indicate resorbing roots. (E): Cementum are resorbed by odontoclasts (arrows) and periodontal ligament space is narrow with loss of normal fibre arrangement. (F): Both cementum and dentine are resorbed, which is replaced by newly produced mineralised tissues (*).This bony reparative process forms an ankylosis between the alveolar bone and the cementum or dentine. Scale bars = 100 µm.

1.4.2 **The microenvironment in tooth resorption**

As discussed in section 1.1.3.3 osteoclast/odontoclast differentiation and activity are tightly regulated by the bone and tooth microenvironment. Although these cells share many similarities, sometimes they behave differently under certain conditions (*e.g.* their responses differ in the presence of thyroid hormone, parathyroid hormone or an inhibitor of prostanoid synthesis) (21, 24, 140, 141). Administration of thyroid hormone (L-thyroxine) increased bone resorption but did not enhance force induced root resorption in rats (140). In a study investigating the effect of hyperthyroidism in dogs, resorption by odontoclasts were not present. It also reported that parathyroid extract did not cause any morphological changes of odontoclasts residing in the dogs' deciduous teeth (141). Another study reported that indomethacin, an inhibitor of prostanoid synthesis belonging to the group of nonsteroidal anti-inflammatory drugs, inhibited osteoclastic resorption but increased odontoclastic resorption (24). These differences in response to exogenous factors suggest that these two types of resorbing cells may be subjected to alternate regulatory mechanisms due to their niche microenvironments and resident cell populations. Therefore, to better understand TR, there is a need for a thorough investigation of the tooth microenvironment itself. Initially, TR requires stimulatory factors to damage the defence layer of the tooth and attract odontoclast precursors. For example, when the periodontal ligament is damaged by a mechanical load or inflammation, periodontal ligament and alveolar bone cells react via the release of numerous substances such as neurotransmitters, cytokines and growth factors. The released molecules elicit cellular responses in the various dental cells for tooth resorption or repair (23). The supporting role of surrounding cells on odontoclast differentiation has been shown by co-culturing odontoclast precursors with dental pulp or periodontal ligament cells, which lead to spontaneously differentiated odontoclasts without the addition of osteoclast stimulating factors (*e.g.* prostaglandin E_2) (23, 142). Differentiated clastic cells need to attach to the tooth resorption sites. The selective resorption by odontoclasts depends upon ECM

proteins (*e.g.* osteopontin, bone sialoprotein) mediating clastic cell attachment and activation (23, 143).

Lastly, survival and activation of clastic cells largely depend on a favourable microenvironment for osteoclastic activity. *In vitro*, reduced oxygen tension and acidosis (low pH) lead to an increase in osteoclast and resorption pit formation (20). An hypoxic environment is evident in some pathological states (*e.g.* reduction of partial pressure oxygen in diseased mandibles and in fracture hematomas) (144).

1.4.3 Odontoclast dysregulation and pathways involved in TR

As discussed in section1.1.3.3 and 1.1.5.4 osteoclasts and odontoclasts differentiate via CSF-1 and the RANK/RANKL/OPG axis pathway. This central axis is important in both physiological and pathologic TR. However, the microenvironment of physiological and pathologic TR is different. Therefore there has been a focus on identifying co-stimulating factors (*e.g.* growth factors, cytokines and transcription factors) in pathological conditions. The precise origin and activation of odontoclasts during TR is presently unclear however, many possible candidates that directly or indirectly impact on the RANK/RANKL/OPG axis pathway have been postulated (20, 22).

First of all, many intracellular factors have been reported to be involved in the control of osteoclast formation. For example, the disruption of genes coding for transcription factors, PU.1, MITF and c-Fos impaired the early stage of osteoclast differentiation (20, 145-147). Osteoclast stimulatory transmembrane protein (OC-STAMP) and DC-STAMP have been reported to be involved in the fusion of osteoclast precursors (148). The Fos-related protein inversely controls osteoclast survival and size (149). The matrix metalloproteinase (MMPs) including MMP2, 9, 12, 13, and 14 play an important role in osteoclast activity that contribute to bone matrix solubilisation (150). Specifically, MMP9 has been associated with bone resorption and many diseases including cancer, osteoporosis and fibrosis where MMP9 modulates the ECM (151-153).

Secondly, many RANK/RANKL/OPG downstream signalling molecules

have been proposed as co-stimulatory factors (*e.g.* TRAF2, 5, 6, NF-κB and NFATc1). Higher expression of OPG in permanent teeth offers protection against TR (22) and this may be via local factors such as TNF, GM-CSF, IL-1 (IL-1α, β), IL-6, IL-12, IL-17, IL-18, IL-23, TGF-β (20, 43, 154). Although IL-1β is a well-known stimulator of osteoclast formation for example in periodontitis, cytokine expression can be contradictory in certain situations (*e.g.* non-inflammatory resorption, orthodontic related TR). In human TR, especially in EARR it has been suggested that genetic mutations of IL-1β or the purinergic-receptor-P2X, ligand-gated ion channel 7 (P2X7 receptor) might decrease cytokine levels that modulate local inflammation (81, 155). In the pathological process, local damage (*i.e.* orthodontic treatment) of tissue results in ATP release which in turn activates the P2X7 receptor and further release of cytokines. In such cases, cytokines recruit more monocytes and macrophages to eliminate apoptotic cells to prevent further necrosis. However, if this pathway is blocked, there will be defective alveolar resorption and reduced bone turnover so that teeth experience a prolonged stress and strain from for example during orthodontic treatment (156-158). This pathway might be involved in non-inflammatory induced TR (23).

Other locally produced molecules such as hypoxia inducible factors and leukaemia inhibitory factor are involved in the stimulation of osteoclast formation in hypoxic conditions (149). Bone related systemic factors including both stimulators and inhibitors might also impact on TR: parathyroid hormone (PTH), vitamin D_3, calcitonin, calcitonin gene related peptide, and oestrogen (159-161). Recently the WNT signalling pathway and its related molecules (*e.g.* β-catenin, frizzled transmembrane receptors, Low-Density Lipoprotein receptor related protein co-receptor, sclerostin, dickkopf-1) have been identified as important regulators of osteogenesis and osteoclastogenesis via indirect mechanisms (162). In summary, a range of molecules might be involved in the re-activation of osteoclasts/odontoclasts in TR. Further work is required to elucidate the main pathways responsible.

1.5 Aetiology of tooth resorption

Even though many researchers have sought to elucidate the aetiology of TR in cats, the precise cause(s) remain unknown. Exhaustive studies have been performed to identify local and systemic factors involved (*e.g.* structural characteristics of TR, diet, gender, biomechanical stress, and anatomical defects in tooth morphology) (9, 92, 98, 100, 163-165).

1.5.1 Inflammation

As osteoclasts/odontoclasts are of monocyte/macrophage lineage, inflammation has been most frequently suggested as an initiating factor of feline TR. Inflammatory cytokines have been considered to play a role in the recruitment of progenitors. TR in cats has often been detected concurrent with other oral inflammatory diseases (99, 108, 112). A study reported that messenger RNA (mRNA) levels of inflammatory cytokines including *IL1B* and *IL6* increase in the areas of active dental resorption concurrent with feline TR (163). Although these cytokines are known as potent stimulators of osteoclast/odontoclast differentiation *in vitro* and *in vivo* (23), it is worth noting that increased expression of these cytokines can be a result of inflammation due to TR rather than an initiation factor. Also these stimulators fail to alter the expression of downstream regulators of osteoclast/odontoclast differentiation, RANKL and OPG. Moreover, this inflammatory cytokine study in feline TR possesses technical limitation in terms of measurement of gene expression since mRNA of cytokines were measured by semi-quantitative RT-PCR (163).

Recently another study addressed the involvement of inflammatory cytokines and the possible role of vitamin D in the pathophysiology of TR using quantitative PCR (100). This study reported increased mRNA expression of stimulatory cytokines including *IL1B*, *IL6* and *TNF*, and the nuclear vitamin D receptor (*VDR*) in tissues from TR lesions compared to those of healthy controls. However, paradoxically IL-10 known as anti-inflammatory and interferon gamma

(*IFNG*) possessing an inhibitory effect on osteoclastogenesis, or anti-resorptive cytokines also increased in TR affected teeth and mRNA levels of *RANKL* and *OPG* were not different between TR and control group (100). Therefore, at present it is difficult to conclude if inflammatory cytokines lead to tooth resorption via increased osteoclastogenesis. One study demonstrated the potential role of mast cells and compared the three most common periodontal diseases (chronic gingivostomatitis, periodontitis and TR) in cats (112). All three conditions revealed increased mast cell populations in gingival tissues compared to the gingiva of specific pathogen-free cats. Therefore, it is possible the presence of mast cells might be correlated to these oral diseases. Another finding of this study was the inflammatory scores were significantly lower in TR compared to chronic gingivostomatitis or periodontitis (112). Although most TR lesions are associated with inflammatory cells, the early lesion covered by an apparently normal gingiva does not seem to be. This has led some researchers to believe that the appearance of inflammatory cells is a secondary rather than primary event during development of TR. Concurrent inflammatory, a two feline osteoclast studies demonstrated that hypoxia and local change of pH may play an important role in pathogenesis of feline TR (166, 167).

1.5.2 **Diet**

TR has been reported in wild cats as described in section 1.3.4, but due to the higher prevalence of TR in domestic cats, it has been suggested that their diet is an aetiological factor. According to a previous study TR may be correlated with low calcium or low magnesium intake from homemade food and this is consistent with another cross sectional study where cats fed a high content of minerals (*e.g.* magnesium, calcium, phosphorus, and potassium) experience less TR (104). However as most cats are fed commercially prepared foods, which are balanced in both calcium and magnesium this should no longer be an issue (164). A consumption of foods containing cheese, milk and butter has been associated with an increased risk of TR whereas dry food with an acid surface was not found to contribute to the pathogenesis of TR (168). In a more recent study, indoor or city cats

which have less chance to hunt prey, were found to have a higher risk of developing TR but commercial treats reduced the risk approximately threefold (165). The current findings on the effects of domestic diets on the incidence of TR are inconsistent which might be due to bias or incorrect data collected via questionnaires of owners. At present there are no longitudinal studies reporting the incidence of feline TR on defined diets with known mineral concentrations and therefore it is unknown whether TR prevalence can be modulated by diet.

1.5.3 Bone turnover markers and hormonal influences

Bone resorption by osteoclasts is largely associated with endocrine and metabolic imbalances in humans. One of the most well-known stimulators of osteoclastic bone resorption is chronic PTH which stimulates the RANK/RANKL system (169). The thyroid hormones, and PTH-related peptides (PTHrP) also increase osteoclastic activity in bone (169). These hormones play critical roles in the maintenance of calcium and phosphate homeostasis as well as maintenance of bone health (78, 169, 170). Although the anabolic and catabolic actions of these hormones and their derivatives are complicated due to their dual roles of bone formation and resorption depending on given situations (*e.g.* primary and secondary hyperthyroidism and osteoporosis), hyperparathyroidism primarily causes extensive bone loss and resorption (171). Primary osteoporosis has not been reported in cats and dogs yet. Cats and dogs are also resistant to oestrogen deficient-related bone loss corresponding with postmenopausal osteoporosis in elderly women (172).

Thyroid hormones are also known as stimulators of osteoclastogenesis (173). Various systemic levels of bone turnover markers including the bone formation and degradation markers can be used to assess specific bone pathology.

It is not fully known whether TR is correlated with systemic hormonal related bone diseases in cats (98). Similarly, in humans the relationship between TR and systemic bone disorders are not clear. Only limited literature is available describing oral manifestations with hormone related diseases including increased

periodontitis in hyperparathyroidism, delayed tooth eruption in childhood hypothyroidism, and maxillary and mandibular osteoporosis in hyperthyroidism (174, 175).

To investigate a link between pathological bone remodelling and feline TR, biochemical bone turnover markers were measured in aged cats with or without TR. The bone formation marker, bone alkaline phosphatase (BAP) produced by osteoblast was measured by wheat germ lectin precipitation and human enzyme-linked immunosorbent assay (ELISA). In terms of bone resorption markers serum deoxypyridinoline (DPD) was measured by an automated analyser and urine DPD was measured by a human ELISA. Another resorption marker carboxy terminal telopeptide (CTx) was measured in urine using high-performance liquid chromatography (HPLC) and in serum CTx was quantified by a commercial human ELISA. Serum DPD levels were inconsistent, possibly due to lack of cross-reactivity with the human DPD antibody. Although there were technical limitations to measuring cat serum and urine levels of DPD, there was no difference reported of the three bone turnover markers in serum or urine between control and TR cats (176). In another study on systemic hormonal imbalances, serum calciotropic hormones were measured by previously validated gold standard immunoradiometric assays in cats (177). There was no significant difference in PTH, PTHrP and free thyroxine between control and TR affected cats (178). For other systemic biochemical factors, the mean serum level of blood urea nitrogen and phosphorus were higher in TR cats but multivariate logistic regression model revealed that higher concentrations of these might be due to other factors, such as age. Low urine specific gravity was correlated with TR status but the importance of this has not been determined (178).

It is therefore unlikely that a link exists between systemic bone diseases and TR. This implies that the dentition is generally resistant to resorption under systemic bone resorption. As previously mentioned, bone resorbing stimulators such as prostaglandin E2 (PGE2) and IL-1 can stimulate increased osteoclastic

activity in the local dental environment (43, 179). In one orthodontic study in cats, the level of PGE2 and IL-1β secreted from gingival fluid increased with experimentally induced orthodontic tooth movement (180). Another finding of this study was that in a group of cats where oestrous was induced by gonadotropin hormone injection, it resulted in reduced PGE2 and IL-1β levels and less tooth movement. This suggests a potential ovarian protection activity on orthodontic tooth movement. However, other epidemiological studies in cats have shown there is no correlation between TR and neuter status or gender (98, 103, 178, 181). Due to the limitations of the available studies and the tools available for measuring feline hormone levels any links between these hormones and feline TR remain speculative.

1.5.4 **Vitamin D and its metabolites**

Vitamin D is a known stimulator of osteoclastic bone resorption and an essential ingredient of commercial cat foods and therefore the role of Vitamin D has drawn a great deal of interest in the aetiology and progression of feline TR (92, 100). Vitamin D is a calciotropic hormone and together with PTH they cooperatively mobilise calcium from the bone and conserve calcium from urine (170). Although vitamin D exists in the diet as two forms: ergocalciferol (vitamin D_2) and cholecalciferol (vitamin D_3), the major source of vitamin D_3 in herbivores and omnivores including humans, rats, pigs and sheep is photosynthesised from cholesterol in their skin under sufficient sunlight (182). However, cats and dogs cannot produce sufficient vitamin D_3 precursors (7-dehydrocholesterol) and lack the ability for synthesis of vitamin D_3 in their skin (183). Cats and dogs therefore require supplementation of vitamin D_2 or vitamin D_3 in their diets. Dietary or synthesised vitamin D (D represents either D_2 or D_3) is converted to 25-hydroxyvitamin (25(OH)D) by 25-hydroxylases (*e.g.* coded by the genes *CYP2R1* or *CYP27A1*) in the liver and transported in blood by the vitamin-D binding protein. 25(OH)D comprises the major metabolite of vitamin D in serum as the most useful index of vitamin D status (184). 25(OH)D is further metabolised to its biologically active form, 1,25-dihydroxyvitamin D ($1,25(OH)_2D$) in the kidney by 1α-hydroxylase

(coded by the gene *CYP27B1*) (160). Both 25(OH)D and 1,25(OH)2D are catabolized by 24-hydroxylase (coded by the gene *CYP24A1*) (184). 1,25(OH)2D acts via its receptor VDR which is expressed in many tissues including kidney, bone, and skin as well as in immune cells (185, 186). The role of $1,25(OH)_2D$ in bone is complex; it has a dual activity of bone formation and resorption regulating calcium levels depending on body conditions (170). *In vitro*, $1,25(OH)_2D$ indirectly increases osteoclast activity via RANKL expression but paradoxically, *in vivo* $1,25(OH)_2D$ increases bone mineral density via increased calcium absorption and the subsequent suppression of bone resorption and therefore it has been used as a therapeutic drug for osteoporosis (160). Reiter et al. (2005) first suggested that vitamin D and their metabolites might be involved in the pathogenesis of feline TR. They found that the mean serum level of 25(OH)D in TR cats was significantly higher than controls although both mean serum levels were within the normal reference range (178). Providing high vitamin D_3 in diet caused an increase in serum $25(OH)D_3$ in kitten and adult cats and therefore it was speculated that excessive supplement of vitamin D_3 can lead to hypervitaminosis D and renal impairment that might be correlated with TR (92, 187). However, several vitamin D_3 diet studies demonstrated that high vitamin D_3 diets (up to 63 times of the maximum recommended vitamin D_3) did not cause any apparent adverse effects in kittens and adult cats (188, 189). In addition, results of other studies on vitamin D and their metabolites in TR were not consistent. Girard et al (2010) revealed that there was no significant difference in serum $25(OH)D_3$ between control and TR cats with at least one or more TR teeth, instead it was mentioned that cats possessing multiple (> 5) TR lesions had lower serum $25(OH)D_3$ concentrations than controls (190). Booij-Vrieling and colleagues reported there was no difference in 25(OH)D serum levels whereas $1,25(OH)_2D$ levels were higher in the controls than TR cats (122). There have been many methods developed to measure total serum 25(OH)D (e.g. competitive binding methods, high-performance liquid chromatography, and radioimmunoassay) (191). Overall the radioimmunoassay was considered the gold standard which has been

used in many reference laboratories in the past decades (192). Recently, newer chromatography methods have been developed which improved sensitivity and enabled measurements of all forms of vitamin D (191). One of the new methods, liquid chromatography tandem mass spectrophotometry (LC-MS/MS) is a recommended method for vitamin D analysis by UK Food Standards Agency Workshop Consensus Report (193) and this method has been used in a veterinary diagnostic laboratory (NationWide Laboratories accredited by United Kingdom accreditation Service). Although it is now possible to measure various vitamin D metabolites, vitamin D status was typically only assessed by measuring 25(OH)D because the life span of 25(OH)D is long (approximately 2–3 weeks) and it exists in serum at levels more than 1,000 times higher than $1,25(OH)_2D$ (184). This means that serum 25(OH)D directly reflects dietary vitamin D intake and/or cutaneous vitamin D synthesis. It is therefore assumed that 25(OH)D provides the most meaningful information regarding vitamin D sufficiency or deficiency in the body (184). However, as it is not the most active form of vitamin D, it would be desirable to measure both 25(OH)D and $1,25(OH)_2D$.

In feline TR studies, various methods were used for measuring 25(OH)D which may account for the different results and variations between the various studies (100, 178, 190). Unfortunately, although there many efforts have been made to measure $1,25(OH)_2D$ in feline serum using new techniques including LC-MS or LC-MS/MS, currently there are currently no one gold standard assay for measurement of $1,25(OH)_2D$ in cats and its reference range has not been documented in text although different labs have developed their own cat reference intervals (personal communications, Prof. Danielle Gunn-Moore). Hence, feline studies did demonstrate that systemic levels of vitamin D including 25(OH)D and $1,25(OH)_2D$ varies greatly and that the impact on bone and dentition is unclear. Until further studies can firmly confirm its role, vitamin D still has to be considered to possibly play a role in TR (185).

$1,25(OH)_2D$ has been shown to have a direct effect on the dental

microenvironment in cats (194). Following repeated injections of $1,25(OH)_2D$ into the periodontal ligament of teeth which had gentle orthodontic traction applied to them, the $1,25(OH)_2D$ treated teeth had moved 60% further than the controls. An increase in osteoclast numbers and resorption could be seen histologically in $1,25(OH)_2D$ treated teeth (194). Booij-Vrieling and colleagues demonstrated increased levels of both *VDR* gene and protein expression in TR affected teeth, which may imply possible involvement of vitamin D signalling in TR progression (100, 122). To answer whether vitamin D and their metabolites are involved in TR progression, further investigations on vitamin D metabolism and signalling pathways in the dental environment are required.

1.5.5 **Mechanical load**

Mechanical load, microfracture of cementum and malocclusion have been proposed as possible cause of TR in cats (92). In humans, the occlusal stress theory emerged to postulate tooth wear at the cervical portion of teeth; repeated compressive and occlusal stress during mastication or due to malocclusion disrupt the bond between enamel and dentine, resulting in a form of non-carious tissue loss (195). This can lead to cemental or periodontal ligament inflammation and the attraction of odontoclast progenitors to the site. *In vitro*, human periodontal ligament cells expressed odontoclastic factors, RANKL and OPG (142). RANKL expression constitutively increased depending on occlusal stress (196, 197). In a similar way, occlusal stressors could develop TR in cats. Some orthodontic treatment studies have previously been performed in cats (180, 194, 198). After application of mechanical forces to the canines, numerous resorption lacunae were found in the apical region of the alveolar bone socket and wide areas of root resorption were clearly visible. The histological patterns corresponded to those seen in mice and human following orthodontic treatment. This suggests that mechanical load and malocclusion could be a contributing factor in feline TR.

1.5.6 Other factors

TR increases with age (92, 102), and older TR affected cats have significantly more teeth missing (92), which is similar to aging related tooth loss seen in humans. There are possible anatomical features of the feline dentition that might contribute to this age related onset. As previously mentioned in section 1.1.1, feline teeth have relatively poor levels of mineralisation on their surface. An electron scanning electron microscopy study of feline permanent teeth revealed a thin enamel and cementum, and exposed dentine at the ECJ with evidence of tooth wear. The areas with lowest dentine mineralisation were the ECJ and cervical roots. These observations indicate that the ECJ and the cervical dentine may be at a greater risk of odontoclastic resorption compared with other regions of the tooth (199).

An early study on the role of viral infections as a possible factor focussed on some commonly diagnosed feline viruses; they reported that feline immunodeficiency virus (FIV) infection may be involved in feline TR aetiology (200). However this study was performed in a small number of cats and it was not clear how they confirmed the presence of TR. Despite the weakness of the study, their findings of a possible involvement of immune deficiency is potentially interesting (200). Oral bacterial infections were also investigated in several studies but there is no clear evidence of a correlation between bacterial infections and TR (92). The cumulative evidence suggests that the initiation and progression of TR is complex and multifactorial and is also mediated by local rather than a systemic mechanisms.

1.6 Genetic investigations into tooth resorption

1.6.1 Gene expression studies of dental environment

As discussed in section1.1.3 and 1.1.5 dental tissues contain specialised cells and their differentiation and fate are programmed spatiotemporally during tooth development. Studies using transgenic animals (usually single gene knockouts) have identified the main pathways and contributed to a better understating of

mammalian dentition, however, the level of complexity quickly becomes evident and a single gene null mouse is not sufficient to determine the function of sets of genes especially when they are correlated with each other or members of a large family with potential functional crossover (201). Moreover, the anatomic difference between species (*e.g.* type of tooth, variation of dentition) might have impact on species-specific disease or different response to the microenvironment, as demonstrated for example by the extensive cementosis observed in equine odontoclastic tooth resorption and hypercementosis. For these reasons, gene expression studies using dental tissues in the same species is of great interest to help map normal dental physiological pathways as well as dissect out the pathways involved in pathological conditions at the cellular and molecular level. Recently, dental gene expression studies have started to fill in the gaps in our knowledge of the already well defined molecular complexity of the dental microenvironment (201-203). For example, gene expression profiling studies of human tooth buds which included odontoblasts and ameloblasts identified the involvement of a much larger portion of the human genome in the development of the human tooth than previously known (201, 202). Although the majority of gene expression and genetic studies in dentistry have been perform to gain knowledge of tooth development, one clinical exploratory study reported differential gene expression in human pulpitis and these findings enhance our understanding of pulpal inflammation. It also provides a biological reference for future treatment strategies based on pulpal biology (203).

1.6.2 **Genetic studies of TR**

In humans, EARR is a relatively common adverse complication of orthodontic treatment and 30% of orthodontic patients have more than 5 mm resorption at the end of treatment (129, 204). Risk factors for root resorption have been suggested including patient gender, severity of malocclusion, force and duration of treatment together with a genetic predisposition (23, 205). Variable susceptibilities to root resorption concurrent with orthodontic treatment had been

observed within families and populations, so a potential genetic predisposition was predicted (206). The hypothesis that siblings experience similar levels of EARR in response to orthodontic treatment was supported by estimation of heritability in the sib-pair model (206). As heritability is defined as the proportion of the phenotypic variance attributable to genetic control , its estimation is the first step in the genetic study of a quantitative trait (155). The estimation of heritability averaged about 50% for the total phenotypic variation in EARR (155, 206).

Genetic variables of *IL1B*, *RANK*, *RANKL*, *OPG* and *P2X7R* and heritability including a combination of environmental and host factors have been suggested predispositions to develop the complex phenotype of root resorption in orthodontic patients (81, 156, 157, 207). *IL1B* (rs1143634) and *P2X7R* (rs1718119) polymorphisms have been reported as EARR susceptible markers in several sibling pair studies (156, 207). The cytosine (C) variant of *IL1B* accounted for 15% of total variation of EARR in maxilla incisors and this genotype was associated with decreased levels of IL-1β expression (155, 156). Although positive associations between *IL1B* and *P2X7R* polymorphisms and EARR have been reported in other similar studies and confirmed in knockout animal models, *IL1B* polymorphisms have not always been replicated whereas more consensus has been observed with the *P2X7R* (rs1718119) polymorphism (158, 207). This inconsistency in the *IL1B* might be due to use of different population (*e.g.* families vs. extended random populations), size of population and complexity of analysis models (*e.g.* multivariate analysis) (156, 158, 207). Determining genetic causes of TR is complicated, and it is likely that it is a multifactorial trait. Future studies should therefore aim to include additional genetic factors beyond the current candidate genes.

In terms of feline TR, there has been no studies to elucidate possible genetic predispositions. A cohort study demonstrated that there were a high incidence in purebred cats and a widespread presence in siblings within the population, which might suggest a genetic predisposition for feline TR (102).

1.6.3 **Next generation sequencing**

Traditional genetic studies like the ones reported in previous section 1.6.2 usually utilise DNA samples from a defined population, use genotyping based on PCR, Sanger sequencing or restriction fragment length polymorphism followed by a final analysis of genotype and phenotype taking account of variables. This process is time consuming and can only be performed on a limited number of genes. Next generation sequencing (NGS), also known as high-throughput sequencing technologies) refers to a technique of sequencing massive amounts of DNA at once. The advent of this has led to remarkable progress in genetics. RNA sequencing also called whole transcriptome shotgun sequencing (RNA-seq) is a recently developed NGS approach which aids us in the understanding of the functional elements of the genome by mapping and quantifying the transcriptome. This technique has revealed tissue-specific alternative splicing, novel transcripts and genomic variations in structure (208). The data from RNA-seq allows researchers to measure differential gene expression with greater sensitivity than microarrays (208). It is particularly useful for studying non-model organisms with genome sequences that are yet to be fully determined or annotated. In addition, it can be applied to identify SNPs in the transcribed regions. The major challenges with RNA-seq are how to properly analyse the massive data sets generated with a biological meaningful interpretation (209). Recently bioinformaticians have contributed to the development of a variety of algorithms and analytic soft wares (*e.g.* SAMtools, Picard, Pysam, Galaxy and R *etc.*) leading to the successful application of RNA-seq to elucidate biological findings in a wide range of animals. Using next generation sequencing, around 300 novel miRNAs as regulators of gene expression were identified in equine osteochondrosis physiopathology and in the cellular response to biomechanical stress in cartilage and bone between healthy and osteochondrosis affected foals (210). The successful application of this new technique produced results in agreement with the findings of a previous preliminary proteomics study showing equine osteochondrosis to be associated with combined cartilage and bone

defects (210).

In another RNA-seq study, transcriptome analysis of ameloblasts during amelogenesis disclosed differentially expressed genes and provided a good starting point to identifying genes and proteins that are critical for dental enamel formation (202). RNAseq was also used to investigate the transcriptional changes that take place during diet-induced phenotypical changes in cichlid fish (211). The study fed the fish two types of diet (hard and soft), and RNA samples were collected simultaneously to allow the analysis of the whole transcriptome of the two groups. The data displayed significantly differentially expressed genes in response to diet induced mechanical strain. These massive data sets are hugely beneficial when elucidating comprehensive pathways and when identify novel genes involved in normal physiological processes as well as in pathological conditions.

1.7 Aims and Hypothesis

The general aims of this study was to design and optimise a method for 1) RNA-seq of feline tooth samples, 2) develop a model to study odontoclast dysregulation, 3) identify candidate genes correlated with feline tooth resorption and 4) test genes *in vitro* for a better understanding of odontoclast biology and microenvironment in feline TR. These aims will test the hypothesis that feline teeth with TR reveal transcriptomic differences compared to feline teeth without TR. Specifically, I will:

- Optimise a method of RNA isolation from feline teeth collected in a clinical setting and at post mortem to produce high quality RNA suitable for gene expression studies.
- Determine mRNA expression of pro-inflammatory cytokines, VDR, and RANKL using quantitative PCR.
- Establish an *in vitro* feline osteoclast differentiation system to investigate the functional role of candidate TR proteins and others identified via the RNA –seq approach
- Perform RNA-seq from feline teeth with or without TR to generate a list of differentially expressed genes and verify their expression by quantitative PCR to identify a short list of candidate genes related to TR and osteoclast biology.
- Further analyse the gene sets by propriety software to identify gene pathways and circuits and provide a biological context to the transcriptome analysis.
- Identify protein expression of candidate genes in histological tooth sections.
- Test the functional role of one of the candidate gene (*MMP9*) identified from the RNA-seq data in its ability to influence osteoclast biology and bone resorption. This will be done using an MMP9 inhibitor and siRNAs targeting the feline *MMP9* sequence.

Chapter 2 Materials and methods

2.1 RNA and DNA methods

2.1.1 RNA extraction from cells

Total RNA was isolated from cells utilising the RNeasy Mini kit (Qiagen, Sussex, UK) with or without QIAshredder according to the manufacturer's protocol. To minimize DNA contamination of RNA samples, a DNase on-column digestion step was included using RNase-Free DNase Set (Qiagen). This commercial kit is based on the principle that combines the RNA selective binding properties of a silica membrane column with microspin technology. In brief, up to 1×10^7 cells were lysed in 350 µl to 600 µl of RLT lysis buffer containing guanidine thiocyanate which stabilises RNA by inactivating RNases. Alternatively, the cell monolayer in the culture vessel was lysed by adding RLT lysis buffer directly to the well. Samples were mixed thoroughly by pipetting or vortexed. The cell lysate was homogenised in a QIAshredder by centrifugation at full speed for 2 min before 70% of ethanol was added and mixed thoroughly. The lysate was applied to the spin column and centrifuged at 8,000 x *g* for 15 s. The flow through containing protein and cellular debris was discarded. A wash step using 350 µl of RW1 buffer was performed at 8,000 x *g* for 15 s. To decontaminate DNA, a mixture of 10 µl of DNase and 70 µl of RDD buffer was added directly to the spin column membrane. After 15 min of incubation at room temperature (RT) a further wash step with 350 µl of RW1 buffer was performed. Two wash steps with 500 µl of RPE buffer containing 80% of ethanol were then performed at 8,000 x *g* for 15 s and for 2 min respectively. To evaporate the ethanol, a further centrifugation step at full speed was performed for 1 min. RNA was eluted in 30 µl to 50 µl of RNase-free water by centrifugation at 8,000 x *g* for 1 min. RNA was stored at -80C until analysed.

2.1.2 Determination of quantity and purity of RNA

Yield of RNA was determined based on absorbance at 260 nm (A_{260}) using a NanoDrop™ 1000 Spectrophotometer. The purity of RNA was assessed based on

the ratios of absorbance at 260 and 280 nm ($A_{260:280}$ ratio) and 260 and 230 nm ($A_{260:230}$ ratio).

2.1.3 Reverse transcription reaction

For first strand complementary DNA (cDNA) synthesis, Omniscript® Reverse Transcription kit (Qiagen) was used. RNA was diluted in 7 µl of RNase free water containing 0.25 to 0.5 µg of RNA. Aliquots were denatured at 65°C on a heat block and cooled on ice. A master mix was prepared consisting of 10× RT buffer, 0.5 µM of dNTP mix, either 1 µM of Oligo-dT primer or 10 µM of random hexamers (Qiagen), 10 unit of RNasin®Plus RNase inhibitor (Promega), RNase-free water and 4 unit of the Omniscript reverse transcriptase (Omniscript RT) and 100 mM of dithiothreitol (DTT, Thermo Fisher Scientific) according to the manufacturer's instructions. The denatured RNA was added to a master mix with a total volume of 20 µl. The cDNA was reverse transcribed at 37°C for 1 h in G-Storm Thermal Cycler (Labtech Ltd, Sussex, UK) and stored at -20C.

2.1.4 Primer design

Primers used in this study were chosen based on published data or designed using online tools. To design effective primers, two online tools of PCR primer design were used: PCR Primer Design Tool (Eurofins Genomics) and Primer-BLAST combining Primer3 and Basic Local Alignment Search Tool (BLAST) (National Center for Biotechnology Information). To screen complementarity and secondary structure of primers including self-dimers and hetero-dimers against the two primers, online OligoAnalyzer software was used. BLAST searches were performed for primers against the feline whole genome shotgun (wgs) sequence and nucleotide collection (NCBI, 2017). Newly designed primers were purchased from Eurofins MWG Operon (eurofinsgenomincs.eu).

2.1.5 Polymerase Chain Reaction (PCR)

PCR reactions were performed using a commercially available kit (HotStarTaq® DNA polymerase kit, Qiagen) following the manufacturer's

protocols. The master mix was prepared on ice and each aliquot had 2 µl of cDNA template, 10× PCR buffer, 200 µM of each dNTP, 2.5 units of HotStart Taq DNA polymerase, 0.5 µM of each primer and nuclease free water added in 25 µl total reaction volume. PCR reactions were performed on the G-Strom thermal cycler (Labtech Ltd). To assess consistency of sample loading and PCR conditions, a reference gene (beta-actin) previously designed and tested for feline beta-actin and no RNA control (NTC) were included in every reaction. The thermal conditions were: initial denaturation at 95°C for 15 min, 30 to 40 cycles of denaturation at 94°C, annealing at 50 to 56°C and extension at 72°C for 1 min, and final extension at 72°C for 1 min. PCR products were analysed using gel electrophoresis with 1.2 to 3% agarose gels (Sigma-Aldrich®) dissolved in TAE buffer (Appendix). The solution was cooled and mixed with GelRed™ Nucleic Acid Gel Stain (10,000x, Biotium, UK). The agarose was poured into gel casting trays with gel combs and allowed to set. PCR products and 100 bp DNA ladder (Promega) were loaded with 6× loading dye (Promega, UK). The gel was run in TAE buffer at 60 to 80 V for 30 to 60 min. Gels were visualised utilising Kodak Gel Logic 200 Imaging (Kodak, USA) and images were recorded using Kodak 1D 3.6 Gel Logic software.

2.1.6 **Quantitative PCR**

A real-time PCR known as quantitative PCR (qPCR) was performed with high affinity, double stranded DNA-binding dye SYBR Green using Stratagene MX3000P qPCR system (Agilent Technologies). Two commercially available kits were used: 2×Takyon for SYBR Assay - Low ROX (Eurogentec, Belgium) or Precision™ 2× qPCR Mastermix (Primer design, Southampton, UK). Each qPCR reaction contained 300 nM of gene of interest or reference gene primers, 2× Mastermix and 4 µl of nuclease free water in a 96 well plate format. The cDNA template from each treatment group was diluted 1:5 or 1:10 from cDNA and 5 µl was added to the reaction, producing a final volume of 20 µl for each reaction. The thermal cycling conditions followed manufacturer's instructions. All samples were performed in duplicate or triplicate and cycling threshold (Ct) values for each gene

were generated.

2.1.7 Optimisation of qPCR primers

All primers were tested to check efficiency of primers using Stratagene MX3000P qPCR system. The cDNA was serially diluted with nuclease free water 4 or 10-fold depending on genes and primer sets. Primer efficiency and melt curve (association curve peak) were generated using MxPro QPCR Software (Mx3000P, Agilent Technologies).

2.1.8 Quantification of gene expression

Calculation of relative gene expression analysis was based on delta-delta method (212, 213). Analysis were performed using cycling threshold (Ct) values for each target and RGs. Relative gene expression was calculated using Microsoft Excel 2013. The delta Ct value for each sample was calculated and the relative expression level of the target gene was calculated as shown in Table 2.1. Relative gene expression was calculated as fold change as calculation of $2^{-\Delta\Delta Ct}$.

ΔCt = Ct for target gene - Ct for reference gene
ΔΔCt = ΔCt of TR positive (+ve) sample – ΔCt of TR negative (-ve) sample
Relative expression = $2^{-\Delta\Delta Ct}$

Table 2.1 Calculation of relative gene expression based on delta-delta method

2.1.9 Purification of PCR product

Synthesised cDNA from PCR product was purified using the Wizard® SV Gel and PCR Clean-Up System (Promega) according to the manufacturer's protocol. In brief, for direct purification of PCR products, an equal volume of membrane binding solution was added to the PCR reaction mix, transferred to SV minicolumn assembly and incubated for 1 min at RT. Then the column was centrifuged at 16,000 x g for 1 min and the flow through was discarded. The column was washed with 700 µl of membrane wash solution containing 95% ethanol by centrifugation at 16,000 x g for 1 min. A further wash was carried out with 500 µl of membrane wash

solution by centrifugation at 16,000 x g for 5 min. The column was set with lid open to dry the ethanol residue for 1 min. The column was transferred into a clean microcentrifuge tube and DNA was eluted with 30-50 µl of nuclease free water during centrifugation for 1 min at 16,000 x g. Eluted cDNA was stored at -20°C.

2.1.10 DNA sequencing

DNA sequencing was performed in The University of Edinburgh sequencing facility (Edinburgh Genomics, Kings Buildings, Edinburgh). Samples for submission were prepared in labelled PCR strip tubes. Varying amounts of DNA were required depending on the length of the DNA fragment (Table 2.2). Five µl of nuclease free water containing the maximum amount of DNA was added to 1 µl of nuclease free water containing 3.2 pmol of primer. Sequencing was performed in both directions using the BigDye® Terminator v3.1 (Applied Biosystems, UK) sequencing reaction based on the Sanger sequencing technique. It utilises dideoxy-nucleotides that terminate chain elongation after their incorporation into the DNA strand. This reaction is followed by clean-up and capillary analysis using the ABI3730 DNA analyser (Applied Biosystems). Sequences obtained underwent BLAST searches against the feline wgs sequence and nucleotide collection (NCBI, 2017).

For purified PCR product	Amount of DNA template
100- 200 bp	1.5-3 ng
200- 500 bp	4.5-10 ng
500- 1000 bp	7.5-20 ng
1,000- 2,000 bp	15-40 ng
>2,000 bp	60-100 ng

Table 2.2 DNA amount for DNA sequencing.

2.2 RNA Sequencing (RNA-Seq)

2.2.1 Tooth collection and TR phenotyping

Teeth were collected from patients with full owner's consent presented to Hospital for Small Animals, The Royal (Dick) School of Veterinary Studies, The

University of Edinburgh, UK. TR was diagnosed by the combination of oral examination and intraoral dental radiography (97). The TR affected teeth were extracted by a veterinary surgeon using standard dental equipment under full general anaesthesia. Further research samples including teeth, maxilla, mandibles and various tissues were collected at post mortem from cats and dogs euthanized for a wide range of medical reasons and donated to the school for research. To phenotype TR status in research samples, frozen jaws were delivered to the radiographic facility in a liquid nitrogen carrier and radiographed. TR type and staging were confirmed by a veterinary dental specialist, Dr Norman Johnston (MRCVS. RCVS, American & European Specialist in Veterinary Dentistry, DentalVets, North Berwick) and Dr Susan Thorne (MRCVS, Dentistry and Oral Surgery Resident, DentalVets, North Berwick).

2.2.2 **Tissue processing and RNA extraction**

Clinical samples were immediately stored in RNA*later*® solution (Thermo Fisher Scientific) at RT or snap frozen in liquid nitrogen before stored in - 80°C freezer. Post mortem samples, consisting of mandibles, maxilla, trimmed bones or soft tissues were snap frozen in liquid nitrogen before stored at -80°C until RNA extraction. Teeth were extracted from the alveolar sockets using dental equipment (214) or bone cutters and forceps while maintaining cold temperatures by working over dry ice. TRIzol® reagent (Thermo Fisher Scientific) was used to extract RNA from tissues based on a guanidinium thiocyanate-phenol-chloroform extraction method (215). RNA extraction method was modified from the manufacturer's protocol. In brief, tissues filled with TRIzol® reagent (1 ml/100 mg of tissue) were homogenised in a beaded tube (Lysing Matrix D tube) placed in FastPrep FP120 (Thermo Savant) to agitate at a speed of 4 m/s for 20 s or in a stainless steel jar and ball (Mixer Mill MM200, Retsch, Germany) set at 30 Hz for 2 min to perform radial oscillations in a horizontal position. Homogenised tissues were incubated for 30 min and centrifuged at 10,000 x *g* for 10 min at 4°C. Supernatant was transferred into a clean tube and 200 µl of chloroform was added, mixed and incubated at RT for 10

min. A further centrifugation step of 15 min at 10,000 x *g* at 4°C was performed and the clear supernatant was transferred into a clean tube. An equal volume of 70% ethanol was added to each tube and mixed by pipetting. The mixture was transferred to Qiagen RNeasy Mini spin column (Qiagen, Sussex, UK). RNA washing and DNase digestion were performed according to the manufacturer's instruction. Details were described in section 2.1.1. RNA was eluted with 30 - 50 μl of RNase free water and stored at -80°C.

2.2.3 RNA quantity and quality control

Quantity and purity of RNA were measured as described in section 2.1.2. The RNA Integrity Number equivalent (RIN^e) was determined by RNA analysis ScreenTape kit on Agilent 2200 TapeStation for quality control. RNA samples were sent to Edinburgh Genomics for further quality control of RNA and RNA sequencing.

2.2.4 cDNA library and RNA sequencing

The Illumina TruSeq stranded mRNA sample preparation kit was used for cDNA libraries. To generate cDNA libraries, 0.8 μg - 1 μg of total RNA was used according to the manufacturer's instructions (Illumina, San Diego, CA, USA). Briefly, purified poly-A containing mRNA molecules using poly T oligo magnetic beads were fragmented using divalent cations on a pre-heated block at 94°C for 8 min. The cleaved RNA fragments were copied into first strand cDNA using reverse transcriptase and random primers and then followed by second strand cDNA synthesis using DNA polymerase I and RNase H. These cDNA fragments were added with a single 'A' base and underwent subsequent ligation of the adapter. The products were then purified and amplified in 10 cycles to create the final cDNA library. Paired-end sequencing was performed using the Hiseq 4000 system (Illumina).

2.2.5 Mapping to feline reference genome

Annotation and alignment were performed using STAR (version 2.5) comparison to the *Felis catus* genome (version 6.2) in the Ensembl database (216). Alignment files were generated in the bam format for each sample. The RNA-seq expression profile was represented by a table of raw read counts for tens of thousands of genes in all TR -/+ samples using HTSeq (version 0.6.0.1) with mode 'union' (217). Duplicate reads were found using picard tools (version 1.141). Generation of MDS plot were generated using plotMDS function from edgeR package (version 3.12.1) to visualize the level of similarity of individual cases of a dataset.

2.2.6 Differentially expressed genes

Differentially expressed genes were identified through comparisons between TR -ve and TR +ve groups using edgeR (version 3.12.0) (218). Genes with less than 20 reads were discarded from this analysis. The trimmed mean of M-values normalization method was used. To explore sample dispersion between control and TR +ve group, distance plot of biological coefficient of variation samples were generated and outliers were exclude for differential expression gene analysis. Significantly DE genes were identified using the threshold of false discovery rate (FDR)-adjusted p-value < 0.05.

2.2.7 Gene sets and pathways analysis

To identify gene sets and pathways analysis, two enrichment analyses on the set of up- and down-regulated DE genes were performed: Kyoto Encyclopaedia of Genes and Genomes metabolic pathways (KEGG) (219) and gene ontology (220).

2.2.8 Identification of single nucleotide polymorphisms

SNPs were identified using Genome Analysis Toolkit with mode 'HaplotypeCaller' (GATK, version 3.5)(221) and the NCBI database of genetic variation (dbSNP build ID 148) (222) performing local realignments and base quality score recalibration. The resulting variant call format files (VCFs), one per sample,

were merged to create a single gVCF file using GATK GenotypeGVCFs. This allows variants to be called on all samples simultaneously. Finally, genomic locations and prediction of coding effects on these SNPs were identified using SNPEff (version 4.2) (223).

2.3 Cell culture

2.3.1 Reagents

All cell culture reagents including cell culture media, supplements and foetal bovine serum (FBS) were obtained from Gibco (Thermo Fisher Scientific, UK) unless otherwise stated. Tissue culture plastics were obtained from a variety of sources *e.g.* conical sterile polypropylene centrifuge tubes (Becton Dickinson Biosciences, UK), cell culture flasks, multiple well plates, microplate, pipette tips, cell strainer and cryogenic vials (Corning® Sigma-Aldrich., UK or Thermo Fischer Scientific., UK) and microcentrifuge tubes (Eppendorf tubes, Axygene, VWR, USA).

2.3.2 Cell lines

Osteoclasts are terminally differentiated cells from haematopoietic progenitors, and there are no currently available immortalised osteoclast cell lines. To establish authentic osteoclasts, initially non-adherent mononuclear cells derived from bone marrow or peripheral blood were used as a source, and two critical cytokines, M-CSF (CSF-1) (224) and RANKL (30, 225) were added. One commercially available cell line, RAW 264.7 cells which were established from the ascites from a mouse tumour by injection of Abelson leukaemia virus (226) and are reported that they are capable of differentiation into osteoclasts in the presence of RANKL (226).

2.3.3 Cell passaging

Cell lines including RAW 264.7 cells and primary periodontal ligament cells were maintained in T25 flasks or T75 flasks. Cells were routinely passaged when they reached 85 to 95% confluency. To passage cells, medium was removed by pipetting and the cells were washed twice with PBS by centrifugation at 400 x g for 5

min. Following washing, 0.25% trypsin- ethylenediaminetetraacetic acid (EDTA) (Table 2.3) was added to cells and incubated at 37°C until cells were detached. Trypsinization was terminated by adding double volume of FBS containing media to the cells to neutralise the trypsin. Cells were split as required (1:5 to 1:20) and seeded directly into new culture vessels with fresh media.

2.3.4 Cell counting and viability

Ten µl of cell suspension were transferred to a microcentrifuge tube, mixed with 10 µl of trypan blue stain, and incubated for 2 min. Ten µl of cell suspension was added to the counting chamber of a haemocytometer and the cells were counted. Dead cells were recognised as dark blue stained cells and non-refractile. Cell density were then determined using following formula: Cell density (cells per ml) = Average number of cells in one square × dilution factor × 10^4.

Cell culture vessel	Surface area (cm2)	Total volume of media (ml)	Volume of 0.25% Trypsin-EDTA (ml)
T75	75	13	3
T25	25	8	2
10 cm plate	55	10	3
6 well plate	9.6	2 - 2.5	1
24 well plate	1.9	1	0.5
96 well plate	0.32	0.2	N/A

Table 2.3 Information of a variety of cell culture vessels including cell number seeded, total volume of media and 0.25% trypsin-EDTA.

2.3.5 Freezing/thawing cells

Cells were counted, up to 1×10^6 were suspended in cryogenic tube vials containing 1 ml of 10% dimethyl sulfoxide (DMSO) in FBS. Vials were transferred to a Freezing Container (Mr Frosty™, Thermo Fisher Scientific) in -80°C for 24 h. This container enables slow cooling at a rate of -1°C/min, the optimal rate for cell preservation. After 24 h, the freezing container was transferred to -150°C.

For thawing cells from frozen vial, cells were quickly defrosted in a 37°C water bath and transferred into Falcon tubes containing 5 ml of warm medium. The

cell suspension was centrifuged at 400 x g for 5 min. The supernatant was discarded and the cell pellets were resuspended in their respective media, transferred to appropriate cell culture vessel, T25 or T75 and incubated at 37°C/5% CO_2 overnight.

2.3.6 Peripheral blood mononuclear cells (PBMCs) isolation and osteoclast culture

For the primary cell culture, peripheral blood was obtained at post mortem from cats euthanized for clinical reasons and donated to the School for research purposes. This protocol was modified from previously published protocols (227, 228). The osteoclast differentiation protocol is illustrated in Figure 2.1 and Figure 2.2, A. Blood was heparinised and transported on wet ice. Peripheral blood mononuclear cells (PBMCs) sedimented at the interface between plasma and Ficoll-paque solution with a density of 1.077 ± 0.001 g/ml (Ficoll Hypaque Plus, GE Health care, Buckinghamshire, UK) following centrifugation for 30 min at 400 x *g* at RT (Figure 2.1). Mononuclear cells were carefully isolated and washed twice in alpha Minimum Essential Medium (α-MEM) by centrifugation at 400 x *g* for 5 min. Isolated PBMCs were resuspended in α-MEM supplemented with 10% heat-inactivated FBS (F1 -3 of three different serum batches, Gibco), 2 mM L-glutamine, 100 IU/ml benzyl penicillin, 100 mg/ml streptomycin and plated on plastic vessels ($1 \times 10^5/cm^2$) with CSF-1 (human CSF-1, 30-100ng/ml or mouse CSF-1, 10 to 25ng/ml, R&D systems) at 37°C/5% CO_2. On day 4, 90% of the medium was changed and, replaced with a new α-MEM containing CSF-1 (concentrations as above)and RANKL (human RANKL , 25-100ng/ml, mouse RANKL, 3-20 ng/ml, R&D systems) and half of medium were changed with new medium twice weekly for up to 10 -14 days.

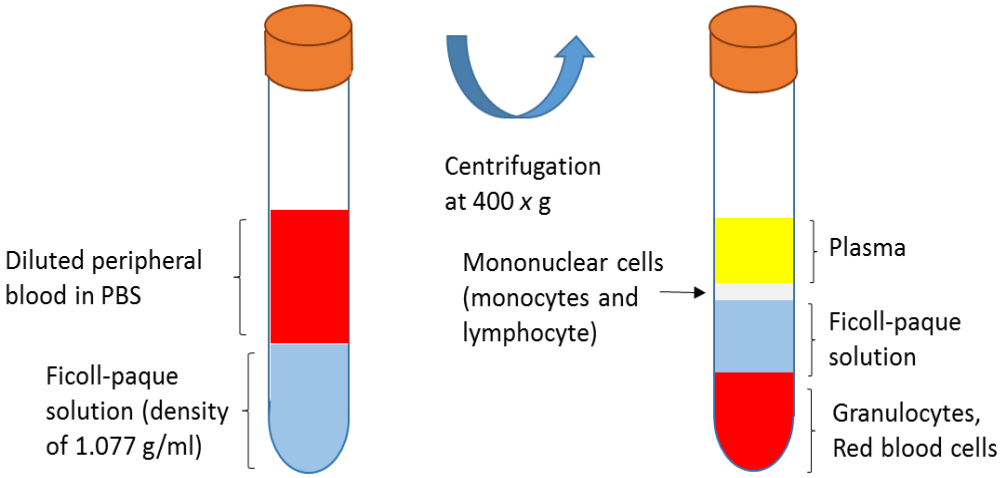

Figure 2.1 Isolation of mononuclear cells from peripheral blood. Diluted whole blood in Ficoll-paque solution, the density gradient media is centrifuged and mononuclear cells including osteoclast precursors are layered at the interface between plasma and Ficoll-paque solution.

2.3.7 Bone marrow isolation and osteoclast culture

This protocol was modified from a published rodent/feline osteoclast culture protocols (228, 229) (Figure 2.2, B). The femurs, tibiae, and humeri were dissected from the cats, dogs or mice, washed in 70% ethanol and cut off at the proximal and distal ends. Bone marrow was flushed out using a 25 G needle in α-MEM containing 10% FBS. The bone marrow suspension was passed through a cell strainer and followed by lysis of red cells using 5 ml of Lysis Buffer (150 mM NH4Cl, 10 mM NaHCO3, 0.1 mM EDTA) for 5 min, on ice. The cells were washed and resuspended by centrifugation at 400 x g for 5 min in α-MEM containing 10% FBS, 2 mM L glutamine, 100 IU/ml benzyl penicillin, 100 mg/ml streptomycin, and CSF-1 (human CSF-1, 30-100ng/ml or mouse CSF-1, 10 to 25ng/ml, R&D systems) and plated into T 75 flasks for 24 h at 37°C/5% CO_2 for attachment of stromal cells. On the following day, non-adherent cells were collected and washed once in α-MEM (concentrations as above)containing 10% FBS by centrifugation at 400 *x g* for 5 min. Resuspended cells were plated on new plastic vessels ($1\times10^5/cm^2$) with CSF-1 (at 37°C/5% CO_2. On day 4, 90% of the medium was changed and, replaced with a new α-MEM containing CSF-1 (concentrations as above) and RANKL (human RANKL , 25-

100ng/ml, mouse RANKL, 3-20 ng/ml, R&D systems). The culture medium was subsequently change twice weekly by replacing half of the volume with fresh media up 10 to 14 days.

2.3.8 **RAW 264.7 cells-osteoclast differentiation**

RAW 264.7 cells have the potential to differentiate into osteoclasts in the presence of RANKL but independently of CSF1. This protocol was modified based on a published paper (226). On day 0, 1×10^4 cells/cm^2 were plated on plastic or dentin discs in α-MEM containing 10% FBS, 2 mM L glutamine, 100 IU/ml benzyl penicillin, 100 mg/ml streptomycin supplemented with 5-10 ng/ml of mouse RANKL. Half of medium was changed every other day until osteoclast formation occurred (days 4 -6).

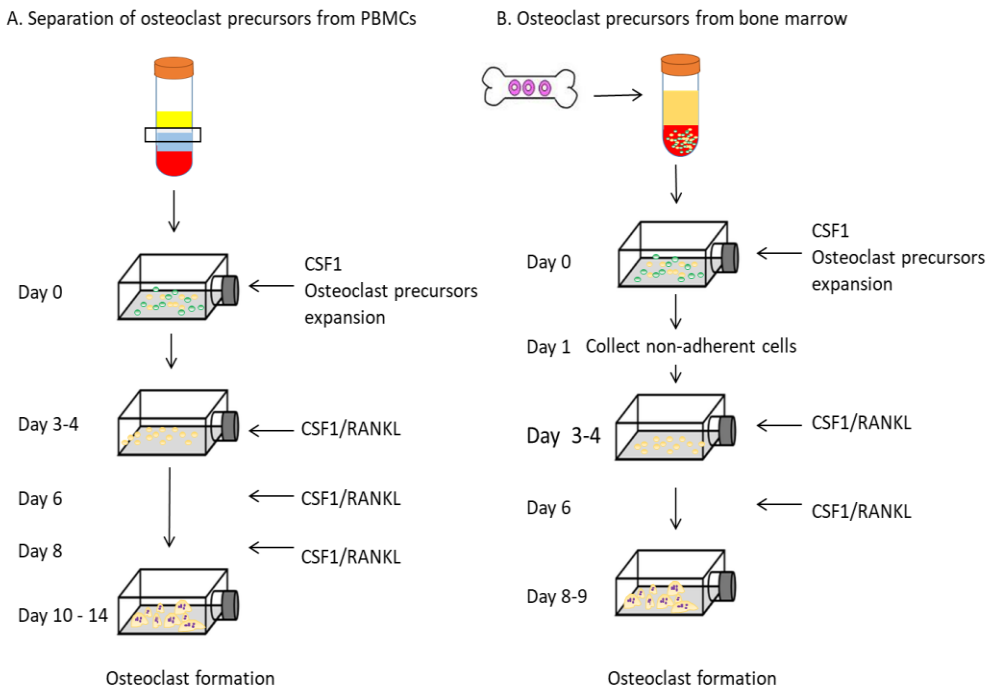

Figure 2.2 Illustration of osteoclast differentiation from peripheral blood mononuclear cells and bone marrow. (A) Differentiation osteoclasts derived from blood precursors (B) Separation of bone marrow cells and stepwise differentiation of osteoclasts. See text for more details.

2.3.9 Primary feline periodontal ligament cells

Feline teeth were extracted at post mortem and dissected into small pieces. Periodontal ligament cells were shaved off utilising a surgical knife and gingival tissues near the cemento-enamel junction were dissected into small pieces. The periodontal ligament tissue, shattered teeth and gingival tissues were incubated in a 15 ml conical tube containing α-MEM with 0.2% collagenase at 37°C for overnight in a roller incubator. All cells containing collagen digested tissues were put through a cell strainer with 70 μm pore size to obtain a uniform single-cell suspension and remove tissue debris. Cells suspension were centrifuged and pelleted cells were subsequently cultured in α-MEM, containing 10% FBS at 37°C/5% CO_2 on dishes 100 mm in diameter until 80% confluency. These cells were collected with 0.05% trypsin-EDTA and transferred to a new plastic vessel or frozen as described in section 2.3.5.

2.3.10 Osteoclast-periodontal ligament cells co-culture

For indirect culture, bone marrow derived mononuclear cells (10^5 cells/ well) as described in section 2.3.7 were seeded onto 24 well plate and Corning® Transwell® polyester membrane cell culture inserts (0.4 μm pore size) were placed on the seeded plate (Figure 2.3, A). The periodontal ligament cells were seeded onto transwell inserts (1×10^4 cells/well), and cultured in α-MEM, containing 10% FBS, at 37°C/5% CO_2 for 14 -20 days. Co-culture was also performed directly mixing the two cell types in 24 well plate; bone marrow derived mononuclear cells (10^5 cells/ well) and periodontal ligament cells (1×10^4 cells/well) (Figure 2.3 B).

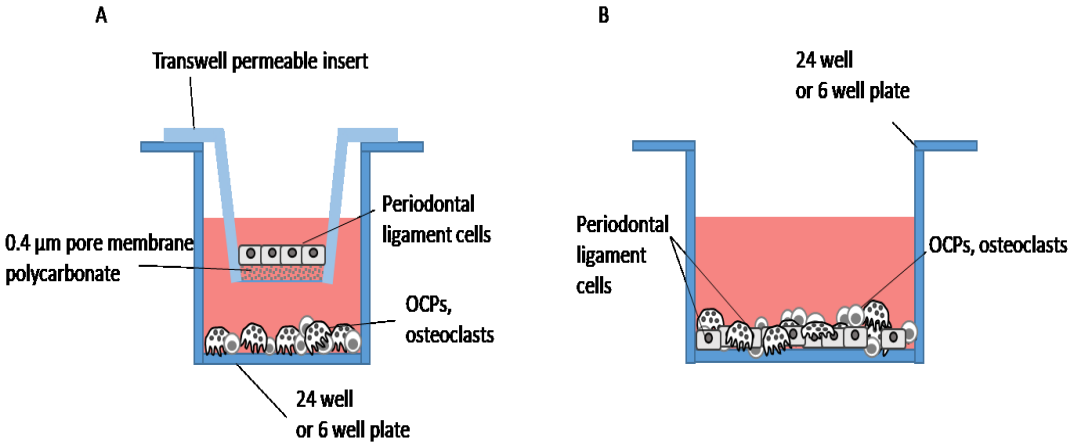

Figure 2.3 Co-culture of feline osteoclast precursors and periodontal ligament cells in indirect or direct culture setting. (A) Osteoclast precursors are seeded and periodontal ligament cells were seeded onto a transwell insert in indirect co-culturing system. (B) Two cells are mixed and seeded in direct co-culturing. OCPs: osteoclast precursors.

2.4 Characterisation of feline osteoclast

2.4.1 Tartrate resistant acid phosphatase (TRAP) reaction

Cultured osteoclasts on plastic or dentin discs were washed twice with PBS and fixed in 2.5% glutaraldehyde for 5 min. TRAP reactivity was performed using Acid phosphatise leukocyte kit (Sigma-Aldrich Ltd) according to the manufacturer's protocol with some modification including reduced incubation time (30 min) and with or without haematoxylin staining. TRAP positive cells were imaged via light microscopy (Leica DM LB2, Milton Keynes, UK). Cells were considered to be osteoclast like cells when they were TRAP positive and contained more than two nuclei when manually counted.

2.4.2 Immunocytochemistry and antibodies

Cells were seeded onto chamber slides at a density of $5x10^4$ cells per well containing 200 µl of media and incubated at 37°C/5% CO_2 until to form multinucleated cells. Following differentiation of osteoclasts, the media was discarded and the cells were washed twice in cold PBS. Cells were fixed in cold acetone or methanol (500 µl/chamber) for 5 min at RT then washed twice in cold PBS for 10 min. PBS was removed from the chambers and 500 µl of 10% goat serum

blocking solution was added. The cells were incubated at RT for 1 h and blocking solution was removed. Primary antibodies were diluted in 0.1% goat serum blocking solution and added to the chambers (100 µl/chamber) (Appendix). Negative controls consisted of 0.1% goat serum blocking solution without primary antibodies or with immunoglobulin isotype. The slides were incubated in a humid chamber overnight at 4°C. Following incubation the slides were washed three times in PBS containing 0.1% Tween 20 (PBST) for 10 min. Secondary antibodies were diluted in 0.1% goat serum blocking solution and added to the chambers (100 µl/chamber). Secondary antibodies raised against the species in which the primary antibody was produced were chosen (Appendix). The slides were incubated at RT for 1 h in a humid chamber in the dark. Following secondary antibody incubation slides were separated, put in a staining jar covered in foil and washed with PBST three times for 10 min each time on the orbital shaker. Then the slides were stained with DAPI (Invitrogen D1306) 1:10,000 dilution in PBST for 5 min. After final washing with PBS three times for 2 min, the slides were mounted using the anti-fade mount media (Vectashield hardset mounting medium) and cover slips were applied gently and dried overnight at 4°C covered with foil. The slides were stored at 4°C for a few days or stored at -20°C for long term storage.

2.4.3 **Actin ring staining**

Cultured osteoclasts on chamber slides was fixed using acetone or methanol and washed in PBST three times. Two drops of Actinred™ 555 ReadyProbes® Reagent which include high-affinity F-actin probe conjugated to the red-orange fluorescent dye tetramethylrhodamine (TRITC) was diluted in 1 ml of PBST. The diluted Actinred was directly added onto slide or place (300 µl/sample) and incubated for 30 min, protected from light. Cells were washed in PBST and nuclei was stained as described in 2.4.2 and cover slips were applied with anti-fade mount media, dried and stored with covered foil until viewed under the fluorescent microscope.

2.4.4 Source of mineralised substrates

To evaluate resorption activities, osteoclasts require mineralized substrates. The block of dentine and discs were generous gifts from Prof. Timothy R. Arnett (University College London, London, UK). To generate authentic osteoclasts with resorption pits, osteoclast precursors were transferred onto dentine discs. To activate the osteoclast, culture medium was acidified to pH 7.0 by addition of 11.5 M HCl (229). Resorption pits are normally easily detected by reflected light. If necessary, cells were removed from the discs using sonication for 5 min in 0.25 M ammonium hydroxide. Discs may require additional staining for 2 min in toluidine blue solution to improve visualisation of pits. Resorption pits were measured as area. Alternatively, Corning Osteo Assay Surface multiple well plates can be used as a source of mineralised substrate. This plate has bone-like mineral surface coated with a proprietary hydroxyapatite mineral surface that is highly uniform and microscopically fine-grained. This unique plate has been used for both routine resorption assays and high-throughput screening for the study of both osteoclast and osteoblast function.

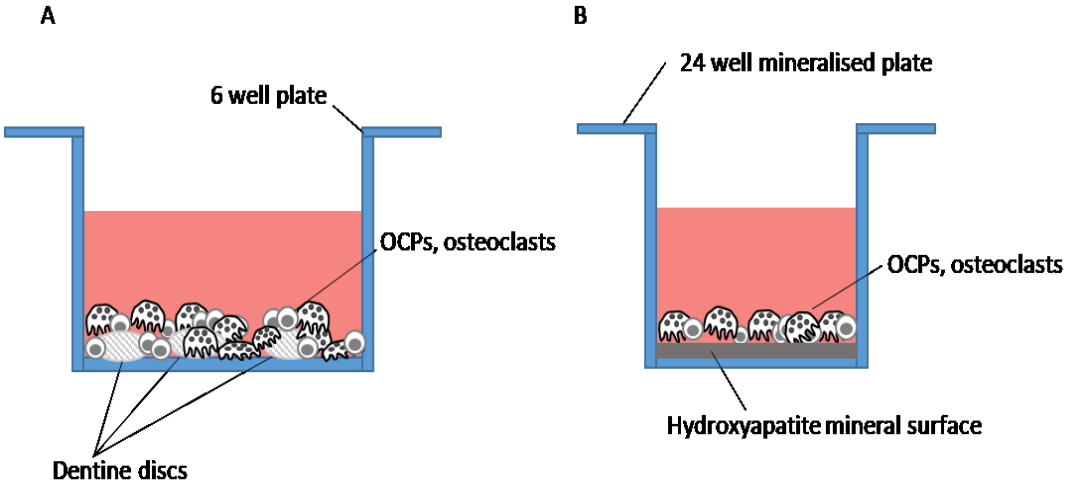

Figure 2.4 Osteoclast resorption activity. (A) Resorption activity of osteoclasts is tested on the dentine discs. (B) Alternately, osteoclasts are seeded in a mineralised plate coated with hydroxyapatite for resorption activity. OCPs: osteoclast precursor.

2.4.5 Resorption activity on mineralised plate

To visualise resorption pits, Corning Osteo Assay Surface multiple well

plates was bleached and the contrast enhanced to assess resorbed surface area. In brief, 10% bleach solution was added to the wells and incubated for 5 min at RT. After washing cells twice with distilled water, plates were allowed to dry at RT for 3 to 5 h. Individual pits can be visualised using a microscope. The modified von Kossa staining protocol was performed to improve the contrast for resorbed pit by adding 5% (w/v) aqueous silver nitrate solution to each of the bleached wells and incubated for 30 min at RT in the dark. The silver nitrate solution was discarded and plates were soaked in distilled water for 5 min. When the mineral surface turned yellow, 5% sodium carbonate (w/v in commercial buffered formalin) was added and incubated for 4 min at RT. As the ionic silver (I) was reduced to metallic silver, the plate appeared a dark colour. The plates were dried at 50°C for 1 h. Resorption pits were assessed using light microscopy (Axiocam 105 color).

2.4.6 **Resorption activity on dentin discs**

Resorption pits can be visualised by reflected light microscopy following TRAP reactivity as described in section 2.4.1 without the removal of cells. Alternatively, cells from discs were removed by vigorous sonication for 5 min in 0.25 M ammonium hydroxide. The discs were stained for 2 min in toluidine blue solution followed by rinsing in water and air drying to improve visualisation of pits. Counting of the pits or measurement of the pits surface area were performed by scanning the entire surface of each disc using reflected light microscopy (Nikon Eclipse Ni).

2.4.7 **Vitamin D treatment**

1,25-dihydroxyvitamin D_3 (1,25$(OH)_2$ D), the biologically active form of Vitamin D was purchased from Sigma-Adrich (UK). Ten mg of 1,25$(OH)_2D_3$ was made up to a 10 μM stock solution in ethanol and stored at -20°C. The primary feline, canine, murine osteoclast precursors from bone marrow were treated, in addition to CSF-1 and RANKL, with a range of concentrations from 0.1 nM to 100 nM diluted in α- MEM until termination of osteoclast differentiation. Vehicle

controls were treated at the equivalent concentrations of ethanol corresponding to the ethanol concentrations used for the highest $1,25(OH)_2D_3$ concentration in the experiment. Untreated control cells were also included in each experiment.

2.4.8 MMP9 inhibitor

The MMP9 inhibitor containing hydroxamate (-CONHOH) group binds the zinc atom in the active site of the MMP enzyme. This molecule is a cell permeable, potent, semi-selective, and reversible MMP-9 Inhibitor (IC50 = 5 nM). At high concentrations, it can inhibit MMP1 and MMP13 as well. Five hundred μg Calbiochem (Merck Millipore, UK) was made up to 1 mg/ml stock solution in DMSO and stored at -20°C. The primary feline, canine, murine osteoclast precursors from bone marrow were treated, in addition to CSF-1 and RANKL, with a range of concentrations from 5 nM to 1 μM diluted in α- MEM until termination of osteoclast differentiation. Vehicle controls were treated with DMSO concentrations corresponding to the highest MMP9 concentration used in the experiment. Untreated control cells were also included in each experiment.

2.5 RNA interference

2.5.1 Designing siRNA targeting feline MMP9

The siRNA sequence against the feline MMP9 were designed using an online design tool, i-Score designer (i-score web service program). Potential siRNAs were evaluated for GC content and Reynolds scores were obtained (230). BLAST searches were then performed for selected siRNAs against the feline wgs sequence and nucleotide collection (NCBI, 2017). DNA oligonucleotide templates were purchased from eurofins MWG Operon (eurofinsdna.com). DNA oligonucleotide templates were designed by adding an eight nucleotide T7 Promoter sequence (5′ CCTGTCTC 3′) to the 3′ end of both the sense and antisense template strands.

2.5.2 Construction of siRNA targeting feline MMP9

MMP9 feline siRNA was constructed using the Silencer® siRNA Construction Kit (Ambion) according to the manufacturer's protocol. In brief, the

sense and antisense DNA oligonucleotide templates were resuspended to a concentration of 100 μM and each aliquot of sense and antisense templates were mixed with the T7 promoter primer in 8 μl of the DNA hybridisation buffer in separate tubes. The reaction was heated to 70°C for 5 min and cooled at RT for 5 min to anneal the eight nucleotide leader sequence of the DNA oligonucleotide template with the T7 Promoter primer. Following hybridisation, Exo-Klenow Reaction buffer, dNTPs, nuclease-free water and Exo-Klenow were added to each reaction and incubated at 37°C for 30 min. Two μl of the sense and antisense siRNA templates were transcribed for 2 h at 37°C in separate reactions. Then the templates were mixed with nuclease-free water, NTPs, T7 reaction buffer and T7 enzyme mix. The sense and antisense transcription reactions were then mixed and incubated overnight. Double stranded RNA solutions were digested with RNase and DNase for 2 h at 37°C. Four hundred μl of siRNA binding buffer containing ethanol was added to the Double stranded RNA and incubated for 5 min at RT. For each siRNA sample a filter cartridge was placed into a 2 ml collection tube that was pre-wet with 100 μl of siRNA wash buffer. The siRNA-binding buffer mix was added to the filter cartridge and centrifuged at 80,000 x *g* for 1 min. The column was washed twice in 500 μl of siRNA wash buffer and centrifuged each time at 80,000 x *g* for 1 min. The filter cartridge was placed into a new collection tube and 100 μl of pre-heated 75°C nuclease-free water was added and incubated at RT for 2 min before centrifuging at 8,000 x *g* for 2 min. Purified siRNAs were quantified as previously described in section 2.1.2. Each 20 μM siRNA aliquot was stored at -20°. Commercially available negative control siRNA, scrambled non-targeting siRNA (Silencer® Negative control number 1, Life Technologies™) was purchased.

2.5.3 **Electroporation of RNA and DNA**

Osteoclast precursors were seeded in fresh isolated bone marrow as described in section 2.3.7 or frozen vials containing bone marrow precursors in section 2.3.5. Cells were seeded in 10 cm coated plate including α-MEM with GlutaMAX, 10%FBS, penicillin/Gentamicin (50μg/ml) and CSF-1 (10ng/ml) added incubate

overnight at 37°C/5% CO_2 to allow stromal cells to attach. Non adherent cells including the osteoclast precursor enriched population was collected and transferred into new non-coated plates and incubated further 2 days at 37°C/5% CO_2. On day 3, cells were detached by flushing using a syringe and needle before they were counted for electroporation. The cell pellet was suspended in 100 µl Mouse Macrophage Nucleofector™ Solution and transferred to a microcentrifuge tube containing siRNA. The cell suspension–DNA mixture was transferred to Amaxa™ electrode cuvettes and electroporated in an Amaxa™ Nucleofector II™ using program Y-001. Following electroporation, cells were immediately transferred to a bijou tube using the Amaxa™ Pasteur pipette and 2.5 ml medium containing 10ng/ml CSF1 and 3 ng/ml RANKL was added. The cell suspension was cooled on ice for 5 min and seeded into 96-well plates at 2×10^5 cells/ cm^2 or onto dentine discs. Cells were incubated at 37°C/5% CO_2 until formation of osteoclasts was observed in control cultures. Media were changed every 2 days. Green fluorescence expression was observed using fluorescence microscopy. For transfection efficiency test, cells were trypsinased and collected for flow cytometry.

2.5.4 Liposome-mediated transient transfection

Bone marrow derived osteoclasts cultures were performed according to a standard protocol in section 2.3.7. Osteoclast precursors were seeded in T 75 flasks and incubated for 24 h at 37°C/5% CO_2 with addition of mouse CSF-1 10 ng/ml to allow stromal cells attachment. On day 2, Cells were seeded on plastic ($5x10^5$ cells/24 well) supplemented with CSF-1, and incubated further 24 h. On day 3, osteoclast precursors were transfected using RNAiMAX with appropriate DNA (pEGFP) or siRNA. medium was changed with CSF-1 (mouse CSF-1 10 ng/ml) and RANKL (mouse 3 ng/ml). During transfection, medium was treated without antibiotics. Lipofectamine reagent was mixed in Opti-MEM medium and incubated for 5 min at RT. Mixtures of DNA (pEGFP vector from Amaxa Cell line Nucleofector kit V) or siRNA and Opti-MEM medium were prepared. Then the lipofectamin mixture and RNA or DNA mixture were combined in 1:1 ratio and incubated for 20 min. This

GFP or siRNA-lipid complex was directly added to cells. Cells were further incubated in medium containing 10ng/ml CSF1 and 3 ng/ml RANKL until appearance of mature osteoclasts and media were changed every 2 days. Green fluorescence expression was analysed under the fluorescence microscopy. For transfection efficiency test, cells were collected by trypsinisation and collected for flow cytometry.

2.5.5 Flow cytometry

Flow cytometry was performed to evaluate transfection efficiency and cell viability using BD FACSCalibur (BD Biosciences, San Jose, USA). Cell viability was assessed using 7-AAD (7-amino-actinomycin D) (eBiosciences, Hatfield, UK) and incubated for 5 min before analysis. Data was analysed using FlowJo ™ software. During the process, technical helps were supported by skilled people (Mrs Iren Mcguinnes).

2.6 Protein Methods

2.6.1 Protein extraction

Protein extraction was carried out either by lysis of cell pellets or direct lysis of cultured cell monolayer. To harvest cells from culture plastic, media was discarded and the cells were washed twice in PBS, scraped from the culture plastic in PBS, transferred into a microcentrifuge tube and centrifuged at 4,000 x *g* for 4 min at 4°C. The supernatant was discarded and the cell pellet was either used immediately or snap frozen on dry ice and stored at -70°C. Chilled urea buffer was added to cell pellets. The volume of urea buffer was variable depending on the amount of cell pellet (30 -100 µl). Monolayers of cells were scraped using urea lysis buffer (50 to 100 µl per well in 24 well plate). The mixture of cells and urea buffer was mixed gently by repeated pipetting and incubated on ice for 15 min. The solution was centrifuged at 10,000 x *g* for 15 min at 4°C. The lysate was either snap frozen on dry ice and stored at -70°C or placed on ice for immediate use.

2.6.2 **Quantification of protein**

Five μl of diluted protein lysates or known bovine serum albumin (BSA) protein standards were mixed with 250 μl of Quick Start™ Bradford Dye Reagent (Bio-Rad) in a 96 well plate. All samples were performed in duplicate and the absorbance at 595 nm was measured on a plate reader (Perkin Elmer 1420 Multilabel Counter Victor 3™) using the Wallac 1420 Manager program (Perkin Elmer). Lysate protein concentrations were determined from a standard curve generated from the known BSA concentrations.

2.6.3 **Western blot**

Protein samples were resolved on SDS-polyacrylamide gels using electrophoresis. Ten percent SDS-polyacrylamide gels were used. The SDS-polyacrylamide gels were prepared using the Bio-Rad Protean II mini-gel system. The resolving gel was prepared (Appendix), poured between the plates and allowed to set at RT. The stacking gel (Appendix) was layered on top of the resolving gel and a loading comb was then inserted into the stacking gel. Once the stacking gel was set, the comb was removed. The gel was placed into the running module and immersed in SDS-PAGE running buffer (Appendix) prior to protein loading. Ten to 30 μg of protein lysates were mixed with 4x SDS sample buffer (Appendix). The mixtures were denatured in 95°C for 3 min and then loaded into the wells in the stacking gel. Five μl of a pre-stained Full Range Rainbow Marker (Amersham Pharmacia Biotech) was placed in parallel to indicate protein bands by size. The gel electrophoresis was performed at 180 V until the dye reached the bottom of the resolving gel. Then the resolved proteins were electrophoretically transferred onto nitrocellulose membranes (Hybond™-C, Amersham Biosciences, UK) in transfer buffer (Appendix) at 300 mA for 1 h using an ice block to reduce heat during electrophoresis. The nitrocellulose membrane was incubated in 5% milk in PBST (appendix) for 1 h at RT to reduce non-specific antibody binding. The membranes were subsequently probed with primary antibodies overnight at 4°C. Following primary antibody incubation, the membranes were washed three times in PBST for

5 min. Then the membranes were incubated for 1 h at RT with a secondary horseradish peroxidase (HRP) conjugated antibody diluted 1:1000 in blocking solution. All primary and secondary antibodies used in this study are listed in Appendix. The membranes were washed three times in PBST for 15 min. The membranes were developed using ECLTM Western Blotting Detection Kit (Amersham Bioscience) and protein bands visualised by exposure to X-ray film (Hybond™-ECL™ Film, Amersham Biosciences). For the further application of different antibodies, the membranes were stripped at RT for 15 min using Restore™ Plus Western Blot Stripping Buffer (Thermo Fisher Scientific). The membranes were re-developed to ensure the bands had been removed then blocked and probed as previously described.

2.7 Immunohistochemistry

2.7.1 Tissue processing and paraffin embedding

Feline tooth samples were collected post mortem as described in section 2.2.1 and samples were fixed by immersion in 10% neutral buffered formalin for 48 h before being processed. All fixed teeth were demineralised in EDTA pH 7.0 for 4 to 6 weeks at RT. Demineralised samples were dehydrated in a series of ascending alcohol dehydration steps including washing with xylene and infiltrated by immersion in liquid paraffin wax. From the paraffin tooth block, eight micron sections were cut, mounted onto electrostatically charged slides (Superfrost plus, Thermo Fisher Scientific), dried overnight at 60°C and stored in RT until use.

2.7.2 Haematoxylin and Eosin (H&E) staining

Paraffin sections were dewaxed rehydrated and stained using an autostainer machine (Leica Autostainer XL) according to its programmed protocol in Table 2.4.

2.7.3 Immunohistochemistry and antibodies

Sections were prepared as described above (section 2.7.1). Antigen retrieval was performed in 0.1M citrate buffer pH 6.0 for 90 min at 70°C. Endogenous peroxidase was blocked using 1% hydrogen peroxidase in methanol for 30 min at

RT. A further blocking was carried out using a normal goat serum 1:5 in 5% of FBS for 30 min. Primary antibodies were diluted at 1:50 to 1:200 dilution (Table 2.5) in 5% FBS/PBS and incubated at 4°C overnight. Sections were washed and horseradish appropriately diluted peroxidase labelled secondary antibodies (Envision Kit, Dako UK Ltd.) were added to the sections (Table 2.6) and incubated for 1 h at RT. Sections were washed 3 times with PBS for 5 min. Labelling was developed using ImmPACT™ DAB (Vector Labs Ltd., UK) at RT for 10 min producing a brown colour in positive sections. All samples were count-stained with haematoxylin prior to dehydrating, clearing and mounting under PERTEX Mounting Media (CellPath, UK).

Processing Stage	Reagent	Time
Dewax	Xylene	3 times for 5 min
Rehydration	100% ethanol	3 min
	100% ethanol	2 min
	95% ethanol	2 min
Wash	H_2O	5 min
Haematoxylin	Haematoxylin	3 min
Wash	H_2O	3 times for 3 min
Eosin	Eosin	2 min
Wash	H_2O	45 s
Dehydration	75%, 95%, 95% ethanol	Each 30 s
	100% ethanol	2 times for 1 min
Wash	Xylene	3 times for 1 min

Table 2.4 Tissue processing.

2.7.4 Cytokeratin immunolabelling

To distinguish osteoclasts from epithelial cells, decalcified feline teeth slides were presented into Easter Bush Pathology laboratory for cytokeratin immunohistochemistry. The brief protocol follows; antigen retrieve was performed using proteinase K ready to use from Agilent for 30 min at RT. The monoclonal Pan

cytokeratin (Agilent, MNF116) was diluted 1 in 50 and incubated for 30 min at RT. Secondary antibody(Envision anti-mouse HRP, Agilent) was applied for 40 min at RT and labelling was developed by DAB for 10 min at RT.

Primary Antibody	**Host**	**Manufacturer**	**Dilution**
MMP9	Rabbit Polyclonal	Abnova, PAB12714	1: 50, 100, 200
SPI.1	Rabbit EPR3158Y Monoclonal	Abcam, AB76543	1:50, 100, 200
P2XR4	Goat Polyclonal	Abcam, AB134559	1: 100, 200, 400
CTSK	Mouse IgG2a Monoclonal	Abcam, AB66237	1: 50, 100, 200
OPG	Mouse IgG1 kappa Monoclonal	OPG (E-10): sc-390518. Santa Cruz Biotechnology, Inc.	1: 100, 200
RANKL	Rabbit	ProSci, XP-5273Bt	1: 50, 100
RANK	Mouse IgG1 kappa Monoclonal	RANK (H-7): sc-374360. Santa Cruz Biotechnology, Inc.	1: 50, 100
Isotype		**Manufacturer**	
Rabbit IgG	-	Sigma-Aldrich, SAB5500149	#
Goat IgG	-	Biorad, 5160-2104	#
Mouse IgG	-	Abcam, ab37355	#

Table 2.5 List of primary antibodies and isotypes for immunohistochemistry. #: Corresponding concentration to primary antibody.

Secondary Antibody	Host	Manufacturer	Dilution
Anti-rabbit immunoglobulins	Goat	Peroxidase-Conjugated Goat Anti-Rabbit Immunoglobulins, Dako, P0448	1:100
Anti-mouse immunoglobulins	Rabbit	Peroxidase-Conjugated Rabbit Anti-Mouse Immunoglobulins, Dako	1:200
Anti-goat immunoglobulins	Rabbit	Peroxidase-Conjugated Rabbit Anti-Goat Immunoglobulins, Dako	1:200 – 1:500

Table 2.6 List of secondary antibodies for immunohistochemistry.

2.8 Statistical analysis

All experiments were repeated at least twice on two separate occasions gaining similar results (except RNA-seq). All quantitative analysis included triple to five technical replicates. *In vitro* experiment and qPCR data were analysed using Minitab® 15 Statistical Software (Minitab Ltd., UK) and all graphs and diagrams were generated using Microsoft Office® 2013 (Microsoft Corporation) or GraphPad prism v5 software. *P* values of less than 0.05 were deemed statistically significant. Data following a normal distribution was analysed with parametric tests, however if data are not normally distributed then non-parametric tests were performed. One-way ANOVA tests were used to compare differences between more than two groups. The two sample t-test or Mann Whitney U-tests were used to compare differences between two groups.

Chapter 3 Optimisation of RNA isolation method suitable for gene expression study and RNA sequencing in feline tooth

3.1 Introduction and aims

The main interest of this study was to identify transcriptome changes during feline tooth resorption. To do this, I used RNA-seq technique on RNA extracted from feline teeth. RNA-seq is a widely available technique for the quantification of transcriptomes as well as for the identification of genetic variations (e.g. SNPs) (208, 211). In order to obtain reliable data, very high quality of RNA as well as sufficient amounts of RNA are essential (231-233). There are several published RNA isolation protocols available but vary according to study design and mainly describe the extraction of RNA from soft tissues (215, 234-237). To the best of my knowledge, a RNA-seq study using feline teeth has not been published and therefore an optimised protocol for feline tooth RNA extraction does not exist. As clinical archived dental samples derived from animals are a valuable resource, there is a necessity to maximise utility of such samples. Mineralised tissues are notoriously difficult to obtain good quality RNA due to the added complication of extracting tissue itself from the whole bone or tooth (238). This makes slow permeabilisation of protein denaturants or RNAse retarding solutions which minimise the effects of RNAses during cell lysis (239). Therefore prior to performing RNA-seq from feline teeth, I developed a RNA extraction methodology that was capable of extracting RNA of RNA-seq quality from feline tooth samples.

This chapter describes the development of an optimised RNA extraction protocol suitable for use on mineralised tissues to produce RNA of a high quality, and how to test the RNA to ensure that it was of a quality suitable for RNA-seq.

The following manuscript was submitted to Veterinary Research Communications on 08/01/2018. The inclusion of this manuscript as part of this thesis does not cause any potential conflict with Springer editorial policies. In this

study, all work was performed by myself except individual contributions as specified: (i) Sample collection from cats and dogs, and subsequent RNA extractions were performed by myself with the help of Craig Johnson. (ii) RNA sequencing and quality control for RNA-seq were performed by Dr Urmi Trivedi at Edinburgh Genomics. (iii) The manuscript authors advised on the paper design and wording.

3.2 Submitted manuscript

The following manuscript was submitted to Veterinary Research Communications on 08/01/2018.

This submitted manuscript is included as a part of this thesis as described in 'GUIDANCE FOR THE INCLUSION OF PUBLICATIONS IN POSTGRADUATE RESEARCH THESES' (1.7. Articles which have been submitted for publication but not yet accepted may be included as the submitted format.).

Optimised isolation method for RNA extraction suitable for RNA sequencing from feline teeth collected in a clinical setting and at post mortem

Authors:

Lee, S. [1], Trivedi, U. [2], Johnson, C. [3], Farquharson, C. [1], Bergkvist, G.T. [1]

Affiliations and addresses:

1. The Royal (Dick) School of Veterinary Studies and The Roslin Institute, The University of Edinburgh Easter Bush Campus, Midlothian, EH25 9RG, UK

2. Edinburgh Genomics, The University of Edinburgh, Charlotte Auerbach Road, Edinburgh, EH9 3FL, UK

3. Centre for Applied Anatomy, University of Bristol, Southwell Street, Bristol, BS2 8EJ, UK

Corresponding Author: Lee, S.

Email Address:

seungmee.lee@ed.ac.uk

Abstract

Advanced next generation sequencing approaches have started to reveal the cellular and molecular complexity of the microenvironment in many tissues. It is challenging to obtain high quality RNA in mineralised tissues. We developed an optimised method of RNA extraction from feline teeth collected in a clinical setting and at post mortem. Teeth were homogenised in phenol-guanidinium solution at near-freezing temperatures and followed by solid-phase nucleic acid extraction utilising a commercially available kit. This method produced good RNA yields and improved RNA quality based on RNA integrity numbers equivalent (RIN^e) from an average of 3.6 to 5.6. No correlation was found between RNA purity parameters measured by $A_{260:280}$ or $A_{230:260}$ ratios and degree of RNA degradation. This implies that RNA purity indicators cannot be reliably used as parameters of RNA integrity. The stability of reference gene expression varied depending on reference genes used rather than degree of RNA degradation. Furthermore, we investigated effect of quantity and quality of RNA on RNA sequencing (RNA-Seq) results. Thirteen RNA-seq data showed similar duplication and mapping rates (94 to 95%) against the feline genome regardless of RIN^e values. However one low yield sample with a high RIN^e value showed a high duplication rate and was an outlier on the RNA-seq multidimensional scaling plot. We conclude that overall yield of RNA was more important than quality of RNA for RNA-seq quality control. These results guide others who wish to perform RNA extractions from mineralised tissues, especially if collecting in a clinical setting with the restraints that impose.

Introduction

Teeth consist of connective tissues and highly specialised cells that produce a unique extracellular matrix composed of organic matrix proteins and inorganic minerals. Tooth development and alveolar bone and deciduous teeth resorption during tooth eruption and shedding is a complex process that is tightly regulated at the molecular level (Ten Cate and Nanci, 2003, Bei, 2009). In permanent teeth, mineralised tissues such as enamel, cementum and dentine do not turn over or have limited regeneration capacities. The hard tissues of the tooth can be resorbed and structurally damaged under pathologic conditions such as inflammation, mechanical trauma or idiopathic tooth resorption (TR) (Darcey and Qualtrough, 2013). The exact mechanisms behind the pathological resorption observed in idiopathic TR are still unclear. Gene expression profiling of dental samples is of great interest to help map physiological pathways as well as dissect out the pathways involved in pathological conditions at the cellular and molecular level. Recent studies of the oral and dental transcriptome have started to unveil the molecular complexity of the dental microenvironment (Simmer et al., 2014, Hu et al., 2015). Whilst *in vitro* studies are fundamental to the study of these cellular and molecular events and genetically engineered rodents have been important models in dentistry, there is a necessity to utilize human or companion animal derived tissues from clinical archives. Since both ethical and logistical considerations can limit the sourcing of human and companion animal derived tissues from clinics, it is important to maximize utility of collected tissue samples for research purposes.

As high-throughput sequencing techniques are used more frequently and the cost of such studies is continuing to decrease, it is likely that more clinical veterinary studies will be able to utilise these evolving and cutting-edge approaches. Advanced high-throughput systems especially next generation sequencing, require high quality of RNA. However, in some cases it can be hard to avoid RNA degradation during sampling. For example, due to the practical limitations samples may be stored at suboptimal conditions for a period of time. Certain tissue types, in particular mineralised tissues, are difficult to homogenise. In addition, the collection procedure itself may accelerate RNA degradation, for example heat generated by a dental bur during tooth extraction can be detrimental to RNA quality.

Routinely total RNA yield, purity and integrity is evaluated for RNA quality control. The most rapid and commonly used method for quantification of nucleic acids is to measure ultraviolet (UV) absorption of RNA sample using a spectrophotometer (Manchester, 1996, Desjardins and Conklin, 2010). One commonly applied metrics for assessment of RNA purity is to calculate the ratio of absorbance at 260 and 280 nm (the $A_{260:280}$ ratio) and at 260 and 230 nm (the $A_{260:230}$ ratio). The development of microfluidic capillary electrophoresis has allowed the assessment of RNA quality

with low volumes of sample (1 µl) through direct trace observation and automated calculation of the 28S:18S ratio (Schroeder et al., 2006). Currently the RNA Integrity Number (RIN) algorithm is the industry standard for RNA quality assessment.

Degradation of RNA might be a minor problem in hybridization-based microarray, in which each expressed gene is measured by a few short and distinct probes. One microarray study reported that only a small portion of probes (0.67%, 275/ 41,000) were significantly affected by RNA degradation and biological differences far outweighed RNA degradation (Opitz et al., 2010). In recent years, sequencing based platforms like RNA-seq have been extensively applied, in which RNA degradation can be more problematic as degraded RNA can distort yield of sequencing reads which represents abundance of transcripts. Thus RNA degradation could be a major source of variation when measuring gene expression using RNA-seq data (Wang et al., 2016). There is still an ongoing controversy as to what extent gene expression results are affected by various degrees of RNA degradation in order to decide which partially degraded samples to include in an analysis, but for some tissues, in particular mineralised tissues, it can be difficult to obtain high quality RNA with the conventional phenol- chloroform protocols or commercial kits. Several protocols have been suggested to improve RNA quality including preserving samples in liquid nitrogen (Carter et al., 2012). The purpose of this study was to develop an improved protocol for processing samples and extracting RNA from hard tissues collected in a clinical setting with the limitations that entailed. Here we evaluate the quantity and quality of RNA extracted from feline tissues focusing on teeth from TR free or TR affected cats for next generation sequencing. We also assessed the impact of RNA degradation on reference gene expression by quantitative PCR and the quality of the RNA sequencing data.

Material and methods

Sample collection and tissue processing

Teeth were collected from patients with full owner's consent presented to the Hospital for Small Animals, The Royal (Dick) School of Veterinary Studies, The University of Edinburgh, UK. TR was diagnosed by the combination of oral examination and intraoral dental radiography (Heaton et al., 2004). The TR affected teeth were extracted by a veterinary surgeon using standard dental equipment under full general anaesthesia (Reiter and Soltero-Rivera, 2014). Further research samples including teeth, maxilla, mandibles and various soft tissues were collected at post mortem from cats and dogs euthanized for a wide range of medical reasons and donated to the school for research. The clinical samples underwent one of the following processes: A) immediately stored in RNA*later*® solution (Thermo Fisher Scientific) (Figure 1, Step 1. A) at room temperature or B) snap

frozen in liquid nitrogen before storage at -80°C (Figure 1, Step 1. B). Post mortem samples consisting of mandibles or maxillae were snap frozen in liquid nitrogen before storage at -80°C until further investigation (Figure 1, Step 1. C). Bones and other soft tissues were trimmed into small pieces, snap frozen in liquid nitrogen and stored at -80°C until RNA extraction (Figure 1, Step 1. D). Teeth were collected as part of a study into TR in cats, so all teeth samples were phenotyped for their TR status. To phenotype TR status in research samples collected at post mortem, frozen jaws were delivered to the radiographic facility in a liquid nitrogen carrier, radiographed, and then immediately put back into the liquid nitrogen. In order to extract the teeth from the frozen jaws, a standard dental extraction technique using dental equipment was used (Reiter and Soltero-Rivera, 2014). However, RNA extracted using this technique was badly degraded (average RIN^e = 4.0), which might have been caused by the heat produced by the dental burs during tooth extractions from the frozen samples. An alternative method was therefore developed where teeth were extracted from the alveolar sockets of the jaws using bone cutters and forceps while maintaining cold temperatures by working over dry ice (Figure 1, Step 1. C).

RNA extraction

Two different RNA isolation protocols were compared. TRIzol reagent is a commonly used solution for soft tissues based on a guanidinium thiocyanate-phenol-chloroform extraction method (Chomczynski and Sacchi, 1987). Protocol 1 was a modified version of the manufacturer's protocol (TRIzol® reagent, Thermo Fisher Scientific, Figure 1, Step 2). In brief, frozen tissues were placed in a beaded tube (Lysing Matrix D tubes, Fisher) with TRIzol® reagent (1 ml/100 mg of tissue). The sample tube was placed in the FastPrep FP120 (Thermo Savant) to agitate at a speed of 4 m/s for 20 s. Each tube was incubated at room temperature for 5 min before adding 0.2 ml of 1-bromo-3-chloropropane (BCP B9673, Sigma). After vigorously shaking the tube by hand for 15 s, the tube was left to stand at room temperature for 3 min. For phase separation, samples were centrifuged at 12,000 rpm for 15 min at room temperature and the upper aqueous layer was transferred to a new tube. An equal volume of isopropyl alcohol was added and incubated for 10 min on ice. To precipitate the RNA, the tube was centrifuged for 30 min at 12,000 rpm at room temperature. Supernatant was removed and the RNA pellet was washed with 1 ml of 75% ethanol. The sample was briefly vortexed and centrifuged for 30 min at room temperature at 12,000 rpm. The supernatant was removed and the RNA pellet was air-dried for 5 to 10 min before RNA was re-suspended in RNase free water.

Protocol 2 was modified from a previous study (Reno et al., 1997) and optimised for cartilage and tendon in our lab (Clements et al., 2006) (Figure 1, Step 2). To facilitate disruption and pulverisation of hard tissues, we used a grinding machine consisting of a stainless steel jar and ball (Mixer Mill

MM200, Retsch, Germany). The grinding jar and ball were submerged in liquid nitrogen for a few minutes before use to keep the sample frozen during homogenisation. TRIzol reagent (0.5 ml/100 mg of tissue) was added to the pre-chilled jar and allowed to freeze. Frozen tissue and the pre-chilled ball were placed into the jar and the lid firmly closed. The Mixer Mill MM200 was set at 30 Hz for 2 min to perform radial oscillations in a horizontal position. The pulverized tissue was transferred to a pre-chilled centrifuge tube containing TRIzol® reagent (0.5 ml/100 mg of tissue). After a brief mix, the mixture was left to stand for 30 min before being centrifuged at 12,000 rpm for 10 min at 4°C. The supernatant was transferred into a clean tube and 200 µl of chloroform was added, mixed and left to stand at room temperature for 10 min. A further centrifugation step of 15 min at 12,000 rpm at 4°C was performed and the clear supernatant was transferred into a clean tube. An equal volume of 70% ethanol was added to each tube and mixed by pipetting. RNA was washed and DNase digestion was performed according to the manufacturer's instruction (RNeasy Mini Kit, Qiagen). RNA was eluted with 30 to 50 µl of RNase free water, and stored at - 80°C.

Measurement of RNA yields, purity and integrity

RNA yield was measured based on absorbance at 260 nm, and the $A_{260:280}$ and the $A_{260:230}$ ratios were used to assess the purity of RNA using NanoDrop™ 1000 Spectrophotometer (Thermo Fisher Scientific Inc.). The RNA Integrity Number equivalent (RIN^e) was determined by RNA analysis ScreenTape kit on Agilent 2200 TapeStation. RIN^e is a comparable value to RIN generated by industry standard 2100 Bioanalyzer system for quality assessment of RNA on a microcapillary electrophoretic RNA separation platform (Schroeder et al., 2006). The software produces a separate RNA integrity number, the correlating electropherogram, and a gel image for each sample.

Reference gene expression by qPCR and RNA integrity

To investigate the suitability of including the feline tooth RNA samples in our gene expression study, RNA samples were divided into three categories based on RIN^e values (High ≥ 6, 5 < Moderate < 6, and Low ≤ 5) and quantitative real time RT PCR was performed for each sample. In brief, 400 ng of RNA was reversed transcribed using Omniscript® Reverse transcription (Qiagen) with random primers at 37°C for 1 h according to the manufacturer's instructions. Real-time PCR was performed with high affinity, double stranded DNA-binding dye SYBR green (Takyon™ qPCR MasterMixes for SYBR® assays, Eurogentec) using Stratagene MX3000P qPCR system (Agilent Technologies). The sets of reference gene primers were selected from previously validated feline reference genes (Penning et al., 2007) under universal cycling conditions including pre-incubation at 50°C for 2 min and 95°C for 3 min, 40 cycles of amplification at 95°C for 10 s, 60°C for 20 s and 72°C for 30 s, and followed by data analysis at 95°C for 1 min, 60°C for 15 s and 95°C for 15 s. All samples were performed in

triplicate and cycling threshold (Ct) values of reference genes were generated to compare gene expression level of each RIN^{e} category.

Generation of cDNA libraries and RNA sequencing

Tested RNA samples were sent to our academic facility (Edinburgh Genomics, The University of Edinburgh, UK) for cDNA libraries and RNA sequencing. Briefly, one microgram of RNA from each of the thirteen samples and 0.8 µg of RNA from one low quantity sample were used to generate fourteen cDNA libraries using the Illumina TruSeq stranded mRNA sample preparation kit according to the manufacturer's instructions (Illumina, San Diego, CA, USA). Paired-end sequencing was performed using the Hiseq 4000 system (Illumina). The low quality reads were filtered by Phred quality score (Q score 30) (Ewing and Green, 1998) and 3' adapter were trimmed with cutadapt (version 1.8.3)(Martin, 2011) . All the raw reads have been submitted to the European Nucleotide Archive (ENA) under accession PRJEB24183 (ENA, https://www.ebi.ac.uk/ena).

Mapping to reference genome, generation of mapping statistics, and generation of Multidimensional scaling (MDS)

Annotation and alignment were performed using STAR (version 2.5) comparison to the *Felis catus* genome (version 6.2) in the Ensembl database (Hubbard et al., 2002). Alignment files were generated in the bam format for each sample. The read counts from each sample were generated using HTSeq (version 0.6.0.1) (Anders et al., 2015) with mode 'union'. Reads were mapped to Felis_catus_6.2 using STAR (version 2.5). Duplicate reads were found using picard tools (version 1.141). Generation of MDS plot were generated using plotMDS function from edgeR package (version 3.12.1) to visualise the level of similarity of individual cases of a dataset.

Statistical analysis for RIN^{e} values and reference gene expression by qPCR

Statistical data were analysed using Minitab® 17 Statistical Software (Minitab Ltd., UK). P values below 0.05 were considered statistically significant and specific P values were noted. When data followed a normal distribution, parametric tests were performed. If parametric tests could not be applied, non-parametric testing was performed. One-way ANOVA was used to compare differences between more than two treatment groups. Two sample t-tests or Mann Whitney U-tests were used to compare differences between two groups. Correlations between two groups were assessed using Pearson's correlation coefficient.

Result

Good RNA yields were obtained from tooth samples regardless of homogenisation step used

Obtaining a good yield of RNA from dental tissues is a challenge because individual teeth are relatively small and acellular compared to soft tissues. The wet weight of teeth varied widely and ranged from 10 to 500 mg depending on the type of tooth (incisors, molars, canines or premolars vary greatly in size) or to which extent the teeth were affected by TR. In this study, the protocols described produced good yields of total RNA regardless of the homogenisation step used. Samples between 100 - 500 mg of wet weight produced 2.0 to 12 µg of total RNA which was higher than the minimum requirement of quantity control for next generation sequencing. However, small teeth and some clinical samples weighing less than 50 mg produced low yields of RNA with total RNA less than 1.0 µg (50 to 60 ng/µL). These samples failed to reach the minimum yield of total RNA required (1.2 to 2.2 µg of total RNA) for assessment of RNA quality for standard RNA-seq (Genomics, 2017).

Tissue processing at collection significantly impacted RNA integrity

The tissue processing procedures were performed according to four different tissue processing protocols depending on the type of tissue and source of samples (Figure 1, Step 1. A, B, C, and D). Teeth preserved in RNA*later*® solution (Protocol A) obtained the lowest RIN^e values with high variations (3.04 ± 1.8) indicating highly degraded RNA (Figure 2). A representative electrogram is shown in Figure 2 and shows how the two distinct peaks of 28S and 18S had disappeared and combined into one peak (Figure 2, top right panel). Tissue processing protocols B, C and D showed improved RIN^e values (Figure 2) but still with partially degraded RNA. Partial degradation of RNA can be seen as several extra small peaks left of the 18S peak (Figure 2, bottom right panel). The main difference between protocol A and the other three protocols was the method of tissue storage and RNA stabilisation following collection. While protocol A used RNA*later*® solution for RNA stabilisation at room temperature, in the other protocols the tissues were immediately snap frozen in liquid nitrogen.

The homogenisation steps and tissue type had a significant impact on RNA integrity

One of the critical time points when significant RNA degradation can occur is at the time of tissue homogenisation**.** Protocol 1 (Figure 1, Step 2, homogenisation at room temperature using beaded tubes) resulted in incomplete homogenisation of the mineralised samples. This indicated that the procedure in Protocol 1 was insufficient for these highly mineralised tissues. When Protocol 2 (Figure 1, Step 2) was applied, teeth were pulverized in cold TRIzol® reagent. RIN^e values were improved when Protocol 2 was used for cat teeth. In parallel, we also extracted RNA from dog teeth and we

also obtained improved results with Protocol 2 for these tooth samples (Table 1). There were two reasons why we wanted to test dog tissues. One was due to the greater availability of dogs' teeth available to test our protocols, and secondly to test if these protocols were applicable for dog's teeth as well. Dog's teeth are bigger and harder than cat's teeth, and testing these teeth ensured a larger application of our protocol for other animals including humans and large animals.

To compare the different homogenisation steps on different tissue types, teeth and soft tissues from dogs were used. Regardless of protocol used, RNA from soft tissues consistently achieved higher RIN^e values (Table 2), suggesting that the less vigorous homogenisation step using beads was sufficient to prevent significant RNA degradation when processing soft tissues. RNA from cat soft tissues such as muscle, liver, intestine and gingiva extracted using Protocol 2 also showed improved RIN^e values (average 6.9) when compared to RNA obtained from hard tissues such as bone and teeth (average 4.9, Table 2). In order to compare across species we processed some dog tissues according to the same protocols; dog soft tissues yielded higher RIN^e values (average 7.1 and 6.6 with Protocol 1 and 2 respectively) than those of tooth samples (Average 2.7 and 4.7 in Table 2) demonstrating how the protocols used are a lot less critical when working with soft tissues compared to mineralised tissues.

There was no correlation between RNA purity parameters and RNA integrity values.

To investigate if there is a correlation between RNA purity and integrity, extracted RNA samples from clinical samples collected according to protocol B (snap frozen in liquid nitrogen) and post mortem samples collected according to protocol C (snap frozen within the jaw) were categorised into High, Moderate, and Low RIN^e groups according to their RIN^e values. Five RNA samples from each category were chosen and shown that there was statistically difference of average RIN^e values among the groups (Figure 3, B). All samples in the high RIN^e group presented on the gel images and electropherograms with characteristics typical of intact RNA: tall 28S ribosome peaks double the height of the 18S peak, short 18S ribosome peaks and with only a few small peaks of small RNAs and minor signs of degraded RNA. The moderate RIN^e group showed partially degraded ribosome peaks with moderate height of 28S peaks and with extra peaks observed below the 18S peak. In the low RIN^e group, 28S peaks were shorter than the 18S peaks and there were several background peaks present. We then compared the $A_{260:280}$ ratios between the three groups using Spearman's correlation coefficient. There was no statistically significant difference between any two groups which suggests the $A_{260:280}$ ratio does not correlate with or represent RNA integrity ($P = 0.781$, Spearman's correlation coefficient). Similar patterns were observed when the $A_{260:230}$ ratio was used (Figure 3, Table 3), and no correlation was observed between the ratio and the RIN^e values ($P = 0.197$, Spearman's correlation coefficient).

RNA degradation levels had an impact on reference genes expression by qPCR

To investigate the impact of RNA degradation on gene expression levels, the three groups were tested for expression of three reference genes, glyceraldehyde-3-phosphatedehydrogenase (GAPDH), ribosomal protein S17 (RLP17) and ribosomal protein S19 (RPS19) using quantitative PCR (qPCR). qPCR was performed using the same amount of synthesized cDNA from each RNA sample and cycling threshold (Ct) values for each reference gene were generated. There was no significant difference in the expression of GAPDH between high and moderate RIN^e groups, however the low RIN^e group revealed significantly higher Ct values indicating low expression of GAPDH (Figure 4). For RPS19 the Ct values were significantly different between the high and the moderate RIN^e groups (Figure 4). As high Ct value indicates lower expression of gene, degraded RNA correlated with a lower expression of reference genes. Whereas expression of GAPDH and RPS19 in this study was affected by RNA degradation, expression of RLP17 was less affected by the level of RNA degradation.

Low yield affects quality of RNA-seq data regardless of RNA integrity

Fourteen RNA samples from TR free (7 samples collected at post mortem according to Protocol C) and TR affected teeth (4 samples collected at post mortem according to Protocol C and 3 clinical samples collected as described in Protocol B) were chosen from the feline tooth resorption study. The quality of cDNA libraries and sequencing was measured by percentage of duplicated reads and mapped reads (Table 4) (Supplementary Table S1). As cDNA library complexity is determined by duplication rate, high duplication rate is often caused by degraded and fragmented RNA. Interestingly one sample that yielded low quantity of RNA but achieved a high RIN^e value (RIN^e = 7.3) showed much higher duplication rate than any of the other samples. After annotation to *Felis catus* genome, sequencing reads of all libraries except for the one library with the low input RNA mapped to 94 to 95 % of the feline genome. The low quantity RNA sample with a high RIN^e value only mapped 87.53 % of reads to the feline genome. RNA-seq data from each sample as genome wide expression were plotted to investigate similarity of whole genome expression profile within the given samples (Figure 5). Interestingly the low yielding RNA sample with a high RIN (Supplementary Table S1) was defined as an outlier from the other samples which might have been caused by the low expression of genes and low quality of the cDNA library due to low yield of RNA rather than quality of RNA (Figure 5).

Discussion

Selection of a high quality and quantity of RNA is important for downstream gene expression studies using next generation sequencing. The first challenge of extracting RNA from certain types of clinical samples, in this example dental tissues, is to obtain a good yield of RNA from potentially small

quantities of tissue. The wet weights of intact adult teeth range from 100 to 200 mg for mandibular premolars, 400 to 550 mg for canines, and 10 to 40 mg for incisors. The carnassial tooth (the third molar in the maxillary arcades and the first molar in mandibular arcades) were often less than 500 mg. Like other mineralised tissues, dental tissues are relatively acellular compared to soft tissues as they contain a large amount of hydroxyapatite and collagen (Ten Cate and Nanci, 2003). In cases of clinical samples, only small quantities are available due to loss of tissues during TR progression or treatment of TR such as partial crown amputation in case of type 2 TR (Reiter and Soltero-Rivera, 2014). Furthermore, TR affected tissues undergo apoptotic processes and stimulate inflammation which can lead to extensive loss of tissues (DuPont and DeBowes, 2002, Booij-Vrieling et al., 2010). Here we compared tissue processing and RNA isolation protocols to maximise the yield of RNA and improve the quality of the RNA obtained from feline teeth. In our study, the average yield of RNA from feline tooth samples with a wet weight of less than 50 mg was below 1.0 µg of total RNA. This quantity of RNA limits the application for expression studies. For example, in many gene expression studies (DeLaurier et al., 2002, Kessler et al., 2009, Gunter et al., 2013), an input of 0.5 to 2 µg of RNA for reverse transcription was used. Microarray or RNA sequencing studies require a relatively low amount of RNA due to its high sensitivity. For instance, for cDNA library using the TruSeq stranded mRNA kit, according to the manufacturer's protocol 100 ng of RNA can be used as a minimum input. However, practically larger quantities of RNA are required in order to be able to assess the quality and quantity of RNA (e.g. the minimum required by our facility, Edinburgh Genomics is 1.2 µg: 0.2 µg for quality control and 1 µg for library preparation). Therefore the total recommended amount of RNA is 2.2 µg to allow for two attempts at library preparation. In this study, we used 0.8 – 1 µg of total RNA. As tooth samples with wet weights of 100 to 500 mg yielded more than 1.0 µg of total RNA, we would recommend that gene expression or sequencing studies aim for at least 100 mg of wet weight as a minimum tooth sample size.

Different tissue processing methods were compared based on the RNA quality obtained. As endogenous ribonucleases (RNAse) are widely present in tissues, RNA in collected tissues can be rapidly degraded. To minimize RNA degradation in the tissue samples, they are firstly required to be frozen by immersion in liquid nitrogen immediately upon collection and secondly to be homogenized by a powerful protein denaturant (chaotropic agent usually guanidinium isothiocyanate). RNAlater® is a commonly used RNA stabilization solution because of the convenience of storage at room temperature. Liquid nitrogen or dry ice is often not readily available if collecting clinical samples from most veterinary practices. When tooth samples were extracted and stored in RNAlater®, the extracted RNA was highly degraded. This was likely to be due to poor permeability of RNAlater® into the hard tissues like teeth. In order to achieve effective preservation of tissue using this reagent,

tissues need to be dissected into small pieces to allow adequate diffusion of the chemical into the tissues (Lader, 2012). Other studies have also mentioned the limited application of RNAlater® in hard tissues (Clements et al., 2006, Carter et al., 2012). Our data showed that snap freezing using liquid nitrogen improved RNA quality. However, the necessity for liquid nitrogen is likely to limit the application of this processing protocol outside of the laboratory environment. In order to collect large number of samples in a clinical setting, the ability to collect and store samples at room temperature would be a great advantage. For example it allows for recruitment of several practices to contribute samples to clinical studies even if they have no access to liquid nitrogen. Our study does however suggest that for soft tissue samples that can be trimmed into small pieces, collection and storage in RNAlater® is likely to be adequate.

In our study, tissue samples that were stored at suboptimal temperatures during phenotyping (assessment of TR status, i.e. became defrosted during the dental radiographic procedure) or were subjected to potentially high temperature during processing (i.e. while extracting the teeth using dental burs at post mortem) also showed marked RNA degradation. By optimising our protocols, we managed to achieve average RIN^e values of between 5 and 6. The average RIN^e value reported in this study is lower than what is reported in other studies using soft tissues. However other studies extracting RNA from mineralised tissues reported similar limitations and showed the same pattern where RNA from hard tissues was more degraded compared to those from soft tissues (Sun et al., 2012, Carter et al., 2012).

We also investigated if there were any correlation between RNA purity as measured by the $A_{260:280}$ and $A_{230:260}$ ratios and RNA integrity as measured by RIN^e values. The $A_{260:280}$ ratios were consistent and similar among all RNA samples regardless of RIN^e value. In terms of $A_{230:260}$ ratio, although these values were more variable between samples with high standard deviation compared to the $A_{260:280}$ ratios, there was no correlation to the RIN^e values of the samples. This implies that these two indicators cannot be reliably used as parameters of RNA integrity or quality.

To investigate the impact of RNA integrity and quality on gene expression, expression of three reference genes was compared. In theory, reference genes are expressed stably across the samples. When equal amount of RNA is reverse-transcribed and analysed by qPCR, the values of Ct of the reference gene is expected to be similar across samples (Conde et al., 2012, Belluoccio et al., 2013, Chapman and Waldenstrom, 2015). Also, it should show minimal variability in its expression. Two reference genes, GAPDH and RPS19 showed different expression levels depending on the degradation of RNA with the high RIN^e value group showing the highest expression with the lowest Ct. Only RLP17 was similar between the three groups. We recognise that reference genes may intrinsically vary between samples or tissues, but these reference genes have been extensively

tested and used in our lab on a range of feline tissues and cell lines and have overall proved the most consistent. The difference in reference gene expression might be affected by the extent of degradation of RNA, but it may also imply that certain genes have a more stable gene expression in a specific type of tissue (Penning et al., 2007).

For further investigation of the impact of RNA quality and quantity on RNA sequencing, we evaluated RNA-seq data related to RNA quantity and quality. We collected 13 RNA samples with RNA yields of more than 1.0 µg of total RNA and one clinical sample with very low yield. Thirteen TruSeq stranded mRNA libraries were generated using 1.0 µg of total RNA, while for the low yielding sample only 0.8 µg of total RNA was used. Although manufacturer tested using low amount of input, (0.1 µg of total human RNA for cDNA library generation was reported), our data revealed that the RNA-seq data from the low input RNA sample was an outlier which skewed the data set of the whole genome expression profiles. It was documented that degraded RNA samples using poly A selection for preparation of cDNA library are likely to cause 3' mapping bias that might have effect on false positives in differential expression and the quantification of duplicate reads (Sigurgeirsson et al., 2014). In our data, duplication rates and percentage of mapped reads were similar across a range of RIN^e values. The cDNA library complexity and duplication profiles were affected by the low input of RNA rather than by RNA integrity. Therefore the low yield of RNA was not suitable for RNA-seq and was excluded in the final data analysis. We concluded that the overall yield of the RNA for input into RNA-seq was more important than quality of RNA for RNA-seq quality control. Recently, there have been technical advances made to allow for low input of RNA or degraded RNA from clinical samples, formalin-fixed paraffin-embedded samples or single cell samples (DeLuca et al., 2012, Adiconis et al., 2013, Gallego Romero et al., 2014, Wu et al., 2014) to be used. Therefore for gene expression study especially high throughput sequencing, RNA extraction protocols, generation of cDNA library, RNA-seq and bioinformatics need to be considered and customised. There is likely there will be further opportunities to overcome these limitations in the future.

The goal of this study was to identify improved protocols for RNA extraction from calcified tissues to maximise its application for gene expression studies using precious clinical samples. Here we optimised a protocol to maximise RNA yield and improve quality extracted from feline teeth in a clinical setting and at post mortem. We suggest that minimum amounts of sample are required for a conventional gene expression study. We identified that it was critical to keep the samples frozen in liquid nitrogen and /or dry ice during the entire tissue processing procedure including during tissue homogenisation. We further investigated parameters commonly utilised to assess RNA purity and integrity and its correlation to gene expression and RNA-seq. Overall the degradation of RNA was inevitable to some extent when extracting RNA from mineralised tissues such as teeth, but with our

optimised protocol we managed to extract RNA with signs of only moderate degradation, and the RNA-seq data from these samples were still worth analysing for the first reported feline sequencing study of molecular pathways of the feline dental environment. Furthermore this detailed protocol should have beneficial applications for RNA processing and analysis in mineralised tissue from many animal species either obtained via the clinic or in a research environment.

Notes

Acknowledgements

This work was supported by the BBSRC and Fiona and Ian Russell Seed Corn Grant Fund. In addition, the PhD studentship of S. Lee was funded by The University of Edinburgh under Edinburgh Global Research Scholarship and The Sym Charitable Trust.

Disclosure of potential conflicts interest

The authors declare that they have no conflict of interest.

References

ADICONIS, X., BORGES-RIVERA, D., SATIJA, R., DELUCA, D. S., BUSBY, M. A., BERLIN, A. M., SIVACHENKO, A., THOMPSON, D. A., WYSOKER, A., FENNELL, T., GNIRKE, A., POCHET, N., REGEV, A. & LEVIN, J. Z. 2013. Comparative analysis of RNA sequencing methods for degraded or low-input samples. *Nat Methods,* 10**,** 623-9.

ANDERS, S., PYL, P. T. & HUBER, W. 2015. HTSeq—a Python framework to work with high-throughput sequencing data. *Bioinformatics,* 31**,** 166-169.

BEI, M. 2009. Molecular genetics of tooth development. *Curr Opin Genet Dev,* 19**,** 504-10.

BELLUOCCIO, D., ROWLEY, L., LITTLE, C. B. & BATEMAN, J. F. 2013. Maintaining mRNA integrity during decalcification of mineralized tissues. *PLoS One,* 8**,** e58154.

BOOIJ-VRIELING, H. E., FERBUS, D., TRYFONIDOU, M. A., RIEMERS, F. M., PENNING, L. C., BERDAL, A., EVERTS, V. & HAZEWINKEL, H. A. 2010. Increased vitamin D-driven signalling and expression of the vitamin D receptor, MSX2, and RANKL in tooth resorption in cats. *Eur J Oral Sci,* 118**,** 39-46.

CARTER, L. E., KILROY, G., GIMBLE, J. M. & FLOYD, Z. E. 2012. An improved method for isolation of RNA from bone. *BMC Biotechnol,* 12**,** 5.

CHAPMAN, J. R. & WALDENSTROM, J. 2015. With Reference to Reference Genes: A Systematic Review of Endogenous Controls in Gene Expression Studies. *PLoS One,* 10**,** e0141853.

CHOMCZYNSKI, P. & SACCHI, N. 1987. Single-step method of RNA isolation by acid guanidinium thiocyanate-phenol-chloroform extraction. *Anal Biochem,* 162**,** 156-9.

CLEMENTS, D. N., VAUGHAN-THOMAS, A., PEANSUKMANEE, S., CARTER, S. D., INNES, J. F., OLLIER, W. E. & CLEGG, P. D. 2006. Assessment of the use of RNA quality metrics for the screening of articular cartilage specimens from clinically normal dogs and dogs with osteoarthritis. *Am J Vet Res,* 67**,** 1438-44.

CONDE, M. C., NEDEL, F., CAMPOS, V. F., SMITH, A. J., NOR, J. E., DEMARCO, F. F. & TARQUINIO, S. B. 2012. Odontoblast RNA stability in different temperature-based protocols for tooth storage. *Int Endod J,* 45**,** 266-72.

DARCEY, J. & QUALTROUGH, A. 2013. Resorption: part 1. Pathology, classification and aetiology. *Br Dent J,* 214**,** 439-51.

DELAURIER, A., ALLEN, S., DEFLANDRE, C., HORTON, M. A. & PRICE, J. S. 2002. Cytokine expression in feline osteoclastic resorptive lesions. *J Comp Pathol,* 127**,** 169-77.

DELUCA, D. S., LEVIN, J. Z., SIVACHENKO, A., FENNELL, T., NAZAIRE, M. D., WILLIAMS, C., REICH, M., WINCKLER, W. & GETZ, G. 2012. RNA-SeQC: RNA-seq metrics for quality control and process optimization. *Bioinformatics,* 28**,** 1530-2.

DESJARDINS, P. & CONKLIN, D. 2010. NanoDrop Microvolume Quantitation of Nucleic Acids. e2565.

DUPONT, G. A. & DEBOWES, L. J. 2002. Comparison of periodontitis and root replacement in cat teeth with resorptive lesions. *J Vet Dent,* 19**,** 71-5.

EWING, B. & GREEN, P. 1998. Base-calling of automated sequencer traces using phred. II. Error probabilities. *Genome Res,* 8**,** 186-94.

GALLEGO ROMERO, I., PAI, A. A., TUNG, J. & GILAD, Y. 2014. RNA-seq: impact of RNA degradation on transcript quantification. *BMC Biol,* 12**,** 42.

GENOMICS, E. 2017. *Sample requirements* [Online]. Available: https://genomics.ed.ac.uk/resources/sample-requirements [Accessed 08 Aug 2017.

GUNTER, H. M., FAN, S., XIONG, F., FRANCHINI, P., FRUCIANO, C. & MEYER, A. 2013. Shaping development through mechanical strain: the transcriptional basis of diet-induced phenotypic plasticity in a cichlid fish. *Mol Ecol,* 22**,** 4516-31.

HEATON, M., WILKINSON, J., GORREL, C. & BUTTERWICK, R. 2004. A rapid screening technique for feline odontoclastic resorptive lesions. *J Small Anim Pract,* 45**,** 598-601.

HU, S., PARKER, J. & WRIGHT, J. T. 2015. Towards unraveling the human tooth transcriptome: the dentome. *PLoS One,* 10**,** e0124801.

HUBBARD, T., BARKER, D., BIRNEY, E., CAMERON, G., CHEN, Y., CLARK, L., COX, T., CUFF, J., CURWEN, V., DOWN, T., DURBIN, R., EYRAS, E., GILBERT, J., HAMMOND, M., HUMINIECKI, L., KASPRZYK, A., LEHVASLAIHO, H., LIJNZAAD, P., MELSOPP, C., MONGIN, E., PETTETT, R., POCOCK, M., POTTER, S., RUST, A., SCHMIDT, E., SEARLE, S., SLATER, G., SMITH, J., SPOONER, W., STABENAU, A., STALKER, J., STUPKA, E., URETA-VIDAL, A., VASTRIK, I. & CLAMP, M. 2002. The Ensembl genome database project. *Nucleic Acids Res,* 30**,** 38-41.

KESSLER, Y., HELFER-HUNGERBUEHLER, A. K., CATTORI, V., MELI, M. L., ZELLWEGER, B., OSSENT, P., RIOND, B., REUSCH, C. E., LUTZ, H. & HOFMANN-LEHMANN, R. 2009. Quantitative TaqMan real-time PCR assays for gene expression normalisation in feline tissues. *BMC Mol Biol,* 10**,** 106.

LADER, E. S. 2012. Methods and reagents for preserving RNA in cell and tissue samples. Google Patents.

MANCHESTER, K. L. 1996. Use of UV methods for measurement of protein and nucleic acid concentrations. *Biotechniques,* 20**,** 968-70.

MARTIN, M. 2011. Cutadapt removes adapter sequences from high-throughput sequencing reads. *2011,* 17.

OPITZ, L., SALINAS-RIESTER, G., GRADE, M., JUNG, K., JO, P., EMONS, G., GHADIMI, B. M., BEISSBARTH, T. & GAEDCKE, J. 2010. Impact of RNA degradation on gene expression profiling. *BMC Med Genomics,* 3**,** 36.

PENNING, L. C., VRIELING, H. E., BRINKHOF, B., RIEMERS, F. M., ROTHUIZEN, J., RUTTEMAN, G. R. & HAZEWINKEL, H. A. W. 2007. A validation of 10 feline reference genes for gene expression measurements in snap-frozen tissues. *Veterinary Immunology and Immunopathology,* 120**,** 212-222.

REITER, A. M. & SOLTERO-RIVERA, M. M. 2014. Applied feline oral anatomy and tooth extraction techniques: an illustrated guide. *J Feline Med Surg,* 16**,** 900-13.

RENO, C., MARCHUK, L., SCIORE, P., FRANK, C. B. & HART, D. A. 1997. Rapid isolation of total RNA from small samples of hypocellular, dense connective tissues. *Biotechniques,* 22**,** 1082-6.

SCHROEDER, A., MUELLER, O., STOCKER, S., SALOWSKY, R., LEIBER, M., GASSMANN, M., LIGHTFOOT, S., MENZEL, W., GRANZOW, M. & RAGG, T. 2006. The RIN: an RNA integrity number for assigning integrity values to RNA measurements. *BMC Mol Biol,* 7**,** 3.

SIGURGEIRSSON, B., EMANUELSSON, O. & LUNDEBERG, J. 2014. Sequencing Degraded RNA Addressed by 3' Tag Counting. *PLOS ONE,* 9**,** e91851.

SIMMER, J. P., RICHARDSON, A. S., WANG, S. K., REID, B. M., BAI, Y., HU, Y. & HU, J. C. 2014. Ameloblast transcriptome changes from secretory to maturation stages. *Connect Tissue Res,* 55 Suppl 1**,** 29-32.

SUN, J. X., HORST, O. V., BUMGARNER, R., LAKELY, B., SOMERMAN, M. J. & ZHANG, H. 2012. Laser capture microdissection enables cellular and molecular studies of tooth root development. *Int J Oral Sci,* 4**,** 7-13.

TEN CATE, A. R. & NANCI, A. 2003. Structure of the Oral Tissues. *In:* NANCI, A. & TEN CATE, A. R. (eds.) *Ten Cate's oral histology : development, structure, and function.* Sixth edition. ed. St. Louis, Mo.: Mosby,.

WANG, L., NIE, J., SICOTTE, H., LI, Y., ECKEL-PASSOW, J. E., DASARI, S., VEDELL, P. T., BARMAN, P., WANG, L., WEINSHIBOUM, R., JEN, J., HUANG, H., KOHLI, M. & KOCHER, J. P. 2016. Measure transcript integrity using RNA-seq data. *BMC Bioinformatics,* 17**,** 58.

WU, A. R., NEFF, N. F., KALISKY, T., DALERBA, P., TREUTLEIN, B., ROTHENBERG, M. E., MBURU, F. M., MANTALAS, G. L., SIM, S., CLARKE, M. F. & QUAKE, S. R. 2014. Quantitative assessment of single-cell RNA-sequencing methods. *Nat Methods,* 11**,** 41-6.

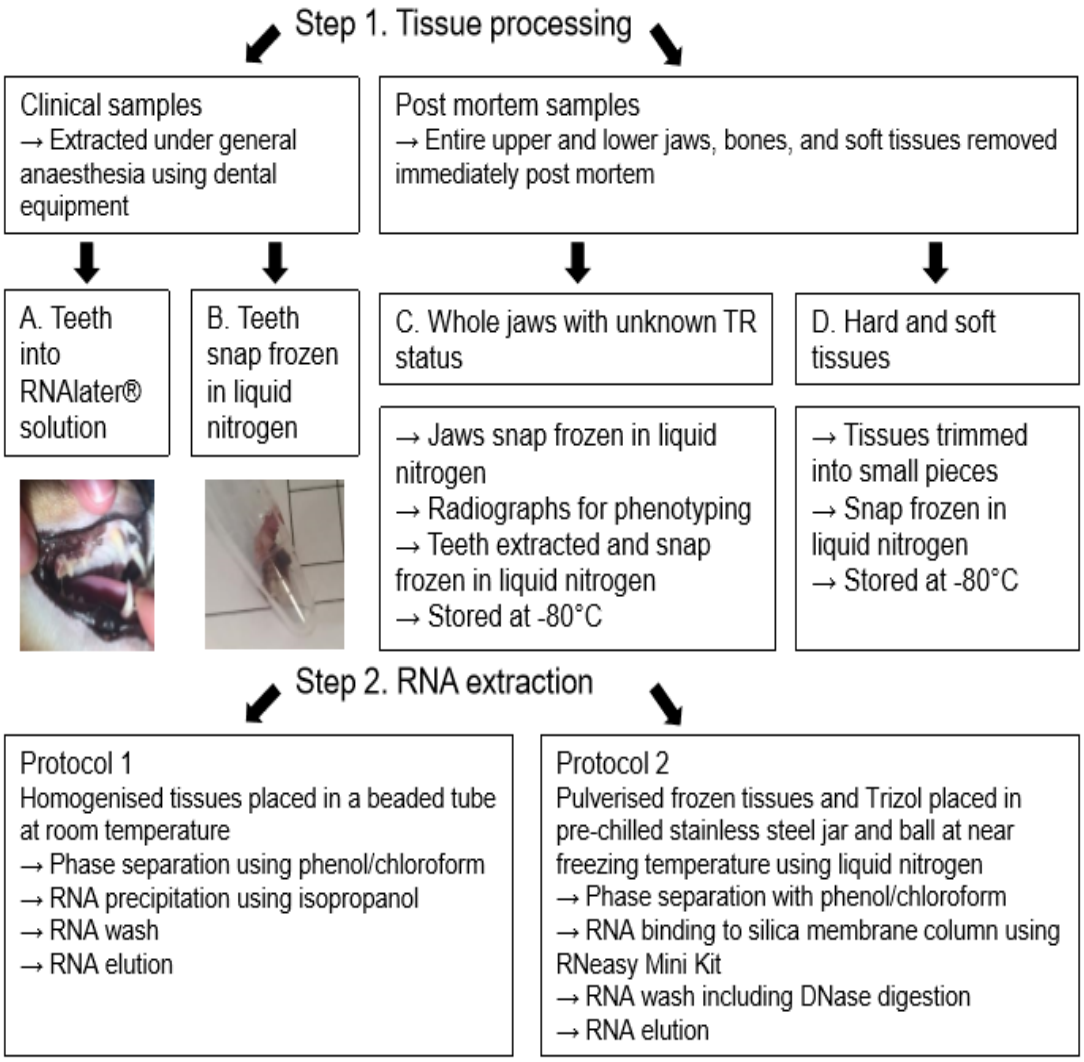

Figure 1. Workflow of tissue processing for RNA extraction

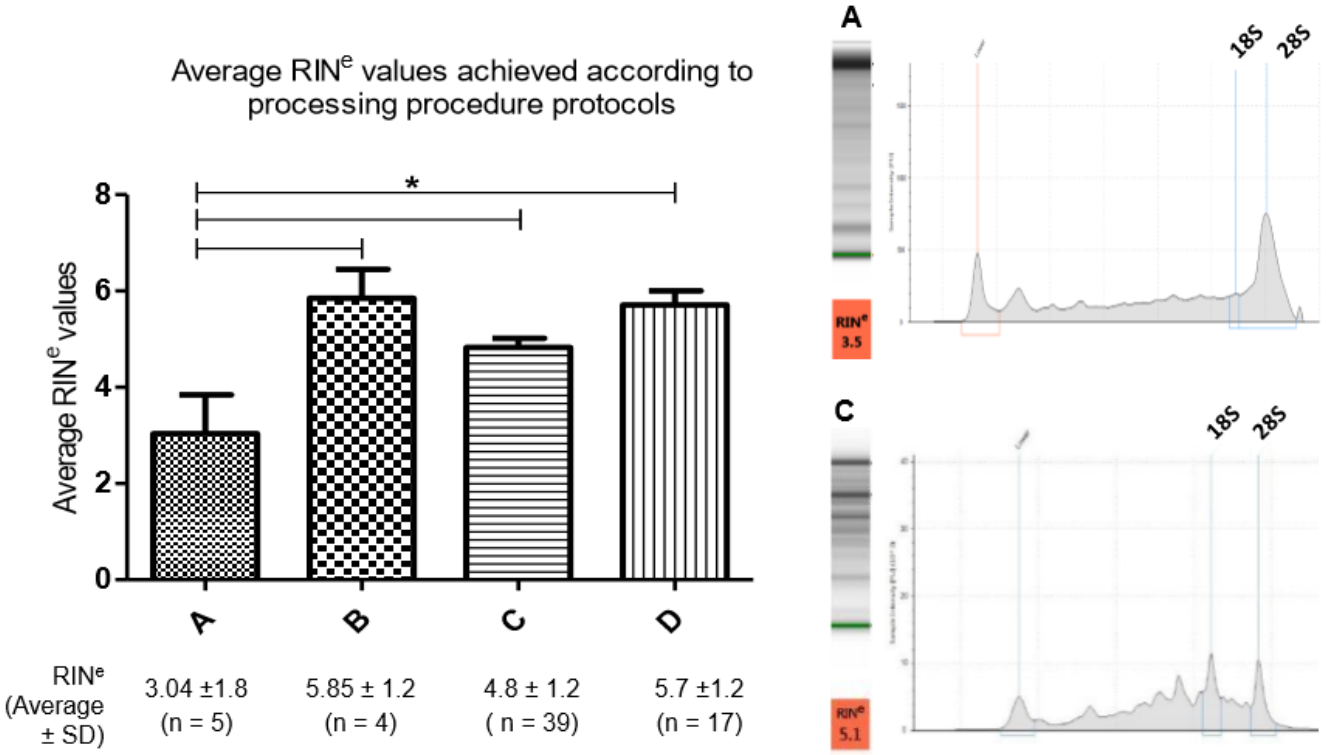

Figure 2. Average RIN^e values under the different sample processing procedures (left). Each RIN^e value is reported at the average with standard deviation (SD). Number of samples tested shown in brackets. When teeth were immediately frozen in liquid nitrogen (B, clinical samples, C and D, post mortem samples), RIN^e values were improved compared to samples stored in RNAlater® at room temperature ($P < 0.01$ by One-way ANOVA). Right panel shows representative electrograms of RNA extracted under protocols A and C. Distinction of 18S and 28S bands and peaks disappeared in highly degraded RNA (top right, protocol A). Protocol C (bottom right) produced only moderately degraded RNA. The 28S and 18S bands are distinguishable on the electrogram but several minor peaks can be seen to the left of the 18S peak.

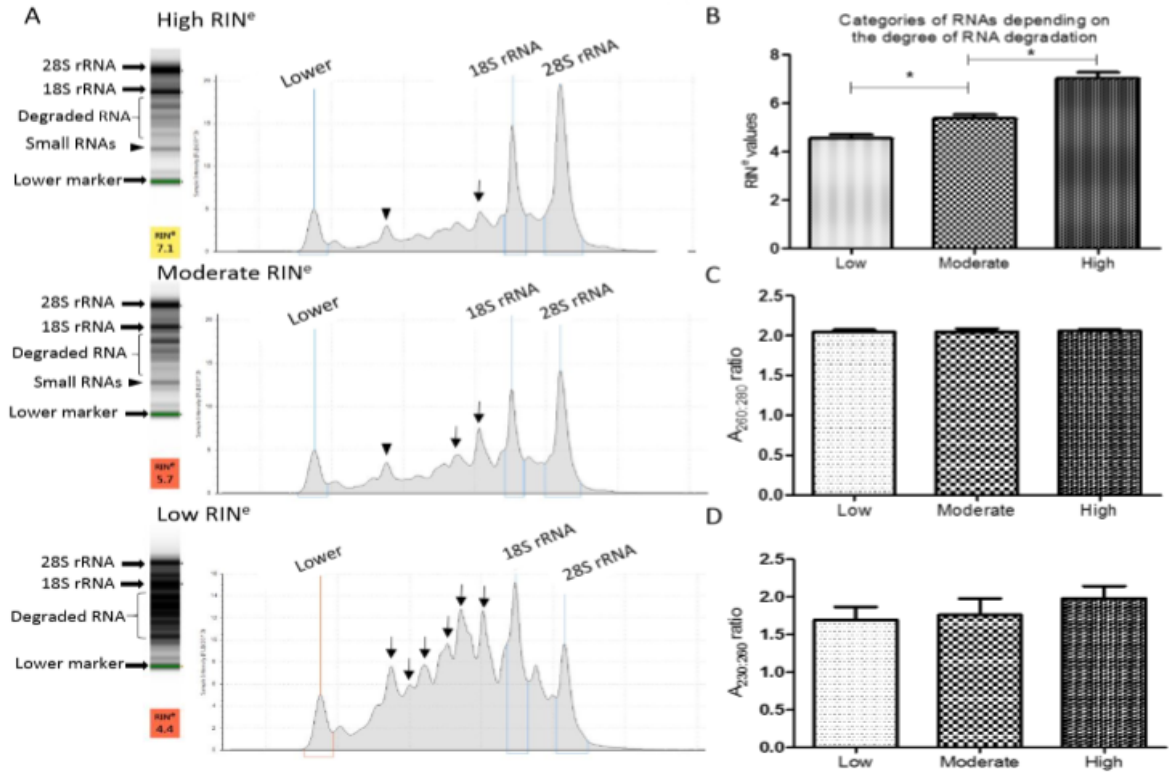

Figure 3. RNA purity and integrity. Fifteen RNAs were divided into three groups, Low, Moderate and High categories according to RIN^e values. On the lef three gel images and electropherograms are shown as representative images of each group (A). Arrow heads indicate small RNAs and arrows indicate degraded RNAs. The average RIN^e values from each category was statistically difference among the groups (*P < 0.05, Mann-Whitney U-test) (B). In terms of both $A_{260:280}$ ratio and $A_{260:230}$ ratio, there were no statistically significant differences between any two groups (P > 0.1, Mann-Whitney U-test) (C and D).

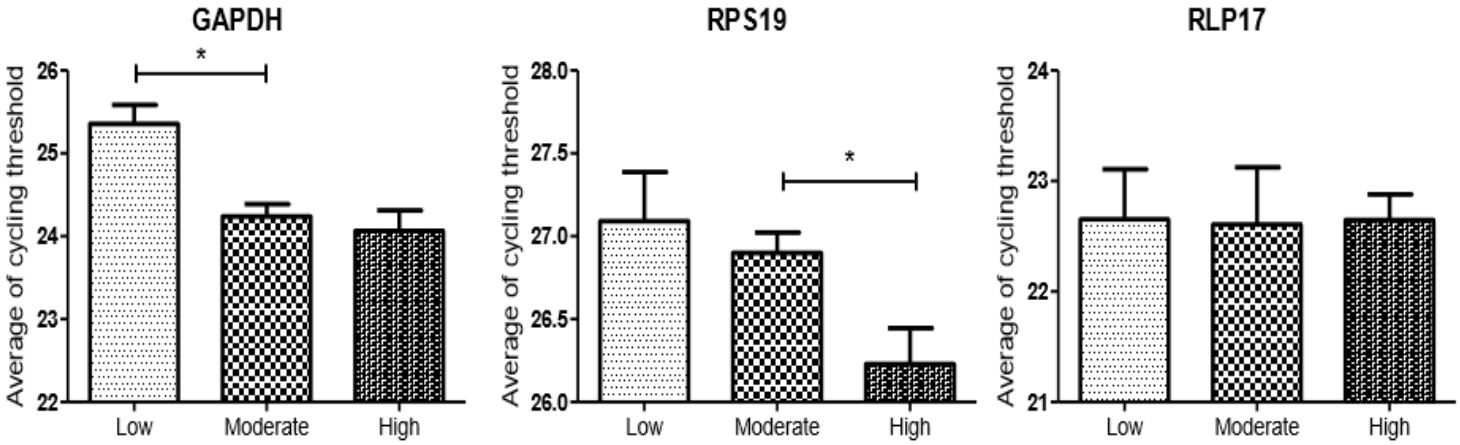

Figure 4. RNA quality and reference gene expression. Expression levels of three reference genes were generated as average of cycling threshold (Ct) with standard deviation. (GAPDH * $p < 0.05$ in Two sample t-tests, RPS19 *$P < 0.05$ in Two sample t-tests, RLP17 $P > 0.1$ in Mann-Whitney U-test)

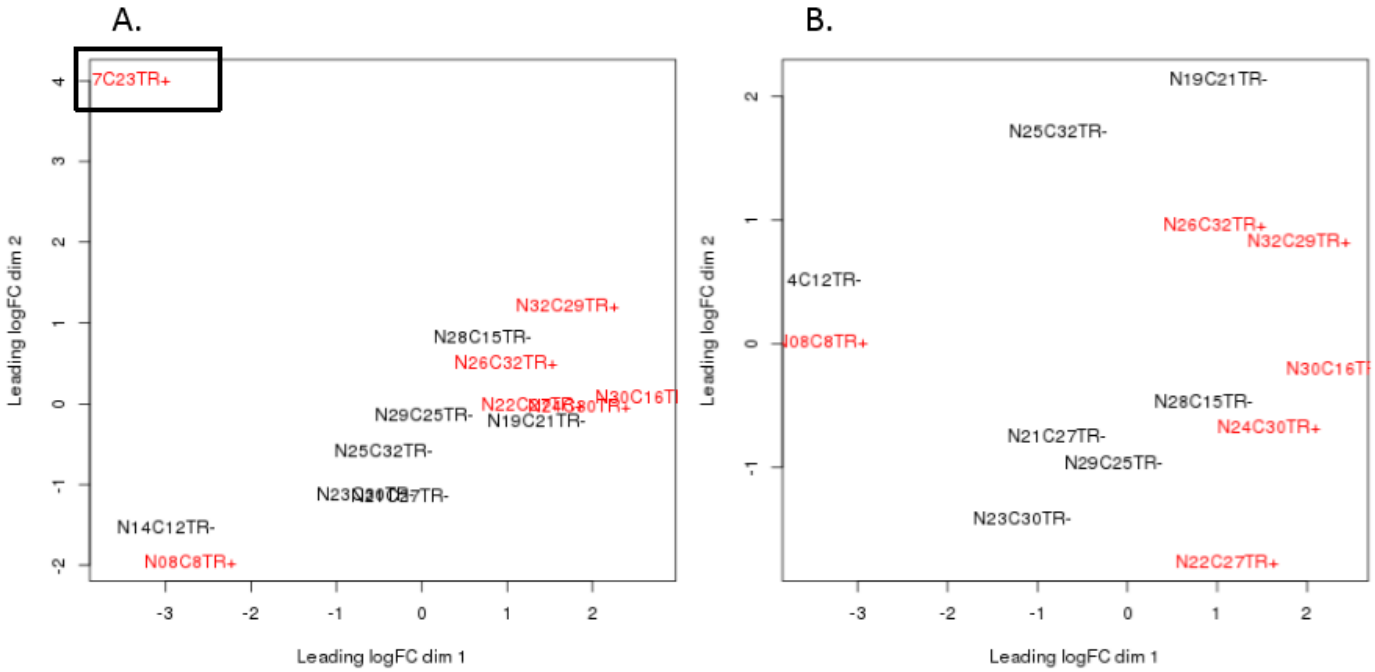

Figure 5. The effect of low yield of RNA sample on RNA-seq two-dimensional MDS plot of genome-wide expression profiles (A) MDS plot showed that the one low quantity RNA sample (highlighted with a square) was displayed as an outlier while other samples were clustered together. (B) When the low yielding RNA sample was excluded from the data set, data from all samples were displayed evenly and clustered. There was no obvious outlier.

Protocol	Feline tooth samples		Canine tooth samples	
	Protocol 1	Protocol 2	Protocol 1	Protocol 2
RIN^e Average ± SD	3.6 ± 1.3 (n = 6)	5.6 ± 1.0 (n = 16)	2.7 ± 1.2 (n = 3)	4.7 ± 1.0 (n = 3)

Table 1. Average RIN^e values achieved following the two different protocols described in feline and canine teeth. All tooth samples were collected following tissue sampling procedures C or D. Each RIN^e value is reported at the average with SD. Number of samples tested shown in brackets.

	Feline tissues using Protocol 2		Canine tissues using Protocol 1		Canine tissues using Protocol 2	
Type of tissues	Hard tissues	Soft tissues	Hard tissues	Soft tissues	Hard tissues	Soft tissues
RIN^e Average ± SD	4.9 ± 1.3 (n = 70)	6.9 ± 0.7 (n = 14)	2.7 ± 1.2 (n = 3)	7.1 ± 0.4 (n = 2)	4.7 ± 1.0 (n = 3)	6.6 ± 1.6 (n = 2)

Table 2. Average RIN^e values achieved using different feline and canine tissues and the two protocols described. Each RIN^e value is reported at the average with SD. Number of samples tested shown in brackets.

Metric used to assess RNA quality	RIN[e]
$A_{260:280}$ ratio	
Correlation coefficient	0.079
P value	0.781
$A_{230:260}$ ratio	
Correlation coefficient	0.353
P value	0.197

Table 3. Spearman correlation coefficients for different metrics used to assess RNA quality of feline teeth. Spearman rho test was performed to assess level of correlation between RIN[e] values and the $A_{260:280}$ ratios or the $A_{260:230}$ ratios obtained for all of the samples.

Categories by RIN[e]	High (n = 5)	Moderate (n = 4)	Low (n = 5)	Total (n = 14)
RIN[e] of RNA	6.9 ± 0.4	5.4 ± 0.3	4.5 ± 0.3	5.6 ± 1.1
Yield	High*	High	High	High*
% duplicate reads	40.4 ± 14.1 [#] 34 ± 7.9 [##]	30.4 ± 5.5	34 ± 7.9	35.3 ± 10.3
% mapped reads	94.2 ± 3.9	95.4± 1.7	95.4± 1.7	95.0 ± 2.5

Table 4. RNA integrity effect on cDNA library and sequencing. Each value is reported at the average with standard deviation.* include one low yield RNA sample. # shows % duplicate reads with the low yield RNA sample included, and ## shows it excluding the low yielding sample.


Click here to access/download
Electronic Supplementary Material
Supplement 1.xlsx

3.3 Discussion

In this chapter, I have reported the development of a RNA extraction protocol capable of producing good yields of RNA and improved RNA quality from mineralised tissues. The information from this chapter is important as it is recognised that RNA is fragile and susceptible to degradation. This is especially true for RNA extracted from specialised tissue such as mineralised teeth Moreover, it remains unclear whether most transcripts of RNA degrade at similar rates under a certain situation (*e.g.* clinical settings or post mortem) or whether rates of RNA degrade are associated in a gene-specific manner (233). Hence, gene expression study is based on the assumption that each nucleotide of the transcript is sequenced equally and the amount of amplicon is proportional to the abundance of the transcript (240, 241). Several studies have been done to elucidate how low quality RNA impacts on gene expression profiling (233, 242, 243). A qPCR study revealed that RNA samples with poor integrity were found highly comparable if integrity of RNA is similar among samples avoiding use of RNA samples with disparate quality (242). Similarly, a study reported that RNA degradation did not preclude microarray analysis if microarray is done using samples of comparable RNA integrity or circumventing probe positions near the 5' end (243). When it comes to RNA-seq, if RNA is partially or completely degraded the corresponding read yield would be distorted in a gene-specific manner, which might have profound influences on whole genome gene expression profiling (241). A RNA-seq study using RNA with a wide range of quality revealed that disparate quality of RNA impacted on measurements of gene expression levels and the more degraded RNA tended to have a significant loss of library complexity (233). Therefore, RNA-seq analysis requires RNA of a much higher quality than for example standard PCR reactions where the overall RNA degradation is of less importance.

In this study I found that RNA with a medium to high RIN^e value was suitable for gene expression and RNA-seq data analysis when extracted with a good

yield. Only one cDNA library was defined as an outlier from the other samples tested. Although it was sequenced from a high RIN^{e} it was a low yielding RNA sample. Due to suboptimal temperatures during sample processing or post mortem apoptosis, RNA cannot be devoid of some degradation. The overall quality of RNA from feline teeth was lower than that achieved from soft tissue but as similar to comparable studies of murine teeth (237). The quality of RNA-seq data will guide which data can be useful for inclusion or exclusion for further data analysis. In the following two chapters of this thesis, this RNA isolation protocol is used throughout. In chapter 4, I focused on the expression levels of inflammatory cytokines which I considered might be correlated to feline TR based on published data from other studies. RNA-seq data will be utilised to investigate the whole dental transcriptome changes between TR -ve and TR +ve teeth in chapter 5. In summary, the technical advances described in this chapter create a strong base for the majority of the work on this PhD project.

Chapter 4 Investigation into the role of inflammatory cytokines and vitamin D in feline tooth resorption

4.1 Abstract

Inflammatory cytokines, vitamin D and vitamin D metabolites have been frequently reported to play important roles in both periodontal disease and tooth resorption in cats. To test this hypothesis, expression of the inflammatory cytokines, the nuclear vitamin D receptor (VDR) and the key regulator of osteoclast/odontoclast differentiation, RANKL expression were investigated by qPCR. Also, an *in vitro* co-culture model system was developed for feline osteoclasts and periodontal ligament cells to study osteoclast differentiation and activation. There was no statistically significant difference in mRNA expression of any of the inflammatory cytokines tested (*e.g. IL1B, IL6, P2X7R, TNF* and *IFNG*), *VDR* or *RANKL* between TR -ve and TR +ve teeth samples when assessed by qPCR. Feline osteoclasts were successfully differentiated from peripheral blood and bone marrow and showed typical characteristics of bone and tooth resorbing cells including mRNA expression of cathepsin K (*CTSK*), tartrate-resistant acid phosphatase type 5 (*ACP5*), d2 isoform of vacuolar ATPase (*ATP6V0D2*) and DC-STAMP (*DCSTAMP*) by PCR, and cathepsin K, calcitonin receptor, c-Src, vitronectin receptor and MMP9 by immunocytochemistry. To test the effect of vitamin D on osteoclast formation and resorption activity feline osteoclasts were treated with physiological levels of the active form of vitamin D_3 ($1,25(OH)_2D_3$). This resulted in increased osteoclast formation and resorption activity, but at a higher dose of $1,25(OH)_2D_3$, resorption activity was inhibited. Primary periodontal ligamnet cells expressed RANKL and induced osteoclast formation without additional exogenous RANKL in co-culture systems of osteoclasts and periodontal ligament cells. Interestingly, osteoclast precursors from TR +ve cats yielded higher numbers of osteoclasts under co-culture conditions compared to TR -ve cats.

4.2 Introduction

Tooth resorption is one of most common oral diseases reported in cats (99, 107, 108, 112). The oral cavity constitutes a moist environment which contains a reservoir of nutrients. This environment is subject to plaque accumulation and bacterial colonisation which can cause dental inflammation (6). When inflammation progresses, cytokines are released locally, which may attract osteoclast progenitors and progress osteoclast induced tooth resorption (163, 244). TR lesions frequently accompany localised gingival inflammation. Therefore inflammation has been proposed as an aetiological factor to trigger progression of TR (92, 100).

As high prevalence of TR has been reported in domestic cats, commercial diets and their levels of vitamin D_3 and its metabolites have also been suggested to be involved in the aetiology of TR (92). Several authors have hypothesised that vitamin D_3 and its catabolic metabolism might induce odontoclastic tooth resorption (92, 122, 178, 245). However, our understanding of the precise mechanisms behind the development and pathophysiology of TR is currently limited, and the roles of vitamin D or vitamin D metabolites and inflammatory cytokines have not been fully elucidated.

In this chapter I will present qPCR data on the mRNA expression levels of various osteoclast stimulatory factors including inflammatory cytokines, *VDR* and *RANKL* between TR –ve and TR +ve teeth to investigate the involvement of these factors in osteoclast dysregulation.

Osteoclasts are terminally differentiated cells and unable to proliferate (20). Therefore there is no available immortalised osteoclast cell line (246). Authentic osteoclasts can be acquired from differentiating them from their precursors or from isolation of primary osteoclasts whose successful isolation is limited to new born animals (246). Initial studies indicated that the *in vitro* long-term culture of osteoclasts required haematopoietic precursor cells as well as osteoblasts/stromal cells and various stimulating factors including $1,25(OH)_2D$, PTH or PGE2 (247, 248).

This indirect method for the differentiation of osteoclasts was superseded by the direct stimulation method using commercially available recombinant CSF-1 and RANKL following the discovery of these critical cytokines (30, 224, 229). This protocol is now established and is the most widely used *in vitro* method for direct osteoclast formation of osteoclast precursors derived from bone marrow, spleen, or peripheral blood (229). These direct *in vitro* techniques are well established in several species including human (227), cat (228), rodents (246) and rabbit (249) and include isolation of primary mature osteoclasts from newborn rabbits (249) or chicks (250), osteoclast derived from peripheral blood (227, 245) or bone marrow (246), and immortalised macrophage cell line such as RAW 264.7 cells (226).

I here present the successful *in vitro* differentiation of feline osteoclasts from both PBMC and bone marrow. This will be a useful tool for studying feline osteoclast biology and testing efficacy of drugs *in vitro*.

In this chapter I will also present the technique of co-culturing osteoclasts and periodontal ligament cells. Feline TR usually occurs on the external tooth surface. Lesions initiate from the external root and invade into the dentine and pulp (9), and histopathology of TR lesions often indicate impairment of periodontal ligament structure (9, 92, 113). Normal periodontal ligament possesses well-developed vascular networks and various cells that play an important role of remodelling of tooth supporting structure (92). To investigate interaction between periodontal ligament cells and osteoclasts, a previously described co-culturing technique was modified and applied (76, 142). Here I will demonstrate successful osteoclast formation and resorption in a co-culture model that mimic the tooth microenvironment.

4.3 Materials and Methods

4.3.1 Samples and phenotyping of TR

Samples of cat tissues in this study were collected as described in section 2.2.1. A total of 24 cats was included in the study. Teeth without dental radiographs

were excluded. All extracted teeth were collected from the mandible (left and right third and fourth premolars and first molar, referred to as 307-9, 407-409 according to the Triadan system). TR type and staging were confirmed by a veterinary dental specialist, Dr Norman Johnston (MRCVS, RCVS, American & European Specialist in Veterinary Dentistry, DentalVets, North Berwick) and Dr Susan Thorne (MRCVS, Dentistry and Oral Surgery Resident, DentalVets, North Berwick).

4.3.2 RNA extraction and preparation of cDNA

Total RNA was isolated from the teeth with/without TR as described in sections 2.1.1 and 2.2.1. The first strand cDNA was synthesised as described in sections 2.1.2 and 2.1.3. After phenotyping and RNA assessment, 24 RNA samples (11 TR –ve teeth and 13 TR +ve teeth) from 16 cats (3 TR –ve cats and 13 TR +ve cats) were included in this study (Table 4.1). TR + teeth were classified into eight of Stage 2, two of Stage 4 and three of Stage 5. All teeth samples were further sub grouped into TR -ve from TR unaffected cats, early stage from Stages 1-2 and advanced stage from Stages 3-5. In terms of types, all TR + teeth were classified Type 2(n = 11) or Type 3 (n = 2) and none of them was identified as Type 1. Available RIN^e values were noted if applicable. Only limited information of other disease was available.

4.3.3 Primer sets for feline inflammatory cytokine genes

The primers used are described in Table 4.2. The previously published primers included *IL6, TNF, IFNG, GAPDH, HPRT, RPL17* and *RPS19*. As the feline genome has not been fully annotated or no validated primers were available, new primer sets for *1L1B, P2X7R* and *RANKL* were designed as described in section 2.1.4 and the sequences were confirmed by sequencing described in section 2.1.10.

4.3.4 Primer efficiency and quantitative PCR

To check the specificity of PCR products, conventional PCR was performed and each product was visualised using agarose gel as described in section 2.1.5. Quantitative PCR was performed using SYBR Green based reagent, Precision™ 2× qPCR Mastermix (Primer design, Southampton, UK) using Stratagene MX3000P

qPCR system (Agilent Technologies) as described in section 2.1.5. The thermal cycling condition was displayed in Figure 4.1. To determine primer efficiency for four reference genes including *GAPDH, HPRT, RPL17* and *RPS19*, 10-fold serial dilutions up to 10,000 were carried out. For seven genes of interest 4-fold serial dilutions up to 4^{-5} were carried out. Following determination of primer efficiency, quantitative PCR was performed and relative mRNA expression as fold change was analysed using the calculation of $2^{-\Delta\Delta Ct}$ as previously described in section 2.1.8. GraphPad prism v5 was used for generation of graphs.

Cat ID	Age	Sex	Breed	Cat TR status	Examined teeth [#]	TR + teeth [#]	Extracted teeth	TR status	TR stage	TR type	RIN[e]	Other disease
C6	>5	F	Mixed	+	7	1	407	+	4	3	5.3	N/A
C8	>5	F	Mixed	+	14	8	307, 407	+	2	2	5.2	N/A
C12	4	F	Mixed	-	14	0	307,308, 407, 408	-	N/A	N/A	4.5	GI tract
C15	9	NF	Mixed	-	14	0	307, 407	-	N/A	N/A	7.3	Chronic cystitis
C16	5	NF	Mixed	+	14	1	308	+	2	2	5.1	N/A
C17	12	NF	Mixed	+	6	2	407	+	5	2	5.6	Age related problems
C18	10	F	Mixed	+	6	3	307	+	5	2	3.8	N/A
C21	16	NF	Mixed	+	8	1	308	-	N/A	N/A	5.3	Age related problems
C25	10	NF	Mixed	-	14	0	307, 407	-	N/A	N/A	6.7	Back pain
C26	>5	NM	Mixed	+	6	1	407	+	5	2	4.6	N/A
C27	7	NF	Mixed	+	14	2	407	-	N/A	N/A	4.1	N/A
							404	+	2	2	5.9	
C30	10	NF	Mixed	+	14	3	309	-	N/A	N/A	3.5	Thyroid problems
							409	-	N/A	N/A	4.4	
							307	+	2	2	5.2	Thyroid problems, overweight
							407	+	2	2	4.4	
C32	6	NF	Mixed	+	14	3	308	-	N/A	N/A	4.9	N/A
							407	+	4	3	6.3	
C34	9	NM	Mixed	+	14	5	309	-	N/A	N/A	N/A	GI and urinary problems
							308	+	2	2	N/A	
C36	10	F	Mixed	+	14	6	309	-	N/A	N/A	N/A	Age related problems
							408	+	2	2	N/A	
C37	5	M	Mixed	+	14	4	309	-	N/A	N/A	N/A	N/A
							407	+	2	2	N/A	

Table 4.1 Description of sample information and TR status for qPCR. #: number, NF: neutered female, NM: neutered male, N/A: not applicable, GI: gastrointestinal.

Primer set	Sequence (5’ -3’)	Amp (bp)	Tm (°C)	Reference
IL6	F; GACTTCCTTCAGTTCAGCCTCAGG	81	64	(100)
	R; AGGAATGCCCGTGAACTACAGC			
IL1B	F; TGGCGGAAGGGGAATAGAAG	427	58	NP_001070882
	R; GCTTGGTATAAAGATGGCACAC			
P2X7R	F; TGTGGAGGATGTGTGAGAG	367	55	XM_003994650
	R; GGGATAAACAAGAGAAGCGAAG			
TNF (TNF-α)	F; TCTTCTCCTTCCTCCTCGTCG	185	65	(100)
	R; GGGGTTTGCTACTACATGGGC			
IFNG	F; CAGATGTAGCAGATGGTGGGTC	176	60	(100)
	R; CATGTCTTCCTTGATGGTGTCC			
VDR	F; TCTCTGACCCTGGACCTGTC	122	62	(100)
	R; GAAGTGAGGTCTCTGAACCCTG			
RANKL	F; CTTCCGGGCAGCTGTACAAA	186	60	XM_023251873
	R; AGGCTCACTTTGTGGGAACC			
HPRT	F; AACTGGAAAGAATGTCTTGATTGTTG	100	56	(251)
	R; GACCATCTTTGGATTATACTGCTTGA			
GAPDH	F; GCCGTGGAATTTGCCGT	82	59	(251)
	R; GCCATCAATGACCCCTTCAT			
RPL17	F; CTCTGGTCATTGAGCACATCC	108	58	(252)
	R; TCAATGTGGCAGGGAGAGC			
RPS19	F; TCATGCCCAGCCACTTTAGC	116	59	(252)
	R; GAGGTGTCAGTTTGCGTCCC			

Table 4.2 List of primer sets used for quantitative PCR.

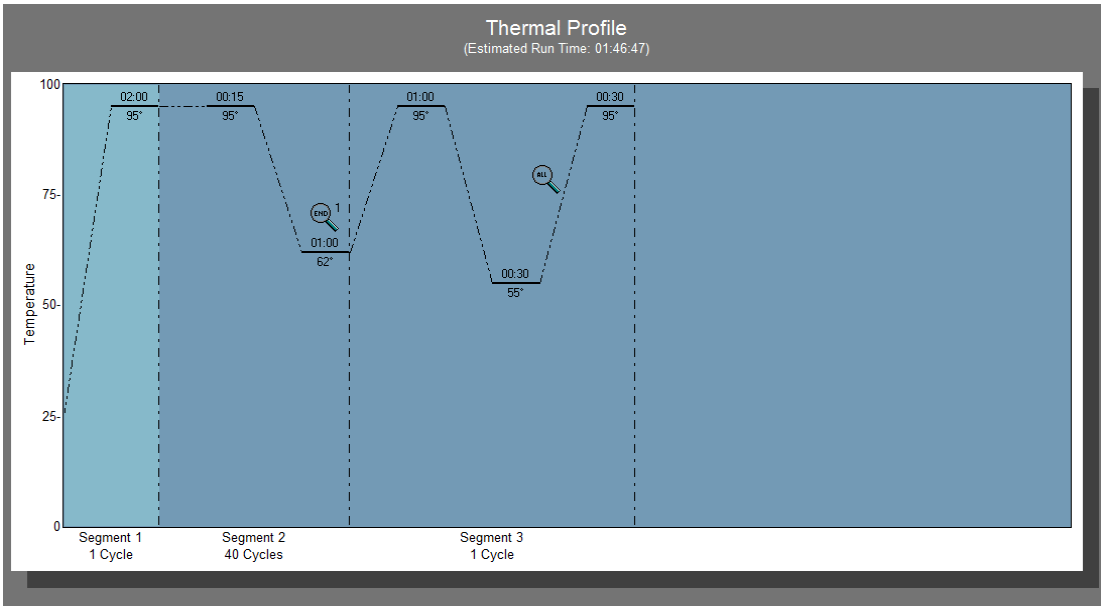

Figure 4.1 Thermal cycling condition used in this chapter.

4.3.5 **Osteoclast culture and characteristics**

In vitro techniques of primary osteoclast cultures from peripheral blood and bone marrow were previously described in sections 2.3.6 and 2.1.6. RAW 264.7 cells were differentiated into osteoclasts according to protocol described in section 2.3.8. To characterise osteoclasts, various techniques including PCR, TRAP activity, and immunocytochemistry were performed as described in section 2.4.2.

To test the effect of the biologically active form of vitamin D on osteoclast formation, $1,25(OH)_2D_3$ was used to treat the cells at different concentrations as described in section 2.4.6.

4.3.6 **Isolation of periodontal ligament cells and co-culture with osteoclasts**

Primary periodontal ligament was isolated in feline periodontium and cultured as previously described in section 2.3.9. Co-culturing of periodontal ligament and osteoclasts were established in section 2.3.10. To characterise periodontal ligament, RANKL PCR and immunocytochemistry were performed as described in section 2.1.5 and 2.7.3.

Primer sets	Sequence (5' -3')	Amp (bp)	Tm (°C)	Reference
ACP5	F; CAATGCCCCGTTCTACACAG	362	59	XM_003981893
	R; TCACCGTGTCCAGCATGAAG			
ATP6V0D2	F;CCAAAATTGACACGGAGATGAG	266	55.2	XM_004001615
	R; AACCAGAACAGCATTGAAGAG			
CTSK	F; CTACATGACCAATGCCTTCC	372	56.8	XM_019837802
	R; TTTCCCCAGTTTTCTCCCC			
DCSTAMP	F; AAATGACACCAAAGGCCAAG	384	57.2	XM_023248441
	R; TCTATGGCTGCAAACAGCAC			
ACTB	F; TTCGAGACCTTCAACACCCC	300	59	AB051104
	R; GCCATCTCCTGCTCAAAATCC			

Table 4.3 List of primer sets used for conventional PCR.

4.4 Results

4.4.1 TR phenotyping and prevalence of study population

A brief description of the prevalence of TR from the 24 cats examined is summarised in Table 4.1. Twenty one of 24 cats were diagnosed with at least one TR lesion (21/24, 87.5%). Seventeen cats had multiple teeth affected with TR (17/24, 70.8%), in total, 82 out of 293 teeth were found with TR (82/293, 28%). Mean age of the cat population was 8.5 years old ranging from 4 to 19. From the 82 TR affected teeth, Stage 2 TR teeth were most frequently detected (45/82, 54.9%), followed by Stage 3 (15/82, 18.3%), Stage 4 and 5 (10/82, 12.2%). Stage 1 TR was least common. In terms of Type of TR, Type 2 TR was the most common Type affecting 67 of 83 teeth (82.7%), followed by Type 1 (9/82, 11%) and Type 3 (6/82, 7.3%).

4.4.2 Inflammatory cytokines, VDR, and RANKL expression in TR

All the genes of interest were expressed in teeth when using a conventional PCR, although *TNF* showed relative low expression in terms of amount of product. All PCR products were of expected size. Except for *INFG*, each amplicon was presented as a single band (Figure 4.2). *INFG* produced a strong band below 100 bp

which might be primer-dimer formation.

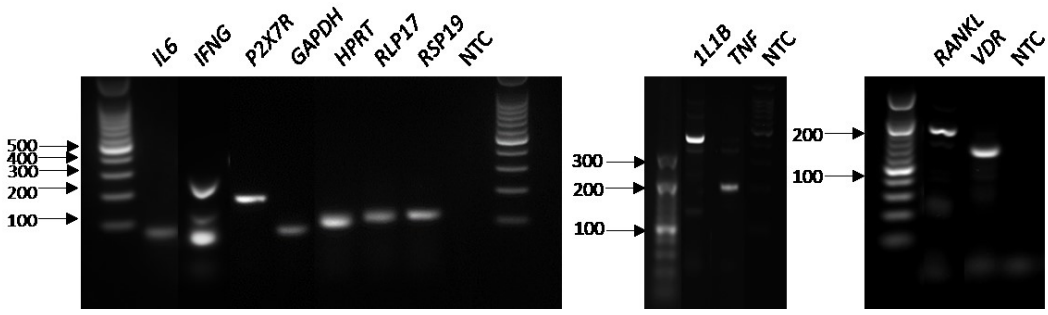

Figure 4.2 Result of PCR to test the primer sets. Teeth expressed mRNA of all cytokines, *RANKL, VDR* and the four reference genes. Note that *IFNG* produce a strong extra band which was presumed to be due to primer-dimer formation. Both amplicons of *IL6* and *TNF* amplicon represent relatively weak bands when compared to other genes. NTC; no template control.

The melt curve for each product by qPCR was generated following melt curve analysis and each curve is shown in Figure 4.3. A single peak on the melt curve implies that the PCR produced a single specific amplicon. Each curve represented a single sharp peak, except for *IL1B* which showed a wide and blunt peak. To check availability of primer, efficiency of each primer was tested and each value is shown in Table 4.4. The efficiencies of primers including *IL6, P2X7R, RANKL, VDR* and all reference genes ranged between 90 to 110%. The efficiencies of *IL1B* and *IFNG* were higher than 110% and that of *TNF* was just below 90%.

Primer set	**Efficiency**	**Primer set**	**Efficiency**	**Primer set**	**Efficiency**
IL6	97.6%	*IL1B*	122.7%	*P2X7R*	**109%**
TNF	**89%**	*IFNG*	124%	*RANKL*	95.5%
VDR	107.8 %	*GAPDH*	93.4%	*HPRT*	102.0%
RPL17	97.9%	*RPS19*	102.8%		

Table 4.4 Primer efficiency for each primer set. Efficiencies > 110% and < 90% are shown in bold.

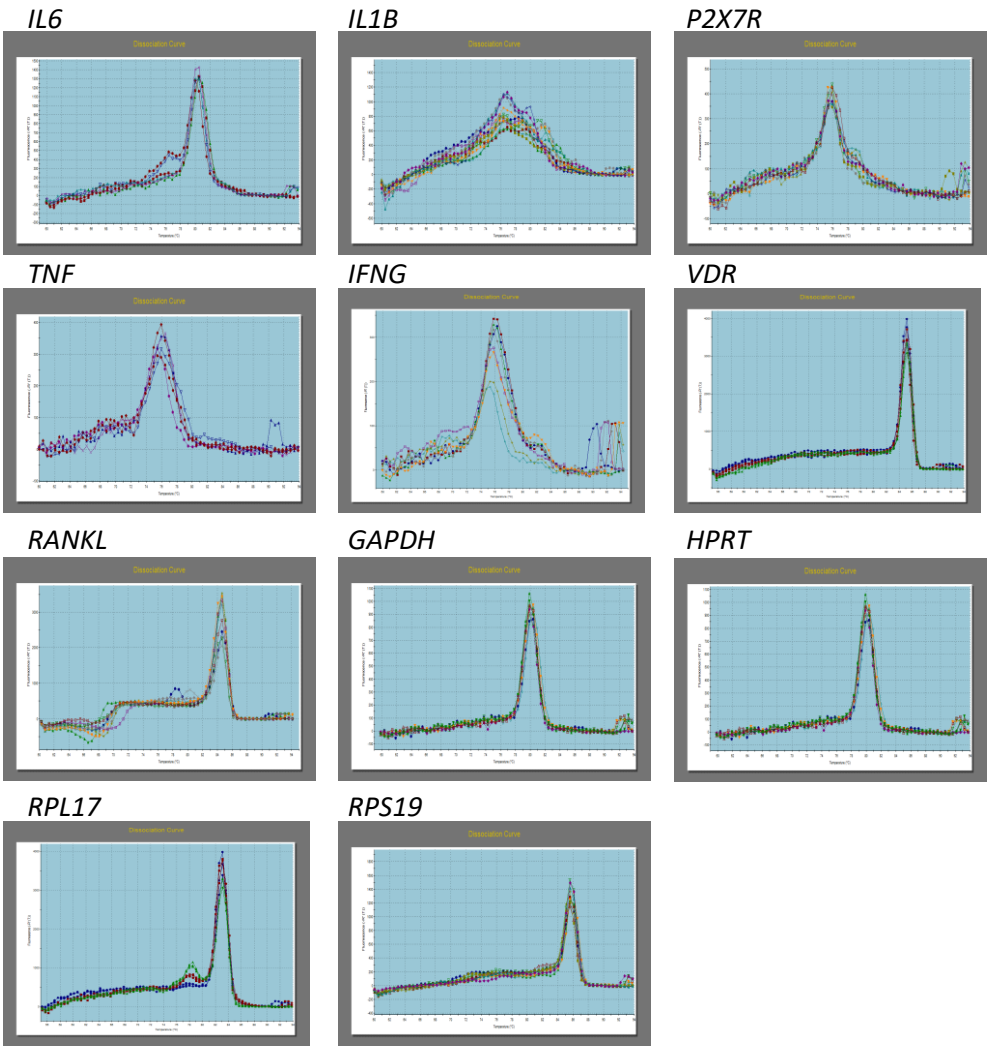

Figure 4.3 Melt curves from qPCR of various genes. Each amplicon reveals a single peak except *IL1B* following melt curve analysis.

To investigate the possible involvement of inflammatory mediators and vitamin D in osteoclastogenesis, qPCR was performed and data were analysed from all RNA samples. Samples were first divided into TR –ve and TR +ve teeth. The relative expression was normalised to geometric mean of the four reference genes. There were no significant differences in inflammatory cytokine expression including *IL6*, *IL1B*, *P2X7R* and *TNF* between TR –ve and TR +ve teeth. Likewise, there were no detectable differences between the samples in their expression of the anti-inflammatory cytokine *INFG*, *VDR*, or *RANKL* ($p > 0.05$) (Figure 4.4).

To investigate inflammatory changes during the progression of TR, samples were divided into subgroups, TR-ve from TR –ve cats, early stage TR, and advanced TR stage. The data were re-analysed (Figure 4.5). Only *IL6* expression showed

statistically difference between TR –ve and early stage TR (p = 0.043) but no difference in expression levels were seen between TR –ve and advanced stage or between early and advanced stage of TR.

4.4.3 Development of an *in vitro* model of feline osteoclastogenesis

Isolated cells from peripheral blood or bone marrow samples including enriched osteoclast precursors were seeded at the same density ($5x10^5$/24 well plate). In the early stages of *in vitro* osteoclast differentiation cells were mononuclear and non-adherent on the culture vessels (Figure 4.6, A and D). In the presence of mouse recombinant CSF-1 and RANKL, mononuclear osteoclasts started to fuse and formed multinucleated cells. Maximum generation of osteoclasts from PBMCs occurred on day 11 (Figure 4.6, B) while bone marrow derived osteoclasts usually formed within 9 days (Figure 4.6, E). Multinucleated cells from both sources were TRAP positive (Figure 4.6, C and F). When osteoclast precursors were cultured only CSF-1 without RANKL, there were only few multinucleated cells generated (Data not shown).

To optimise culture conditions for feline osteoclast generation *in vitro* cytokines derived from human or mouse were compared. The optimal amount of RANKL for osteoclast formation was 30 ng/ml and 3 ng/ml for human and mouse cytokines respectively while mouse recombinant CSF-1 was used at the same concentration (10 ng/ml) (Figure 4.7, A and B). Similar numbers of osteoclasts were generated in the given condition (Figure 4.7, C). RAW 264.7 cells were tested for usage as an immortalised osteoclast precursor line. Treatment with mouse RANKL at 30 ng/ml resulted in multinucleated TRAP positive osteoclasts in a limited population within 5 days (Figure 4.7, D). However, RAW 246.7 meditated

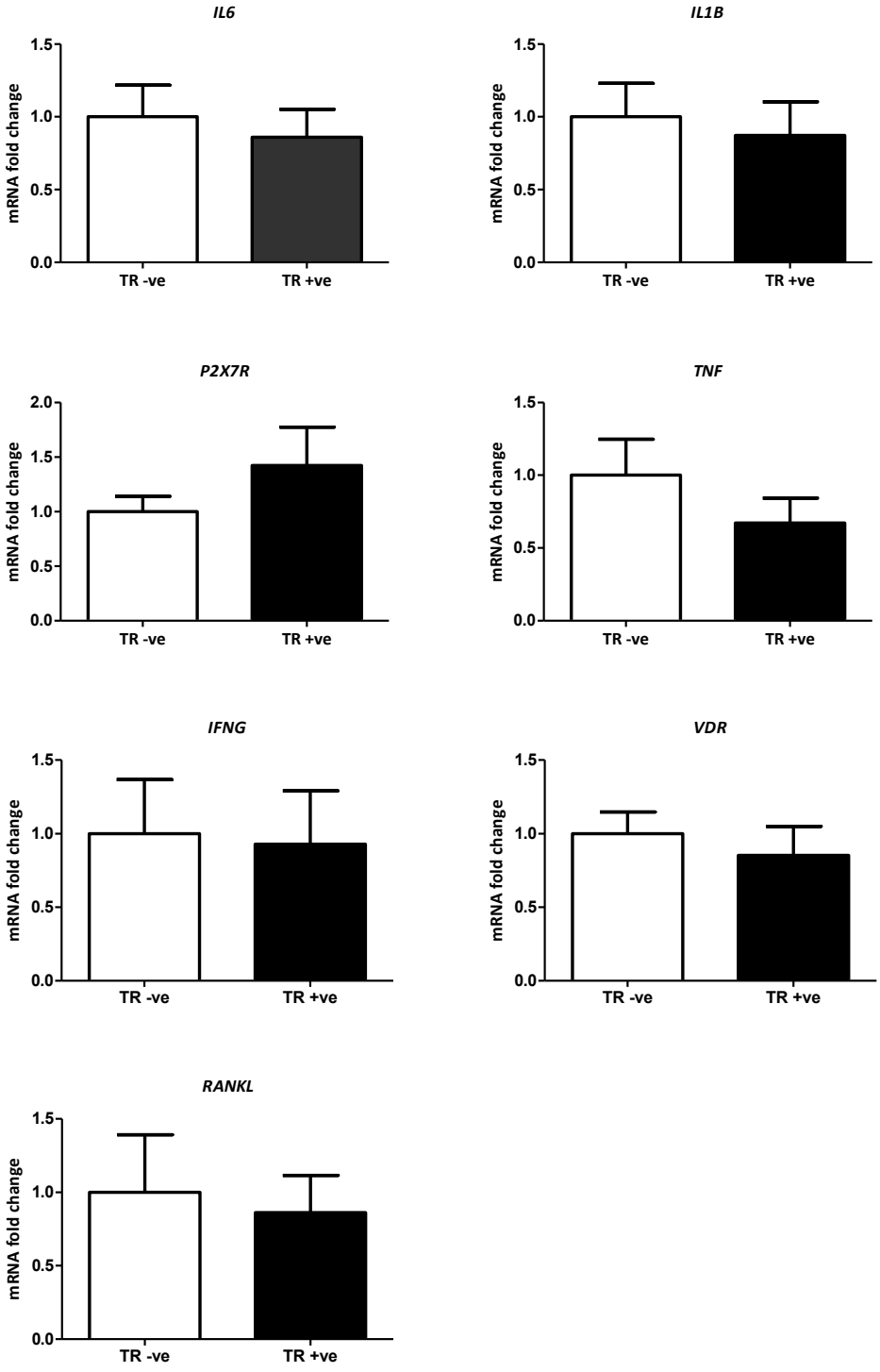

Figure 4.4 Relative expression of inflammatory cytokines, *VDR* and *RANKL* between TR –ve and TR +ve teeth. Each gene of interest was normalised to four reference genes. None of the genes showed any statistical differences in expression by the two sample t-test (P > 0.05). Graphs represent relative expression as fold changes with SEM bars (n= 11 for TR –ve teeth and n=13 for TR +ve teeth).

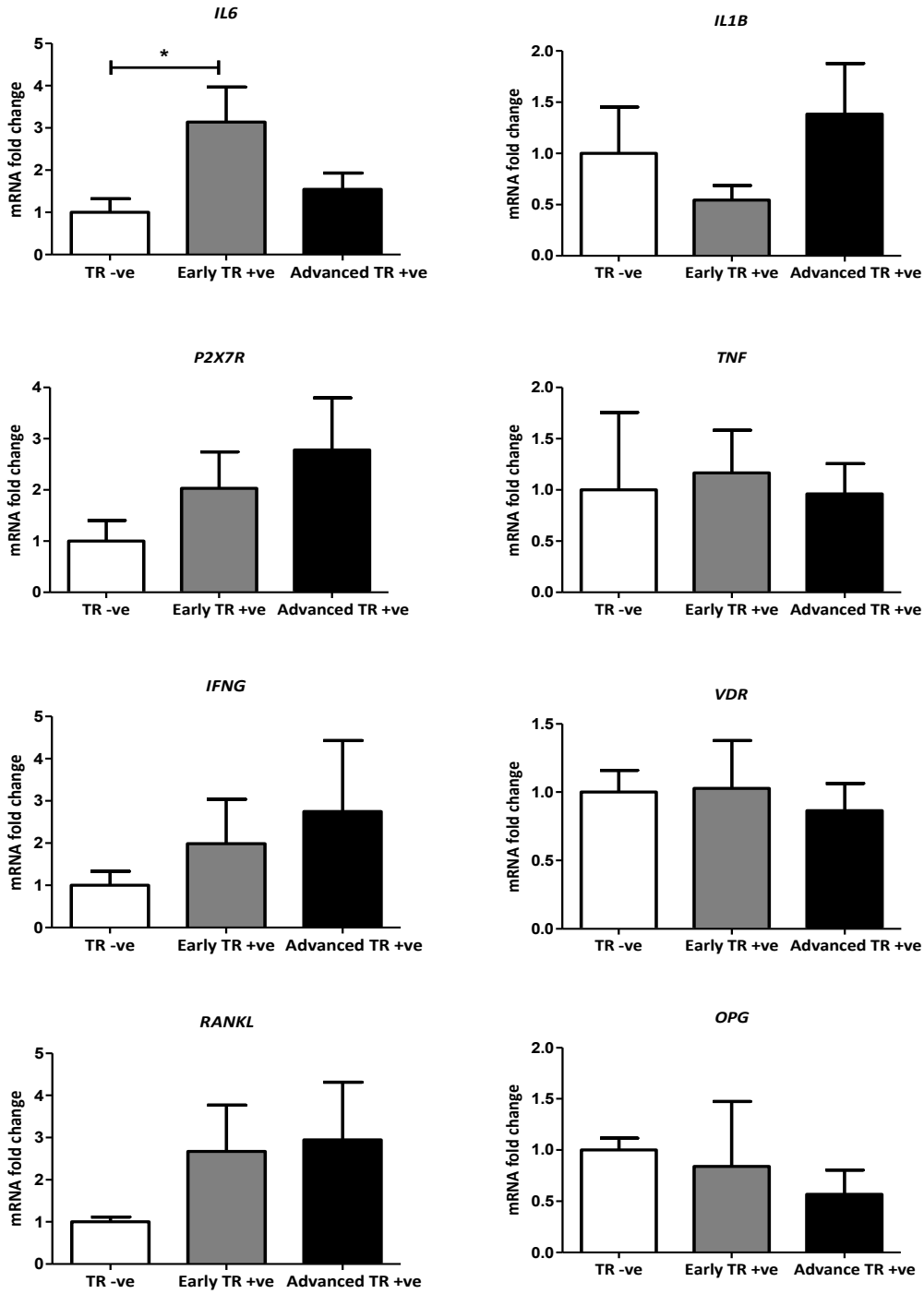

Figure 4.5 Relative expression of inflammatory cytokines, *VDR* and *RANKL* among subgroups: TR –ve, early stage TR +ve, and advanced stage TR +ve. Each gene of interest was normalised to four reference genes. Only early stage TR +ve showed significantly higher expression of *IL6* when compared to TR-ve teeth (* $p < 0.05$) by two sample t-test. There were no statistically significant differences found for any of the other genes ($p > 0.05$) by one-way Anova for three comparisons or two sample *t*-test for two comparisons. Graphs represent relative expression as fold changes with SEM bars (n = 3 for TR -ve, n = 8 for early TR +ve, and n= 5 for advanced TR +ve).

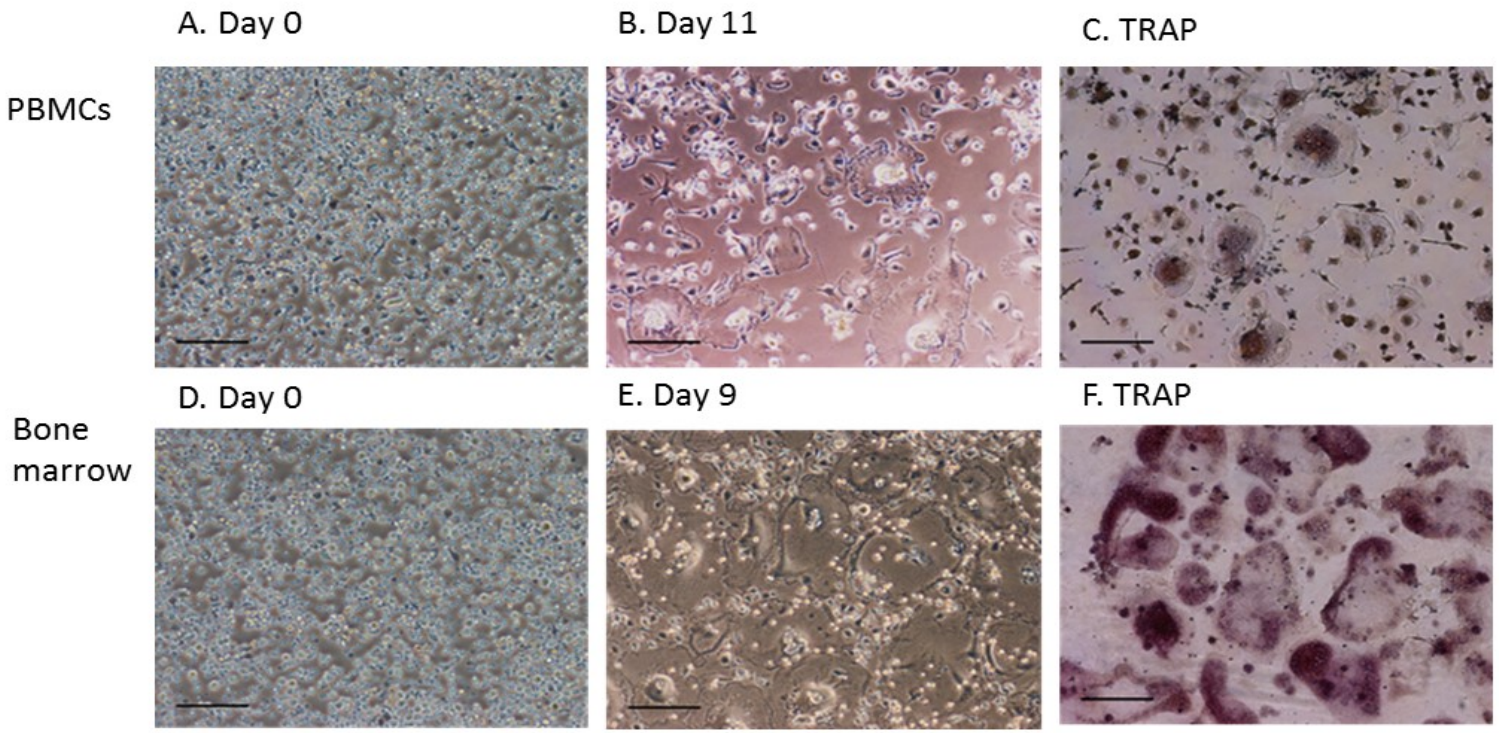

Figure 4.6 *In vitro* feline osteoclast generation from blood and bone marrow on plastic. (A) - (C): osteoclast differentiation from PBMCs. (D) - (F): osteoclast differentiation from bone marrow cells. Both osteoclast precursors were seeded at the same density in the growth vessel ($5x10^5$/24 well plate). On day 0, isolated mononuclear cells from both PBMCs (A) and bone marrow (D) are small and non-adherent on the culture plastic. Under the presence of CSF-1 (10 ng/ml) and RANKL (3 ng/ml), mononuclear osteoclast progenitors adhered onto the plastic and started to fuse into multinuclear giant osteoclasts. Osteoclasts from PBMCs formed on day 11 (B) and osteoclasts derived from bone marrow reached maximum differentiation earlier at day 9 (E). Both osteoclast-like cells expressed TRAP positivity (C and F). Scale bars = 100 µm.

osteoclasts were generated inconsistently, and when passaged cells failed to differentiate into osteoclasts.

This *in vitro* osteoclast generation protocol was also applied to canine and murine osteoclast precursors using bone marrow derived precursors (Figure 4.8). *In vitro* canine (Figure 4.8, B) and murine osteoclast (Figure 4.8, C) required higher RANKL concentrations (mouse recombinant RANKL 5-10 ng/ml) compared to feline osteoclast (mouse recombinant RANKL 3 ng/ml) (Figure 4.8, A) while maintaining the same concentration of mouse recombinant CSF-1 (10 ng/ml) to efficiently generate osteoclasts. The size of feline osteoclasts were relatively larger and contained more nuclei than osteoclasts from other species (mouse and dog).

Feline osteoclasts were successfully differentiated using mouse recombinant CSF-1 and RANKL at a lower concentration than with the equivalent human cytokines. , I therefore decided to use mouse recombinant CSF-1 and RANKL throughout this study. Unless otherwise specified CSF-1 or RANKL refers to mouse recombinant CSF-1 or RANKL throughout this study. The optimal concentrations of CSF-1 and RANKL for *in vitro* feline osteoclast were 10 ng/ml and 3 ng/ml, respectively. I refer to this optimised medium as osteoclast formation medium.

Feline bone marrow derived osteoclasts

A. Human RANKL 30 ng/mL

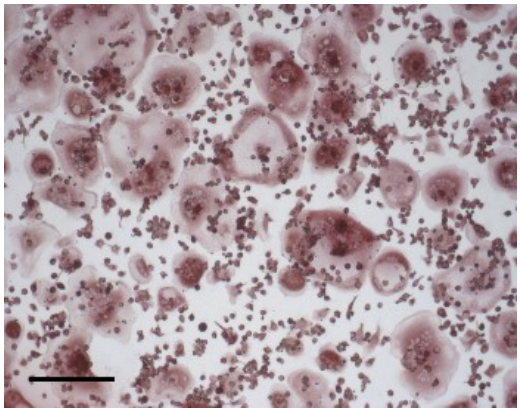

B. Mouse RANKL 3 ng/mL

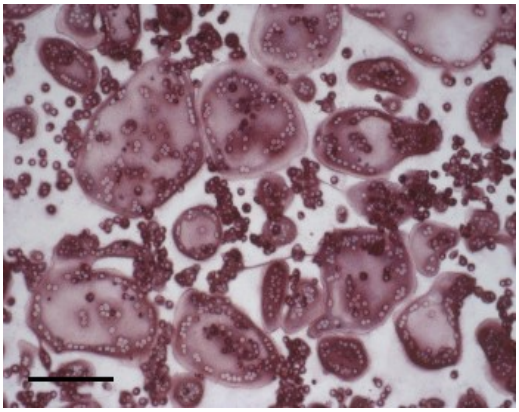

C. Number of TRAP positive osteoclast cells

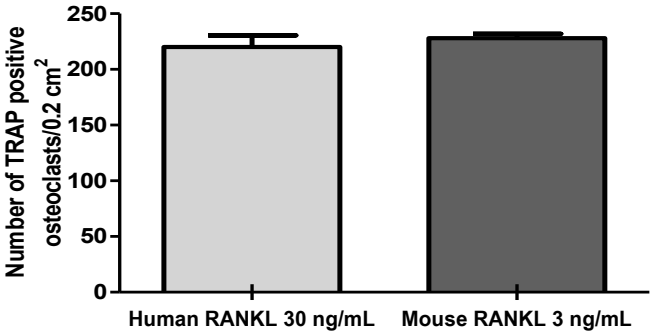

D. RANKL mediated osteoclast formation from RAW 264.7 cells

Control no RANKL

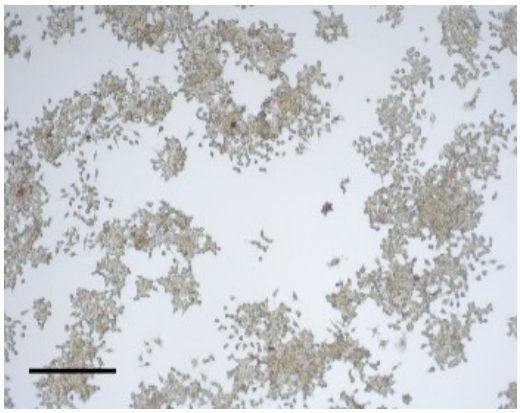

Mouse RANKL 30 ng/mL

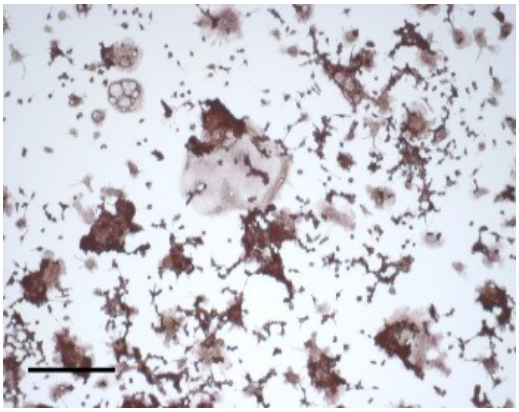

Figure 4.7 Optimisation of *in vitro* feline osteoclast differentiation and RAW 264.7 mediated osteoclastogenesis. (A) Osteoclast formation using human recombinant RANKL at 30 ng/ml, (B) Osteoclast formation using mouse recombinant RANKL at 3 ng/ml. (C) When the optimum RANKL concentrations was used for human and mouse cytokines, similar number of osteoclasts were generated. (D) A population of RAW 264.7 cells were able to differentiate into TRAP positive osteoclasts using high mouse RANKL concentration (30 ng/ml). Data represent mean + SEM bars. Scale bars = 100 µm.

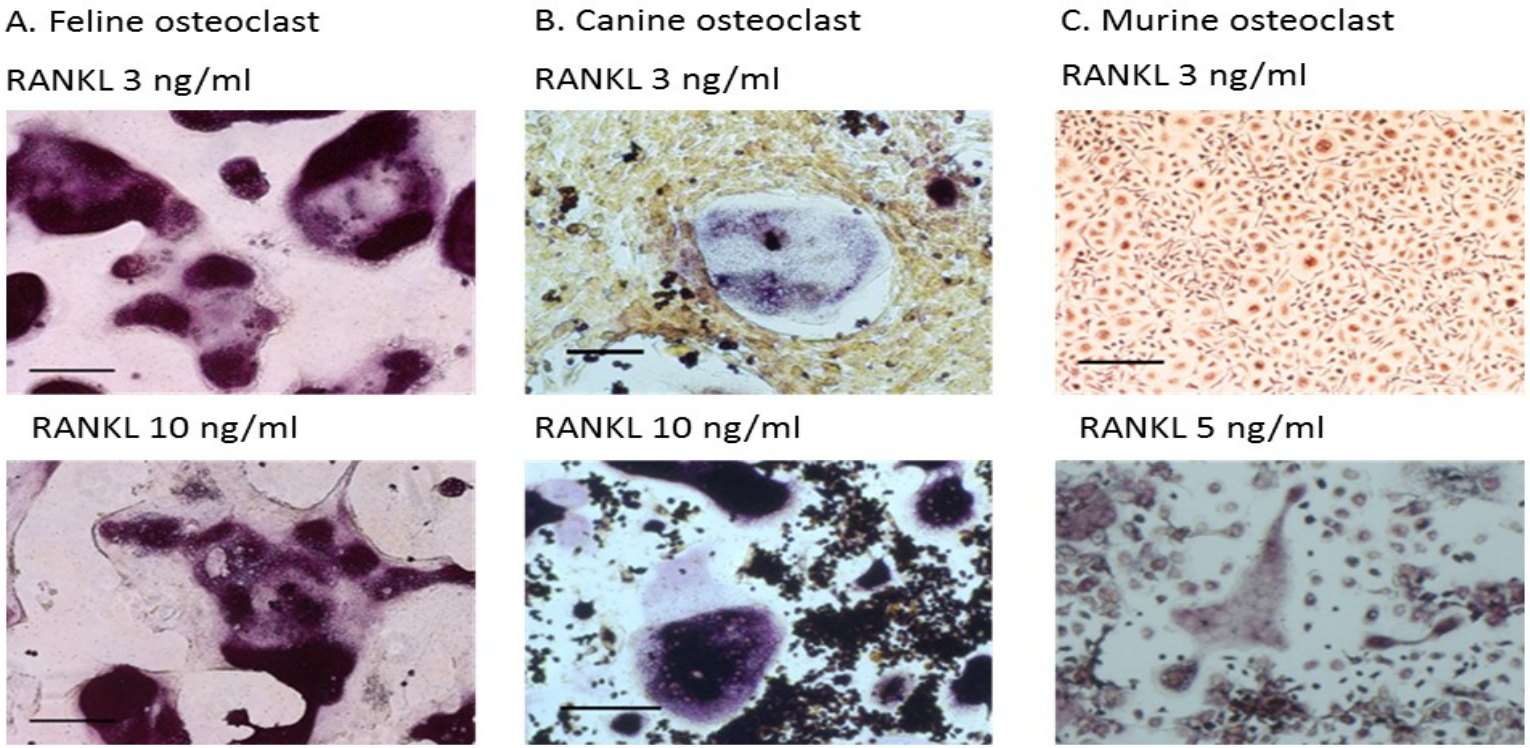

Figure 4.8 *In vitro* feline, canine and murine osteoclast differentiation. (A) Feline osteoclasts were able to differentiate into TRAP positive osteoclasts using mouse recombinant CSF-1 10 ng/ml and mouse recombinant RANKL at 3 -10 ng/ml. High concentration of RANKL induced feline osteoclasts fusion more quickly leading to the formation of giant osteoclasts and subsequent apoptosis. (B) When RANKL was used at the same concentrations as those used for feline osteoclast generation, only a few canine osteoclasts were generated. Higher RANKL concentration (10 ng/ml) was required for efficient canine osteoclast generation. (C) In mouse, a low RANKL concentration (3 ng/ml) caused the differentiation of small osteoclasts with two to three nuclei. Murine osteoclasts also required a higher RANKL concentration (5 ng/ml) for successful differentiation.

4.4.4 **Feline osteoclast characteristics *in vitro***

To further characterise the cultured osteoclasts, a number of criteria were tested: formation of an actin ring, and demonstration of expression of the vitronectin and calcitonin receptors, cathepsin K, c-Src and MMP9 by immunocytochemistry (Figure 4.9, A). PCR was able to confirm expression of osteoclast specific genes *ACP5*, *CTSK, ATP6V0D2* and *DCSTAMP* whose expression was not seen in the bone marrow mononuclear cells (Figure 4.9, B). For functional assessment of resorption activity of cultured osteoclasts, the cells were cultured on mineralised substrates using dentine discs or mineralised coated (hydroxyapatite) plates. Resorbed areas can be visualised clearly by light microscopy following toluidine blue staining (Figure 4.9, C). On mineralised plates the morphology of the osteoclasts were similar to that of osteoclast grown on plastic. The resorbed areas were identified as paler spots after a modified von Kossa procedure which stain mineralised areas a dark colour (Figure 4.9, C).

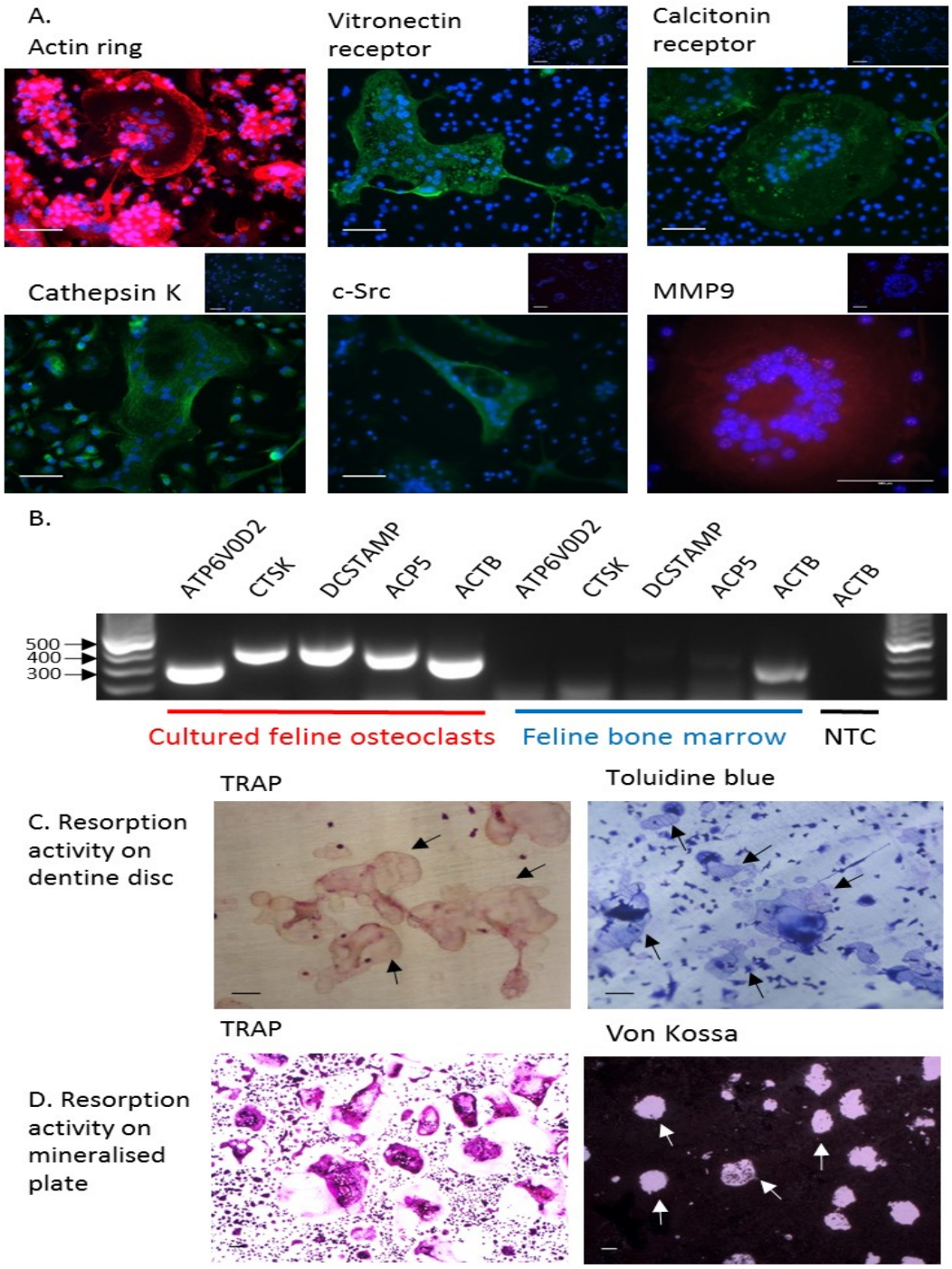

Figure 4.9 *In vitro* feline osteoclast like cells revealed typical characteristics of osteoclasts. (A) Immunocytochemistry reveals that cultured feline osteoclasts possess osteoclast characteristics such as formation of an actin ring, expression of vitronectin receptor, calcitonin receptor, cathepsin K, c-Src and MMP9. Small upper Insert images show corresponding negative isotope controls. (B) Expression of osteoclast specific genes ACP5, CTSK, ATP6V0D2 and DCSTAMP by PCR. Note that no expression of these genes in bone marrow mononuclear cells. (C) Resorption activity of cultured osteoclasts on a dentine disc shows resorption pit formation (black arrows) (D) Resorption activity of cultured osteoclasts on a mineralised substrate (hydroxyapatite plate) show resorption (white arrows). See text for further details. Scale bars = 100 µm.

4.4.5 Effect of $1,25(OH)_2D_3$ on feline osteoclastogenesis

As reported in section 4.4.2, there was no difference in *VDR* mRNA expression between TR –ve and TR +ve teeth. To further investigate any effect of $1,25(OH)_2D_3$ on feline osteoclast formation I used an *in vitro* system in which osteoclasts were generated from bone marrow derived osteoclast precursors with addition of $1,25(OH)_2D_3$ at various concentrations, ranging from physiological level (0.1 nM) to high dose (10 nM), to the osteoclast formation medium. Data of number of osteoclasts formed, resorption pits and resorption area were presented as percentage compared to control. The number of osteoclasts formed were similar in the presence of low concentration of $1,25(OH)_2D_3$ (0.1 nM) and control cultures (the osteoclast formation medium, supplemented with ethanol as a vehicle). The number of osteoclasts were increased compared to vehicle control with the addition of 1 nM of $1,25(OH)_2D_3$ treatment (115.0%, $p<0.05$) whereas osteoclast formation at higher doses of $1,25(OH)_2D_3$ (5 and 10 nM) was decreased (78.1% and 53.0% respectively, $p < 0.05$) in a dose dependent manner (Figure 4.10, A). In parallel, osteoclast precursors were seeded on mineralised plates to compare the effect of $1,25(OH)_2D_3$ on resorption activity (Figure 4.10, B). Resorption areas were seen as paled areas following a modified von Kossa staining. Low $1,25(OH)_2D_3$ doses (0.1 and 1 nM) produced an increased number of resorption pits compared to vehicle treated controls at 111% and 131% respectively but high doses (5 and 10 nM) led to a decreased number of resorption pits (56% and 32.8% respectively). A similar pattern was seen for resorption area; it increased at low $1,25(OH)_2D_3$ doses (133% at 0.1 nM and 160.1% at 1 nM) and decreased dose dependently at concentrations of 5 and 10 nM (67.3% and 37.4% respectively) (Figure 4.10, C).

A.

Vehicle

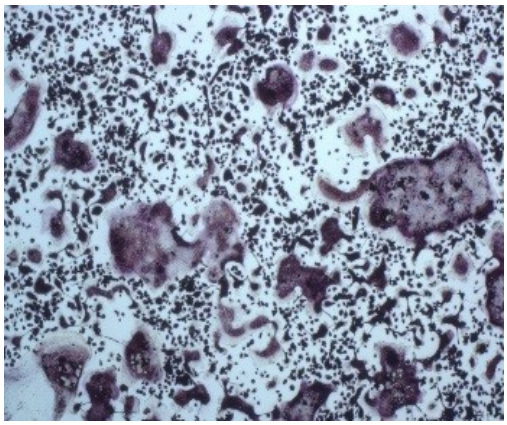

$1,25(OH)_2D_3$: 0.1 nM

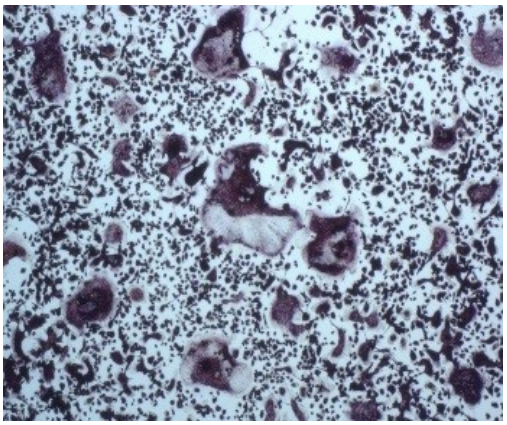

$1,25(OH)_2D_3$: 1 nM

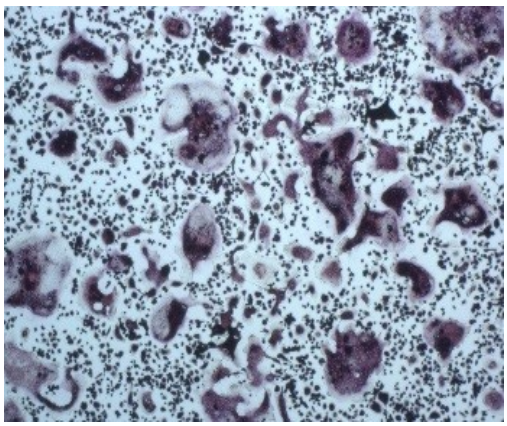

$1,25(OH)_2D_3$: 5 nM

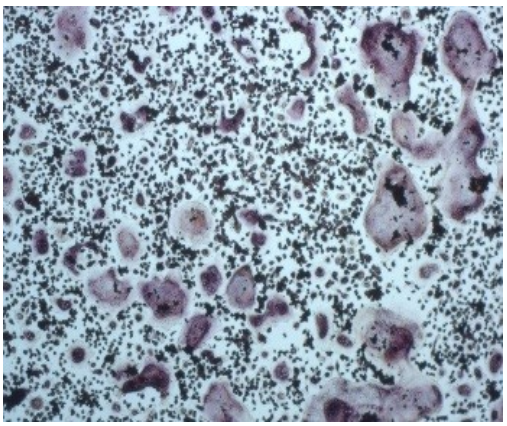

B.

Feline osteoclast formation with $1,25(OH)_2D_3$

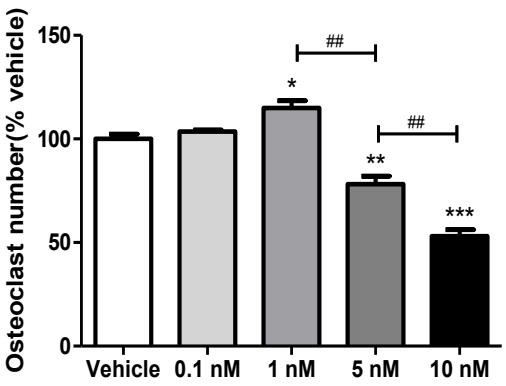

$1,25(OH)_2D_3$: 10 nM

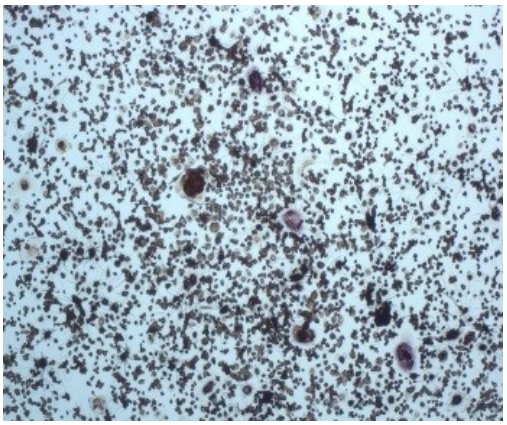

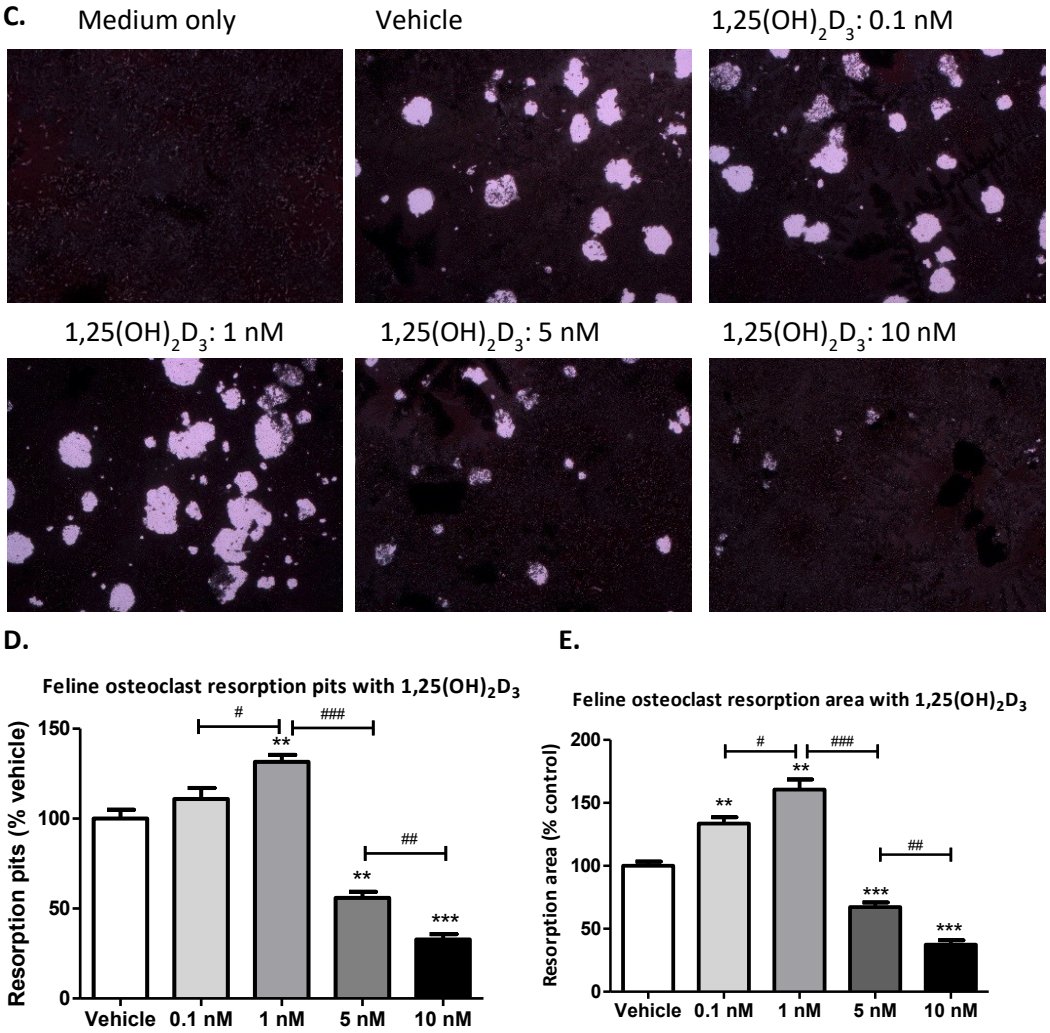

Figure 4.10 Low dose of $1,25(OH)_2D_3$ induced feline osteoclast formation and resorption but high dose of $1,25(OH)_2D_3$ showed an inhibitory effect on feline osteoclast formation and resorption. (A) Feline osteoclasts formation in the presence of various $1,25(OH)_2D_3$ concentrations and quantified result was generated as as bar graph (B). The osteoclasts formed a similar level at 0.1 nM of $1,25(OH)_2D_3$ compared to negative control (osteoclast formation medium, ethanol added as a vehicle) and it increased at 1 nM of $1,25(OH)_2D_3$. However higher doses of $1,25(OH)_2D_3$ (5 and 10 nM) inhibited osteoclast formation ($P < 0.05$) by two sample t-test. (C) Representative images of $1,25(OH)_2D_3$ effect on resorption activity of feline osteoclasts. Graphs of number of resorption pits (D) and resorption area (E) under the various $1,25(OH)_2D_3$ treatment. Low $1,25(OH)_2D_3$ showed increased resorption activity seen as increased resorption pits and area. High $1,25(OH)_2D_3$ induced inhibition of resorption activity by resorption pits and area. Data were combined from 3 independent experiments with technical replicates (n = 3). Data represent mean ± SDs bars. Images from (A) and (B) are shown as representative pictures. See the text for further details. Medium only: medium without CSF-1 and RANKL, Vehicle: osteoclast formation medium, ethanol added at the same concentration as diluted $1,25(OH)_2D_3$.

4.4.6 The role of periodontal ligament cells in osteoclastogenesis

Periodontal ligament cells were isolated at post mortem from the teeth of a cat with no TR lesions. Periodontal ligament cells were grown on plastic and their morphology revealed fibroblast-like cells with elongated shapes that attached to the culture plastic vessel. The cells expressed vimentin (a mesenchymal marker) and RANKL (to support osteoclast generation) by immunocytochemistry and PCR (Figure 4.11, A). Periodontal ligament cells were co-cultured with bone marrow osteoclast precursors and CSF-1 but without the addition of RANKL. This led to the *in vitro* generation of osteoclasts which were TRAP positive, multinucleated, exhibited actin staining, as well as expressed cathepsin K and vitronectin receptor (Figure 4.11, B). Lastly, they were capable of hydroxyapatite resorption on a mineralised substrate. The resorption area was seen on mineralised plate after removal of osteoclasts as a pale spot (Figure 4.11, C).

After confirmation of the presence of typical osteoclast characteristics for the cells generated in the co-culturing system, I compared osteoclast generation ability between osteoclast precursors from TR –ve and TR +ve cats using the same co-culture system (Figure 4.12, A). The number of TRAP positive multinucleated osteoclasts were higher in those derived from osteoclast precursors from TR + cats in the co-culturing system, under the osteoclast formation medium containing RANKL (Figure 4.12, B left graph). When osteoclast numbers were normalised to RANKL treated control TR +ve or TR -ve cells, the number of osteoclasts formed remained higher in the wells with osteoclast precursors derived from TR +ve cats than from TR –ve cat under the RANKL deprived co-culture condition (Figure 4.12, B, right graph). I then used this co-culturing system to test the effect of $1,25(OH)_2D_3$ on osteoclast generation in both population of cells; osteoclast precursors from TR + and periodontal ligament cells. $1,25(OH)_2D_3$ treatment using a high dose (10 nM) resulted in reduced osteoclast formation in the presence of periodontal ligament cells (Figure 4.13).

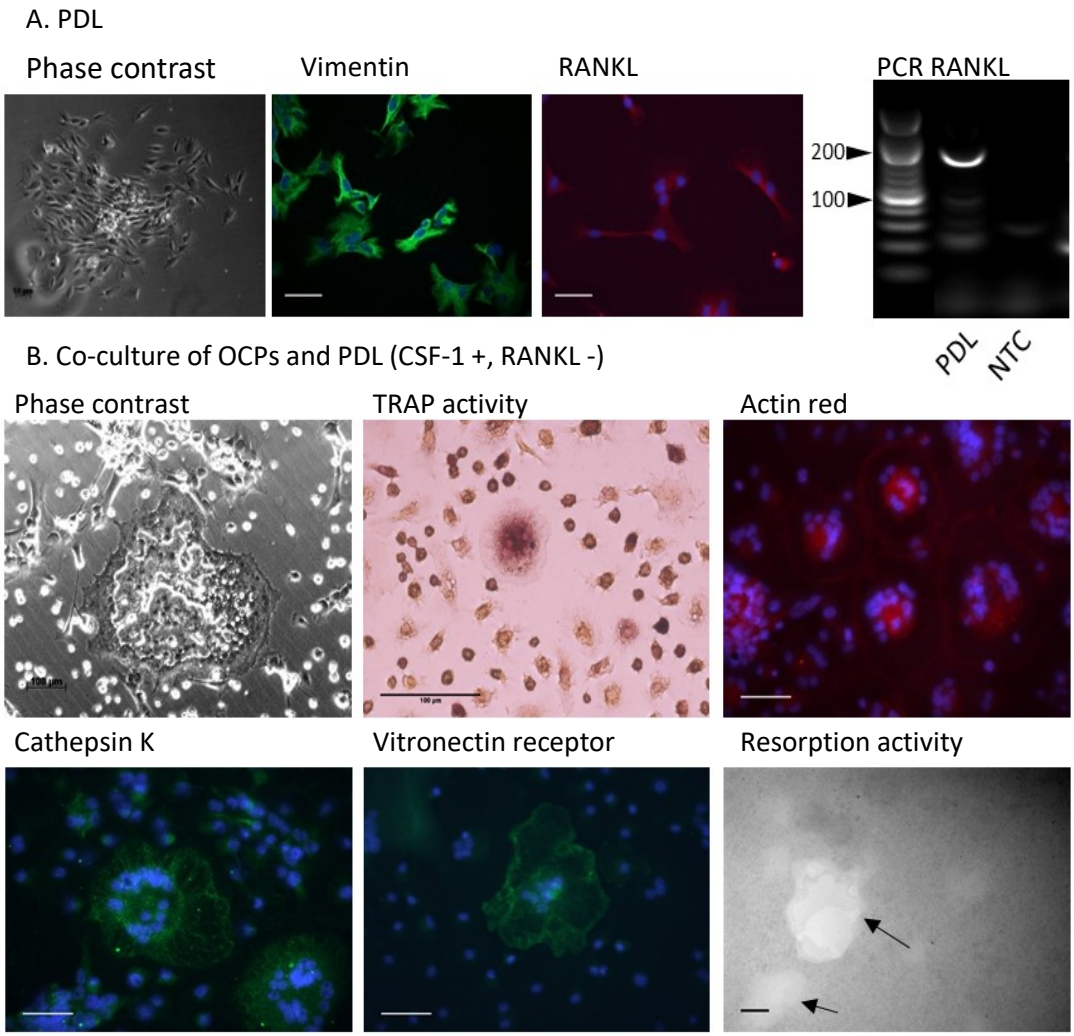

Figure 4.11 Functional feline osteoclasts were generated under the co-culture system of osteoclasts precursors and periodontal ligament without RANKL treatment. (A) Isolated fibroblast-like periodontal ligament cells expressed vimentin (a mesenchymal marker) and RANKL. (B) Co-culturing system of periodontal ligament cells and bone marrow osteoclast precursors successfully produced osteoclasts in CSF-1 (10 ng/ml) supplemented medium without RANKL. Cultured osteoclasts disclosed an osteoclast specific phenotype including TRAP positivity, multiple nuclei, as well as expression of CTSK and vitronectin receptor. Finally, they also revealed resorption activity seen as paled areas (arrows) on a mineralised plate. Scale bars = 100 µm.

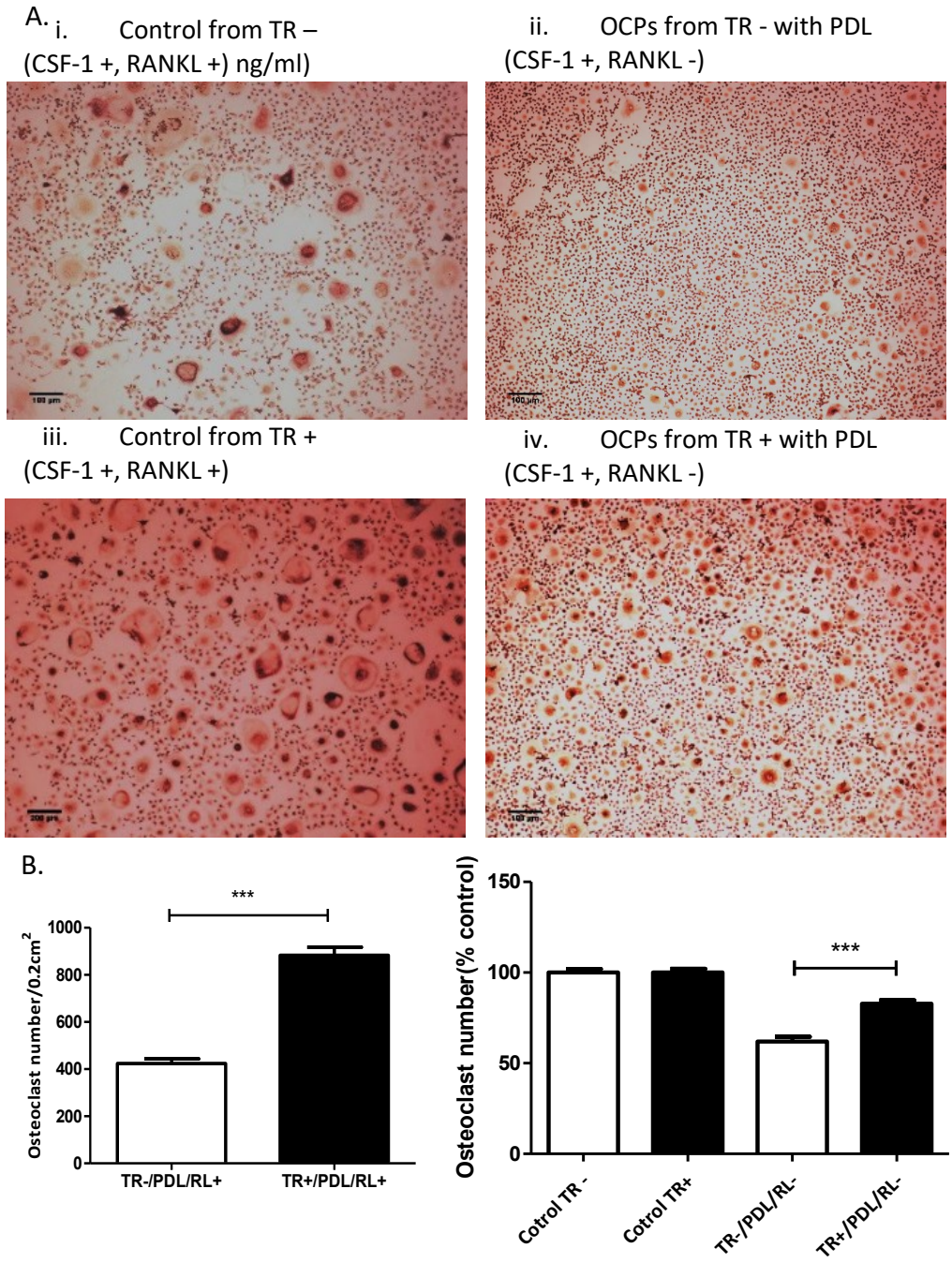

Figure 4.12 More osteoclasts were generated derived from TR +ve cats compared to TR –ve cat in the co-culturing system. (A) Co-culturing of periodontal ligament and osteoclast precursors from TR -ve or TR +ve cats. i. Osteoclast precursors from TR -ve were cultured with periodontal ligament cells in osteoclast formation medium (control). ii. Osteoclast precursors from TR -ve were cultured with periodontal ligament cells in medium supplemented CSF-1 only (10 ng/ml) without RANKL. iii. Osteoclast precursors from TR +ve were cultured with periodontal ligament cells in osteoclast formation medium as a control. iv. Osteoclast precursors from TR +ve were cultured with periodontal ligament cells in medium supplemented CSF-1 only (10 ng/ml) without RANKL. (B) Each treatment of A was quantified by number of TRAP positive osteoclasts and two graphs were generated.

Number of TRAP positive osteoclasts were higher in those derived from osteoclast precursors from TR +ve cats compared to from TR -ve cats under the presence of RANKL (B, left). When number of osteoclasts were normalised to control (RANKL treatment), osteoclast precursors from TR +ve cats produced more TRAP positive osteoclasts in co-culturing system without RANKL (B, lower graph). Data were combined from 3 independent experiments TR -ve or +ve cats (n = 3) with technical replicates (n = 3). Data represent mean with SEM bars ***; $p < 0.001$ by two sample t-test. Scale bars = 100 µm.

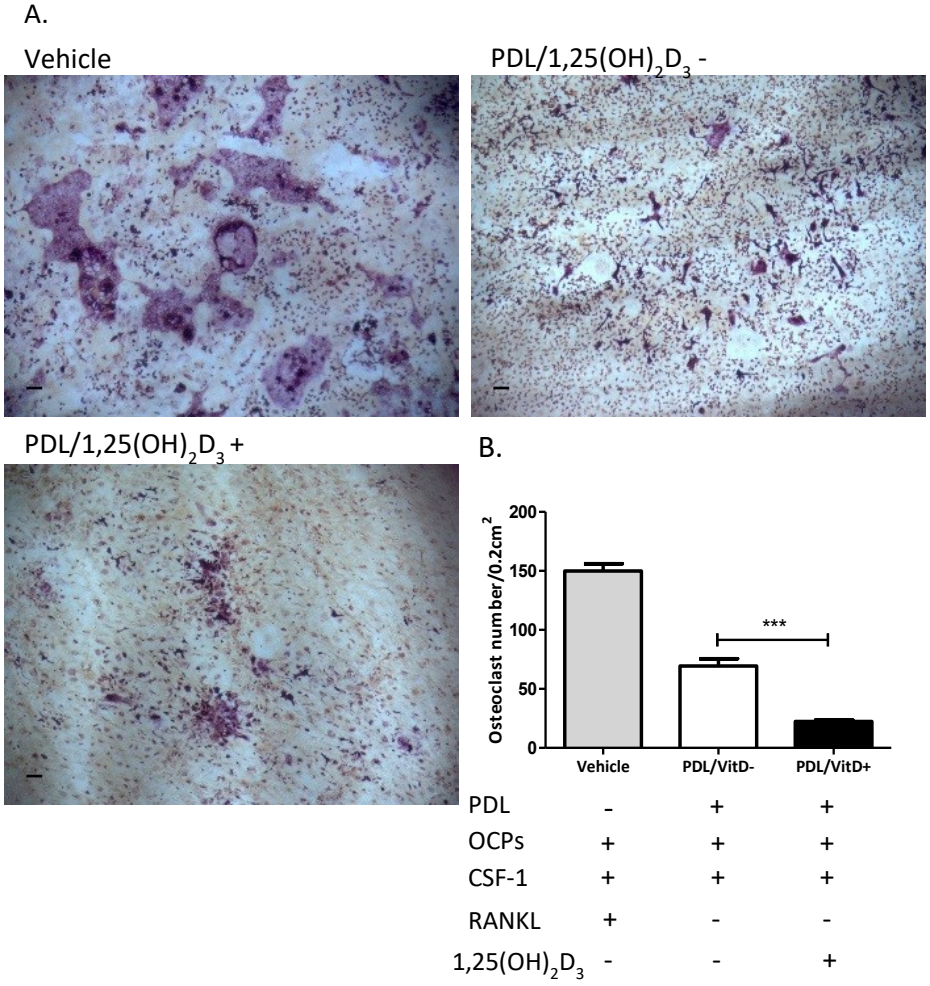

Figure 4.13 High dose of $1,25(OH)_2D_3$ revealed inhibitory effect on osteoclastogenesis in co-culture system. (A) shows the representative photos of on osteoclast formation in the presence of $1,25(OH)_2D_3$ in co-culture system osteoclast formation are shown in vehicle (upper left), co-culture without $1,25(OH)_2D_3$ (upper right) and with $1,25(OH)_2D_3$ (lower left). Graph (B) shows osteoclast formation in co-culture with periodontal ligament cells with/without $1,25(OH)_2D_3$. High dose $1,25(OH)_2D_3$ treatment (10 nM) reduced osteoclast formation on dentine discs under the presence of periodontal ligament cells compared to control (no $1,25(OH)_2D_3$ added). Data were combined from cells of 3 different TR +ve cats (n = 3) with technical replicates (n = 3). Data represent mean ± SEM bars *** $p < 0.001$ by two sample t-test. Vehicle: osteoclast formation medium, ethanol added as a vehicle. VitD: $1,25(OH)_2D_3$, OCPs: osteoclast precursors, PDL: periodontal ligament, RL: RANKL.
Scale bars = 100 µm.

4.5 Discussion

Both inflammation and vitamin D have been suggested as possible contributors to the development of tooth resorption in cats, however it has not been conclusively shown. The aim of the experiments shown in this chapter was to investigate the potential role of inflammation and vitamin D in tooth resorption. The prevalence of TR (87.5%) found in this study is higher than the reported prevalence (29 - 58%, average 43%) (102-105) although the population size of this present study is small (n = 24). The study population did have a higher mean cat age (8.5 years) than other studies (3.6 – 6.5 years) (102, 103, 105). Bias of small sample size and aged population may contribute to high prevalence. It has been reported in many studies that the incidence of TR increased with age and therefore TR could be considered as an age related condition. (103, 108, 114). In this study more than half of the samples were in the early stages (stage 1 and 2). Stage 1 is hardly detected by radiography and both stage 1 and stage 2 are not usually associated with any clinical signs (97, 106, 114). This implies that early stages of TR without clinical signs are possibly underdiagnosed in practice. Since feline TR has a progressive nature early lesions will develop to advanced stages (9), so this result would support performing survey radiographs of clinically normal teeth in animals that are in for dental treatments. Another finding is that the major type of TR in this study comprises Type 2 (81.7%) and the remainder is Type 1 or Type 3 (18.3 %). This contrasts with other published studies on much larger populations of cats (ref). One study of 543 cats showed that Type 1 (49.4%) and Type 2 (50.6%) had similar prevalence while another study reported a slightly higher percentage of type 2 (60%) than type 1 (40%) in 109 cats (99, 102). In Type 1 TR, the root of the tooth is not yet affected so it possess a normal radiographic appearance of roots and periodontal ligament space. In Type 2 TR, roots are attacked so present on radiographs lacking a clear periodontal ligament space although the lesions do not extend to the crown.

Although each study shows variable compositions of types in feline TR, authors agree that Type 1 TR are found more frequently with periodontitis and Type 2 TR are not. Therefore, Type 2 TR sometimes is considered as idiopathic TR rather than inflammatory. As our study population contained mainly Type 2 TR it is possible it may have caused a bias towards the idiopathic type of TR.

This chapter investigated the local expression of inflammatory cytokines *IL1B, IL6, P2X7R, TNF* and *IFNG*, as well as *RANKL*. Conventional PCR and melt curve by post analysis of qPCR revealed expression of all genes of interest in feline teeth, but there were no difference in expression detected for any inflammatory cytokines, and RANKL between TR –ve and TR +ve teeth. When sub-group comparisons were performed, only early TR showed higher IL-6 expression than TR –ve teeth but it did not when compared to advanced TR +ve teeth. This result implies that there is no major inflammatory process involved in TR +ve teeth when compared to TR –ve teeth, but IL-6 could potentially be re-considered to contribute to initiate TR. In terms of inflammatory cytokines, two studies have revealed higher expression of IL-1β and IL-6 and one study reported higher expression of IFN-γ and TNF-α in TR +ve teeth (100, 163). These results differ to what I found in my study.

With regards to RANKL however, the results were consistent with what has been reported in the literature, with RANKL expression not increasing in TR +ve teeth when compared to unaffected control (100, 163). There could be a couple of reasons for this; one reason for no observed difference in RANKL expression between groups is possibly that the lifespan of osteoclasts (about 2 weeks) and the process of differentiation of osteoclasts is relatively short so that it is hard to capture the moment of osteoclast formation (253). This is supported by a histological study where authors mentioned the difficulty of identifying odontoclasts and osteoclasts in sections of TR affected teeth due to the relatively quick process of osteoclast formation and activation (9). Another point is that samples used for qPCR comprise Type 2 as the major type. Type 2 is characterised by a narrowing or disappearance of the periodontal ligament and replacement resorption whose features might be considered to be non-inflammatory and idiopathic (113). Another possible

explanation is the technical limitations of this study. Most primers were based on sequences from published papers in order to allow for a comparison of results. However, the efficiency of several primers was beyond the recommended range (90-110%) (254). The *IL-1β* primer in the published paper was found to be against *IL-1α* rather than *IL-1β*. When new primers were designed their primer efficiency was not optimal. This is one of the major concerns reported when using intercalating dye (*e.g*. SYBR™ green), because intercalating dyes bind to any double-stranded DNA product and suboptimal primer efficiency can be due to non-specific sequence binding of dye (*i.e.* primer-dimer formation). Data can be reanalysed using a data analysis model which takes efficiency into account for the calculations suggested by Hellemans et al. (255, 256). Another way to overcome this technical limitation is the use of probe-based assays. The hydrolysis probe based assay has additional specificity from the probe amplicon specific primers which is a third sequence that has to bind within the amplicon of the target sequence in order to generate a fluorescent signal (251, 257). In future studies it would be recommended to use hydrolysis probes to confirm these results.

Another aim of this study was to set up an *in vitro* feline osteoclast model applicable for studying feline osteoclast biology. There are successful methods available for osteoclast formation in a range of animals. However, efficiency of osteoclast formation largely relies on components of growth medium (e.g. CSF-1, RANKL and serum as a major source of nutrient) (229, 258). Therefore each laboratory needs to develop an optimised culture system on their own. I modified previously developed osteoclast culture protocols (227-229). Here I used peripheral blood and bone marrow as a source of osteoclast precursors. Obtaining sufficient blood from cats for osteoclast culture was for ethical reasons not possible in our set up. The monocytes, the source of osteoclast precursors in peripheral blood occupy less than 10% of the white blood cells in the buffy coat layer. Hence the total volume required to gain sufficient monocytes was not ethically viable to withdraw as residual blood from the cats coming through the clinic. For this reason, sufficient amount of blood was accessible only at post mortem. Blood quickly coagulates

when taken at post mortem and the drug used for euthanasia (e.g. pentobarbital) might affect circulating monocytes. A previous study showed pentobarbital modulated several inflammatory cytokines including IL-1, IL-6 and monocyte chemotactic protein-1 (MCP-1) (259). Blood derived osteoclast formation was less efficient and non-accessible compared with bone marrow. On the other hand, bone marrow from long bones possessed enriched haematopoietic cells and *in vitro* generation of osteoclasts was robust, quick and efficient. The number of osteoclasts differentiated in this model system was similar to that reported in other studies (167, 245). The high efficiency of osteoclast formation from bone marrow derived osteoclast precursors might be a consequence of high numbers of haematopoietic stem cells which upon addition of CSF-1 osteoclast cell linage commitment is stimulated. However, morphologically TRAP positive multinuclear cells are easily detected and this gold standard indication of osteoclasts was efficient to distinguish the osteoclasts from other stromal cells (227, 229, 260). In terms of osteoclast formation in cats, feline osteoclasts effectively were differentiated from precursors with low amount of RANKL addition (3 ng/ml) compared to murine or canine osteoclasts (10 ng/ml). The relative size of osteoclasts with more number of nuclei in cats were larger than other osteoclasts derived from other species (mouse and dog). This was also documented in other feline osteoclast study which demonstrated that feline osteoclasts appeared earlier *in vitro* feline osteoclast formation with greater numbers of nuclei than in human osteoclasts cultures (228).

I also tested RAW 264.7 the mouse macrophage cell line as it is a widely used cell line (226). However, it required high concentrations of RANKL and osteoclast differentiation was not consistent, and the cell line lost its osteoclast differentiation ability when passaged. The RAW cell line is highly heterogenetic so only a certain population of cells was able to differentiate into osteoclasts. This heterogeneity and the problem with the higher passages (18–20 passages) were mentioned in other studies (226, 261). It is also considered that bone marrow derived osteoclasts and RAW cell derived osteoclast are different as the RAW cells can produce CSF-1 themselves and they already express high RANK which are equivalent of mid-stage

of precursors during osteoclast differentiation. The RAW cells may differ in terms of osteoclast biology for example their resorption activity, survival and apoptosis (226).

I tested the characteristics of the cultured feline osteoclasts to demonstrate they had genuine osteoclastic features. The cultured feline osteoclasts expressed a range of osteoclast markers, consistent with markers reported in other studies (227, 228, 245). This provides strong support that my cultured osteoclasts were authentic osteoclasts similar to findings in other studies (228, 262, 263). For resorption activity, I used dentine discs and mineralised plates. Dentine discs are similar to bone as it consists collagen and hydroxyapatite whereas mineralised plate was made up with hydroxyapatite with no collagen present. Dentine discs or bone slices are the gold standards for testing resorption activity however, due to the limited accessibility of these animal derived sources alternative methods have been used (264-266). One benefit to using mineral coated plates is easy handling and early non-adherent osteoclast precursors are distributed equally. Dentine discs need to be transferred from smaller into larger plastic vessels and a decent number of osteoclast precursors can be lost during this step.

A previous study found an increased expression of VDR mRNA in TR +ve teeth. This suggested, that $1,25(OH)_2D$ might play a role in pathological tooth resorption in cats since $1,25(OH)_2D$ induces RANKL mediated osteoclast activation and it acts through VDR (100, 122). They also reported that increased VDR was correlated with increased mRNA expression of inflammatory cytokines (IL-6 and IL-1β) (100). However, the results did not reflect increased odontoclast activity because RANKL or OPG expression did not change (100). To investigate the role of VDR in feline TR, I also performed conventional PCR and qPCR and showed that feline teeth from TR -ve or TR +ve expressed VDR mRNA. The VDR expression in teeth was consistent with the previous studies. This might support the concept that teeth can use $1,25(OH)_2D$ directly in a paracrine manner whereas the local level of $1,25(OH)_2D$ might affect odontoclast activity (186, 194, 267). However, mRNA expression of VDR expression was not different between TR –ve and TR + teeth in

this study. To confirm this, further studies using a larger number of samples may be required. To further investigate the effect of vitamin D on feline osteoclasts, active vitamin D, $1,25(OH)_2D_3$ was used at concentrations ranging from physiological serum levels up to 100 times that level since $1,25(OH)_2D_3$ is known to act as a direct stimulator of osteoclasts *in vitro* (100). When doses just above a physiological level of $1,25(OH)_2D_3$ (1nM) was used, stimulation of osteoclast formation was observed but at high doses of $1,25(OH)_2D_3$ a decrease in osteoclast formation was observed. When testing their resorption activity, both number of resorption pits and resorption area showed the same trend i.e. low doses induced an increase in resorption activity and high doses decreased the resorption activity of the osteoclasts. $1,25(OH)_2D_3$ is known as a stimulator of osteoclastic bone resorption (160, 194). This is thought to occur via direct stimulation of osteoblasts/stromal cells to increase their RANKL production leading to osteoclast formation rather than through osteoclasts themselves *in vitro*. However, *in vivo* vitamin D has a dual activity of bone formation and resorption, hence its role in the body is complex (170, 185). It has been shown that osteoclasts are capable of metabolising $1,25(OH)_2D$ and $25(OH)_2D$ as they showed mRNA expression of VDR and anabolic/metabolic enzymes (122, 186, 267). However molecular mechanisms involved in this process are still uncertain.

Periodontal ligament cells were isolated from a TR -ve cat at post mortem. The primary periodontal ligament cells were cultured and maintained in limited passages (no more than four passages). The periodontal ligament cells expressed RANKL by immunocytochemistry and PCR, which indicates periodontal ligament cells may be capable of inducing osteoclast formation. Co-culturing of periodontal ligament cells and osteoclast precursors in a long term culture (2-3 weeks) supported this concept. Osteoclast progenitors were capable of differentiating into osteoclasts under the presence of periodontal ligament cells without the addition of RANKL. The osteoclastogenesis occurred both when the cells were directly and indirectly co-cultured. Direct co-culturing requires a direct contact of two populations of cells, osteoclast precursors and RANKL providing cells while

indirect co-culturing it is not necessary for the cells to be in physical contact. It has been shown that dental cells, and especially periodontal ligament cells, increase their RANKL expression as a response to a mechanical load (*e.g.* orthodontic treatment) and induce alveolar bone resorption for effective tooth movement (142, 196, 268). RANKL exists in two forms; soluble RANKL and as a transmembrane protein (269). As transmembrane RANKL is more powerful than the soluble form of RANKL for osteoclastogenesis, direct contact between osteoblasts and osteoclast progenitors was considered a necessity for osteoclast formation (269-271). However, here feline osteoclast formation occurred when indirect culture of the two cell populations were performed which implies soluble RANKL efficiently lead to osteoclast formation. RANKL protein was not detected by western blot (data not shown) I tried two commercially available antibodies however, none of them were capable for detecting feline RANKL at the predicted molecular size of the protein. Interestingly, osteoclast precursors from TR +ve cats yielded higher numbers of osteoclasts under co-culture conditions compared to TR -ve cats. These data suggest that TR +ve osteoclast precursors were more responsive to RANKL expressed by periodontal ligament cells. If this is the case, it may explain why some cats are prone to attack by odontoclasts and get tooth resorption. Co-culturing of periodontal ligament and osteoclast precursors was used to test the effects of $1,25(OH)_2D_3$ in this system. High dose of $1,25(OH)_2D_3$ inhibited periodontal ligament cells induced osteoclast formation. However, the RANKL or OPG expression of periodontal ligament cells was not investigated and therefore it is noit possible without further study to explain how this inhibitory effect of $1,25(OH)_2D_3$ on osteoclast work. In future studies, the effects of various concentrations of $1,25(OH)_2D_3$ on *in vitro* osteoclast formation and osteoclast related gene expression *e.g.* RANK/RANKL/OPG are required.

In this chapter, differentially expressed genes between TR –ve and TR +ve teeth were investigated for inflammatory cytokines and VDR. The genes investigated were selected based on previously reported links to TR. This approach is however rather limited as it is dependent upon prior knowledge and therefore in

the following chapter, I will examine RNA-seq data between TR –ve and TR +ve teeth so as to identify all transcriptomic changes which might reflect odontoclast dysregulation in TR.

Chapter 5 Identification of feline tooth transcriptomic changes in TR

5.1 Abstract

Gross and histological features of tooth resorption lesions in cats are well described. However, few studies have explored the cellular and molecular aspects of TR. There is no transcriptome analysis of feline teeth to the best of the author's knowledge. The aim of this chapter was to investigate transcriptome changes using RNA sequencing (RNA-seq) and identify candidate genes which might be responsible for the development of TR. Fourteen cDNA libraries from seven TR -ve and seven TR +ve teeth from eleven cats were generated and sequenced. Data were analysed under three comparisons: TR cat (TR -ve vs.TR +ve cats)[1], TR tooth (TR -ve vs. TR +ve teeth)[2], and paired TR (TR -ve vs. TR +ve teeth from the same cat)[3]. Of these the paired comparison proved the most powerful comparison and revealed 1,732 significantly differentially expressed genes (up-regulated genes; n = 1,286, down-regulated genes; n = 446). Pathway analysis revealed up-regulated genes that are involved in osteoclast differentiation and calcium signalling. Gene ontology enrichment analysis as a reflection of over represented set of genes presented many gene sets involved in muscle physiology including actin binding, myofibril, actin cytoskeleton, muscle contraction, heart contraction, muscle fibre development, skeletal muscle cell differentiation and muscle organ morphogenesis which are also abundantly expressed in developing teeth and bone. These features of the transcriptome might suggest that TR +ve teeth undergo reparative or remodelling processes mediated by dental, periodontal ligament, or alveolar bone cells in response to resorption and similar to tooth development, bone remodelling and repair.

[1] 'TR -ve cats' means teeth collected from a cat without any TR lesion and 'TR +ve cats' means teeth collected from a cat with at least one TR lesion.

[2] 'TR tooth' compares TR status of individual teeth. TR -ve teeth can be collected from TR free cats or TR diagnosed cats. TR +ve teeth are collected from TR +ve cats

[3] 'Paired TR' compares TR -ve teeth and TR +ve teeth from same cat.

A list of candidate genes for further investigation were chosen due to their involvement in osteoclast differentiation, a crucial step in tooth resorption and development. These included *SPI1*, *CTSK*, *ACP5*, *MMP9*, *RANKL*, *OPG* and P2XR genes. These genes were highly expressed in TR +ve teeth and the RNA-seq data were validated by quantitative PCR. Although *RANKL* expression was not different, *OPG* was highly expressed in TR -ve teeth, which resulted in a relative increase in the *RANKL*/*OPG* ratio in TR +ve teeth. Of these, *MMP9* was regarded as one of target genes related to feline TR since it showed consistent up-regulation with a high fold change in TR +ve teeth by qPCR and RNA-seq. Many SNPs in candidate genes were identified by RNA-seq data and some missense variations were also detected by Sanger sequencing. The functional effect of these SNPs requires further investigation.

5.2 Introduction

It has been well documented that pathogenesis of feline TR is caused by dysregulation of odontoclasts (92, 98, 113). However, the cellular and molecular changes present in TR are still unknown as previous studies have been limited to the investigation of predetermined factors including inflammatory cytokines, hormones, or specific markers in blood. All these studies relied on the use of primers or antibodies suitable for feline genes and protein targets respectively (100, 163, 176). Although qPCR is the most effective way to quantify each transcript among samples, the overall set of transcripts defined as the transcriptome cannot be accomplished by qPCR approaches. The development of high-throughput next generation sequencing methods (*e.g*. RNA-seq) have overcome these technical limitations and are capable of mapping and quantifying transcriptomes (208). RNA-seq has gained popularity in the last decade and is now widely used in *in vitro* experiments investigating developmental or disease status in many species (211, 272). However, no transcriptome analysis of feline teeth has been previously reported. The aim of this chapter was to perform RNA-seq in feline teeth and identify transcriptome changes in TR teeth compared with controls.

As Chapter 3 demonstrated, a RNA isolation protocol for use on feline teeth was optimised to produce a high yield of good quality RNA suitable for RNAs-seq. Chapter 4 showed that previously reported genes of interest including inflammatory cytokines and VDR did not show differences in expression between TR -ve and TR +ve teeth in contrast to findings in previous studies (100, 163). Since RNA-seq is a highly technical and sensitive tool, preparation of cDNA libraries, sequencing and initial data analysis, including differentially expressed genes were performed by Edinburgh Genomics. Data analysis of RNA-seq requires professional computational skills (bioinformatics) so the RNA-seq data analysis including gene sets and pathways analysis was supported by bioinformatician Dr Stephen Bush. Since computer programing and developing pipelines for a specific analysis are beyond the scope of my study, I did not write and run software programs by myself. However during data analysis, I was involved at every step of output data and guided how to use the data. My role in this chapter was to design the study, collect samples, identify problems or errors, decide how to use RNA-seq data and summarise the data so as to maximise the meaningful output from the generated RNA-seq data.

In this chapter the transcriptomic analysis revealed important information about tooth resorption pathogenesis, and helped to develop a list of candidate genes that are potentially involved in osteoclast biology. These candidates could be potential targets for treatment of odontoclast dysregulation.

5.3 Materials and methods

5.3.1 Selection of samples and RNA-seq

RNA isolation and RNA-seq methods were detailed in section 2.2.2. Information of samples for RNA-seq are described in Table 5.1.

Sample ID	Extracted teeth	TR status	TR type	TR stage	Description of TR status	RIN[e]	RNA yield (mg)	Age	Sex
N14C12TR-	307,308, 407, 408	-	N/A	N/A	No TR lesion	4.5	10.3	4	F
N28C15TR-	307, 407	-	N/A	N/A	No TR lesion	7.3	9.0	9	FN
N29C25TR-	307, 407	-	N/A	N/A	No TR lesion	6.7	8.0	10	FN
N19C21TR-	308	-	N/A	N/A	TR - tooth	5.3	8.2	16	FN
N21C27TR-	407	-	N/A	N/A	Paired TR - tooth	4.1	8.4	7	FN
N23C30TR-	309	-	N/A	N/A	Paired TR - tooth	4.4	9.0	10	FN
N25C32TR-	308	-	N/A	N/A	Paired TR - tooth	4.9	8.7	9	FN
N08C8TR+	307, 407	+	2	2	TR + tooth from TR +cat	5.2	5.8	> 5	F
N30C16TR+	308	+	2	2	TR + tooth from TR +cat	4.7	9.1	5	FN
N27C23TR+	108	+	3	4	TR + tooth from TR +cat	7.3	0.8	6	FN
N32C29TR+	108	+	3	4	TR + tooth from TR +cat	7	9.7	7	FN
N22C27TR+	404	+	2	2	Paired TR + tooth	5.9	7.4	7	FN
N24C30TR+	307	+	2	2	Paired TR + tooth	5.2	9.0	10	FN
N26C32TR+	407	+	3	4	Paired TR + tooth	6.3	8.5	9	FN

Table 5.1 Phenotyping of TR and selection of samples for RNA sequencing. N/A: not applicable, F: female, FN: female neutered, RNA yield shows total yield.

5.3.2 **RNA-seq Data analysis**

Mapping to the feline reference genome, generation of a Table of read counts, and MDS plots were previously described in section in section 2.2.5. As discussed in Chapter 3, clustering of RNA samples by MDS plot was visualised to explore the overall expression profiles between samples. MDS plots can be used for analysis and quality control. When data are plotted in a default mode, leading fold-change is set as the root-mean-square of the largest 500 log2-fold changes between samples (218, 273). Therefore, the distance between samples in a MDS plot means the leading log-fold change of genes that best distinguish each pair of samples. The sample **N27C23TR+** (a low yield RNA) was seen to be separated from the other 13

samples, occupying the top left corner of the MDS plot (Figure 5.1, A). Therefore this sample was considered as an outlier. Figure 5.1, B shows the MDS plot with the outlier excluded. All samples distributed evenly. MDS of samples from TR -ve teeth which are labelled in black are located to the left of samples from TR +ve teeth (labelled in red) except the sample **N08C8TR+**. Even though the **N08C8TR+** was re-confirmed as TR +ve teeth, its transcriptome shows more similarity to the TR -ve group. Therefore two samples from the 14 RNA-seq samples were excluded from further analysis.

A. MDS plot from all 14 samples

B. MDS plot excluding the outlier sample

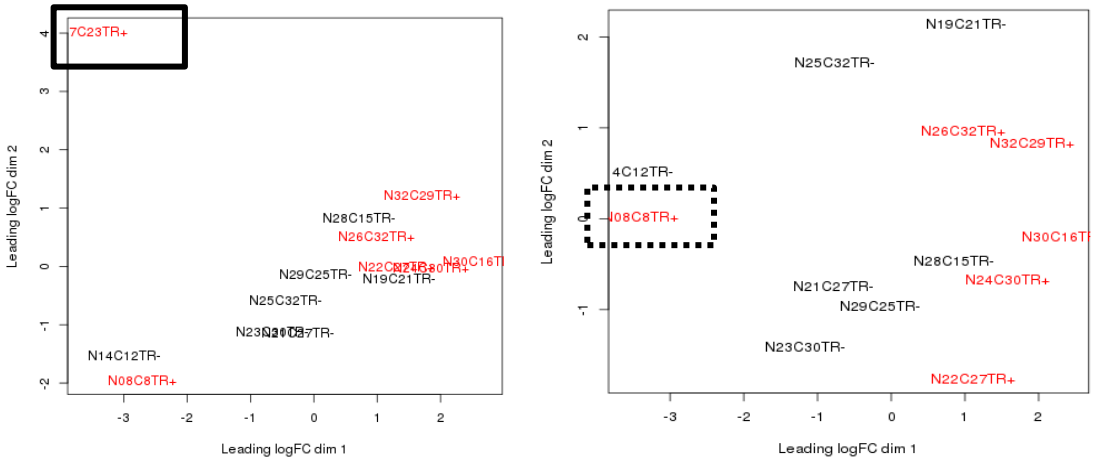

Figure 5.1 Sample selection for data analysis. (A) MDS plots for RNA-seq data from all 14 samples. Lined square indicates an outlier. Distance between samples indicates similarity. (B) MDS plots of RNA-seq data excluding the outlier (**N27C23TR+**). Dotted square, the sample **N08C8TR+**, shows similar data to TR -ve samples.

From the remaining 12 samples, three comparisons were performed as displayed in Figure 5.2, (1) TR -ve cats (n= 3 from TR -ve cats) and TR +ve cats (n = 5 from TR +ve cats)[1], (2) TR -ve teeth (n = 7 from TR –ve teeth) and TR +ve teeth (n = 5 from TR +ve teeth)[2], and (3) paired TR, TR -ve (n =3 from TR –ve teeth) and TR +ve (n= 3 from TR +ve teeth)[3]. Differentially expressed genes, gene sets and pathways were identified as described in section 2.2.6 and 2.2.7, respectively.

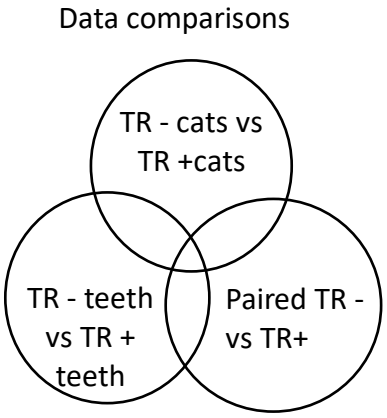

Figure 5.2 Data comparisons. Twelve RNA samples were divided into three comparisons.

5.3.3 Validation of a RNA-seq result

The list of differentially expressed genes were validated by qPCR. Primer sets were designed as described in section 2.1.4. Primers used in this Chapter are listed in Table 5.2. Primers for the reference genes, CTSK, and RANKL were previously shown in Table 4.1. Primer efficiency and specificity of PCR products were confirmed as described in section 4.3.4. Quantitative PCR was performed using SYBR™ Green based reagent, 2×Takyon for SYBR™ Assay - Low ROX (Eurogentec, Belgium) using Stratagene MX3000P qPCR system (Agilent Technologies) as described in section 2.1.6. The thermal cycling conditions are shown in Figure 5.3.

5.3.4 Identification of SNPs

SNPs were identified using the RNA-seq data as described in section 2.2.8. Sanger sequencing was used for a direct identification using TR +ve teeth samples as described in section 2.1.10.

Primer sets	Sequence (5’ -3’)	Amp (bp)	Tm (°C)	Reference
SPI1	F; GAAACAGGCAGCAAAAAGAAG	125	53.9	XM_019812398
	R; TTGGACGAGAACTGGAAGG			
OPG	F; TGTCCAGATGGGTTCTTCTCG	175	57	KX610462
	R; CGCACAGGGTGACATCTATTC			
MMP9	F; TGCCACTTCCCTTTCACCTTC	170	58	XM_003983412
	R; TTGCCTTCTCCATTGCCGTC			
P2X2R	F; GCTCCTCATCCTGCTCTACTTC	153	56.7	XM_023241231
	R; TTCACGTACTCCTCCACGTC			
P2X4R	F; TCACCCCAGAGAAAGTTCC	93	54.5	XM_023241408
	R; CGCCCTACACACAAAACAC			
P2X6R	F; ACTTCAGGACAGCCACTCAC	198	56.6	XM_023241697
	R; ACAACAGCAGCAGATCACAG			
PLCB4	F; CACTACTTCATCAGTTCTTCCC	144	53.1	XM_023251453
	R; GTCTTCACCTTTTCCATCCC			
CA6	F; CTGAAGGCTCTGAAACTGAC	180	54.2	XM_003989566
	R; GCTGATCTCTGAGGACTCAC			
CA4	F; CCAGACCCAAGATGAACACC	141	55.2	XM_003996604
	R; CAGTCCAGACAACCTTCTCC			

Table 5.2 Primers used in this chapter.

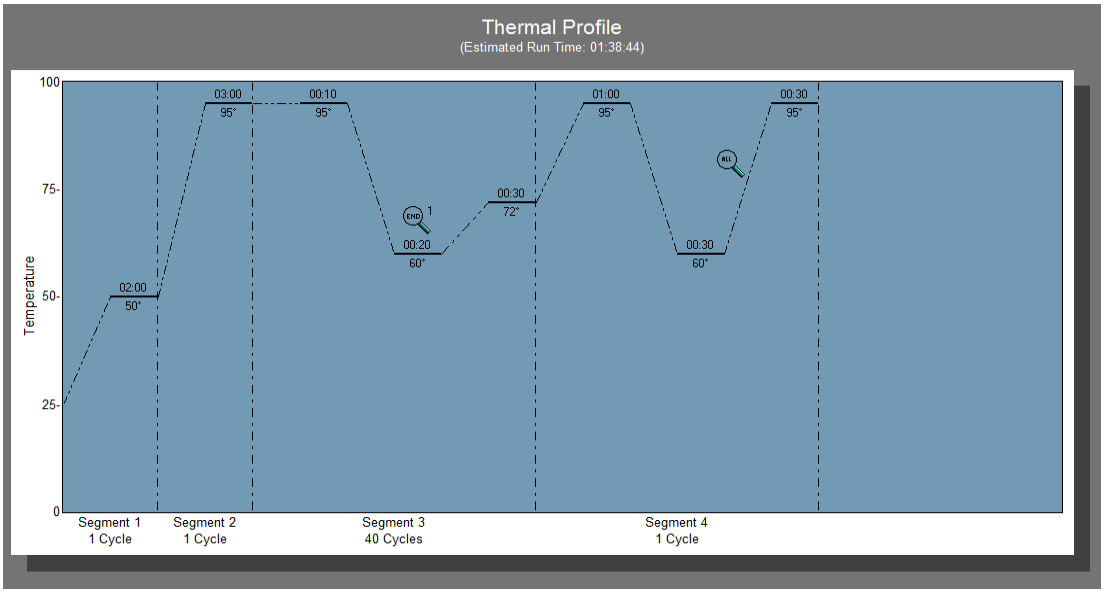

Figure 5.3 Thermal cycling condition used in this chapter.

5.4 Results

5.4.1 Data comparisons of RNA-seq results

The raw RNA-seq data were made publically available (European Nucleotide Archive, accession PRJEB24183, https://www.ebi.ac.uk/ena) as previously described in Chapter 3. MDS plots of each comparison, TR -/+ve cats, TR -/+ve teeth or paired TR are shown in Figure 5.4. In all three plots, the clustered TR - ve group is separate from the TR +ve group. Given that the distance between samples reflects similarity *e.g.* the closer they are the more similar they are, TR -ve and TR +ve samples from TR -/+ cats and TR -/+ teeth comparisons are closely plotted which implies their expression levels are similar (Figure 5.4, A and B). On the contrary, in the paired comparison, TR -ve samples are widely separated from TR +ve samples which indicates there are likely to be more significant expression differences between paired TR -/+ than other two comparisons (Figure 5.4, C).

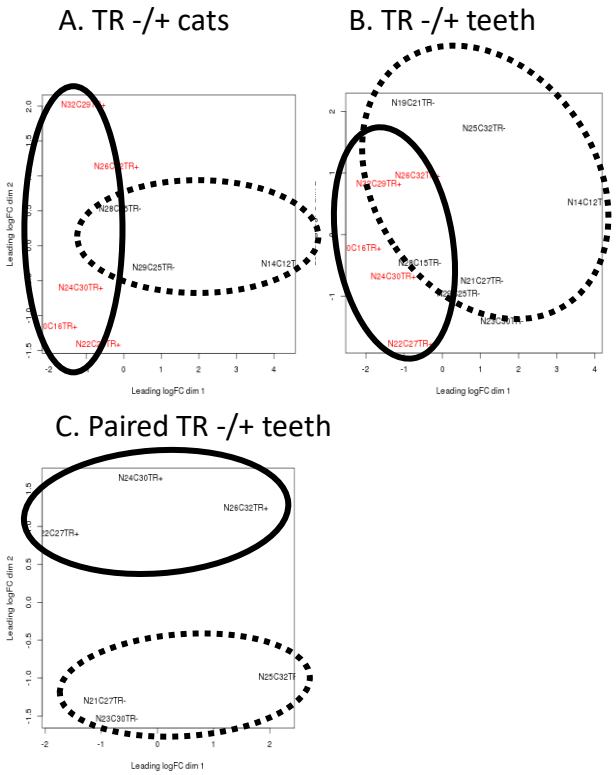

Figure 5.4 MDS plots showing RNA-seq data relationships between samples. (A) MDS plot of TR -/+ cats comparison, (B) MDS plot of TR -/+ teeth comparison, (C) paired TR-/+ comparison (within cat comparison). Lined circle: TR +ve samples, dotted circle: TR –ve (control teeth). See text for more details.

5.4.2 **Differentially expressed genes from RNA-seq**

The raw count reads that map to each transcript sequence were generated for transcript quantification (Supporting information 1). The smear plot visualises the relationship between overall expression level measured in counts per million (CPM) on the x axis and log2 fold-change (FC) on the y axis where differentially expressed genes are displayed in red (Figure 5.5). As expected, the largest number of differentially expressed genes was seen in paired TR -/+ ve teeth (Figure 5.5, C). The total number of transcripts detected amongst teeth samples was 16,366, 16,745, 16,307 in TR-/+ cats, TR -/+ teeth and paired TR -/+ teeth, respectively (Table 5.3Table 5.3). Of these, the largest number of statistically differentially expressed genes was identified in paired TR group yielding a total of 1,732 genes comprising 1,286 up-regulated genes and 466 down-regulated genes (Table 5.3).

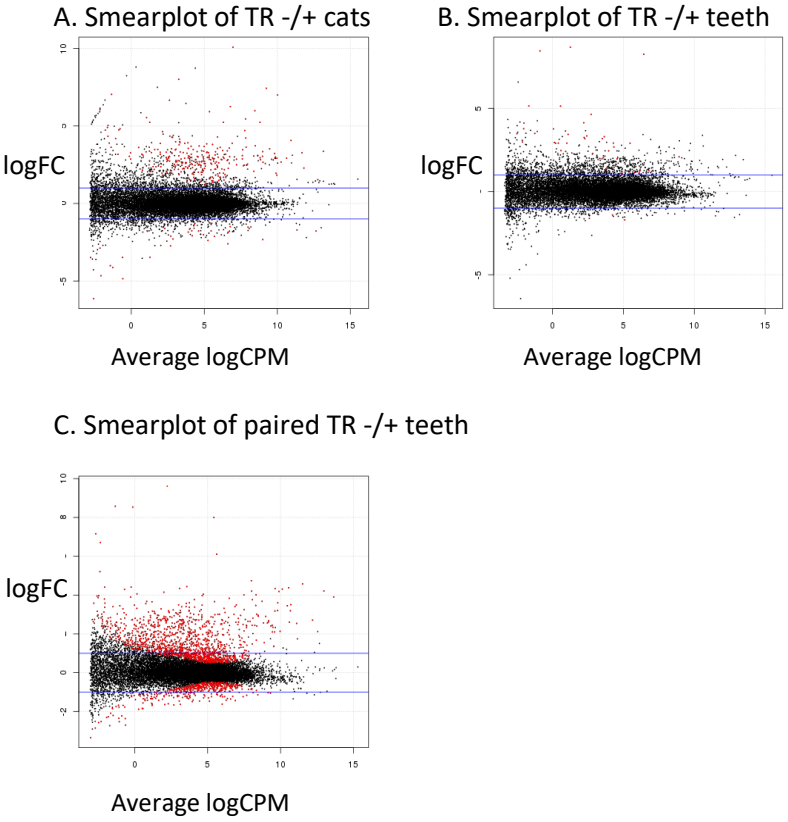

Figure 5.5 Visualisation of gene expression data by smearplots. (A) Plot of average gene expression and fold-change in TR -/+ cats. Horizontal blue lines indicate fold-change of two. Red dot indicates each differentially expressed gene at False Discovery Rate or corrected P-value (FDR) of 0.05 or smaller. (B) Smearplot of TR -/+ teeth. (C) Smearplot of paired TR -/+ teeth. The largest number of differentially expressed genes labelled in red was found in paired TR -/+ teeth.

Set	# total expressed genes	# significantly DE genes (FDR < 0.05)	# up-regulated genes	# down-regulated genes
TR- vs TR+ cats	16,366	315	279	36
TR- vs TR+ teeth	16,745	44	41	3
Paired TR- vs TR+	16,307	1,732	1,286	446

Table 5.3 Summary of differentially expressed genes from all comparisons. DE: differentially expressed.

The significantly differentially expressed genes and fold changes are displayed graphically (Figure 5.5 and Figure 5.6) and details of differentially expressed genes are listed in Supporting information 2. Given that the genes labelled by the same colour represent a similar gene expression pattern e.g. a relative up-regulation (green) or down-regulation (red), biological samples (TR -ve samples or TR +ve samples) clustered together which implies each sample possess a similar transcriptome (Figure 5.6, A). There are much more up-regulated genes (1,286 genes) than down-regulated genes (446 genes). The heatmap in Figure 5.6, B shows the top 50 differentially expressed genes by descending order of FDR. Of 1,732 differentially expressed genes, none of the inflammatory cytokines (e. g. *IL1B, IL6, TNF, IFNG* and *P2X7R*) or *VDR* were included, which was consistent with the result found in Chapter 4.

Twenty seven differentially expressed genes were common for all three comparisons, and included 25 up-regulated genes and 2 down-regulated genes (Table 5.4). However, the majority of remaining genes were uncharacterised or were not reported to be involved in tooth or osteoclast biology. For further characterisation of the transcriptome in TR, 1,732 of the listed differentially expressed genes between paired TR groups (Supporting information 2) were utilised to identify pathways and gene sets.

5.4.3 **Pathway and gene ontology analysis of RNA-seq data**

To gain more biological insight into downstream pathways in the paired TR

comparison, KEGG pathway enrichment was performed using the R/Bioconductor package SPIA (Signalling Pathway Impact Analysis) (274). SPIA uses a list of differentially expressed genes and takes into account the fold changes of genes along with signalling pathways topology to identify pathways that are relevant to the condition under study. It showed that the transcription profile of TR +ve teeth was enriched for a total of 28 metabolic pathways (Supporting information 3). Of these, 25 pathways were involved in sets of up-regulated genes and three pathways were related to sets of down-regulated genes. The most interesting pathways were osteoclast differentiation (Supporting information 3, KEGG pathway 04380; $p = 0.03$) and calcium signalling (Supporting information 3, KEGG pathway 04020; $p = 1.1 \times 10^{-4}$) which promote the differentiation of osteoclast precursors and induce osteoclastic tooth resorption in teeth. Relative expression of each gene in each pathway was visualised with colour labels in Figure 5.7 and Figure 5.8.

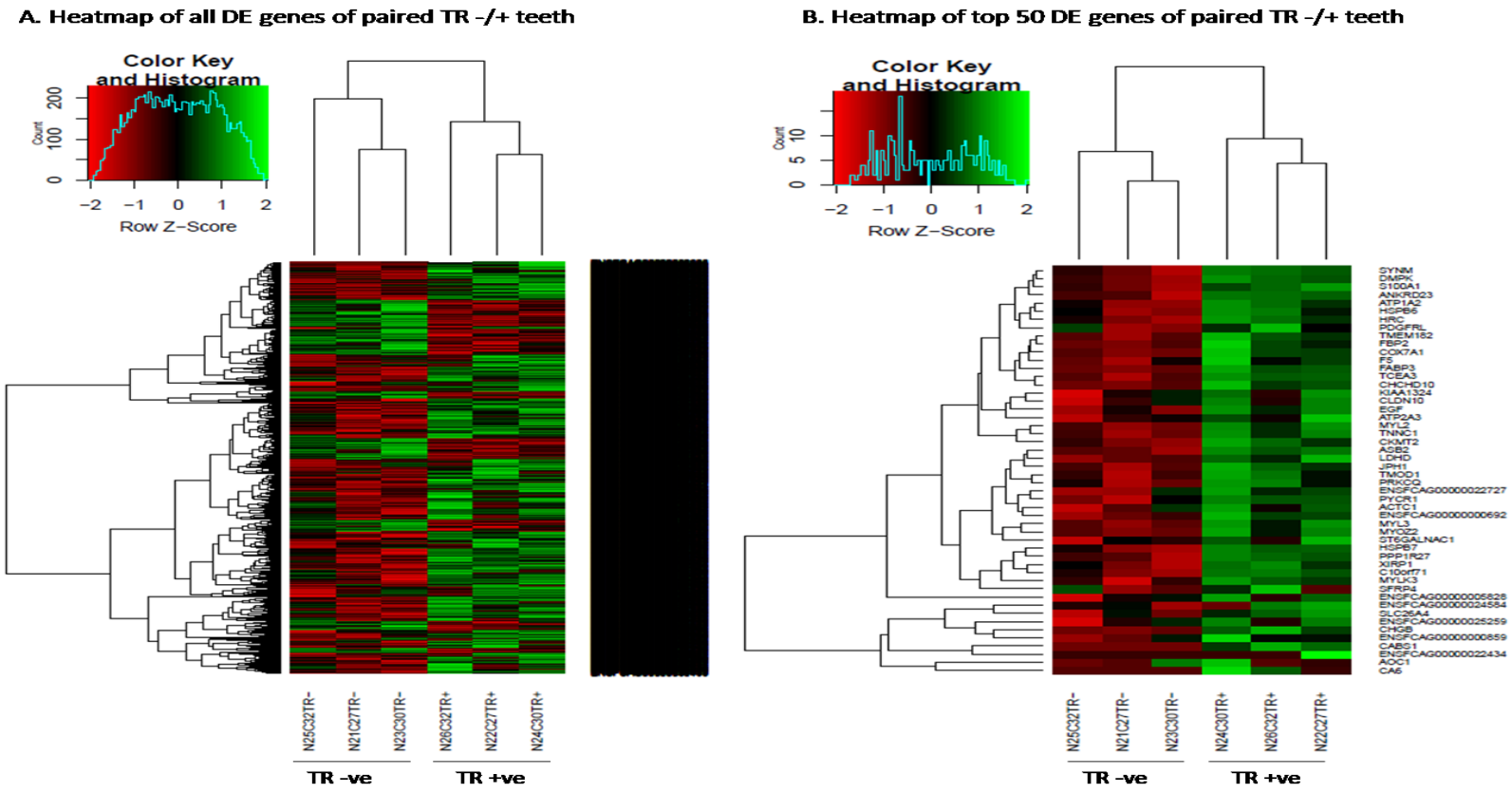

Figure 5.6 Transcriptome differences between TR -ve and TR +ve teeth in paired cats. (A) Heatmap of total significantly differentially expressed genes. (B) Heatmap of top 50 significantly differentially expressed genes. Each row represents a gene and each column represents a sample. The colour scale illustrates the relative expression level of differentially expressed genes based on gene-level counts. See text for more details.

Upregulated genes					
Gene	Description	LogFC	Gene	Description	LogFC
CA6	carbonic anhydrase VI	10.45	*MUCIN7*	mucin 7, secreted	8.00
ARX	aristaless related homeobox	6.70	*CHGB*	chromogranin B	4.14
HOXA4	homeobox A4	3.79	*TECRL*	trans-2,3-enoyl-CoA reductase-like	3.55
PPP1R27	protein phosphatase 1 regulatory subunit 27	3.38	*LBX1*	ladybird homeobox 1	3.12
METTL7B	methyltransferase like 7B	2.71	*ATP1A3*	ATPase, Na+/K+ transporting, alpha 3 polypeptide	2.54
CA4	carbonic anhydrase IV	2.53	*ETNPPL*	ethanolamine-phosphate phospho-lyase	2.52
SLC9A2	solute carrier family 9, subfamily A (NHE2, cation proton antiporter 2), member 2	2.41	*CLDN10*	claudin 10	2.35
SMCO1	single-pass membrane protein with coiled-coil domains 1	2.24	*FAM166B*	family with sequence similarity 166 member B	1.97
LDHD	lactate dehydrogenase D	1.96	*TLX1*	T-cell leukaemia homeobox 1	1.91
GRB14 Novel gene	growth factor receptor bound protein 14	1.62	*CHCHD10*	coiled-coil-helix-coiled-coil-helix domain containing 10	1.58
ATP2A2	sarcoplasmic/endoplasmic reticulum calcium ATPase 2	1.48	*CES2*	carboxylesterase 2	1.21
IVD	isovaleryl-CoA dehydrogenase	1.08	*KIF19*	kinesin family member 19	1.05
Downregulated gene					
Gene	Description	Log FC	Gene	Description	Log FC
SOSTDC1	sclerostin domain containing 1	-1.05	*KLK5*	kallikrein related peptidase 5	-1.19

Table 5.4 Common genes from all three comparisons. LogFC; log 2 fold change. Upregulated genes have log2 fold change > 0 and downregulated genes have log2 fold change < 0.

SPIA also discloses whether the differentially expressed genes themselves impact upon the function of that pathway. As many of the genes related to osteoclast differentiation were highly expressed in TR +ve teeth (Supporting information 3, total number of genes in osteoclast differentiation pathway = 93, number of up-regulated differentially expressed genes = 15, down-regulated differentially expressed genes = 3), it was hypothesised that osteoclast differentiation was activated. Osteoclast differentiation is controlled by the RANK/RANKL/OPG axis. *RANKL* is highly expressed but not significantly up-regulated (Table 5.5, log2 fold change = 0.810) and *RANK* is significantly up-regulated (Table 5.5, log2 fold change = 1.157) in TR +ve teeth. However, *OPG* is down-regulated (Table 5.5, log2 fold change = -1.326), which means the *RANKL*/*OPG* ratio increases in favour of *RANKL* which is likely to promote osteoclast differentiation. This could be part of the explanation why osteoclast differentiation occurs more in TR +ve teeth and results in the phenotypic consequence of tooth resorption.

The highlighted differentially expressed genes in osteoclast differentiation and calcium pathway are listed in Table 5.5.

The gene ontology terms reflect the best-annotated roles of certain genes. The gene ontology describes function in three aspects: molecular function, cellular component and biological process (220). The enriched gene ontology terms are only listed if more than 50 genes are assigned that term. Many of the enriched gene ontology terms are involved in muscle physiology (molecular function gene ontology terms include 'actin binding', cellular component gene ontology terms include 'myofibril' and 'actin cytoskeleton', and biological process gene ontology terms include 'muscle contraction', 'heart contraction', 'muscle fibre development', 'skeletal muscle cell differentiation' and 'muscle organ morphogenesis') (Supporting information 4).

In particular, in the TR +ve teeth, the structural myofibril components *ACTA1*, *ACTN2*, *ATP2A1*, *CSRP3*, *MYH11*, *MYOZ2*, *PDLIM3*, *SYNC*, *TCAP*, *TNNI1*,

TNNT3 and *TPM2* are up-regulated.

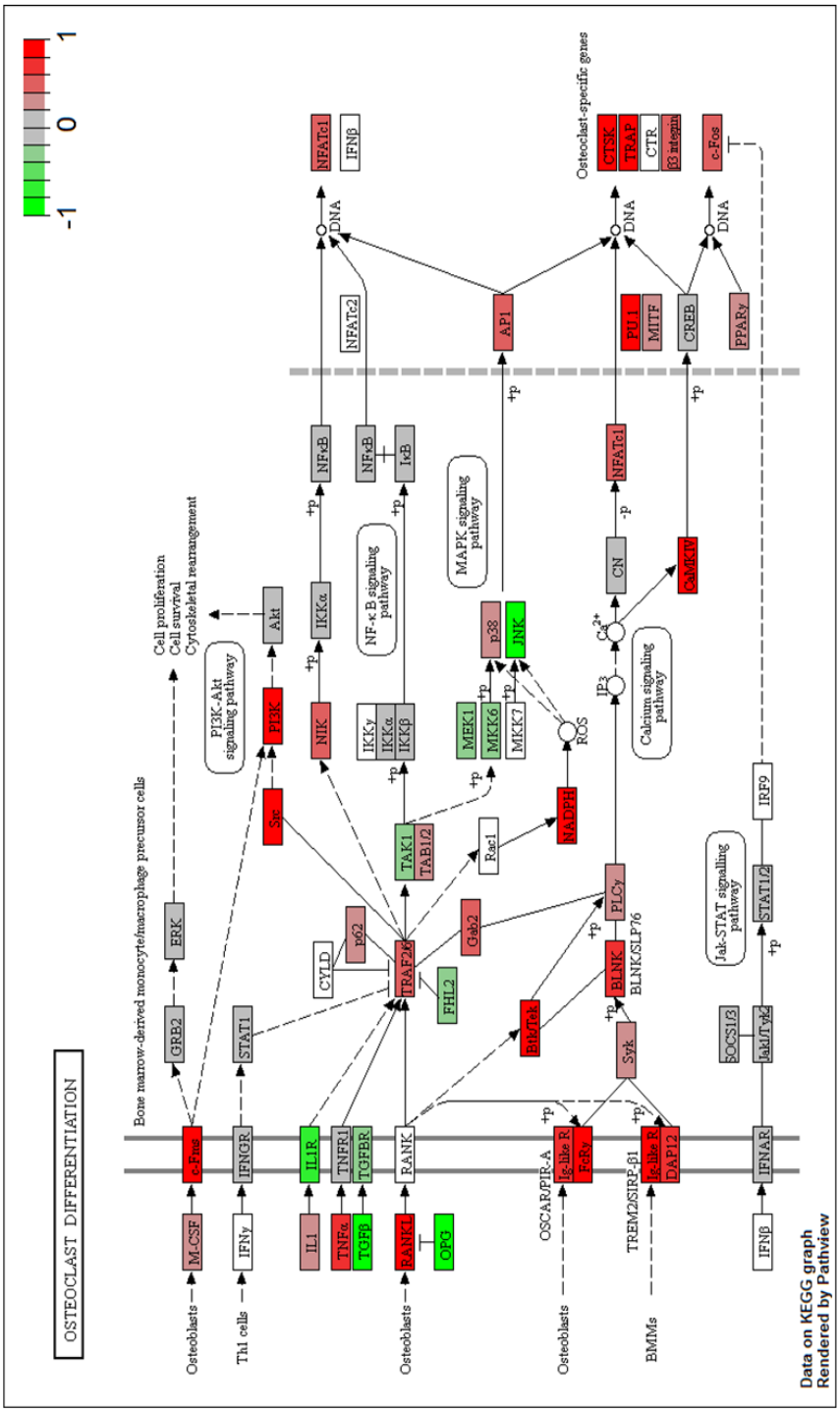

Figure 5.7 Osteoclast differentiation pathway. Expressed genes are coloured with red indicating relative up-regulation and with green indicating down-regulation in TR +ve teeth.

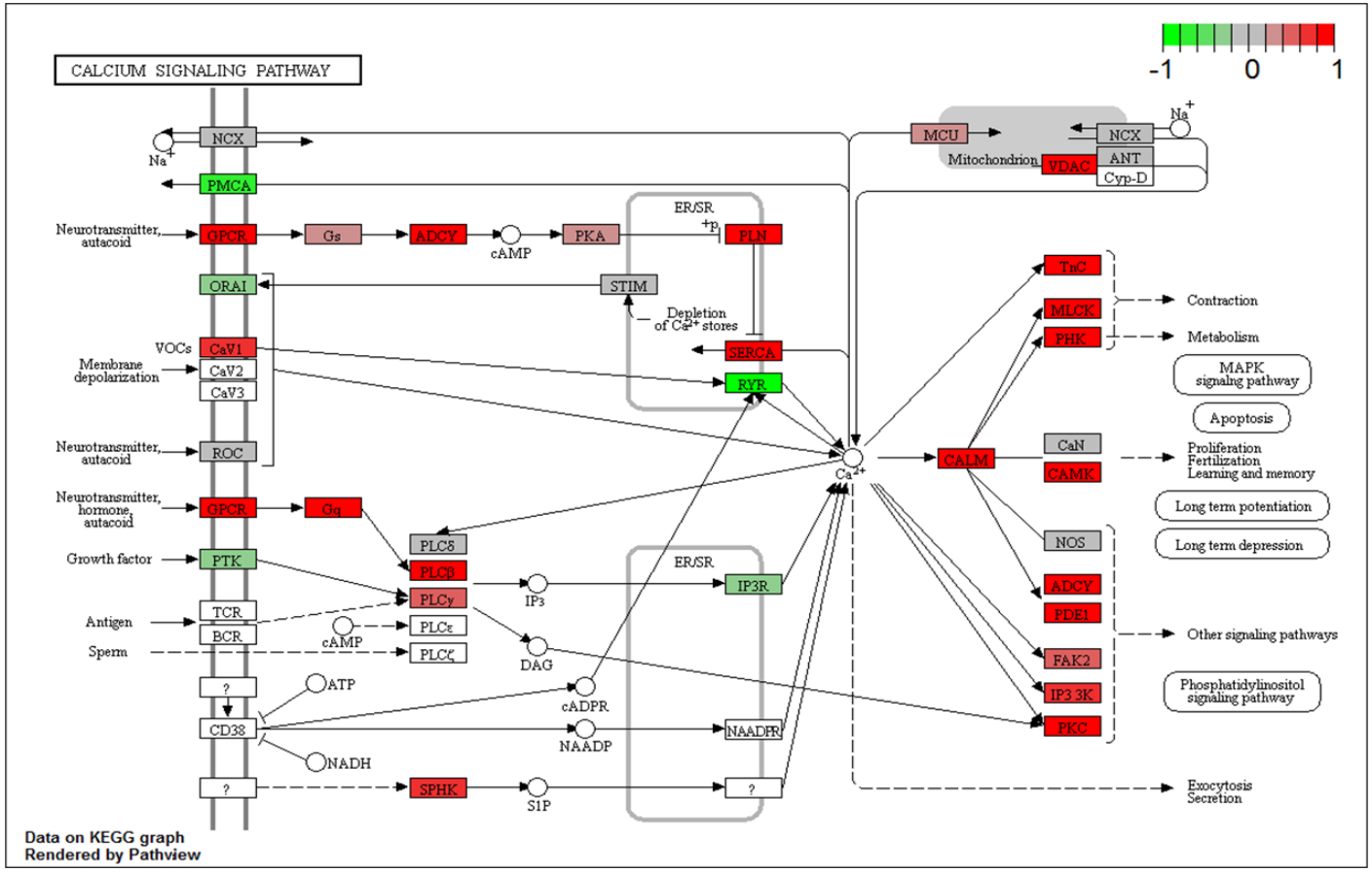

Figure 5.8 Calcium signalling pathway. Expressed genes are coloured with red indicating relative up-regulation and with green indicating down-regulation in TR +ve teeth.

Putative pathway: Osteoclast differentiation					
Gene status	Gene name	Description	logFC	FDR	Putative function (reference)
↑	*SPI1 (PU.1)*	Spi-1 proto-oncogene	1.028	0.0014	induction of osteoclast formation (145)
↑	*C-FMS (CSF1R)*	colony stimulating factor 1 receptor	1.026	$1.37x10^{-6}$	a trigger event leading to osteoclast differentiation via the c-Fms receptor (275)
↑	*TNFRSF11A (RANK)*	TNF receptor superfamily member 11a	1.157	0.0013	RANK/RANKL signalling is a central regulator of osteoclastogenesis (51)
↑	*TNFSF11 (RANKL)*	TNF superfamily member 11	0.810	#0.253	
↑	*OCSTAMP*	osteoclast stimulatory transmembrane protein	2.329	0.0030	lack of cell–cell fusion of osteoclasts in OC-STAMP deficient mice (148)
↑	*ACP5*	acid phosphatase 5, tartrate resistant	2.149	0.007	a cytochemical marker of osteoclast (276)
↑	*MMP9*	matrix metallopeptidase 9	2.326	0.010	high expression in RANKL induced osteoclasts (153)
↑	*CALCR*	calcitonin receptor	1.896	0.036	increase of calcitonin receptor during osteoclast formation (277)
↑	*CTSK*	cathepsin K	1.099	*0.059	degradation of type I collagen by osteoclast-mediated bone resorption (278)
↑	*TREM2*	triggering receptor expressed on myeloid cells 2	1.293	0.0027	Co-stimulatory receptor of RANK signalling (279)
↑	*TYROBP (DAP12)*	TYRO protein tyrosine kinase binding protein	0.764	0.0011	osteopenia due to increase of osteoclasts in DAP12 overexpression mice (280)
↑	*CYBA (Nox1)*	cytochrome b-245 alpha chain	0.639	0.0080	MAPK activation via Nox1 in osteoclast differentiation (279)

Gene status	Gene name	Description	logFC	FDR	Putative function (reference)
↑	*CYBB (Nox2)*	cytochrome b-245 beta chain	1.014	0.0146	increase of Nox2 during RANKL induced osteoclasts (281)
↓	*TNFRSF11B (OPG)*	TNF receptor superfamily member 11b	-1.326	$7.0x10^{-8}$	A negative regulator of osteoclastogenesis (51)
↓	*TGFB1*	transforming growth factor beta 1	-0.626	0.024	inhibitory effect of TGF-β on osteoclast differentiation (282)
↓	*TGFB2*	transforming growth factor beta 2	-0.697	0.0055	
Putative pathway: Calcium signalling					
↑	*P2X2R*	purinergic receptor P2X2	1.962	$4.3x10^{-4}$	induction of Ca^{2+} influx in osteoclast precursors and osteoclasts via extracellular ATP via various purinergic receptors (283-285)
↑	*P2X4R*	purinergic receptor P2X4	0.786	0.0029	
↑	*P2X6R*	purinergic receptor P2X 6	2.700	$1.26x10^{-5}$	
↑	*PLCB4*	phospholipase C beta 4	1.106	$3.36x10^{-5}$	activated by GPLC (284, 285)
↓	*P2X7R*	purinergic receptor P2X7	-0.271	$^{\#}0.639$	increased bone resorption by loss of function of P2x7r (286)

Table 5.5 Listed candidate genes identified by RNA-seq were correlated to osteoclast differentiation and calcium signalling. List of representative genes were extracted from two pathways and displayed with log fold change and corrected *p* value (FDR). *; *p* value is larger than 0.05 but close to 0.05. # $p > 0.1$.

5.4.4 **Validation of candidate genes by qPCR**

Twelve of the candidate genes identified in section 5.4.3 were selected for confirmation of expression by qPCR analysis (Table 5.6). The genes selected were correlated to osteoclast differentiation, osteoclast function and calcium signalling or they were genes common to all TR +ve teeth identified in section 5.4.2. All genes that displayed significant differentially expressed genes in RNA-seq (*SPI1, MMP9, ACP5, P2X2R, P2X4R, P2X6R, PCLB4, CA4* and *CA6*) were found to be up-regulated in TR +ve teeth confirming the result of RNA-seq. However, the expression levels of *P2X6R*, *PCLB4* and *CA4* were not significantly different when further samples were tested with qPCR ($p > 0.05$) (Table 5.6). As previously predicted, *RANKL* expression was unchanged but the gene expression ratio of *RANKL*/*OPG* was higher in TR +ve teeth (Fold change = 3.10, $p = 0.036$). *CA6* was identified as the most highly expressed gene in TR +ve teeth (Fold change = 5.51), followed by *MMP9* (Fold change = 4.52), *P2X2R* (Fold change = 3.04), *ACP5* (Fold change = 2.95), SPI1 (Fold change = 2.28) and P2x4r (Fold change = 2.28). CTSK was highly expressed in TR +ve teeth by qPCR ($p = 0.003$) but not by RNA-seq (FDR = 0.059). Overall the gene expression profile of TR identified by RNA-seq was consistent to that of the qPCR analysis.

Putative function	Gene	RNA-seq	qPCR		
		Expression in TR +ve	Expression in TR +ve	Fold change normalised to TR -ve	*p* value
Osteoclast differentiation	*SPI1*	↑**	↑ **	2.60	0.024
	RANKL	↑	↑	1.35	0.279
	OPG	↓**	↓ **	0.44	0.037
	RANKL/OPG	-	↑ **	3.10	0.036
Osteoclast genes	*MMP9*	↑**	↑ **	4.52	0.016
	ACP5	↑**	↑ **	2.95	0.019
	CTSK	↑*	↑ **	2.81	0.003
Calcium signalling in osteoclast	*P2X2R*	↑**	↑ **	3.04	0.025
	P2X4R	↑**	↑ **	2.28	0.039
	P2X6R	↑**	↑ *	2.81	0.079
	PCLB4	↑**	↑	1.83	0.100
Genes common to allTR + teeth (pH homeostasis)	*CA4*	↑**	↑ *	2.67	0.052
	CA6	↑**	↑ **	5.51	0.040

Table 5.6 RNA-seq results were validated by qPCR. Total n = 6 from TR –ve = 3, from TR +ve =3, *; 0.05 < p < 0.1, **; p < 0.05 by student t-test.

5.4.5 SNPs from RNA-Seq data and validation

The qPCR results from and RNA-seq analysis in section 5.4.2 showed that there was no differences in the mRNA levels of pro- inflammatory and anti-inflammatory cytokines, VDR or RANKL between TR -ve and +ve teeth. Nevertheless, I wanted to further investigate if there were any variations in any of these genes which might affect the function of the translated protein without changing gene expression levels.

Gene	Putative function (reference)
TNFRSF11A/RANK	mutations resulting in autosomal dominant bone disorder and spontaneous TR in humans (287)
TNFRSF11/RANKL	Two SNPs significantly associated with bone turnover marker (CTX-I) in men (288)
TNFRSF11B/OPG	SNPs correlated with EARR (207)
IL1B	SNPs more susceptible to EARR in orthodontic treatment (156)
VDR	Increased VDR protein and relative increase mRNA of VDR and its metabolic target genes in feline TR (122)
CYP27B1	
CYP24A1	
P2xR7	Knockout mice induce greater TR (289)
MMP9	Increase of MMP9 expression response to orthodontic treatment (290)

Table 5.7 Candidate genes reported to potentially correlate with human or feline TR.

As RNA-seq data contain actual sequences of expressed genes, it can be useful for the identification of SNPs as well as for quantification of transcripts. Based on the literature (Table 5.7) and listed candidate genes in section 5.4.4, twelve genes were included in this investigation and all variants in each gene of the samples are given in Supporting information 5. Variations were assessed by the extent of impact (low, modifier, moderate and high)[4] and effect type (location of variants, synonymous and missense).

The gene variations that were assessed as high impact and missense were selected (Table 5.8). *VDR* contained the highest number of variations (n = 63) with three missense variations. *SPI1* also have 44 variations but there was no missense or high impact variations. Seventeen variations in RANK included four missense and one splice variation. *OPG* possessed one high impact splice and two missense out of 29 variations. *IL1B* had one missense out of 25 variations. *MMP9* contained 4 missense and 1 high impact splice of a total of 16 variations. One variation was found in RANKL (low impact splice), *CYP24A1* (low impact synonymous) and

[4]low – synonymous changes, modifier – changes outside coding regions, moderate - codon change, deletion or insertion, high - frame shifts, addition or deletion of stop codons.

P2X7R (missense), respectively. There was no variation in *CYP27B1*. In order to see any correlation between these SNPs and TR status, the presence of each variant was investigated between TR -ve and TR +ve teeth. Most of the variations were present in both TR -ve and TR +ve teeth with different frequencies. One variation in *RANK* and *RANKL*, was found only in one TR –ve tooth. Each variation of *IL1B* was found in only one TR +ve tooth. One high impact SNP in *OPG* was found in all TR –ve teeth but not in TR +ve teeth. One *VDR* SNP which showed high impact was identified in two TR –ve teeth. One *MMP9* variation was identified in one TR +ve tooth with high impact effect. Two missense variations of *CA6* were found in one TR +ve tooth. Overall, none of the SNPs identified were only present in TR +ve teeth at a high frequency.

Due to time restraints, only targets that I already had optimised primers available for were validated by Sanger sequencing, these were *RANK*, *OPG*, *IL1B*, *VDR* and *P2X7R* from TR +ve teeth. The SNPs validated were; RANK (2 synonymous), *IL1B* (2 synonymous) and *VDR* (2 missense and 2 synonymous) (Table 5.9). There were no variations identified in *OPG* and *P2X7R*. Except for one synonymous variation, all SNPs were identical to the result of RNA-seq.

Gene (Chr: Gene start- end)	Number of SNPs in total	Highlighted variant (Position)	Effect impact	Variant (R→V)	Effect type	Identified in TR –ve vs. TR +ve teeth (number of teeth)
SPI1 (D1: 101264916-101280263)	44	-	Low or Modifier	-	-	-
TNFRSF11A/RANK (D3: 81404471-81436043)	17	81405965	High	T→C	Splice	TR –ve (1)
		81423363	Moderate	G→A	Missense	TR –ve (3) TR +ve (4)
		81423375	Moderate	G→A	Missense	TR –ve (5) TR +ve (3)
		81423418	Moderate	C→T	Missense	TR –ve (5) TR +ve (4)
		81423463	Moderate	T→C	Missense	TR –ve (4) TR +ve (3)
TNFRSF11/RANKL (A1:27831687-27855725)	1	27832113	Low	G→T	Splice	TR –ve (1)
TNFRSF11B/OPG (F2: 62243175-62253922)	29	62246655	High	C→T	Splice	TR –ve (5)
		62243992	Moderate	A→G	Missense	All TR –ve and +ve (12)
		62244037	Moderate	G→A	Missense	All TR –ve and +ve (12)
IL1B (A3: 104672921-104679186)	25	104675275	Moderate	C→G	Missense	TR +ve (1)
		104675987	Low	A→G	Synonymous	TR +ve (1)
		104677446	Low	T→C	Synonymous	TR +ve (1)
VDR (B4:77248710-77278649)	63	77250610	High	C→G	Splice	TR -ve (2)
		77259936	Moderate	T→C	Missense	TR –ve (6) TR +ve (3)
		77259949	Moderate	A→C	Missense	TR –ve (2) TR +ve (4)

Gene (Chr: Gene start- end)	Number of SNPs in total	Highlighted variant (Position)	Effect impact	Variant (R→V)	Effect type	Identified in TR –ve vs. TR +ve teeth (number of teeth)
VDR (B4:77248710-77278649)	63	77259972	High	T→C	Splice	TR –ve (1) TR +ve (1)
		77260306	Moderate	T→C	Missense	All TR –ve and +ve (12)
		77260415	Low	T→C	Synonymous	TR –ve (5) TR +ve (2)
CYP27B1 (B4: 86,470,520 - 86,474,390)	0	-	-	-	-	-
CYP24A1 (A3: 8241386-8257342)	1	8255607	Low	A→C	Synonymous	TR -ve (1)
P2X7R (D3: 8111906 - 8158046)	27	8112271	Moderate	T→G	Missense	All TR –ve (7) TR +ve (3)
MMP9 (A3: 14893716 - 14900785)	16	14895972	Moderate	C→G	Missense	All TR –ve and +ve (12)
		14896183	Moderate	C→T	Missense	All TR –ve (7) TR +ve (4)
		14896231	Moderate	C→T	Missense	TR –ve (5) All TR +ve (5)
		14898306	High	C→G	Splice	TR +ve (1)
		14898414	Moderate	T→C	Missense	TR –ve (5) All TR +ve (5)
CA6 (C1: 5524897 - 5545144)	4	5535001	Moderate	A→G	Missense	TR +ve (1)
		5545125	Moderate	G→A	Missense	TR +ve (1)
P2X4R (D3: 8068413 - 8083858)	2	-	-	-	-	-

Table 5.8 SNPs in the candidate genes were identified by RNA-seq and potential effects were summarised.

Gene	Identity to feline whole genome nucleotides	Position	Variant (R→V)	Effect type	RNA-seq
TNFRSF11A/RANK	482/484 (99.5%)	81423452	T→C	synonymous	Detected
		81423545	A→G	synonymous	Detected
TNFRSF11B/OPG	1,751/1,751 (100%)	-	-	-	-
IL1B	1,276/1,278 (99.8%)	104675987	A→G	synonymous	Detected
		104677446	T→C	synonymous	Detected
VDR	754/758 (99.5%)	77259936	T→C	missense	Detected
		77260300	G→A	synonymous	ND
		77260306	T→C	missense	Detected
		77260415	T→C	synonymous	Detected
P2X7R	367/367 (100%)	-	-	-	-

Table 5.9 Variations were validated by Sanger sequencing.

5.5 Discussion

Identification and quantification of transcripts are core activities in molecular biology given that RNA plays the key intermediate role between the genome and the proteome. RNA-seq is a powerful tool for both discovery and quantification in a single high-throughput sequencing assay (208, 232). The benefits of this study were the use of RNA-seq data to present transcriptomic profiles which can profile the cellular and molecular status of a certain condition and bridge the gap between the phenotype and gene expression. As previously discussed in Chapter3, one of the 14 RNA-seq samples was found to be an outlier throughout the data exploring process. This process is performed to identify technical errors *(e.g.* switching of samples due to labelling mistakes, outliers caused by low quality data or phenotyping errors) or sample variations (*e.g.* batch effects which are biased by the time and date of sample collection or individual variations originated from different animals) (232). The outlier identified here was likely due to the inclusion of RNA of potentially high quality, but where the yield was only one in ten of the average yield of the other samples, which was less than a minimum required volume. This quality control check is critical for both reproducible and reliable

results. Here, I also found that one sample from the TR +ve teeth group showed similarities to TR -ve samples even though the phenotype was re-confirmed as TR +ve from the dental radiograph. I therefore had to question whether the dental radiograph was the corresponding image of the tooth the RNA had been extracted from. A wrongly allocated sample into a different group by mistake could happen at any level during sample collection, extraction of RNA or synthesis of cDNA or sequencing. Therefore, I decided to exclude these two samples from the final analysis since this could compromise the resultant data. Samples were collected on different days depending on the availability of cats/tissues so even though the same optimised RNA extraction protocol was used, there exists technical sources of variations (*e.g.* individual sample variation and measurement differences) which are referred as batch effects. In most cases, the biological variations (individual variations) are bigger than technical variations especially when utilising clinical samples from a range of animals (291).

I compared transcriptome changes between TR -ve and TR +ve samples using three comparisons, and found the paired TR -ve and +ve comparison within cats from three individuals showed the highest number of DE genes and increased the statistical power of this study. As teeth do not remodel, it was expected that there would be less dynamic changes present with limited transcripts identified. Surprisingly, a large number of transcripts from the TR +ve teeth differed from TR -ve teeth (n = 1,732) which implies that these transcriptome changes occur locally within the same dentition.

The fact that there was transcriptomic similarity between teeth of the same phenotype and that the different phenotypes could clearly be separated reveals that the TR affected teeth undergo similar cellular and molecular changes. The transcriptome corresponding to the phenotype may suggest that transcriptome changes are at the core of TR pathogenesis, and this knowledge has the potential to increase our understanding of the aetiology of TR. No previous RNA-seq analysis of TR samples has been reported, but a microarray study on the dental transcriptome (dentome) in developing human teeth identified that different locations of the

developing tooth expressed unique transcriptome profiles, especially between odontoblasts and pre-secretory ameloblasts (201). Two further microarray studies also reported the differences in gene expression patterns between human deciduous and permanent periodontal ligament and pulp, respectively (292, 293).

The lack of changes in gene expression of various inflammatory cytokines and *VDR* in TR was consistent with the finding in Chapter 4 and support a non-inflammatory pathogenesis aetiology for TR. It is also possible that inflammation only appears at a particular stage of TR development so that the overall oral environment possesses a similar extent of inflammation within this study population. To further investigate this, subgroups of RNA-seq data between different TR stages may be enlightening. For this, current RNA-seq data fromfrom TR –ve and early and advanced TR +ve teeth could be re-analysed. However, more informative may be gleaned from the study of teeth from early, advanced, and end stage TR+ve teeth which would improve the power of this study. Another possible explanation for the lack of any changes in the expression levels of inflammatory cytokines could be due to a bias of TR type in this study. In this study, type 2 was the dominant type of TR. It has been proposed that this type might be involved in non-inflammatory or idiopathic TR although other studies have not confirmed this observation (99, 112, 294).

Two previous feline TR studies noted differences in the gene expression of various inflammatory cytokines by qPCR however the changes reported were in both pro- and inhibitory- inflammatory cytokines (100, 163). The local level of actual cytokines (protein) has however never been measured in TR so overall influence of inflammation cannot be conclusively determined (100, 163).

There were only a few changes in gene expression that were common between all three comparisons of TR -ve and TR +ve teeth and this may be due to large individual variations in the samples avbailable. There was no direct evidence that these identified genes are associated with osteoclast formation and activity. Of these, carbonic anhydrase 4 (*CA4*) has been reported to be expressed in the plasma membrane of osteoclasts (295) and *CA6* is known to be abundantly present in

salivary glands and saliva and involved in maintenance of pH homeostasis in oral cavity (296, 297). Some of the genes, including homeobox genes (e.g. *ARX, HOXA4, LBX1, TLX1*) are related to tooth development (298). One of the downregulated genes was *SOSTDC1* which has been reported to be largely related to tooth development as an inhibitor of Wnt signalling to control tooth number and morphogenesis (299, 300). However, the potential role of carbonic anhydrases *CA4* and *CA6* might be involved in oral pH regulation in osteoclast precursors. If so, this microenvironment may favour osteoclast differentiation (295). The many highly expressed homeobox genes included *ARX, HOXA4, LBX1* and *TLX1* and these have been previously associated with tooth development. The implications for this are unclear but may suggest that permanent TR +ve teeth may be undergoing some form of remodelling process (298, 301).

The paired TR comparison gave the most interesting results. The genes that were increased in expression revealed various metabolic pathways including osteoclast differentiation and calcium signalling and this implies TR +ve teeth are prone to dysregulation of osteoclast activity. Specifically, genes in osteoclast differentiation pathway are known to induce osteoclast differentiation (*SPI1, C-FMS, RANK, RANKL, TREM2, DAP12, Nox1 and Nox2*) (51, 145, 275, 279-281) or highly expressed in functional and mature osteoclasts (*OCSTAMP, ACP5, MMP9, CALCR and CTSK*) (148, 153, 276-278). Genes in calcium signalling might induce Ca2+ influx thus contributing to osteoclast differentiation (*P2X2R, P2X4R, P2X6R, PLCB4*) (283-285).

However, the computational calculation of pathway status, the R/Bioconductor package SPIA indicated an overall inhibitory status of the subsequent downstream pathway in TR +ve teeth. Tthis interpretation though requires an understanding of gene expression in context of a given pathway (274). This algorithm is computationally calculated, with no importance given to the relative location of each gene within that pathway. Hence the calculation does not take into account the importance and impact of the gene in the level of pathway (302, 303). For example, OPG and RANKL are the main regulators of osteoclast

differentiation and physiological importance relies on the ratio of RANKL/OPG via the RANK/RANKL/OPG axis (23, 67). Increased RANKL/OPG ratio will promote osteoclast formation in TR teeth. This up-regulation is observed in both permanent tooth eruption and primary tooth shedding (26, 67). When the impact of the pathways are calculated and they are ranked with a global probability, three factors are incorporated; total number of all pathway genes present, total number of genes in a specific pathway and total number of differentially expressed genes (274). By doing so, pathway impact is determined via a comprehensive view rather than via a specific pathway itself. In case of my data the feline genome is not fully annotated and therefore the detected number of genes in the pathway platform are limited. This places limitations on the impact calculation. Another limitation of this analysis comes from technical errors. In the osteoclast differentiation pathway figure (Figure 5.7), RANK is shown as colourless which means this gene was not detected in the pathway analysis even though it existed in the list of DE genes which was used as input data. The input data are associated with a gene ID and then mapped onto a known KEGG pathway (in this case, 'osteoclast differentiation'). Genes can be identified either by, for example, Entrez ID (NCBI's database), Ensembl ID (European Bioinformatics Institute and the Wellcome Trust Sanger Institute) or HGNC gene symbol (HUGO Gene Nomenclature Committee), but problems could arise when synonyms exist or not all genes have the same ID type. In this case, input of TNFRSF11A by Entrez ID was not detected in the KEGG pathway wherein uses RANK by its HGNC gene symbol. Therefore, these technical errors were cautiously examined. As a consequence, the pathway status should be interpreted in the structure of the pathway with list of differentially expressed genes.

Secondly, this discrepancy of status and the phenotype might be due to the fact that not all genes related to a certain pathway are included (232, 302). Calcium signalling controls multiple cellular functions in many cells via release of calcium ions from internal stores and its entry from the extracellular fluid (285). In particular, calcium signals in osteoclasts are responsible for diverse cellular functions including differentiation, bone resorption and gene transcription (284).

On the other hand, gene ontology enrichment analysis showed abundant genes involved in muscle physiology; genes involved in structural myofibril components including *ACTA1, ACTN2, ATP2A1, CSRP3, MYH11, MYOZ2, PDLIM3, SYNC, TCAP, TNNI1, TNNT3* and *TPM2* were up-regulated, however, the exact role of these genes in bone and tooth metabolism is unclear. These genes have been also identified a role in the development and differentiation of osteocytes; mechanosensing cells that coordinate the remodelling process mediated by osteoblasts and osteoclasts as well as developing bone and tooth (304). This manifestation might be due to tooth ankylosis, a fusion of the tooth to bone, following tooth resorption.

From the pathway analysis of differentially expressed genes I focused primarily on genes associated with osteoclast biology (e.g. *SPI1, C-FMS, RANKL, OPG, ACP5, MMP9* and *CTSK*) and inducers of Ca^{2}+ influx contributing to osteoclast differentiation (*P2X2R, P2X4R, P2X6R, PLCB4*). Up-regulation of genes that are recognised to stimulate osteoclast differentiation would strongly implicate altered osteoclast resorption in the aetiology of TR. SPI1, the gene encoding the haematopoietic transcription factor PU.1 is essential for myeloid and B-lymphoid cell development (145). This is known to be the earliest molecule which binds to sites in the promoter and intronic regulatory element (FIRE enhancer) of *c-fms* for commitment to osteoclast lineage in mice (275, 305). The increased expression of *SPI1* and *C-FMS* found in TR +ve teeth may therefore suggest that TR +ve teeth possess more pre-osteoclasts in their environment which would potentially lead to more mature osteoclasts and increased tooth resorption. The RANKL/OPG ratio is recognised as a principal regulator of osteoclast formation in the bone marrow microenvironment, and alterations to this ratio may be a major cause of bone loss in many metabolic disorders (306). In my RNA-seq result, TR +ve teeth had an increased *RANKL*/*OPG* mRNA ratio although this was obtained by measuring the mRNA levels rather than an actual measurement of secreted cytokines. Current available methods to measure feline cytokines from body fluids were developed and commercial ELISA kits for IL1B, IL6 and TNF are now available (307, 308),

however there is no available ELISA kits for feline RANKL or OPG . To measure the local level of cytokines in oral environment, oral fluids (*e.g*. saliva and gingival crevicular fluid) as an indicator of dental disease can be used (309) but no application of this in cats has been reported yet, hence optimisation steps to utilise the ELISA kits would be required.

ACP5 and *CTSK* are recognised osteoclast markers in bone and teeth (276, 278). Up-regulation of these genes also suggest increased osteoclast number and activity in TR teeth. *MMP9* was identified as the second most up-regulated gene in TR +ve teeth. This matrix metallopeptidase enzyme is also known as gelatinase B and type IV collagenase. Its primary role is to degrade and remodel ECM in many tissues including bone and teeth (263). Increased MMP9 activity has been implicated in many diseases including osteoclastomas, Paget's disease, bone fracture repair and dental pulp inflammation (310, 311). It has also been reported that it is highly expressed in early stages of differentiating osteoclasts, mature osteoclasts as well as in odontoclasts in many species including human, mouse, rabbit, horse and cow (152, 312, 313). However, expression of MMP9 and its role in bone and tooth resorption has not been described in cats. One study reported high expression of MMP9 in feline cancer (151). The role of MMP9 in feline TR needs further investigation.

The last important pathway identified in this chapter was the calcium signalling pathway. In this pathway, several purinergic receptor genes including *P2X2R, P2X4R* and *P2X6R* were highly expressed in TR +ve teeth. These genes are known to encode for nonselective cation channels permeable to $Ca^{2}+$ at the cellular level and thereby contribute to osteoclast differentiation. Originally, purinergic receptors were thought to play a role in ATP production which would in turn induce the formation and activation of osteoclasts (283). Purinergic receptors e.g. P2X7 or P2Y have also now been implicated as potent local inhibitors of matrix mineralisation (314). Expression of P2X2 receptor has been reported in both osteoblasts and osteoclasts but its precise role in bone is not clear (283). Up-regulation of P2X4 receptor has been attributed to inflammation via macrophage

invasion (315). Although expression of the P2X6 receptor has not been reported in osteoclasts, its expression was reported to modulate the differentiation and migration of human mesenchymal stem cells (316). The roles of these genes (and their encoded proteins) in the dental microenvironment is largely unknown, so further studies are required to investigate their possible involvement in tooth resorption.

A large number of the differentially expressed genes I identified were confirmed as being differentially expressed by qPCR. This supports the hypothesis that genes related to osteoclast formation and activation are involved in TR pathogenesis. Further studies into the pathways and genes identified here are required to further add to our understanding of TR pathogenesis and to eventually identify a potential treatment target or even a biomarker for TR.

This chapter also demonstrated SNPs in a number of the candidate genes. Each of the genetic variations, especially the high impact or missense mutations should be investigated further. It has been reported that SNPs or genetic variation of *RANK, OPG, IL1B* and *P2X7R* are correlated to susceptibility of TR following orthodontic treatment in man (207, 287, 289), and there are reported SNPs in RANKL related to bone turnover (288). Other candidates were included because of their reported correlation with feline TR (*VDR* and $1,25(OH)_2D$ regulating genes, *CYP27B1* and *CYP24A1*) (122), or orthodontic treatment in humans (*MMP9*) (290). The highest number of SNPs was detected in VDR and among those three SNPs were missense mutations. The presence of missense mutations implies that they would result in a change to the amino acid sequence of the resultant encoded protein and therefore likely to impact the function of protein. There are several SNPs reported in the human VDR. Some of these have been investigated in detail and specific SNPs have been suggested to cause a different susceptibility to osteoporosis (317). Most of the SNPs were identified in both TR –ve and TR +ve teeth while some SNPs (*OPG, VDR* and *MMP9*) were identified only in TR –ve or TR +ve teeth.

There were no clear differences in the expression of specific SNPs between

TR –ve and TR +ve, e.g. some moderate to high impact SNPs were present in only TR –ve or TR +ve teeth. Furthermore, some of the identified SNPs were confirmed by Sanger sequencing, implying the SNPs are real rather than sequencing errors. Nevertheless, caution is required as I only performed sequencing of a very limited region of candidate genes and therefore making any conclusions about the SNP data preliminary at best. Validating more SNPs would contribute to identifying potential genes correlated to the development of TR.

The gene of major interest in this chapter was *MMP9.* It was highly expressed in TR +ve teeth which is consistent with its reported increased expression in many diseases associated with dysregulated osteoclasts (310, 311). In Chapter 6, I will verify again the findings of RNA-seq and qPCR to choose target genes. Once the target genes (*e.g*. *MMP9*) are confirmed, an in vitro model could be used to investigate the role of the target gene in osteoclast biology and osteoclastic resorption.

Chapter 6 MMP9 as a novel candidate target in feline osteoclast differentiation and resorption activity

6.1 Abstract

RNA-seq data revealed that several genes were differentially expressed between TR –ve and TR +ve teeth. Differentially expressed genes *MMP9* and *P2X4R* were re-confirmed by qPCR on a further six paired TR –ve and TR +ve teeth samples. Of these, *MMP9* was of greatest interest since its encoded protein is known to be a highly expressed enzyme in osteoclasts and odontoclasts in many species, although it is not known whether MMP9 is important for feline osteoclast formation and activity. In order to determine which cells in the tooth express MMP9, I first performed immunohistochemistry on feline tooth samples. MMP9 was highly expressed in actively resorbing odontoclasts in TR lesions and in fibroblasts of the periodontal ligament. *MMP9* mRNA expression was also observed during *in vitro* feline osteoclast formation and this expression increased during osteoclast differentiation; it increased in the early stage osteoclasts before RANKL treatment commenced, and its expression level remained high until termination of osteoclast differentiation. To elucidate the role of MMP9 in feline osteoclasts, osteoclast precursors were treated with a semi-selective MMP9 inhibitor (hydroxamate-based MMP inhibitor), and the treatment reduced both the number of osteoclast formed and their resorption activity. Due to the semi-selectivity of the inhibitor and the potential for off-target effects, I constructed a feline specific *MMP9* siRNA. Following electroporation of the osteoclast precursors with the siRNA against *MMP9*, qPCR showed a 44% of reduction in mRNA levels. *MMP9* siRNA produced a reduction in osteoclast formation but it did not produce a statistically significant reduction in resorption activity. These results (together with those of chapter 5) suggest that increased MMP9 expression is central to TR pathogenesis and it may be a potential therapeutic target in feline tooth resorption.

6.2 Introduction

The results in Chapter 5 enabled me to create a shortlist of differentially expressed genes which can be considered potential treatment targets in feline TR. The transcriptional changes showed that many of the up-regulated genes were involved in osteoclast activity and differentiation. Of these, *MMP9* was chosen for further investigation as it is highly expressed in osteoclasts and odontoclasts (152, 312, 313). It was reported that *MMP9* mRNA and its encoded protein were highly expressed in bovine odontoclasts in resorbing deciduous teeth by in situ hybridization and immunohistochemistry, respectively (1). It was however not clear what the role of MMP9 in osteoclasts and osteoclasts precursors was, or how the high MMP9 expression contributed to the degradation of dental matrix proteins (152). When osteoclastic bone resorption occurs local acidification solubilises the inorganic mineral phase and exposes the organic matrix making it accessible to proteinases; cysteine proteinases such as cathepsin K solubilise collagen and MMPs might digest the rest of the bone matrix according to their substrate specificity (*e.g*. collagenases, gelatinases, stromelysins, matrilysins, and membrane type MMPs) when the pH increases slightly. MMP9 belongs to the gelatinase of MMPs family and was considered to act on degradation of bone matrix collagen but its resorption activity may be not significant because cathepsin K is predominantly present to involve collagen degradation of the subosteoclastic resorption zone (150, 318). MMP9 is considered to be involved in osteoclast migration (150). MMP9 deficient mice showed impaired bone development, intra-osseous angiogenesis and fracture repair, suggesting that MMP9 has an important role in developing bone. In the presence of a MMP9 inhibitor, the recruitment of osteoclasts into the core of the diaphysis was dramatically reduced (150, 319, 320).

The role of MMP9 in cancer has been more thoroughly documented, and it is known to be involved in tumour invasion and angiogenesis (310, 321). A significant correlation between the expression of MMP9 and metastatic potential has also been reported in many cancer types (*e.g.* breast cancer, prostate cancer, and melanoma)

(322, 323). MMP9 is reported to have the capacity to activate cellular effectors such as vascular endothelial growth factor and TGF-β which enables the process of invasion and metastases (150, 324). Despite MMP9 being one of the MMPs that has been researched the most, (150), the expression in feline osteoclasts and odontoclasts is unclear.

In this chapter, I aimed to confirm that *MMP9* is highly expressed in feline tooth sections of TR +ve teeth. Next I used a chemical inhibitor to investigate the direct effect of MMP9 inhibition. As the chemical inhibitor was semi-selective for MMP9, temporary targeting of the target using RNA interference was performed next. The utility of RNA interference is extensively used in gene function studies allowing for the rapid and highly specific silencing of the gene of interest to be assessed in both *in vitro* and *in vivo* (325-327).

I designed and constructed feline specific *MMP9* siRNA. After optimisation of different transfection techniques for use in feline pre-osteoclasts, siRNAs targeting feline MMP9 were screened for the assessment of mRNA silencing. In addition, differentiation and resorption activity was investigated post transfection to assess the potential functional role of MMP9 in feline osteoclasts.

Part of the work reported in this chapter was performed by an undergraduate student at the Royal (Dick) School of Veterinary Studies, Miss Nicola Mawson, under my supervision and technical support. She did an undergraduate research project, (A cat and mouth game: can a feline dental condition inform on how human bones weaken with age?) in the summer of 2017. In detail, I designed the student project, and Miss Mawson helped with the quantitative PCR and histological examination of feline teeth including H&E staining and immunohistochemistry. The histological sections were also assessed by a veterinary pathologist, Dr Erika Abbondati (BVSc, MRCVS and Diplomate of the European College of Veterinary Pathologists).

6.3 Materials and Methods

6.3.1 Quantitative PCR for candidate genes

To confirm the expression of the candidate genes, qPCR was performed in six paired TR teeth including three previous samples used in Chapter 5 (n = 6 from TR -ve, n = 6 from TR +ve) using primer sets (*MMP9, P2X4R, SPI1, CTSK, RANKL and OPG*). The conditions for the qPCR and data analysis were the same as described in section 5.3.3. Relative mRNA expression was analysed using the calculation of 2-ΔΔCt as previously described in section 2.1.8. An average fold change of TR +ve teeth was compared to that of TR –ve teeth. GraphPad prism v5 was used for the generation of graphs.

6.3.2 Histological investigation of feline TR

To determine which cells expressed the candidate proteins, feline teeth were demineralised and teeth sections were embedded in paraffin as described in section 2.7.1. H&E staining and immunohistochemistry were performed as described in section 2.7.2 and 2.7.3, respectively. As all antibodies used were raised against human and/or mouse proteins/peptides it was necessary to examine each for their ability to detect the feline protein. Table 6.1 summarises the results of all antibodies tested. Each slide was examined with a light microscope to determine the optimal dilutions of primary and secondary antibody that would provide specific protein binding with minimal background staining. Only the MMP9 antibody successfully labelled specifically to its target in comparisons with isotype control (Table 6.1). All slides were blinded to the observer, without information on their TR status. H&E and MMP9 positive odontoclasts were counted on each slide which contained at least one or two sections each sample to compare to the saved information on the archived samples (n = 16, TR –ve = 4, TR +ve = 12).

To distinguish odontoclasts from other multinucleated cells (*e.g.* clustered epithelial cells known as epithelial cell rests of Malassez (ERM) which are located in periodontal ligament as described in section 1.1.3.4, pan cytokeratin immunolabelling was performed as described in section 1.1.3.4., cytokeratin

immunolabeling was performed as described in section 2.7.4.

Primary Antibody	Host	Manufacturer	Antibody optimisation
MMP9	Rabbit polyclonal	Abnova, PAB12714	Dilution in 1:200
SPI1	Rabbit monoclonal	Abcam, AB76543	Failed optimisation
P2XR4	Goat polyclonal	Abcam, AB134559	Failed optimisation
CTSK	Mouse monoclonal	Abcam, AB66237	Failed optimisation
OPG	Mouse monoclonal	OPG (E-10): sc-390518. Santa Cruz Biotechnology, Inc.	Failed optimisation
RANKL	Rabbit polyclonal	ProSci, XP-5273Bt	Failed optimisation
RANK	Mouse monoclonal	RANK (H-7): sc-374360. Santa Cruz Biotechnology	Failed optimisation

Table 6.1 Antibodies tested for immunolabelling of candidate protein used in this chapter.

6.3.3 *In vitro* feline osteoclast differentiation, MMP9 expression and inhibition

In vitro feline osteoclast formation was performed as described in section 2.3.7. Cultured cells were collected at each time point (Day 0, Day 3, Day 6 and Day 8) for RNA isolation, and qPCR was performed as described in 2.1.6 and 5.3.3 to assess *MMP9* expression during osteoclast differentiation.

During *in vitro* feline osteoclast formation, cells were treated with MMP9 inhibitor ($C_{27}H_{33}N_3O_5S$, Merck Millipore, CAS 1177749-58-4) using a range of concentrations (5, 20 and 1,000 nM) as described in 2.4.8.

6.3.4 Development of RNA interference targeting feline *MMP9*

The protocols to design and construct a siRNA targeting feline *MMP9* were described in section 2.5.1 and 2.5.2. Table 6.2 summarises the 19 base sequences that were used for the construction of RNA duplexes to cleave feline *MMP9* mRNA. To select an effective siRNA target site, Reynold's statistical algorithm was used to

search for efficient siRNA oligonucleotides containing specific residues within the 19 sequences (230). Among the listed siRNAs using the online siRNA design tool, only siRNAs with a Reynold's score higher than 8 were chosen (Table 6.2). For a negative control, a commercially available scrambled siRNA containing a sequence with no known gene target (Silencer® Negative control, Life Technologies) was used. To identify the most efficient siRNA delivery method, both lipid based transfection and electroporation procedures were tested using a plasmid containing enhanced green fluorescence protein (pEGFP). Transfections were performed on day 3 following 48 hrs culture as described in sections 2.5.3 and 2.5.4.

The appropriate amounts of DNA (pEGFP) or RNA (scrambled or *MMP9* siRNA) and lipid based transfection reagent (RNAiMAX) or Nucleofector™ Solution are shown in Table 6.3 and Table 6.4, respectively. The efficiency of siRNA or pEGFP was checked under the fluorescence microscopy or by flow cytometry as described in section 2.5.5.

Following siRNA transfections, bone marrow osteoclast precursors were seeded onto dentine discs in 96-well plates. Cells were incubated at 37°C/5% CO_2 until formation of osteoclasts was observed in control cultures. Media were changed every 2 days. The number of TRAP positive osteoclasts were recorded as described in section 2.4.1 and resorption pits were counted as described in section 2.4.6.

	Sequences 5'-3'	%GC	Reynold score
Target mRNA	CCAGGAGACTTGCGAACTA	52.63	8
Antisense template	AACCAGGAGACTTGCGAACTA(CCTGTCTC)		
Sense template	AATAGTTCGCAAGTCTCCTGG(CCTGTCTC)		

Table 6.2 Summary of target and DNA template sequences used to produce siRNA against feline MMP9 with the Silencer siRNA Construction Kit. The 8 nt sequence marked in bracket indicates complementary sequence to the T7 Promoter Primer for the first step of the synthesis.

Constituent	Number of cells/cm^2	RNAiMAX mixture		RNA mixture	
		Lipofectamine	Opti MEM I	DNA or RNA	Opti MEM I
Untreated	1.0 x 10^5	1.5 µl	25 µl	-	25 µl
pEGFP (0.5 µg)	1.0 x 10^5	1.5 µl	25 µl	1 µl	25 µl
pEGFP (1.0 µg)	1.0 x 10^5	1.5 µl	25 µl	2 µl	25 µl
pEGFP (2.0 µg)	1.0 x 10^5	1.5 µl	25 µl	4 µl	25 µl

Table 6.3 The number of cells, amount of RNA and Lipofectamine solution per well in a 24-well-plate for lipid based transfection.

Constituent	Transfection			Number of cells/cm^2 after transfection
	Number of cells	Nucleofector® Solution	DNA or RNA	
Untreated	1.0 x 10^6	-	-	2.0 x 10^5
pEGFP (0.5 µg)	1.0 x 10^6	100 µl	1 µl	2.0 x 10^5
pEGFP (1.0 µg)	1.0 x 10^6	100 µl	2 µl	2.0 x 10^5
pEGFP (2.0 µg)	1.0 x 10^6	100 µl	4 µl	2.0 x 10^5
Scrambled (scrambled siRNA)	1.0 x 10^6	100 µl	1.5 µl	2.0 x 10^5
MMP9 (300 nM)	1.0 x 10^6	100 µl	1.5 µl	2.0 x 10^5

Table 6.4 The number of cells, the amount of RNA and Nucleofector™ solution used for electroporation experiments.

6.4 Results

6.4.1 *MMP9* mRNA expression is increased in TR +ve teeth

In order to confirm a shortlist of candidate genes for TR, qPCR was performed in a new set of 6 paired samples (Figure 6.1). In TR +ve teeth, mRNA fold change of *MMP9* and *P2X4R* increased by 3.0±0.7 (p=0.0264) and 2.6±0.4 (p=0.0029), respectively. Fold change of mRNA of *SPI1* and *CTSK* increased by 1.4±0.5 (p=0.5818) and 1.1±0.4 (p=0.7905), respectively, but these differences were not statistically significant. RANKL and OPG fold expression decreased by 0.8±0.4 (p=0.1013) and 0.7±0.3 (p=0.0534), respectively, but neither difference was

statistically significant. The RANKL/OPG ratio in TR+ teeth was not significantly different than in TR- teeth (1.9±0.7, p=0.3231). Overall, *MMP9* had the highest fold change observed in TR +ve teeth among the short listed candidate gene, which was consistent with the validated results of RNA-seq as described in section 5.4.4.

6.4.2 MMP9 was expressed in feline tooth sections

Optimisation of immunohistochemistry for candidate proteins was performed. However, none of the antibodies for SPI1, P2X4R, RANKL, OPG and RANK were successfully optimised, despite trying a range of different options (*e.g.* various antibodies concentrations, different antigen retrieval processes and incubation times). Only MMP9 was successfully labelled in feline dental tissues. Multinucleated odontoclast-like cells based on H&E staining and MMP9 immunolabelled sections were quantified. The initial numerical data were summarised in Table 6.6. The total number of odontoclasts counted in H&E and MMP9 sections could not be confirmed by veterinary pathologist Dr Erika Abbondati due to a discrepancy over the true identity of some of the multinucleated cells first identified. The pathologist highlighted that there are other multinucleated cells present in the region, so that all MMP9 positive, multinucleated cells would have to be distinguished from, for example ERM. Following a discussion with the pathologist, a consensus for distinguishing true resorbing cells from ERM was established. To reliably confirm odontoclasts only multinucleated cells within an obvious resorption pit were considered to be odontoclasts (Figure 6.2, C and D).

It was also observed that the majority of TR +ve teeth had disrupted periodontal ligament fibres, narrowed or complete loss of periodontal ligament space and replacement with bone like tissues demonstrating a degree of ankylosis. This was confirmed by Dr Abbondati. In TR +ve teeth, MMP9 protein was most strongly expressed in multinucleated cells which resorbed cementum and dentine (Figure 6.2, E and F). This protein was also expressed in the periodontal ligament fibroblastic cells (Figure 6.2, B) in both TR –ve and TR +ve teeth in comparisons with isotype control (Figure 6.2, H). Other cells including vascular structures of the dental tissue and gingival epithelium also expressed some MMP9, as well as

multinucleated cells out with resorption pits (Figure 6.2, G).

Dental tissue sections did not always contain active resorption lesions regardless of the tooth's TR status. Active odontoclasts with resorption pits were not identified in five of the twelve TR +ve teeth (Table 6.5).

ERM are resident in the periodontal ligament and of epithelial origin, so they express cytokeratin. To distinguish true odontoclasts from clustered ERM cells, the sections were therefore immunolabelled for cytokeratin. Odontoclasts did not express cytokeratin (Figure 6.3, D) while the gingival epithelium was strongly labelled with cytokeratin (Figure 6.3, A and B). Some periodontal ligament cells showed cytokeratin immunoreactivity (C), while odontoclasts were negative (D).

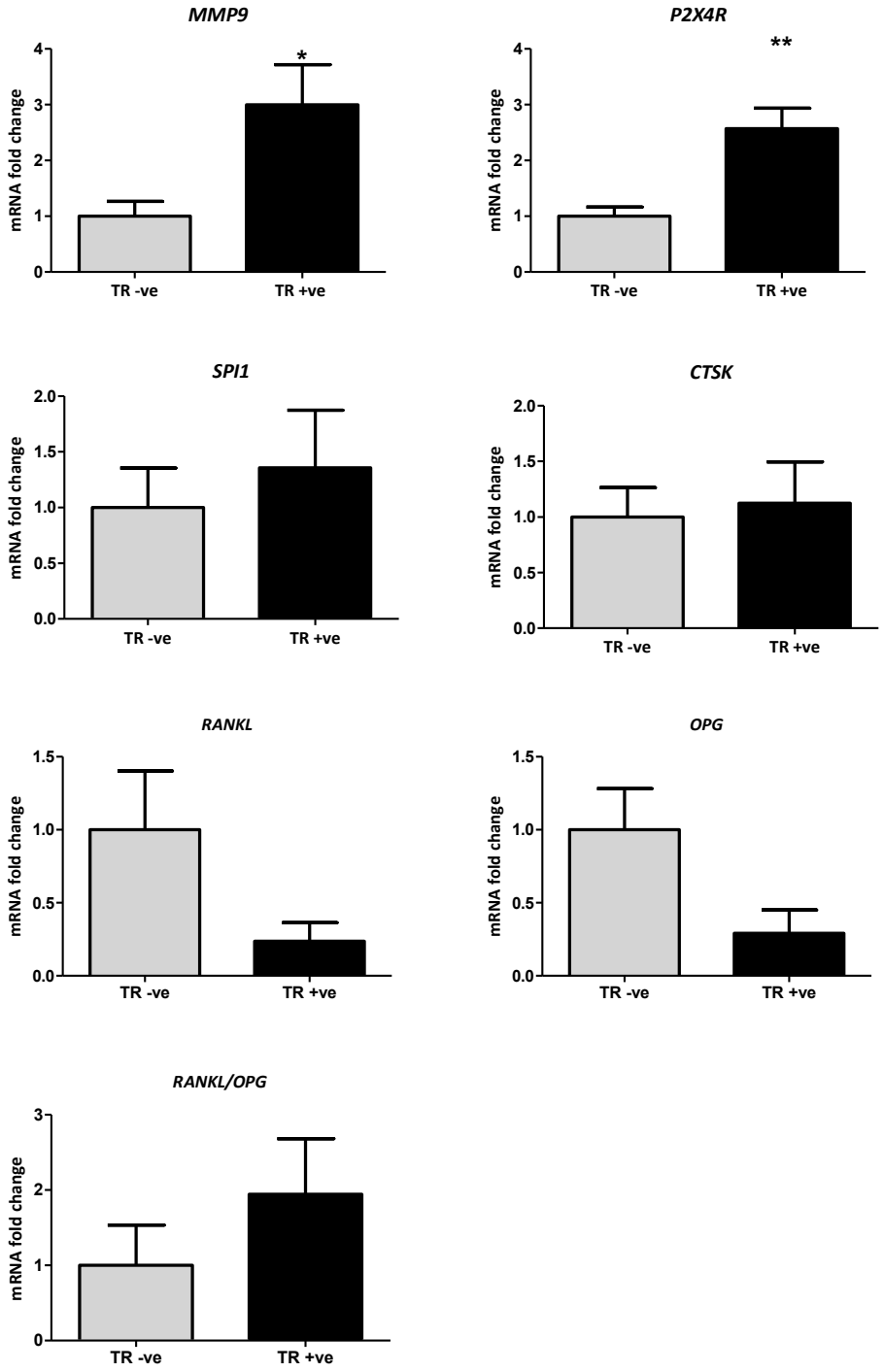

Figure 6.1 *MMP9* and *P2X4R* were highly expressed in TR -ve and TR +ve teeth. Confirmation of gene expression by qPCR in further tooth samples was performed. Graphs represent relative expression as fold changes + SEM bars. (Total n = 12, TR -ve = 6, TR +ve = 6; * $p < 0.05$, ** $p < 0.01$ by the two sample t-test).

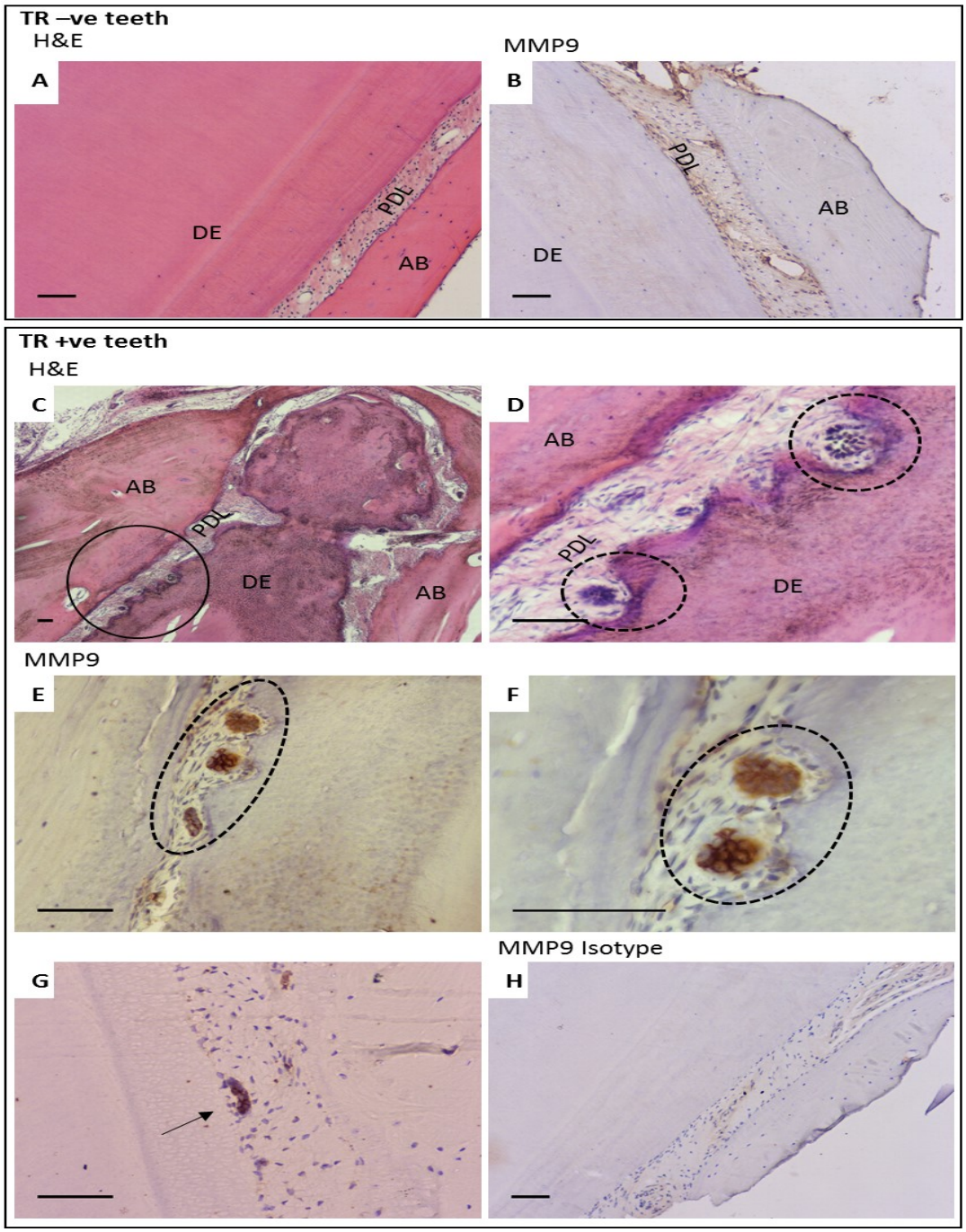

Figure 6.2 MMP9 highly expressed in odontoclasts of feline tooth resorption lesions. H&E from TR –ve teeth (A) and TR +ve teeth (C and D). A shows TR –ve tooth with intact periodontal ligament without resorption pit. C shows root furcation of TR +ve tooth with dentine resorbing odontoclasts (circle area) magnified in D. Immunohistochemical labelling for MMP9 protein with haematoxylin counterstaining TR –ve (B), TR +ve (E, F, and G) and isotype control (H). Most MMP9 expression in TR –ve teeth was observed in periodontal ligament or gingival tissues. TR +ve tooth contains active odontoclasts with resorption pits (dotted circle) with strong MMP9 expression (E), high magnification of this lesion (F). MMP9 expression was less strong, which was similar to TR –ve teeth. MMP9 expression was also found in multinucleated like cell but without resorption pit (G, arrow). AB: alveolar bone, DE: dentine, PDL: periodontal ligament. Scale bars = 100 µm.

Slide number	Number of ODs (H&E)	Number of ODs (MMP9)	Archived TR status	Active ODs with resorption pits	PDL structure /ankylosis
34 307	NA	4	+	+	Partially destroyed and narrowed PDL
35 404	8	10	+	-	Destroyed and narrowed PDL
35 409	17	NA	+	+	-
38 108	6	4	-	-	-
38 204	13	9	-	-	-
38 304	24	9	+	+	-
38 404	12	2	+	-	Disrupted PDL fibre
38 308	15	1	-	-	-
38 307	5	0	+	-	Destroyed and narrowed PDL
38 407	15	3	+	+	Destroyed and narrowed PDL
38 408	4	2	-	-	-
39 108	2	0	+	-	Partially destroyed PDL
39 307	7	2	+	+	Loss of PDL and ankylosis
39 308	25	5	+	+	Destroyed and narrowed PDL
39 309	8	5	+	+	Destroyed and narrowed PDL
39 409	5	3	+	-	Destroyed and narrowed PDL

Table 6.5 The initial quantification of odontoclasts in H&E and MMP9 immunolabelled sections together with their TR status. Total number of teeth sections: n = 16 (TR –ve, n = 4, TR +ve n =12). ODs: odontoclasts, PDL: periodontal ligament.

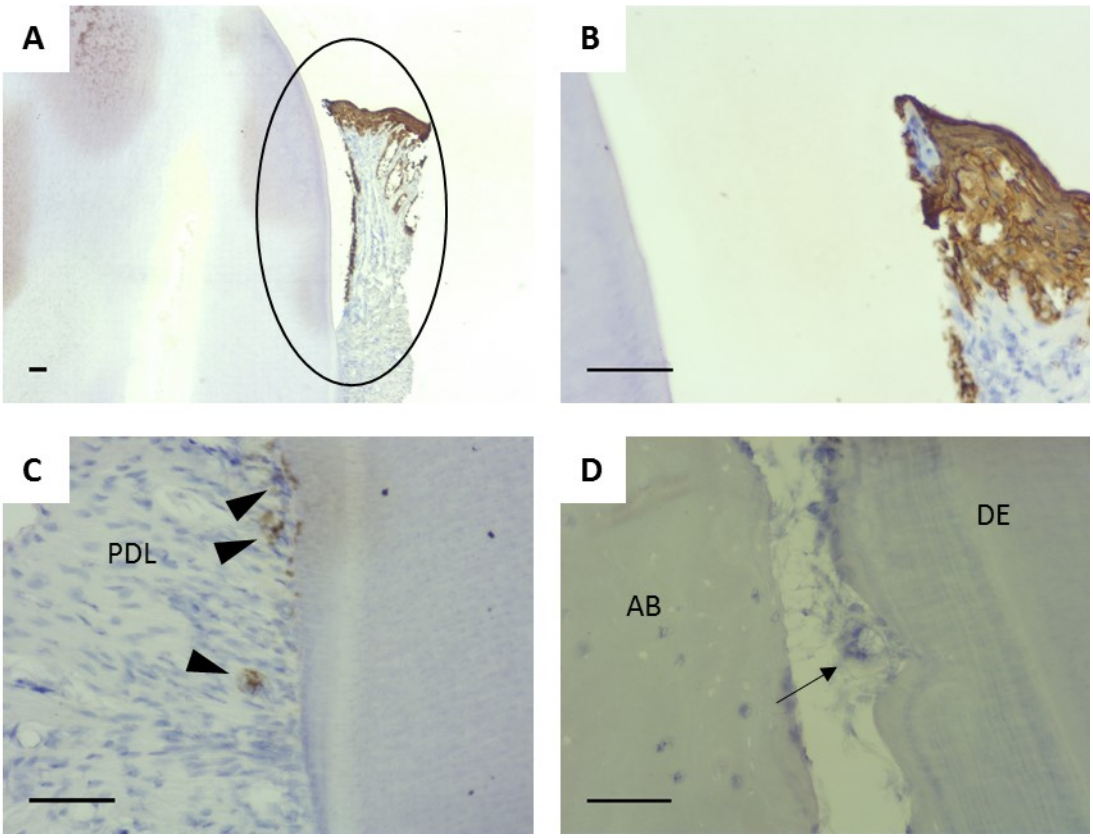

Figure 6.3 No cytokeratin expression was shown in odontoclasts in order to distinguish from epithelial cells. Highly expressed cytokeratin in gingival epithelial cells (circle) at low magnification (A) and high magnification (B). Some cells which are epithelial origin also expressed cytokeratin in periodontal ligament (C, arrow heads). No expression of cytokeratin was observed in resorbing odontoclasts (D, arrows). AB: alveolar bone, DE: dentine, PDL: periodontal ligament. Scale bars = 100 µm.

6.4.3 *MMP9* mRNA is expressed during early feline osteoclast differentiation

MMP9 was highly expressed during osteoclast formation in comparison with control ($p < 0.0001$ by one-way ANOVA). *MMP9* mRNA expression was significantly up-regulated in the early stages of osteoclast differentiation, with a 7.8±0.2 ($p < 0.001$, two sample t-test) fold change on day 3 compared to day 0. MMP9 mRNA expression remained high until day 6 where after it increased further - 8.9±0.2 ($p = 0.0387$, two sample t-test) fold change (from base line control) on day 8 (Figure 6.4).

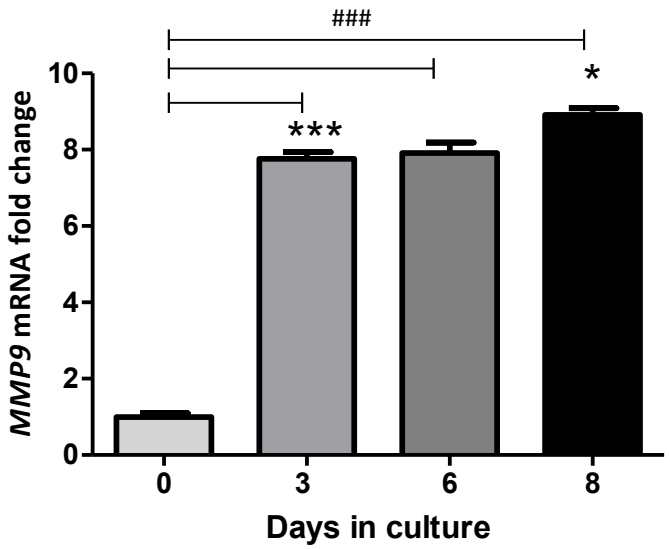

Figure 6.4 *MMP9* mRNA expression increased during *in vitro* feline osteoclast formation over an 8-day culture period. Precursors were treated with M-CSF from day 0, and addition of RANKL from day 3. Graphs represent relative expression as fold changes with + SEM bars. (n= 3; * $p < 0.05$, *** $p < 0.001$ in comparison with the previous time point in culture, ### $p < 0.001$ in comparison with day 0 by two sample t-test).

6.4.4 **Treatment with a semi-selective MMP9 inhibitor reduced osteoclast differentiation and resorption activity**

Since MMP9 was highly expressed in osteoclasts *in vitro* and in odontoclasts in dental tissues, I hypothesised that inhibiting MMP9 would affect osteoclast formation and resorption. *In vitro* osteoclast cultures were treated with a semi-selective MMP9 inhibitor (hydroxamate-based MMP inhibitor). The inhibitor contains hydroxamate (-CONHOH) group which binds to the zinc atom at the active site of MMP9. An inhibitory effect was observed on both osteoclast formation and resorption activity in a dose dependent manner (Figure 6.5, A and B). Osteoclast formation was not significantly reduced at low dose (5 nM, IC50 = 5 nM) compared to vehicle control ($p = 0.802$), but the inhibitor significantly inhibited osteoclast numbers at increased doses, where a 50±6.3% ($p < 0.0001$), and a 48.9±5.8% ($p < 0.0001$) decrease was observed at 20 nM and 1000 nM concentrations respectively (Figure 6.5. A). There was no further reduction in osteoclast numbers observed in the cultures treated with an inhibitor concentration of 20 nM and

1000 nM (p = 0.888). All three concentrations of MMP9 inhibitor resulted in a reduced resorption ability in comparison to vehicle control (Figure 6.5, B), and this was dose dependent (1000 nM) (12.2±2.5%, p = 0.001) and 20 nM (62.2±7.4%, p = 0.0003) and 5 nM (55.4±8.8%, p = 0.002), respectively.

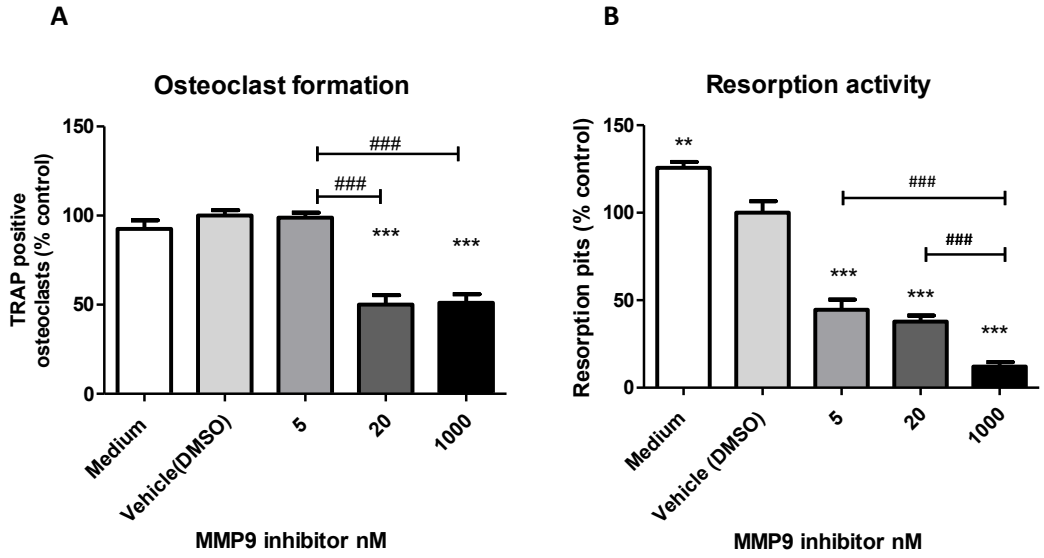

Figure 6.5 A MMP9 semi-selective inhibitor induced decreased feline osteoclast formation and resorption activity. Graphs represent percentage of number of osteoclasts (A) or resorption pits (B) with + SEM bars compared to vehicle (DMSO) control. (n= 3; * $p < 0.05$, ** $p < 0.01$; *** $p < 0.001$ in comparison with vehicle control, ### $p < 0.001$ between individual doses comparison by two sample t-test).

6.4.5 **Electroporation protocols had superior transfection efficiency and cell viability when compared to liposome-based osteoclast transfections**

As the MMP9 inhibitor used above does not specifically inhibit MMP9, the inhibitory effect might be via other members of the MMP family, especially at high concentrations (> 100 nM) according to the manufacturer's instruction. I therefore used RNA interference to specifically target feline *MMP9* mRNA. However, primary cells or terminally differentiated osteoclasts are extremely difficult to transfect using routine protocols. First, I investigated two widely available techniques: liposome-mediated transient transfection and electroporation. Both techniques were assessed utilising pEGFP (20 μg/ml), which expresses green

fluorescence to compare transfection efficiency, effect on osteoclast survival and differentiation. Following lipid-mediated transfection at 24 hrs (osteoclast culture day 3) cells looked viable with 90.15% alive (Figure 6.6, A) but GFP transfection efficiency assessed by flow cytometry was as low as 0.25% (Figure 6.6, B). When differentiated osteoclasts appeared 72 hrs post transfection (osteoclast culture day 5), transfected GFP was only rarely observed in the cells (Figure 6.6, C). The lipid-mediated transfection however seemed to cause minimal effect on osteoclast differentiation following transfection (Figure 6.6, D), probably due to the very low transfection efficiency.

Due to electric shock, after electroporation, some of the precursor cells were observed floating in the culture medium, which indicates that the electroporation protocol itself caused cell damage. Therefore it was recommended to use double the normal number of cells according to manufacturer's protocol. Twenty four hrs following electroporation, cell viability of transfected cells was assessed by flow cytometry, and it was 97.14% in comparisons with cells electoporated with scrambled control siRNA. Transfection efficiency was 40.53% (Figure 6.6, E and F) as measured by flow cytometry for green fluorescence protein. Seventy two hours following electroporation with pEGFP GFP expression was observed in both early stage and differentiated osteoclasts. Electroporation also did not interfere with osteoclast differentiation when viable osteoclasts precursors were cultured (Figure 6.6, H). Transfection efficiency was greatly improved compared to that achieved with lipid mediated transfection.

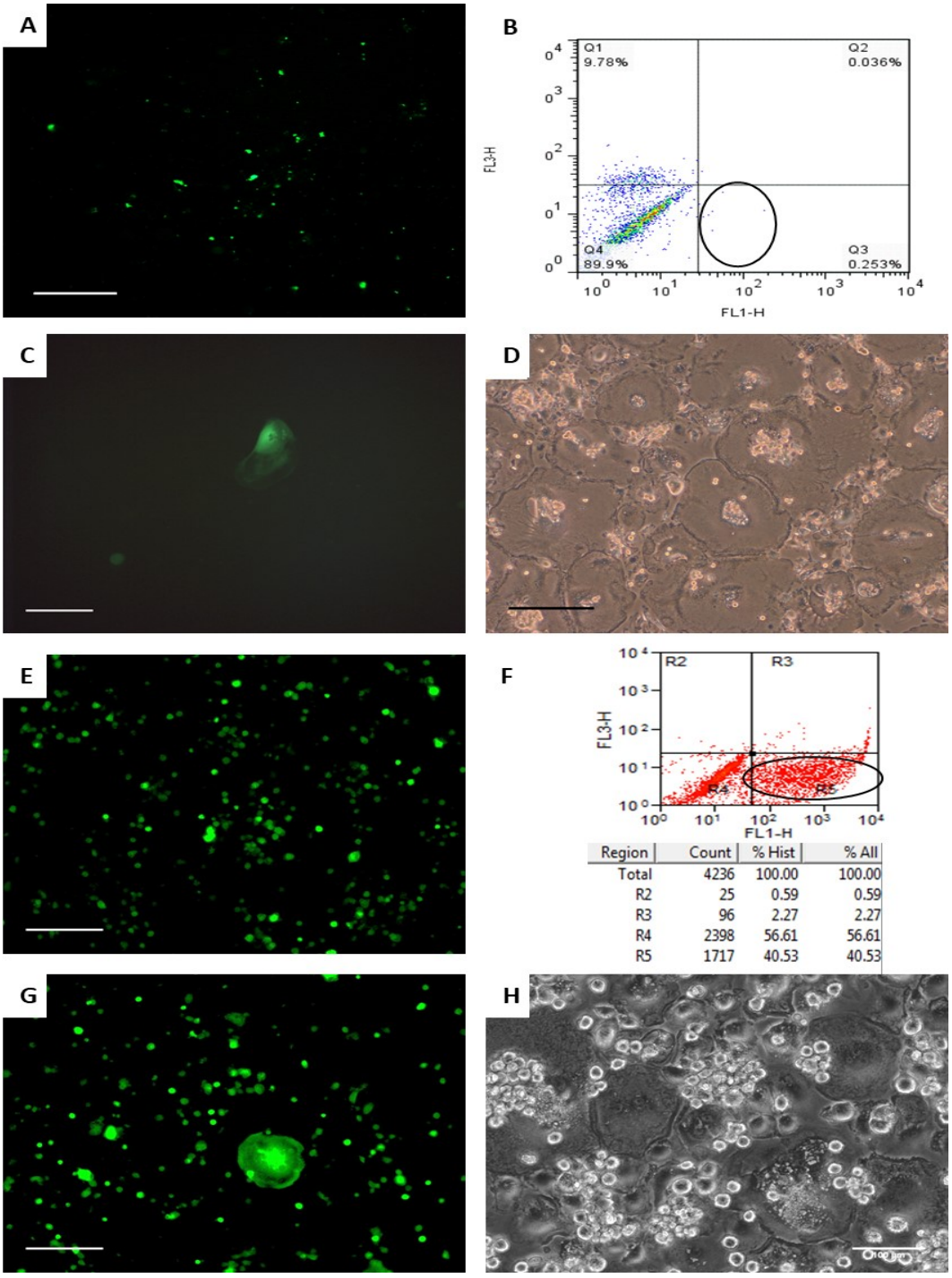

Figure 6.6 Electroporation more efficiently induced temporary transfection of pEGFP in feline osteoclasts compared with a lipid-mediated transfection. Transfection by lipid-mediated protocol (A–D) and electroporation using pEGFP (20 µg/ml) (E-H). A and E represent fluorescence microscope views 24 hrs post transfection (osteoclast culture day 3) in precursors. Transfection efficiencies of lipid-mediated transfection and electroporation by flow cytometry analysis were 0.25% and 40.53%, respectively (B and F, circled area). Fluorescence microscopy of EGFP expression 72 hrs post transfection (C and G; osteoclast culture day 5). D and H show phase contrast images of mature osteoclasts after transfection on day 8. Scale bars =100 µm.

6.4.6 *MMP9* specific siRNAs caused moderate mRNA reductions and reduced the number of osteoclast formed

Following electroporation of the osteoclast precursors with the *MMP9* siRNA, a 44.00±0.03% reduction ($p = 0.0032$) in *MMP9* mRNA levels was observed in the transfected cells as assessed by qPCR at 48 hrs post transfection when compared to negative control transfected precursors (Figure 6.7).

After verifying the efficacy of MMP9 siRNA, feline osteoclast precursors were transfected with feline MMP9 siRNA for treatment or scrambled siRNA for a control and seeded on dentine disc to investigate MMP9's role during osteoclast formation. Electroporation caused some cell death and therefore untransfected cells formed a higher number of osteoclasts and more resorption pits (Figure 6.8, B and D) but all transfected cells were also able to differentiate mature osteoclasts (Figure 6.6., H). *MMP9* siRNA transfected cells resulted in reduced osteoclast formation in comparison with scrambled control. There was a reduction of 74.8±7.2% in the number of osteoclasts formed ($p < 0.0001$) (Figure 6.8, A and B). However, no statistically significant differences in resorption activity was observed between scrambled and siRNA treated wells ($p < 0.2298$) (Figure 6.8).

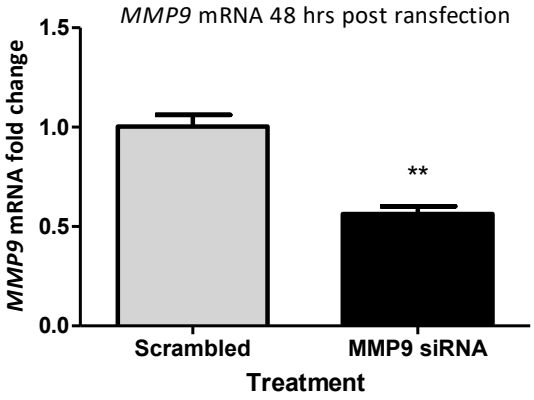

Figure 6.7 *MMP9* mRNA expression levels were reduced (48 hrs post transfection) by *MMP9* siRNA electroporation of feline osteoclast precursors. Graph represents relative expression as fold changes with + SEM bars. (n = 3, ** p < 0.01 by two sample t-test).

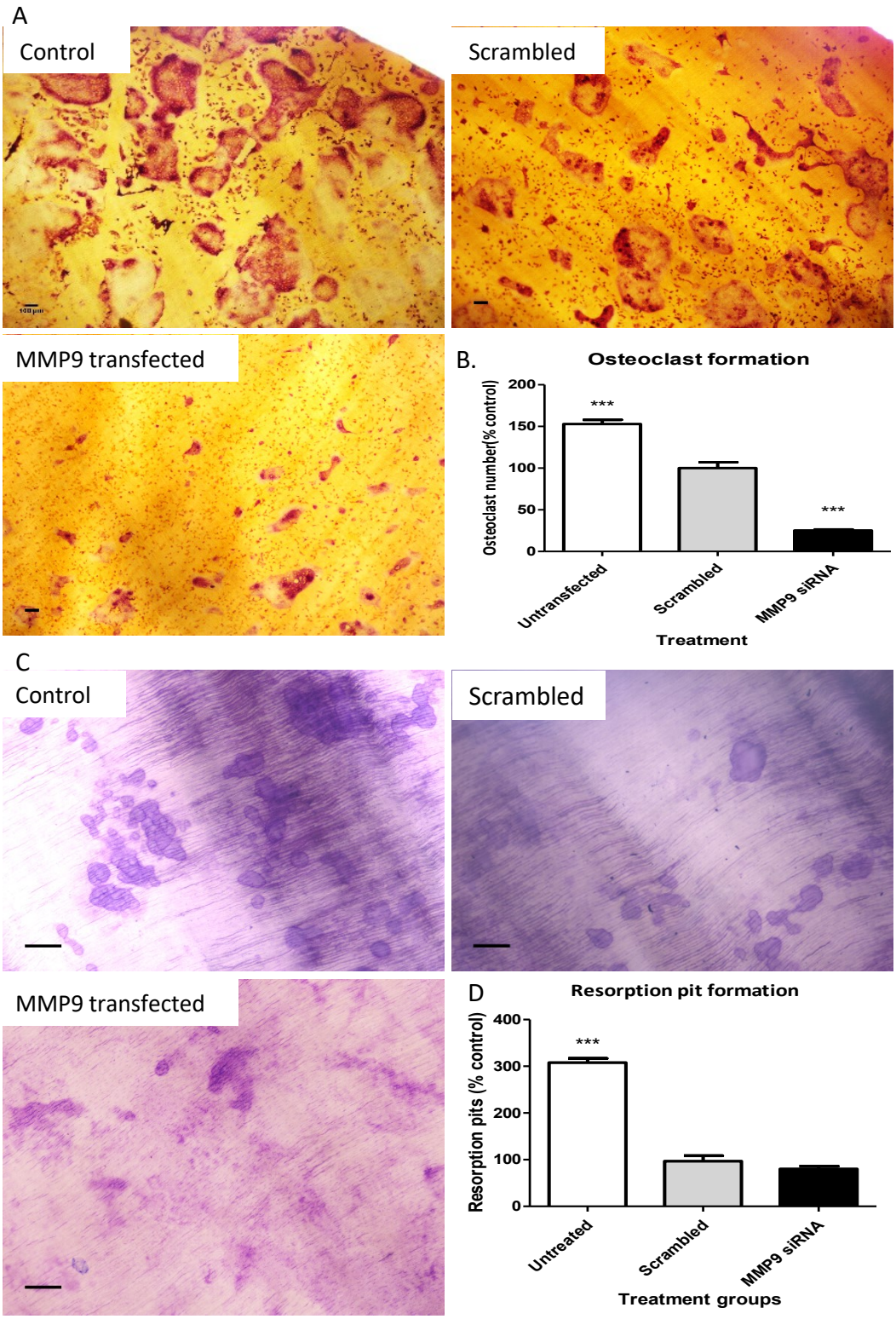

Figure 6.8 *MMP9* siRNA transfected cells resulted in reduced osteoclast formation in comparison with scrambled control but there was no statistically significant differences in resorption activity. Graphs represent percentage of number of osteoclasts (B) and resorption pits (D) with + SEM bars. (n= 3; *** $p < 0.001$ in comparison with scrambled control). Scale bars = 100 µm.

6.5 Discussion

In this chapter, confirmation of TR candidate genes identified by RNA-seq and qPCR in chapter 5 was performed using more TR+ve and TR-ve samples. *MMP9* and *P2X4R* were identified as up-regulated genes in TR +ve teeth by qPCR therefore validating my previous data. To extend these obervations I sought confirmation at the protein level and to identify which cells in the dental tissues expressed these proteins. The relative expression level by immunolabelling intensity was also assessed. Prior to immunohistochemistry, optimisation of antibodies to detect MMP9, RANK, RANKL, P2XR4, OPG, and SPI.1 proteins was attempted. Only MMP9 antibody was successfully optimised and the rest of the antibodies failed to specifically label their targets when compared to isotype controls. Availability of feline specific antibodies is limited, and the antibodies (RANK and OPG) previously reported to have worked in feline tissues were no longer commercially available (328). For example the previously documented polyclonal anti-RANK, RANKL, and OPG antibodies had been replaced by monoclonal antibodies. Hence for these candidate proteins, further optimisation of available antibodies will be necessary or alternatively feline specific antibodies made although this latter option was out with the possibilities in this PhD. Immunohistochemical success is not only down to antigen-antibody specificity, but is also dependent on the tissue processing techniques used preceding the immunohistochemistry. Generally formalin fixed mineralised tissues are required to be demineralised and embedded in paraffin followed by dewaxing and antigen retrieval in order to expose the epitope (the antibody binding site). Due to the several harsh interventions for processing feline tooth samples, antibody epitopes might be masked or destroyed during the extended demineralisation period in EDTA (*e.g*. 6 weeks), the dewaxing or initial immunolabelling steps (*e.g*. or boiling during the antigen retrieval by enzymatic treatment). Although standard protocols for the above procedures were followed (122, 328), the above technical challenges might go some way to answer why difficulties optimising these antibodies were

encountered. These problems are not limited to the study of skeletal tissues of non-routine species (*e.g.* human, mouse and rat). These challenges have been referred to in a previous human bone immunohistochemical study (329).

Although MMP9 is one of the best evaluated MMPs in osteoclasts (324), MMP9 expression in feline teeth has not been previously documented. I found that the intensity of MMP9 expression in odontoclasts was much greater than the surrounding tissues (*e.g.* periodontal ligament fibroblasts). Specifically, odontoclasts actively resorbing dentine were only observed in TR +ve teeth and they were immunolabelled with MMP9. This might indicate that the increase in *MMP9* expression observed in TR +ve tooth samples at the mRNA levels may be due to an increase in odontoclast numbers in the tissues. However, due to the difficulty of obtaining intact teeth sections following a long period of decalcification processing(up to 6 weeks), there was limited number of intact tissue section available with active resorption pits. Importantly MMP9 was also highly expressed in clustered ERM cells, which can be visible in the periodontal ligament and therefore they needed to be distinguished from odontoclasts. The initial quantification data may have overestimated the number of odontoclasts, as when the sections were labelled for cytokeratin, ERM cells in the periodontal ligament were positive while odontoclasts in resorption pits were not.

Disrupted periodontal ligament fibres, loss of periodontal ligament and replacement by ankylosis were predominantly observed in TR +ve teeth. The periodontal ligament has been documented to be part of the biological protection mechanism to prevent tooth resorption and therefore disrupted periodontal ligamnet may be a potential site of odontoclast attack. Similar histological features have been documented in other studies (92, 95, 113). Combination of qPCR data and histological investigation highlights the necessity for further investigation of MMP9 as a potential target in TR.

MMP9 expression in cultured osteoclasts was also shown by immunocytochemistry in Chapter 4. To investigate the expression pattern during osteoclast differentiation, *MMP9* mRNA level was quantitatively measured and it

increased over the culture time period. The increase in *MMP9* expression during osteoclast differentiation has been previously documented in RAW 264.7 cells where the authors showed that RANKL signalling induced *MMP9* mRNA expression through TRAFR6 and that NFATc1 was a downstream effector in mouse osteoclast precursors (153). The RAW 264.7 cells are commonly used in the study of osteoclast biology, but the biology of this cell line is somewhat different from bone marrow derived pre-osteoclasts in terms of different stages of osteoclasts. This cell line is more comparable with mouse macrophages (330). My data in this chapter additionally showed that *MMP9* mRNA expression increased in osteoclast precursors before RANKL treatment commenced on day 3 in comparison to early osteoclast precursors on day 0 and it remained high until osteoclasts were fully differentiated. This might imply MMP9 affects osteoclast biology from the myeloid lineage commitment stage. Further studies on bone marrow derived precursors are required to further elucidate this relationship.

The synthetic MMP9 inhibitor effectively reduced both osteoclast formation and resorption. Synthetic MMP inhibitors have been developed for the treatment of several serious pathologies including periodontitis, although clinical trials gave disappointing results and only a few inhibitors (*e.g*. Periostat™) has been approved by the FDA for the treatment of periodontal disease (331). The synthetic inhibitor possesses a hydroxamic acid analogue which binds to the enzymatic sites of MMPs with high-affinity (331). However, members of MMPs family share a basic structure which comprises an auto-inhibitory pro-domain rendering them enzymatic latency, the catalytic domain, and the C-terminal hemopexin-like domain, for the recognition of MMP substrates (318). Although the inhibition of osteoclastic activity by the MMP9 inhibitor is concentration dependent, it is not clear if the effect of the MMP9 inhibitor is specific to MMP9 or not.

For this reason, I designed a siRNA targeting feline *MMP9*. Prior to application of the siRNA in feline osteoclast precursors, I searched for effective transfection protocols, and electroporation was identified as an improved transfection technique compared to lipid-mediated protocols. A previous study

showed that electroporation in murine bone marrow derived macrophages induced an immediate 20% reduction in cellular metabolism by measuring the reduction of tetrazolium dye by NAD(P)H-dependent oxidoreductase enzyme but their metabolism was recovered after about 24 hrs post transfection (332). The study showed that the introduction of DNA into the cytoplasm is toxic to primary bone marrow derived macrophages rather than the electroporation procedure itself. Although it suggested that the toxicity of DNA was concentration-dependent and sequence-independent, relatively high amount of DNA was tolerated (25 μg/ml). To avoid high toxicity of introduction of foreign DNA, I used the same concentration of DNA (20 μg/ml of endotoxin-free plasmid DNA) based on an optimised electroporation transfection for murine macrophages (333).

Osteoclast formation was significantly inhibited by feline *MMP9* siRNA but resorption activity was not significantly affected. The contribution to osteoclastic resorption by MMP9 may be less than that of CTSK and therefore inhibition of MMP9 expression might have a minor effect on resorption capabilities. It is possible that MMP9 may have a more important role in osteoclast formation and migration. However prior to any conclusions being made, these experiment need to be repeated using various siRNAs together with a precise measurement of resorption activity.

Specifically, MMP9 is secreted as a pro-enzyme that requires activation in the extracellular space (263). Activation of MMP9 is complex and tightly regulated by enzyme inhibition by endogenous inhibitors, the tissue inhibitors of MMPs (TIMPs) and activators of other MMPs (263). In this present study a limited approach was used to investigate the effects of MMP9 inhibition on osteoclast formation and resorption. Therefore, verifying a potential role of MMP9 in osteoclasts and odontoclasts requires further investigation which could include the analyses of pro-enzyme and post enzyme activity, combination effect with other member of MMPs and the use of feline MMP9 specific inhibitors as shown in other species (321).

Meanwhile several studies reported that a selective inhibitor of cathepsin K,

odanacatib was an effective inhibitor of bone resorption *in vivo* and *in vitro* (334, 335) and a clinical study of postmenopausal women demonstrated that it showed increased bone mineral density and reduced biochemical markers of bone resorption (336). Therefore, use of cathepsin K inhibitor or combination of cathepsin K and MM9 inhibitors might have benefits for inhibition of feline osteoclastic resorption activity.

Chapter 7 Discussion

7.1 General discussion

Feline tooth resorption is a common, painful and progressive disease. Domestic cats often suffer multiple TR lesions and lose their permanent teeth due to the progressive nature of the disease. The treatment option of choice is to extract affected teeth. Currently our understanding of the aetiologies is incomplete. Dysregulation of odontoclasts are responsible for TR but the mechanisms underlying their dysregulation are largely unknown. The central aims of this study were to identify candidate genes related to feline odontoclast dysregulation and assess their potential as therapeutic targets. The first step was to complete a RNA-seq investigation to study the molecular characteristics of TR +ve teeth and identify candidate genes correlated with TR. An *in vitro* feline osteoclast model was also established to investigate cellular characteristics of feline osteoclast biology. This model was then used to test potential novel treatment targets for TR.

In Chapter 3, a successful RNA isolation procedure from feline teeth collected in a clinical setting and at post-mortem was developed. The optimised RNA extraction protocol produced sufficient yields of RNA with a medium to high RNA integrity value suitable for gene expression by qPCR of reference genes and RNA-seq data analysis. The RNA-seq technique, as well as the RNA quality introduce potential intrinsic biases due to nucleotide composition, GC contents and PCR, which might directly affect the accuracy of resultant RNA-seq data (241, 337, 338). Therefore, a quality assessment of RNA-seq data prior to subsequent analyses is a critical step for the interpretation of RNA-seq data. In this study, commonly applied factors (*e.g.* yield, sequencing depth, read distribution, duplication rate and alignment rates) in RNA-seq data was first assessed.(231, 337). This analysis guided me in choosing the data to include or exclude for further downstream analysis.

Based on previous studies I also tested putative aetiological factors by qPCR, in particular the involvement of inflammatory cytokines (e.g. *IL1B, IL6, TNF* and *IFNG*) and *RANKL* (100, 163). *P2X7R* was also included as it is considered a

stimulator of osteoclast differentiation in human root resorption (81).

However, my results could not identify any significant changes in the expression of these genes in samples from TR –ve and TR +ve teeth. No change of *RANKL* mRNA levels was consistent with previous feline TR studies (100, 163). It has been reported that RANKL is highly expressed in the periodontal ligament of actively resorbing primary human teeth, (33, 76) whereas the level of *RANKL* mRNA is very low or not expressed in human adult teeth (163, 339). In cats, *RANKL* mRNA levels between adult teeth and bones is similar (163). Since odontoclasts activity is tightly controlled by the OPG/RANKL ratio, the level of *OPG* and *RANKL* mRNA expression should be considered together. In feline healthy permanent teeth, the level of *OPG* mRNA is significantly higher than femoral or alveolar bone, providing evidence that the role of OPG may be a key factor rather than RANKL in modulating odontoclast function in feline TR (163). This is supported by my RNA-seq and qPCR data in the comparison of TR -/+ teeth from the same cat; the level of *OPG* mRNA level was low in the TR +ve teeth thus an increased *RANKL*/*OPG* ratio was observed in TR +ve teeth. However, the observation was not verified when repeated in a larger number of samples, hence the RANKL/OPG involvement in feline TR needs to be further investigated. My data did not show any changes in the expression of pro-inflammatory cytokines between TR –ve and TR +ve teeth but it did show that *IL6* mRNA expression was upregulated in the early stages of TR in comparison with TR –ve teeth or late stage TR. This may suggest that *IL6* is involved in the initiation of TR. The alterative or co-stimulation factors (*e.g.* Toll-like receptors, osteoclast associated receptor, and IL1,4, 6, 10, 23) rather than RANKL itself might play more important roles in osteoclast formation and activation in adult teeth, which is documented in inflammatory arthritis (244). Osteoclast immunology (also referred to as osteoimmunology) has recently gained traction to obtain a more complete understanding of osteoclast biology in various fields of study. This includes; the pathology of bone and cancers and the microenvironment of bone and the immune system in pathological conditions (*e.g*. inflammation or infiltrated cancer cells), which leads immune cells including T cells, B cells and

dendritic cells to release stimulatory cytokines for osteoclast formation (43, 340). In my study population, gene expression studies provided no evidence for an involvement of pro-inflammatory cytokines in TR pathogenesis however, further investigations of various other co-stimulating factors on a larger sample size are required. I also established a protocol for the *in vitro* differentiation of feline osteoclasts from bone marrow derived precursors. *In vitro* feline osteoclasts presented with osteoclast characteristics and resorption activity on mineralised substrate and this is in agreement with other studies (228, 245). I tested the role of $1,25(OH)_2D_3$ on osteoclast formation as a few studies have suggested that vitamin D metabolism could be critical for TR via local effects of $1,25(OH)_2D$ and its receptor (122, 185). My data showed *VDR* mRNA was expressed in teeth but the levels of expression were similar in TR –ve and TR +ve teeth. In my studies, the local effects of $1,25(OH)_2D_3$ on osteoclastogenesis showed dual effects; moderately increased physiological level of $1,25(OH)_2D$ stimulated osteoclast activity whereas high doses of $1,25(OH)_2D_3$ caused a decrease in osteoclast formation. This is similar to *in vivo* findings (170, 185). Functional feline osteoclasts could be generated under co-culture conditions with primary feline periodontal ligament cells but without additional RANKL. Osteoclast precursors from TR +ve cats formed higher numbers of osteoclasts when co-cultured with periodontal ligament compared to TR -ve cats in the absence of RANKL. This might suggest that osteoclast precursors from TR +ve cats are more sensitive/primed to respond to osteoclast stimulating factors released by dental cells and their niche. It has been shown that human primary, adult periodontal ligament and dental pulp have the capacity to differentiate osteoclasts *in vitro* without osteotropic factors (76, 142). Here, I focused on the osteoclast itself but osteoclasts and their interaction with other dental cells need to be considered.

Chapter 5 uncovered the transcriptomic changes between TR -ve and TR +ve teeth. The paired cat comparison identified statistically significant differentially expressed genes and metabolic pathways that promote osteoclast differentiation. These results support my hypothesis that the transcriptome of TR positive teeth is locally different from TR negative teeth. The changes revealed up-regulation of

pathways related to osteoclast formation and calcium signalling in TR +ve teeth. I could only verify a selection of the genes in the differentially expressed genes list including *SPI1, OPG, MMP9, ACP5, CTSK, P2X2R, P2X4R, P2X6R* and *PCLB4* which all might be involved in osteoclast differentiation and activity based on previous studies (207, 260, 263, 283, 285, 290, 315, 341).

In addition to osteoclast biology, many genes associated with dental and bone development were identified (*e.g. ARX, HOXA4, LBX1, TLX1, SOSTDC1, ACTA1, ACTN2, ATP2A1, CSRP3, MYH11, MYOZ2, PDLIM3, SYNC, TCAP, TNNI1, TNNT3, TPM2).* This was unexpected as adult teeth normally possess a limited ability of remodel. However, as TR +ve teeth showed 1) a predominantly disrupted periodontal ligament, 2) new bone formation (ankylosis) and 3) external TR lesions in the root rather than internally, the noted changes in gene expression may reflect repair, limited remodelling or new bone formation.

In the final chapter, MMP9 was chosen as a target for further investigation due to its potential role in osteoclast biology. According to my data, inhibition of MMP9 by a semi-selective synthetic inhibitor caused both a reduction of osteoclast formation and resorption activity. When inhibition of *MMP9* mRNA was successfully performed by feline *MMP9* siRNA, osteoclast formation, but not resorption activity, was inhibited. The reduction of resorption activity by synthetic inhibitors but not by the more specific siRNA approach may be a result of off-target inhibition of other members of the MMP super family. Therefore, MMP9 inhibition experiments by the siRNA approach might be more specific for MMP9. The initial studies suggesting a role for MMP9 in TR pathogenesis require further investigation before any firm conclusions can be reached. Strong MMP9 expression in osteoclasts/odontoclasts has been reported in bovine, rabbit and mice skeletal tissue but its role in osteoclast activity is not clear (152, 342). The major enzyme involved in osteoclastic resorption is CTSK and the role of MMP9 in resorption has not been thoroughly investigated (150). The role of MMP9 in osteoclast precursor's migration has been more thoroughly investigated (150, 319). The underlying mechanism of inhibition of osteoclast formation by MMP9 was not investigated in this present

study.

It was technically very challenging dealing with mineralised samples for histological analysis (*e.g.* precisely identifying the tooth lesions before sectioning and insufficient decalcification of tooth for histology study). Therefore, quantification of MMP9 expression data in TR –ve and TR +ve teeth could not be done due to the limited availability of tooth sections with active odontoclasts. The lack of osteoclasts was mentioned in other studies (92, 93, 98); every tooth section did not contain TR lesion even if the section was originated from TR +ve teeth. This might be because it is difficult to obtain accurate sections of the TR lesions. Also a clear distinction of different TR stages was not possible and larger future studies are required in which a number of tooth sections from multiple teeth at different stages of TR are required.

7.2 Future direction

The *in vitro* model optimised here can be applied to study a range of different pathologies such as periodontitis induced osteoclast activation or bone resorption in invasive cancer. Indeed, an ongoing project in our group is using this *in vitro* system for investigation the role of the microenvironment on osteoclast activation in bone invasive cancers.

Future osteoclast studies should include *in vitro* assay to mimic the *in vivo* environment as osteoclast formation and activation is tightly regulated by other cells in the local vicinity. Likewise, osteoclasts secrete several compounds to promote osteoblast precursor recruitment and differentiation (343). Co-culture system protocols will be useful for these further studies.

The RNA-seq data have now been made publicly available and should be utilised for further investigation of feline dental research. As the feline genome is not fully annotated, the use of these data in the future has the potential to make further insights into feline dental research. In this study, RNA-seq data was aligned to the published feline reference genome. However, since the feline genome is not fully annotated the analysis of the transcriptome without a reference genome would

allow the identification of novel genes. In addition, *de novo* transcriptome assembly could detect transcript isoforms which do not align continuously along the genome and may be erroneously discounted as they may not be identified using a reference-based assembly (208). Due to time limitations, only a relatively small number of samples were included. In future studies are performed, the design of the study should take into account the technical and biological variability and the sample size can be calculated according to a published formula (344). Furthermore, I would suggest that samples in any future studies should include all different stages of TR and be paired within cats. This new data could be combined with my existing data using paired samples. To overcome the technical challenges encountered using mineralised tissues I would propose to use specialised strategies for mineralised tissues processing, and laser capture microdissection, a precise sample dissection technique utilised in mouse and human tooth studies (201, 237).

It would also be valuable to test further candidate genes from the differentially expressed gene list. To verify those candidate genes by qPCR, probe-based assays can be used to improve accuracy, wherein the hydrolysis probe based assay uses the probe amplicon specific primers that bind within the amplicon of the target sequence in order to generate a fluorescent signal (251, 257).

Finally, further investigations aimed at elucidating the functional role of MMP9 in osteoclast biology should include enzyme activity assays and the use of feline MMP9 specific inhibitors (321).

Appendix 1: Supporting information

Additional supporting information is electronically stored in the CD attachment.

Supporting information 1. A table of read counts

Supporting information 2. Differentially expressed genes and fold changes between TR -ve and TR +ve teeth

Supporting information 3. KEGG pathway enrichment for the set of genes differentially expressed between TR- and TR+

Supporting information 4. Gene ontology term enrichment for the set of genes differentially expressed between TR- and TR+

Supporting information 5. SNPs within candidate genes of the TR- and TR+ samples

Appendix 2: Antibodies

Antibodies for immunocytochemistry				
Primary antibody	Raised in species	Manufacturer	Dilution	Incubation time
Vitronectin	Mouse monclonal	Thermoscientific, Integrin alpha V + Integrin beta-3 Antibody (23C6), MA1-33578	1:100	Overnight 4°C
Calcitonin	Rabbit Polyclonal	Thermoscientific, PA5-25594	1:50	Overnight 4°C
Cathepin K	Mouse monoclonal	Abcam, ab66237	1:100	Overnight 4°C
Anti-Src	Mouse	Santa Cruz® Biotechnology, c-Src (B12): sc-8056.	1:100	Overnight 4°C
MMP9	Rabbit Polyclonal	Abnova, PAB12714	1:50	Overnight 4°C
RANKL	Rabbit	ProSci, XP-5273Bt	1: 50, 100	Overnight 4°C
Vimentin	Mouse	Abocam, ab8069	1:100	Overnight 4°C
Secondary	Raised in species	Manufacturer	Dilution	Incubation time
Anti-rabbit IgG	Goat	Thermoscientific AlexaFluro 568, A11011	1:500	1h at room, dark
Anti-Mouse IgG	Goat	Thermoscientific AlexaFluro® 488, A11029	1:500	1h at room, dark
Antibodies used for western blot				
Primary	Raised in species	Manufacturer	Dilution	Incubation time
RANKL	Rabbit	ProSci, XP-5273Bt	1:50, 1:100, 1:200	Overnight 4°C
Secondary	Raised in species	Manufacturer	Dilution	Incubation time
HRP Anti-Rabbit	Swine	Dako, P0217	1:1000	1h at RT

Appendix 3: Solutions and buffers

Resolving gel: 8-10% acrylamide, 375 mM Tris-HCl pH 8.8, 0.1% SDS, 0.1% ammonium persulphate, 0.08% TEMED.

1x SDS-PAGE Running buffer: 192 mM Glycine, 25 mM Tris, 0.1 % SDS.

1xTris-Glycine buffer transfer buffer: 192 mM Glycine, 25 mM Tris.

PBST blocking buffer: 5% Skimmed Milk in PBST.

Urea lysis buffer: 7M urea, 0.1 M DTT, 0.05% Triton x-100, 25 mM NaCl, 20 mM HEPES-KOH, pH 7.6

Tris Buffers: 1.5 M Tris-HCl, pH 8.8 and 1M Tris-HCl, pH 6.8

4X SDS sample buffer: 20 % SDS, 1M Tris pH 6.8, 80% glycerol, 0.1 M EDTA, 1% bromophenol blue

References

1. Ten Cate AR, Nanci A. Structure of the Oral Tissues. In: Nanci A, Ten Cate AR, editors. Ten Cate's oral histology : development, structure, and function. 6th ed. Mosby,; 2003. p.1-16.
2. Wiggs RB, Lobprise HB. Oral Anatomy and Physiology. In: Wiggs RB, Lobprise HB, editors. Veterinary dentistry : principles and practice. Lippincott-Raven Publishers; 1997. p.55-86.
3. Crossley DA. Tooth enamel thickness in the mature dentition of domestic dogs and cats-preliminary study. J Vet Dent. 1995;12(3):111-3.
4. Ginjupally U, Pachigolla R, Sankaran S, Balla S, Pattipati S, Chennoju S. Assessment of age based on the pulp cavity width of the maxillary central incisors. J Indian Acad Oral Med Radiol. 2014;26(1):46-9.
5. Rafter M. Apexification: a review. Dent Traumatol. 2005;21(1):1-8.
6. Bellows J. Feline dentistry : oral assessment, treatment, and preventative care. Ames, Wiley-Blackwell; 2010. p. 314.
7. Lekic P, McCulloch CA. Periodontal ligament cell population: the central role of fibroblasts in creating a unique tissue. The Anatomical record. 1996;245(2):327-41.
8. Nanci A, Whitson S, Bianco P. Bone. In: Nanci A, Ten Cate AR, editors. Ten Cate's oral histology : development, structure, and function. 6th ed. Mosby,; 2003. p. 111-43.
9. Okuda A, Harvey CE. Etiopathogenesis of feline dental resorptive lesions. Vet Clin North Am Small Anim Pract. 1992;22(6):1385-404.
10. Hayashi K, Kiba H. Microhardness of enamel and dentine of cat premolar teeth. Nihon Juigaku Zasshi. 1989;51(5):1033-5.
11. Dixon PM, du Toit N. Dental Anatomy. In: Equine dentistry [Internet]. 3rd ed. Saunders,; 2011. p. 51-76. Available from: http://ezproxy.is.ed.ac.uk/login?url=http://www.sciencedirect.com/science/book/9780702029806.
12. Wiggs RB, Lobprise HB. Dental and Oral Disease in Rodents and Lagomorphs. In: Wiggs RB, Lobprise HB, editors. Veterinary dentistry : principles and practice. Lippincott-Raven Publishers; 1997. p. 518-26.
13. Wiggs RB, Lobprise HB. Domestic Feline Oral and Dental Disease In: Wiggs RB, Lobprise HB, editors. Veterinary dentistry : principles and practice. Lippincott-Raven Publishers; 1997. p. 482-96.
14. Nanci A, Ten Cate AR. Physiologic Tooth Movement: Eruption and Shedding. In: Nanci A, Ten Cate AR, editors. Ten Cate's oral histology : development, structure, and function. 6th ed. Mosby,; 2003. p. 275-98.
15. Floyd MR. The modified Triadan system: nomenclature for veterinary dentistry. J Vet Dent. 1991;8(4):18-9.
16. Nanci A, Whitson S, Bianco P. Dentin-pulp complex. In: Nanci A, Ten Cate AR, editors. Ten Cate's oral histology : development, structure, and function. 6th ed, Mosby,; 2003. p. 157-92.

17. West NX, Lussi A, Seong J, Hellwig E. Dentin hypersensitivity: pain mechanisms and aetiology of exposed cervical dentin. Clinical Oral Investigations. 2013;17(Suppl 1):9-19.
18. Brannstrom M. Sensitivity of dentine. Oral surgery, oral medicine, and oral pathology. 1966;21(4):517-26.
19. Boyce BF, Xing L. Osteoclasts, no longer osteoblast slaves. Nat Med. 2006;12(12):1356-8.
20. Arnett TR. Chapter 8 - Osteoclast Biology. In: Cauley RMFWDLA, editor. Osteoporosis. 4th ed. Academic Press; 2013. p. 149-60.
21. Sahara N, Toyoki A, Ashizawa Y, Deguchi T, Suzuki K. Cytodifferentiation of the odontoclast prior to the shedding of human deciduous teeth: an ultrastructural and cytochemical study. Anat Rec. 1996;244(1):33-49.
22. Boyle WJ, Simonet WS, Lacey DL. Osteoclast differentiation and activation. Nature. 2003;423(6937):337-42.
23. Wang Z, McCauley LK. Osteoclasts and odontoclasts: signaling pathways to development and disease. Oral diseases. 2011;17(2):129-42.
24. Lasfargues JJ, Saffar JL. Inhibition of prostanoid synthesis depresses alveolar bone resorption but enhances root resorption in the rat. Anat Rec. 1993;237(4):458-65.
25. Sasaki T. Differentiation and functions of osteoclasts and odontoclasts in mineralized tissue resorption. Microsc Res Tech. 2003;61(6):483-95.
26. Harokopakis-Hajishengallis E. Physiologic root resorption in primary teeth: molecular and histological events. J Oral Sci. 2007;49(1):1-12.
27. Muto A, Mizoguchi T, Udagawa N, Ito S, Kawahara I, Abiko Y, et al. Lineage-committed osteoclast precursors circulate in blood and settle down into bone. J Bone Miner Res. 2011;26(12):2978-90.
28. Miyamoto T. Identification and characterization of osteoclast precursor cells. IBMS BoneKEy. 2013;10.
29. Takeshita S, Kaji K, Kudo A. Identification and characterization of the new osteoclast progenitor with macrophage phenotypes being able to differentiate into mature osteoclasts. J Bone Miner Res. 2000;15(8):1477-88.
30. Yasuda H, Shima N, Nakagawa N, Yamaguchi K, Kinosaki M, Mochizuki S, et al. Osteoclast differentiation factor is a ligand for osteoprotegerin/osteoclastogenesis-inhibitory factor and is identical to TRANCE/RANKL. Proc Natl Acad Sci. 1998;95(7):3597-602.
31. Simonet WS, Lacey DL, Dunstan CR, Kelley M, Chang MS, Luthy R, et al. Osteoprotegerin: a novel secreted protein involved in the regulation of bone density. Cell. 1997;89(2):309-19.
32. Dougall WC. Molecular pathways: osteoclast-dependent and osteoclast-independent roles of the RANKL/RANK/OPG pathway in tumorigenesis and metastasis. Clin Cancer Res. 2012;18(2):326-35.
33. Fukushima H, Kajiya H, Takada K, Okamoto F, Okabe K. Expression and role of RANKL in periodontal ligament cells during physiological root-resorption in human deciduous teeth. Eur J Oral Sci. 2003;111(4):346-52.
34. O'Brien CA. Control of RANKL gene expression. Bone. 2010;46(4):911-9.

35. Boyce BF. Advances in osteoclast biology reveal potential new drug targets and new roles for osteoclasts. J Bone Miner Res. 2013;28(4):711-22.
36. Boyce BF. Advances in the regulation of osteoclasts and osteoclast functions. J Dent Res. 2013;92(10):860-7.
37. Edwards JR, Mundy GR. Advances in osteoclast biology: old findings and new insights from mouse models. Nat Rev Rheumatol. 2011;7(4):235-43.
38. Vaananen HK, Laitala-Leinonen T. Osteoclast lineage and function. Arch Biochem Biophys. 2008;473(2):132-8.
39. Long CL, Humphrey MB. Osteoimmunology: the expanding role of immunoreceptors in osteoclasts and bone remodeling. Bonekey Rep. 2012;1.
40. Horowitz MC, Xi Y, Wilson K, Kacena MA. Control of osteoclastogenesis and bone resorption by members of the TNF family of receptors and ligands. Cytokine Growth Factor Rev. 2001;12(1):9-18.
41. Lomaga MA, Yeh WC, Sarosi I, Duncan GS, Furlonger C, Ho A, et al. TRAF6 deficiency results in osteopetrosis and defective interleukin-1, CD40, and LPS signaling. Gene Dev. 1999;13(8):1015-24.
42. Naito A, Azuma S, Tanaka S, Miyazaki T, Takaki S, Takatsu K, et al. Severe osteopetrosis, defective interleukin-1 signalling and lymph node organogenesis in TRAF6-deficient mice. Genes Cells. 1999;4(6):353-62.
43. Takayanagi H. Osteoimmunology and the effects of the immune system on bone. Nat Rev Rheumatol. 2009;5(12):667-76.
44. Crockett JC, Mellis DJ, Scott DI, Helfrich MH. New knowledge on critical osteoclast formation and activation pathways from study of rare genetic diseases of osteoclasts: focus on the RANK/RANKL axis. Osteoporos Int. 2011;22(1):1-20.
45. Lacey DL, Boyle WJ, Simonet WS, Kostenuik PJ, Dougall WC, Sullivan JK, et al. Bench to bedside: elucidation of the OPG-RANK-RANKL pathway and the development of denosumab. Nat Rev Drug Discov. 2012;11(5):401-19.
46. Kim JH, Kim N. Signaling Pathways in Osteoclast Differentiation. Chonnam Med J. 2016;52(1):12-7.
47. Mizukami J, Takaesu G, Akatsuka H, Sakurai H, Ninomiya-Tsuji J, Matsumoto K, et al. Receptor Activator of NF-κB Ligand (RANKL) Activates TAK1 Mitogen-Activated Protein Kinase Kinase Kinase through a Signaling Complex Containing RANK, TAB2, and TRAF6. Mol Cell Biol. 2002;22(4):992-1000.
48. DiDonato JA, Mercurio F, Karin M. NF-kappaB and the link between inflammation and cancer. Immunol Rev. 2012;246(1):379-400.
49. Boyce BF, Xing L. Functions of RANKL/RANK/OPG in bone modeling and remodeling. Arch Biochem Biophys. 2008;473(2):139-46.
50. Takayanagi H, Kim S, Koga T, Nishina H, Isshiki M, Yoshida H, et al. Induction and activation of the transcription factor NFATc1 (NFAT2) integrate RANKL signaling in terminal differentiation of osteoclasts. Dev Cell. 2002;3(6):889-901.
51. Wada T, Nakashima T, Hiroshi N, Penninger JM. RANKL-RANK signaling in osteoclastogenesis and bone disease. Trends Mol Med. 2006;12(1):17-25.
52. Kobayashi K, Takahashi N, Jimi E, Udagawa N, Takami M, Kotake S, et al. Tumor necrosis factor alpha stimulates osteoclast differentiation by a mechanism independent of the ODF/RANKL-RANK interaction. J Exp Med. 2000;191(2):275-86.

53. Ten Cate AR, Sharpe PT, Roy S, Nanci A. Development of the Tooth and Its Supporting Tissues. In: Nanci A, Ten Cate AR, editors. Ten Cate's oral histology : development, structure, and function. 6th ed. Mosby,; 2003. p. 79-110.
54. Seo BM, Miura M, Gronthos S, Bartold PM, Batouli S, Brahim J, et al. Investigation of multipotent postnatal stem cells from human periodontal ligament. Lancet. 2004;364(9429):149-55.
55. Moradian-Oldak J. Protein- mediated enamel mineralization. Frontiers in bioscience : a journal and virtual library. 2012;17:1996-2023.
56. McKee MD, Yadav MC, Foster BL, Somerman MJ, Farquharson C, Millan JL. Compounded PHOSPHO1/ALPL deficiencies reduce dentin mineralization. Journal of dental research. 2013;92(8):721-7.
57. Zweifler LE, Ao M, Yadav M, Kuss P, Narisawa S, Kolli TN, et al. Role of PHOSPHO1 in Periodontal Development and Function. Journal of dental research. 2016;95(7):742-51.
58. Foster BL, Nociti FH, Jr., Somerman MJ. The rachitic tooth. Endocrine reviews. 2014;35(1):1-34.
59. Lumsden AG. Spatial organization of the epithelium and the role of neural crest cells in the initiation of the mammalian tooth germ. Development. 1988;103 Suppl:155-69.
60. Fraser GJ, Bloomquist RF, Streelman JT. Common developmental pathways link tooth shape to regeneration. Developmental biology. 2013;377(2):399-414.
61. Thesleff I. Epithelial-mesenchymal signalling regulating tooth morphogenesis. Journal of cell science. 2003;116(Pt 9):1647-8.
62. Zeichner-David M, Oishi K, Su Z, Zakartchenko V, Chen LS, Arzate H, et al. Role of Hertwig's epithelial root sheath cells in tooth root development. Developmental dynamics : an official publication of the American Association of Anatomists. 2003;228(4):651-63.
63. Huang X, Bringas P, Jr., Slavkin HC, Chai Y. Fate of HERS during tooth root development. Developmental biology. 2009;334(1):22-30.
64. Bei M. Molecular genetics of tooth development. Current opinion in genetics & development. 2009;19(5):504-10.
65. Tiffee JC, Xing L, Nilsson S, Boyce BF. Dental abnormalities associated with failure of tooth eruption in src knockout and op/op mice. Calcified tissue international. 1999;65(1):53-8.
66. Yoshino M, Yamazaki H, Yoshida H, Niida S, Nishikawa S, Ryoke K, et al. Reduction of osteoclasts in a critical embryonic period is essential for inhibition of mouse tooth eruption. J Bone Miner Res. 2003;18(1):108-16.
67. Wise GE. Cellular and molecular basis of tooth eruption. Orthodontics & craniofacial research. 2009;12(2):67-73.
68. Heinrich J, Bsoul S, Barnes J, Woodruff K, Abboud S. CSF-1, RANKL and OPG regulate osteoclastogenesis during murine tooth eruption. Archives of oral biology. 2005;50(10):897-908.
69. Wise GE, Yao S. Regional differences of expression of bone morphogenetic protein-2 and RANKL in the rat dental follicle. European journal of oral sciences. 2006;114(6):512-6.

70. Liu D, Wise GE. Expression of endothelial monocyte-activating polypeptide II in the rat dental follicle and its potential role in tooth eruption. European journal of oral sciences. 2008;116(4):334-40.
71. Wise GE, Lumpkin SJ, Huang H, Zhang Q. Osteoprotegerin and osteoclast differentiation factor in tooth eruption. Journal of dental research. 2000;79(12):1937-42.
72. Liu D, Yao S, Pan F, Wise GE. Chronology and regulation of gene expression of RANKL in the rat dental follicle. European journal of oral sciences. 2005;113(5):404-9.
73. Wise GE, Yao S, Odgren PR, Pan F. CSF-1 regulation of osteoclastogenesis for tooth eruption. Journal of dental research. 2005;84(9):837-41.
74. Que BG, Wise GE. Colony-stimulating factor-1 and monocyte chemotactic protein-1 chemotaxis for monocytes in the rat dental follicle. Archives of oral biology. 1997;42(12):855-60.
75. Sahara N. Cellular events at the onset of physiological root resorption in rabbit deciduous teeth. The Anatomical record. 2001;264(4):387-96.
76. Hasegawa T, Kikuiri T, Takeyama S, Yoshimura Y, Mitome M, Oguchi H, et al. Human periodontal ligament cells derived from deciduous teeth induce osteoclastogenesis in vitro. Tissue & cell. 2002;34(1):44-51.
77. Lossdorfer S, Gotz W, Jager A. Immunohistochemical localization of receptor activator of nuclear factor kappaB (RANK) and its ligand (RANKL) in human deciduous teeth. Calcified tissue international. 2002;71(1):45-52.
78. Berry JE, Ealba EL, Pettway GJ, Datta NS, Swanson EC, Somerman MJ, et al. JunB as a downstream mediator of PTHrP actions in cementoblasts. J Bone Miner Res. 2006;21(2):246-57.
79. Rani CS, MacDougall M. Dental cells express factors that regulate bone resorption. Molecular cell biology research communications : MCBRC. 2000;3(3):145-52.
80. Peralta S, Verstraete FJ, Kass PH. Radiographic evaluation of the types of tooth resorption in dogs. American journal of veterinary research. 2010;71(7):784-93.
81. Hartsfield JK, Jr. Pathways in external apical root resorption associated with orthodontia. Orthodontics & craniofacial research. 2009;12(3):236-42.
82. Berger MS, P.; Stich, H.; Lussi, A. Feline dental resorptive lesions in captive and wild leopards and lions. Journal of veterinary dentistry. 1996;13(1):13-21.
83. Darcey J, Qualtrough A. Resorption: part 1. Pathology, classification and aetiology. Br Dent J. 2013;214(9):439-51.
84. Rehrl S, Schroder W, Muller C, Staszyk C, Lischer C. Radiological prevalence of equine odontoclastic tooth resorption and hypercementosis. Equine veterinary journal. 2017.
85. Staszyk C, Bienert A, Kreutzer R, Wohlsein P, Simhofer H. Equine odontoclastic tooth resorption and hypercementosis. Vet J. 2008;178(3):372-9.
86. Hopewell-Smith A. Original Communications; The Process of Osteolysis and Odontolysis, or So-Called Absorption of Calcified Tissues: A New and Original Investigation The Dental Cosmos 1930;72(10):1036-48.

87. Berger M, Schawalder P, Stich H, Lussi A. [Differential diagnosis of resorptive tooth diseases and caries]. Schweizer Archiv fur Tierheilkunde. 1996;138(11):546-51.
88. Berger M, Stich H, Huster H, Roux P, Schawalder P. Feline caries in two cats from a 13th century archeological excavation. Journal of veterinary dentistry. 2006;23(1):13-7.
89. Hale FA. Dental caries in the dog. Journal of veterinary dentistry. 1998;15(2):79-83.
90. Oh C, Lee K, Cheong Y, Lee S-W, Park S-Y, Song C-S, et al. Comparison of the Oral Microbiomes of Canines and Their Owners Using Next-Generation Sequencing. PloS one. 2015;10(7):e0131468.
91. Schneck GW, Osborn JW. Neck lesions in the teeth of cats. The Veterinary record. 1976;99(6):100.
92. Reiter AM, Lewis JR, Okuda A. Update on the etiology of tooth resorption in domestic cats. The Veterinary clinics of North America Small animal practice. 2005;35(4):913-42.
93. Reiter AM. Feline "odontolysis" in the 1920's: the forgotten histopathological study of feline odontoclastic resorptive lesions (FORL). Journal of veterinary dentistry. 1998;15(1):35-41.
94. Berger M, Stich H, Huster H, Roux P, Schawalder P. Feline dental resorptive lesions in the 13th to 14th centuries. Journal of veterinary dentistry. 2004;21(4):206-13.
95. DeLaurier A, Boyde A, Horton MA, Price JS. A scanning electron microscopy study of idiopathic external tooth resorption in the cat. J Periodontol. 2005;76(7):1106-12.
96. Soğur E, Soğur HD, Baksi Akdeniz BG, Sen BH. Idiopathic root resorption of the entire permanent dentition: systematic review and report of a case. Dent Traumatol. 2008;24(4):490-5.
97. Heaton M, Wilkinson J, Gorrel C, Butterwick R. A rapid screening technique for feline odontoclastic resorptive lesions. The Journal of small animal practice. 2004;45(12):598-601.
98. Reiter AM, Mendoza KA. Feline odontoclastic resorptive lesions an unsolved enigma in veterinary dentistry. The Veterinary clinics of North America Small animal practice. 2002;32(4):791-837.
99. DuPont GA, DeBowes LJ. Comparison of periodontitis and root replacement in cat teeth with resorptive lesions. Journal of veterinary dentistry. 2002;19(2):71-5.
100. Booij-Vrieling HE, Tryfonidou MA, Riemers FM, Penning LC, Hazewinkel HA. Inflammatory cytokines and the nuclear vitamin D receptor are implicated in the pathophysiology of dental resorptive lesions in cats. Vet Immunol Immunopathol. 2009;132(2-4):160-6.
101. Cleland WP, Jr. Opportunities and obstacles in veterinary dental drug delivery. Advanced drug delivery reviews. 2001;50(3):261-75.
102. Girard N, Servet E, Biourge V, Hennet P. Feline tooth resorption in a colony of 109 cats. Journal of veterinary dentistry. 2008;25(3):166-74.
103. Ingham KE, Gorrel C, Blackburn J, Farnsworth W. Prevalence of odontoclastic

resorptive lesions in a population of clinically healthy cats. The Journal of small animal practice. 2001;42(9):439-43.
104. Lund EM, Bohacek LK, Dahlke JL, King VL, Kramek BA, Logan EI. Prevalence and risk factors for odontoclastic resorptive lesions in cats. Journal of the American Veterinary Medical Association. 1998;212(3):392-5.
105. Mestrinho LA, Runhau J, Braganca M, Niza MM. Risk assessment of feline tooth resorption: a Portuguese clinical case control study. Journal of veterinary dentistry. 2013;30(2):78-83.
106. Lommer MJ, Verstraete FJ. Prevalence of odontoclastic resorption lesions and periapical radiographic lucencies in cats: 265 cases (1995-1998). Journal of the American Veterinary Medical Association. 2000;217(12):1866-9.
107. van Wessum R, Harvey CE, Hennet P. Feline dental resorptive lesions. Prevalence patterns. The Veterinary clinics of North America Small animal practice. 1992;22(6):1405-16.
108. Farcas N, Lommer MJ, Kass PH, Verstraete FJ. Dental radiographic findings in cats with chronic gingivostomatitis (2002-2012). Journal of the American Veterinary Medical Association. 2014;244(3):339-45.
109. Lommer MJ, Verstraete FJ. Radiographic patterns of periodontitis in cats: 147 cases (1998-1999). Journal of the American Veterinary Medical Association. 2001;218(2):230-4.
110. Harvey CE, Orsini P, McLahan C, Schuster C. Mapping of the radiographic central point of feline dental resorptive lesions. Journal of veterinary dentistry. 2004;21(1):15-21.
111. Bradaschia-Correa V, Moreira MM, Arana-Chavez VE. Reduced RANKL expression impedes osteoclast activation and tooth eruption in alendronate-treated rats. Cell and tissue research. 2013;353(1):79-86.
112. Arzi B, Murphy B, Cox DP, Vapniarsky N, Kass PH, Verstraete FJ. Presence and quantification of mast cells in the gingiva of cats with tooth resorption, periodontitis and chronic stomatitis. Archives of oral biology. 2010;55(2):148-54.
113. Gorrel C, Larsson A. Feline odontoclastic resorptive lesions: unveiling the early lesion. The Journal of small animal practice. 2002;43(11):482-8.
114. Gorrel C. Tooth resorption in cats: pathophysiology and treatment options. Journal of feline medicine and surgery. 2015;17(1):37-43.
115. Logan EI. CHAPTER 28 - Dental Diseases. In: Morgan RV, editor. Handbook of Small Animal Practice, 5th ed, W.B. Saunders; 2008. p. 309-18.
116. Shigeyama Y, Grove TK, Strayhorn C, Somerman MJ. Expression of adhesion molecules during tooth resorption in feline teeth: a model system for aggressive osteoclastic activity. Journal of dental research. 1996;75(9):1650-7.
117. Mohn KL, Jacks TM, Schleim KD, Harvey CE, Miller B, Halley B, et al. Alendronate binds to tooth root surfaces and inhibits progression of feline tooth resorption: a pilot proof-of-concept study. Journal of veterinary dentistry. 2009;26(2):74-81.
118. Rodan GA, Fleisch HA. Bisphosphonates: mechanisms of action. Journal of Clinical Investigation. 1996;97(12):2692-6.
119. Putranto R, Oba Y, Kaneko K, Shioyasono A, Moriyama K. Effects of

bisphosphonates on root resorption and cytokine expression during experimental tooth movement in rats. Orthodontic Waves. 2008;67(4):141-9.
120. Barba-Recreo P, Del Castillo Pardo de Vera JL, Garcia-Arranz M, Yebenes L, Burgueno M. Zoledronic acid - Related osteonecrosis of the jaws. Experimental model with dental extractions in rats. Journal of cranio-maxillo-facial surgery : official publication of the European Association for Cranio-Maxillo-Facial Surgery. 2013.
121. Tomes J, Nowell WS, Tomes CS. A system of dental surgery. Churchill; 1906. p. 780.
122. Booij-Vrieling HE, Ferbus D, Tryfonidou MA, Riemers FM, Penning LC, Berdal A, et al. Increased vitamin D-driven signalling and expression of the vitamin D receptor, MSX2, and RANKL in tooth resorption in cats. European journal of oral sciences. 2010;118(1):39-46.
123. Andreasen JO. Luxation of permanent teeth due to trauma. A clinical and radiographic follow-up study of 189 injured teeth. Scandinavian journal of dental research. 1970;78(3):273-86.
124. Andreasen JO. External root resorption: its implication in dental traumatology, paedodontics, periodontics, orthodontics and endodontics. International endodontic journal. 1985;18(2):109-18.
125. Fernandes M, de Ataide I, Wagle R. Tooth resorption part I - pathogenesis and case series of internal resorption. Journal of conservative dentistry : JCD. 2013;16(1):4-8.
126. Fuss Z, Tsesis I, Lin S. Root resorption--diagnosis, classification and treatment choices based on stimulation factors. Dent Traumatol. 2003;19(4):175-82.
127. Fernandes M, de Ataide I, Wagle R. Tooth resorption part II - external resorption: Case series. Journal of conservative dentistry : JCD. 2013;16(2):180-5.
128. Krishnan V, Davidovitch Z. Cellular, molecular, and tissue-level reactions to orthodontic force. American journal of orthodontics and dentofacial orthopedics : official publication of the American Association of Orthodontists, its constituent societies, and the American Board of Orthodontics. 2006;129(4):469:1-32.
129. Harris EF, Boggan BW, Wheeler DA. Apical root resorption in patients treated with comprehensive orthodontics. J Tenn Dent Assoc. 2001;81(1):30-3.
130. Arnbjerg J. Idiopathic dental root replacement resorption in old dogs. Journal of veterinary dentistry. 1996;13(3):97-9.
131. Hamp S-E, Olsson S-E, Farsø-Madsen K, Viklands P, Fornell J. A macroscopic and radiologic investigation of dental diseases of the dog. Veterinary Radiology. 1984;25(2):86-92.
132. Yoshikawa H, Watanabe K, Ozawa T. Odontoclastic resorptive lesions in a dog. The Journal of veterinary medical science. 2008;70(1):103-5.
133. Kaplan B. Root resorption of the permanent teeth of a dog. Journal of the American Veterinary Medical Association. 1967;151(6):708-9.
134. Sarkiala-Kessel E. Diagnostic imaging in veterinary dental practice. Diagnostic imaging findings and interpretation. Journal of the American Veterinary Medical Association. 2008;233(3):389-91.
135. Verstraete FJ, Kass PH, Terpak CH. Diagnostic value of full-mouth

radiography in dogs. American journal of veterinary research. 1998;59(6):686-91.
136. Peralta S, Verstraete FJ, Kass PH. Radiographic evaluation of the classification of the extent of tooth resorption in dogs. American journal of veterinary research. 2010;71(7):794-8.
137. Roux P, Berger M, Stich H, Schawalder P. Oral examination and radiographic evaluation of the dentition in wild cats from Namibia. Journal of veterinary dentistry. 2009;26(1):16-22.
138. Bellows J. Radiographic signs and diagnosis of dental disease. Seminars in veterinary medicine and surgery (small animal). 1993;8(3):138-45.
139. Roux P, Berger M, Stoffel M, Stich H, Doherr MG, Bosshard D, et al. Observations of the periodontal ligament and cementum in cats with dental resorptive lesions. Journal of veterinary dentistry. 2005;22(2):74-85.
140. Poumpros E, Loberg E, Engstrom C. Thyroid function and root resorption. The Angle orthodontist. 1994;64(5):389-93.
141. Freilich LS. Ultrastructure and Acid Phosphatase Cytochemistry of Odontoclasts: Effects of Parathyroid Extract. Journal of dental research. 1971;50(5):1046-55.
142. Uchiyama M, Nakamichi Y, Nakamura M, Kinugawa S, Yamada H, Udagawa N, et al. Dental pulp and periodontal ligament cells support osteoclastic differentiation. Journal of dental research. 2009;88(7):609-14.
143. Lee A, Schneider G, Finkelstein M, Southard T. Root resorption: the possible role of extracellular matrix proteins. American journal of orthodontics and dentofacial orthopedics : official publication of the American Association of Orthodontists, its constituent societies, and the American Board of Orthodontics. 2004;126(2):173-7.
144. Arnett TR. Acidosis, hypoxia and bone. Archives of biochemistry and biophysics. 2010;503(1):103-9.
145. Tondravi MM, McKercher SR, Anderson K, Erdmann JM, Quiroz M, Maki R, et al. Osteopetrosis in mice lacking haematopoietic transcription factor PU.1. Nature. 1997;386:81.
146. Luchin A, Purdom G, Murphy K, Clark MY, Angel N, Cassady AI, et al. The microphthalmia transcription factor regulates expression of the tartrate-resistant acid phosphatase gene during terminal differentiation of osteoclasts. Journal of Bone and Mineral Research. 2000;15(3):451-60.
147. Grigoriadis AE, Wang ZQ, Cecchini MG, Hofstetter W, Felix R, Fleisch HA, et al. c-Fos: a key regulator of osteoclast-macrophage lineage determination and bone remodeling. Science. 1994;266(5184):443-8.
148. Miyamoto H, Suzuki T, Miyauchi Y, Iwasaki R, Kobayashi T, Sato Y, et al. Osteoclast stimulatory transmembrane protein and dendritic cell-specific transmembrane protein cooperatively modulate cell-cell fusion to form osteoclasts and foreign body giant cells. J Bone Miner Res. 2012;27(6):1289-97.
149. Bozec A, Bakiri L, Hoebertz A, Eferl R, Schilling AF, Komnenovic V, et al. Osteoclast size is controlled by Fra-2 through LIF/LIF-receptor signalling and hypoxia. Nature. 2008;454(7201):221-5.
150. Delaisse JM, Andersen TL, Engsig MT, Henriksen K, Troen T, Blavier L. Matrix

metalloproteinases (MMP) and cathepsin K contribute differently to osteoclastic activities. Microscopy research and technique. 2003;61(6):504-13.
151. Akkoc A, Inan S, Sonmez G. Matrix metalloproteinase (MMP-2 and MMP-9) and steroid receptor expressions in feline mammary tumors. Biotechnic & histochemistry : official publication of the Biological Stain Commission. 2012;87(4):312-9.
152. Linsuwanont B, Takagi Y, Ohya K, Shimokawa H. Expression of matrix metalloproteinase-9 mRNA and protein during deciduous tooth resorption in bovine odontoclasts. Bone. 2002;31(4):472-8.
153. Sundaram K, Nishimura R, Senn J, Youssef RF, London SD, Reddy SV. RANK ligand signaling modulates the matrix metalloproteinase-9 gene expression during osteoclast differentiation. Experimental cell research. 2007;313(1):168-78.
154. Mellis DJ, Itzstein C, Helfrich MH, Crockett JC. The skeleton: a multi-functional complex organ: the role of key signalling pathways in osteoclast differentiation and in bone resorption. The Journal of endocrinology. 2011;211(2):131-43.
155. Hartsfield JK, Everett ET, Al-Qawasmi RA. Genetic factors in external apical root resorption and orthodontic treatment. Crit Rev Oral Biol Med. 2004;15(2):115-22.
156. Al-Qawasmi RA, Hartsfield JK, Jr., Everett ET, Flury L, Liu L, Foroud TM, et al. Genetic predisposition to external apical root resorption. American journal of orthodontics and dentofacial orthopedics : official publication of the American Association of Orthodontists, its constituent societies, and the American Board of Orthodontics. 2003;123(3):242-52.
157. Al-Qawasmi RA, Hartsfield JK, Jr., Everett ET, Flury L, Liu L, Foroud TM, et al. Genetic predisposition to external apical root resorption in orthodontic patients: linkage of chromosome-18 marker. Journal of dental research. 2003;82(5):356-60.
158. Sharab LY, Morford LA, Dempsey J, Falcao-Alencar G, Mason A, Jacobson E, et al. Genetic and treatment-related risk factors associated with external apical root resorption (EARR) concurrent with orthodontia. Orthodontics & craniofacial research. 2015;18(Suppl 1):71-82.
159. Liu B-Y, Wu P-W, Bringhurst FR, Wang J-T. Estrogen Inhibition of PTH-Stimulated Osteoclast Formation and Attachment in Vitro: Involvement of Both PKA and PKC. Endocrinology. 2002;143(2):627-35.
160. Takahashi N, Udagawa N, Suda T. Vitamin D endocrine system and osteoclasts. BoneKEy reports. 2014;3:495.
161. Granholm S, Henning P, Lerner UH. Comparisons between the effects of calcitonin receptor-stimulating peptide and intermedin and other peptides in the calcitonin family on bone resorption and osteoclastogenesis. Journal of cellular biochemistry. 2011;112(11):3300-12.
162. Canalis E. Wnt signalling in osteoporosis: mechanisms and novel therapeutic approaches. Nature reviews Endocrinology. 2013;9(10):575-83.
163. DeLaurier A, Allen S, deFlandre C, Horton MA, Price JS. Cytokine expression in feline osteoclastic resorptive lesions. Journal of comparative pathology. 2002;127(2-3):169-77.

164. Donoghue S, Scarlett JM, Williams CA, Saidla J. Diet as a risk factor for feline external odontoclastic resorption. The Journal of nutrition. 1994;124(12 Suppl):2693S-4S.
165. Scarlett JM, Saidla J, Hess J. Risk factors for odontoclastic resorptive lesions in cats. Journal of the American Animal Hospital Association. 1999;35(3):188-92.
166. Muzylak M, Arnett TR, Price JS, Horton MA. The in vitro effect of pH on osteoclasts and bone resorption in the cat: implications for the pathogenesis of FORL. Journal of cellular physiology. 2007;213(1):144-50.
167. Muzylak M, Price JS, Horton MA. Hypoxia induces giant osteoclast formation and extensive bone resorption in the cat. Calcified tissue international. 2006;79(5):301-9.
168. Zetner K, Steurer I. The influence of dry food on the development of feline neck lesions. Journal of veterinary dentistry. 1992;9(2):4-6.
169. Lombardi G, Di Somma C, Rubino M, Faggiano A, Vuolo L, Guerra E, et al. The roles of parathyroid hormone in bone remodeling: prospects for novel therapeutics. Journal of endocrinological investigation. 2011;34(7):18-22.
170. Bikle DD. Vitamin D and Bone. Current osteoporosis reports. 2012;10(2):151-9.
171. Carter PH, Schipani E. The roles of parathyroid hormone and calcitonin in bone remodeling: prospects for novel therapeutics. Endocrine, metabolic & immune disorders drug targets. 2006;6(1):59-76.
172. Turner AS. Animal models of osteoporosis--necessity and limitations. European cells & materials. 2001;1:66-81.
173. Kanatani M, Sugimoto T, Sowa H, Kobayashi T, Kanzawa M, Chihara K. Thyroid hormone stimulates osteoclast differentiation by a mechanism independent of RANKL-RANK interaction. Journal of cellular physiology. 2004;201(1):17-25.
174. Frankenthal S, Nakhoul F, Machtei EE, Green J, Ardekian L, Laufer D, et al. The effect of secondary hyperparathyroidism and hemodialysis therapy on alveolar bone and periodontium. Journal of clinical periodontology. 2002;29(6):479-83.
175. Chandna S, Bathla M. Oral manifestations of thyroid disorders and its management. Indian Journal of Endocrinology and Metabolism. 2011;15(Suppl2):S113-S6.
176. DeLaurier A, Jackson B, Ingham K, Pfeiffer D, Horton MA, Price JS. Biochemical markers of bone turnover in the domestic cat: relationships with age and feline osteoclastic resorptive lesions. The Journal of nutrition. 2002;132(6 Suppl 2):1742s-4s.
177. Bolliger AP, Graham PA, Richard V, Rosol TJ, Nachreiner RF, Refsal KR. Detection of parathyroid hormone-related protein in cats with humoral hypercalcemia of malignancy. Veterinary clinical pathology. 2002;31(1):3-8.
178. Reiter AM, Lyon KF, Nachreiner RF, Shofer FS. Evaluation of calciotropic hormones in cats with odontoclastic resorptive lesions. Am J Vet Res. 2005;66(8):1446-52.
179. Kaji H, Sugimoto T, Kanatani M, Fukase M, Kumegawa M, Chihara K. Prostaglandin E2 stimulates osteoclast-like cell formation and bone-resorbing activity via osteoblasts: role of cAMP-dependent protein kinase. J Bone Miner Res.

1996;11(1):62-71.
180. Celebi AA, Demirer S, Catalbas B, Arikan S. Effect of ovarian activity on orthodontic tooth movement and gingival crevicular fluid levels of interleukin-1β and prostaglandin E2 in cats. The Angle orthodontist. 2013;83(1):70-5.
181. Girard N, Servet E, Biourge V, Hennet P. Periodontal health status in a colony of 109 cats. Journal of veterinary dentistry. 2009;26(3):147-55.
182. Holick MF, Smith E, Pincus S. Skin as the site of vitamin D synthesis and target tissue for 1,25-dihydroxyvitamin D3. Use of calcitriol (1,25-dihydroxyvitamin D3) for treatment of psoriasis. Archives of dermatology. 1987;123(12):1677-83.
183. How KL, Hazewinkel HA, Mol JA. Dietary vitamin D dependence of cat and dog due to inadequate cutaneous synthesis of vitamin D. General and comparative endocrinology. 1994;96(1):12-8.
184. Bikle DD. Vitamin D Metabolism, Mechanism of Action, and Clinical Applications. Chemistry & biology. 2014;21(3):319-29.
185. Anderson PH, Atkins GJ. The skeleton as an intracrine organ for vitamin D metabolism. Molecular Aspects of Medicine. 2008;29(6):397-406.
186. Zarei A, Morovat A, Javaid K, Brown CP. Vitamin D receptor expression in human bone tissue and dose-dependent activation in resorbing osteoclasts. Bone research. 2016;4:16030.
187. Morita T, Awakura T, Shimada A, Umemura T, Nagai T, Haruna A. Vitamin D toxicosis in cats: natural outbreak and experimental study. The Journal of veterinary medical science. 1995;57(5):831-7.
188. Morris JG, Earle KE, Anderson PA. Plasma 25-hydroxyvitamin D in growing kittens is related to dietary intake of cholecalciferol. The Journal of nutrition. 1999;129(4):909-12.
189. Sih TR, Morris JG, Hickman MA. Chronic ingestion of high concentrations of cholecalciferol in cats. American journal of veterinary research. 2001;62(9):1500-6.
190. Girard N, Servet E, Hennet P, Biourge V. Tooth Resorption and Vitamin D3 Status in Cats Fed Premium Dry Diets. Journal of veterinary dentistry. 2010;27(3):142-7.
191. Arneson WL, Arneson DL. Current Methods for Routine Clinical Laboratory Testing of Vitamin D Levels. Laboratory Medicine. 2013;44(1):38-42.
192. Hollis BW. Assessment and interpretation of circulating 25-hydroxyvitamin D and 1,25-dihydroxyvitamin D in the clinical environment. Endocrinology and metabolism clinics of North America. 2010;39(2):271-86.
193. Hunty Adl, Wallace AM, Gibson S, Viljakainen H, Lamberg-Allardt C, Ashwell M. UK Food Standards Agency Workshop Consensus Report: the choice of method for measuring 25-hydroxyvitamin D to estimate vitamin D status for the UK National Diet and Nutrition Survey. British Journal of Nutrition. 2010;104(4):612-9.
194. Collins MK, Sinclair PM. The local use of vitamin D to increase the rate of orthodontic tooth movement. American Journal of Orthodontics and Dentofacial Orthopedics. 1988;94(4):278-84.
195. Goel VK, Khera SC, Ralston JL, Chang KH. Stresses at the dentinoenamel junction of human teeth--a finite element investigation. The Journal of prosthetic dentistry. 1991;66(4):451-9.

196. Nakano Y, Yamaguchi M, Fujita S, Asano M, Saito K, Kasai K. Expressions of RANKL/RANK and M-CSF/c-fms in root resorption lacunae in rat molar by heavy orthodontic force. European journal of orthodontics. 2011;33(4):335-43.
197. Choi EK, Lee JH, Baek SH, Kim SJ. Gene expression profile altered by orthodontic tooth movement during healing of surgical alveolar defect. American journal of orthodontics and dentofacial orthopedics : official publication of the American Association of Orthodontists, its constituent societies, and the American Board of Orthodontics. 2017;151(6):1107-15.
198. Davidovitch Z, Montgomery PC, Gustafson GT, Eckerdal O. Cellular localization of cyclic AMP in periodontal tissues during experimental tooth movement in cats. Calcified tissue research. 1976;19(4):317-29.
199. DeLaurier A, Boyde A, Horton MA, Price JS. Analysis of the surface characteristics and mineralization status of feline teeth using scanning electron microscopy. Journal of anatomy. 2006;209(5):655-69.
200. Hofmann-Lehmann R, Berger M, Sigrist B, Schawalder P, Lutz H. Feline immunodeficiency virus (FIV) infection leads to increased incidence of feline odontoclastic resorptive lesions (FORL). Vet Immunol Immunopathol. 1998;65(2-4):299-308.
201. Hu S, Parker J, Wright JT. Towards unraveling the human tooth transcriptome: the dentome. PloS one. 2015;10(4):e0124801.
202. Simmer JP, Richardson AS, Wang SK, Reid BM, Bai Y, Hu Y, et al. Ameloblast transcriptome changes from secretory to maturation stages. Connect Tissue Res. 2014;55 Suppl 1:29-32.
203. Galicia JC, Henson BR, Parker JS, Khan AA. Gene expression profile of pulpitis. Genes and immunity. 2016;17(4):239-43.
204. Killiany DM. Root resorption caused by orthodontic treatment: an evidence-based review of literature. Seminars in orthodontics. 1999;5(2):128-33.
205. Segal GR, Schiffman PH, Tuncay OC. Meta analysis of the treatment-related factors of external apical root resorption. Orthodontics & craniofacial research. 2004;7(2):71-8.
206. Harris EF, Kineret SE, Tolley EA. A heritable component for external apical root resorption in patients treated orthodontically. American journal of orthodontics and dentofacial orthopedics : official publication of the American Association of Orthodontists, its constituent societies, and the American Board of Orthodontics. 1997;111(3):301-9.
207. Pereira S, Lavado N, Nogueira L, Lopez M, Abreu J, Silva H. Polymorphisms of genes encoding P2X7R, IL-1B, OPG and RANK in orthodontic-induced apical root resorption. Oral diseases. 2013.
208. Wang Z, Gerstein M, Snyder M. RNA-Seq: a revolutionary tool for transcriptomics. Nature reviews Genetics. 2009;10(1):57-63.
209. Trapnell C, Williams BA, Pertea G, Mortazavi A, Kwan G, van Baren MJ, et al. Transcript assembly and quantification by RNA-Seq reveals unannotated transcripts and isoform switching during cell differentiation. Nat Biotechnol. 2010;28(5):511-5.
210. Desjardin C, Vaiman A, Mata X, Legendre R, Laubier J, Kennedy SP, et al. Next-generation sequencing identifies equine cartilage and subchondral bone

miRNAs and suggests their involvement in osteochondrosis physiopathology. BMC Genomics. 2014;15(1):798.
211. Gunter HM, Fan S, Xiong F, Franchini P, Fruciano C, Meyer A. Shaping development through mechanical strain: the transcriptional basis of diet-induced phenotypic plasticity in a cichlid fish. Molecular ecology. 2013;22(17):4516-31.
212. Pfaffl MW. A new mathematical model for relative quantification in real-time RT-PCR. Nucleic Acids Res. 2001;29(9):45.
213. Rao X, Huang X, Zhou Z, Lin X. An improvement of the 2^(-delta delta CT) method for quantitative real-time polymerase chain reaction data analysis. Biostatistics, bioinformatics and biomathematics. 2013;3(3):71-85.
214. Reiter AM, Soltero-Rivera MM. Applied feline oral anatomy and tooth extraction techniques: an illustrated guide. Journal of feline medicine and surgery. 2014;16(11):900-13.
215. Chomczynski P, Sacchi N. Single-step method of RNA isolation by acid guanidinium thiocyanate-phenol-chloroform extraction. Analytical biochemistry. 1987;162(1):156-9.
216. Hubbard T, Barker D, Birney E, Cameron G, Chen Y, Clark L, et al. The Ensembl genome database project. Nucleic Acids Res. 2002;30(1):38-41.
217. Anders S, Pyl PT, Huber W. HTSeq—a Python framework to work with high-throughput sequencing data. Bioinformatics. 2015;31(2):166-9.
218. Robinson MD, McCarthy DJ, Smyth GK. edgeR: a Bioconductor package for differential expression analysis of digital gene expression data. Bioinformatics. 2010;26(1):139-40.
219. Kanehisa M, Goto S. KEGG: kyoto encyclopedia of genes and genomes. Nucleic Acids Res. 2000;28(1):27-30.
220. Ashburner M, Ball CA, Blake JA, Botstein D, Butler H, Cherry JM, et al. Gene ontology: tool for the unification of biology. The Gene Ontology Consortium. Nat Genet. 2000;25(1):25-9.
221. McKenna A, Hanna M, Banks E, Sivachenko A, Cibulskis K, Kernytsky A, et al. The Genome Analysis Toolkit: a MapReduce framework for analyzing next-generation DNA sequencing data. Genome research. 2010;20(9):1297-303.
222. Sherry ST, Ward MH, Kholodov M, Baker J, Phan L, Smigielski EM, et al. dbSNP: the NCBI database of genetic variation. Nucleic Acids Res. 2001;29(1):308-11.
223. Cingolani P, Platts A, Wang le L, Coon M, Nguyen T, Wang L, et al. A program for annotating and predicting the effects of single nucleotide polymorphisms, SnpEff: SNPs in the genome of Drosophila melanogaster strain w1118; iso-2; iso-3. Fly. 2012;6(2):80-92.
224. Yoshida H, Hayashi S, Kunisada T, Ogawa M, Nishikawa S, Okamura H, et al. The murine mutation osteopetrosis is in the coding region of the macrophage colony stimulating factor gene. Nature. 1990;345(6274):442-4.
225. Lacey DL, Timms E, Tan HL, Kelley MJ, Dunstan CR, Burgess T, et al. Osteoprotegerin ligand is a cytokine that regulates osteoclast differentiation and activation. Cell. 1998;93(2):165-76.
226. Collin-Osdoby P, Osdoby P. RANKL-mediated osteoclast formation from

murine RAW 264.7 cells. Methods in molecular biology. 2012;816:187-202.
227. Henriksen K, Karsdal MA, Taylor A, Tosh D, Coxon FP. Generation of human osteoclasts from peripheral blood. Methods in molecular biology. 2012;816:159-75.
228. Muzylak M, Flanagan AM, Ingham K, Gunn N, Price J, Horton MA. A feline assay using osteoclasts generated in vitro from peripheral blood for screening anti-resorptive agents. Research in Veterinary Science. 2002;73(3):283-90.
229. Orriss IRaA, T.R. Rodent osteoclast cultures. In Bone Research Protocols, Miep H. Helfrich & Stuart H. Ralston, 2nd ed. Humana Press; 2012. p.103-17.
230. Reynolds A, Leake D, Boese Q, Scaringe S, Marshall WS, Khvorova A. Rational siRNA design for RNA interference. Nat Biotechnol. 2004;22(3):326-30.
231. DeLuca DS, Levin JZ, Sivachenko A, Fennell T, Nazaire MD, Williams C, et al. RNA-SeQC: RNA-seq metrics for quality control and process optimization. Bioinformatics. 2012;28(11):1530-2.
232. Conesa A, Madrigal P, Tarazona S, Gomez-Cabrero D, Cervera A, McPherson A, et al. A survey of best practices for RNA-seq data analysis. Genome biology. 2016;17:13.
233. Gallego Romero I, Pai AA, Tung J, Gilad Y. RNA-seq: impact of RNA degradation on transcript quantification. BMC biology. 2014;12:42.
234. Carter LE, Kilroy G, Gimble JM, Floyd ZE. An improved method for isolation of RNA from bone. BMC biotechnology. 2012;12:5.
235. Reno C, Marchuk L, Sciore P, Frank CB, Hart DA. Rapid isolation of total RNA from small samples of hypocellular, dense connective tissues. BioTechniques. 1997;22(6):1082-6.
236. Clements DN, Vaughan-Thomas A, Peansukmanee S, Carter SD, Innes JF, Ollier WE, et al. Assessment of the use of RNA quality metrics for the screening of articular cartilage specimens from clinically normal dogs and dogs with osteoarthritis. American journal of veterinary research. 2006;67(8):1438-44.
237. Sun JX, Horst OV, Bumgarner R, Lakely B, Somerman MJ, Zhang H. Laser capture microdissection enables cellular and molecular studies of tooth root development. International journal of oral science. 2012;4(1):7-13.
238. Conde MC, Nedel F, Campos VF, Smith AJ, Nor JE, Demarco FF, et al. Odontoblast RNA stability in different temperature-based protocols for tooth storage. International endodontic journal. 2012;45(3):266-72.
239. Miyamoto T, Okano S, Kasai N. Irreversible thermoinactivation of ribonuclease-A by soft-hydrothermal processing. Biotechnology progress. 2009;25(6):1678-85.
240. Tarca AL, Romero R, Draghici S. Analysis of microarray experiments of gene expression profiling. American journal of obstetrics and gynecology. 2006;195(2):373-88.
241. Wang L, Nie J, Sicotte H, Li Y, Eckel-Passow JE, Dasari S, et al. Measure transcript integrity using RNA-seq data. BMC bioinformatics. 2016;17:58.
242. Imbeaud S, Graudens E, Boulanger V, Barlet X, Zaborski P, Eveno E, et al. Towards standardization of RNA quality assessment using user-independent classifiers of microcapillary electrophoresis traces. Nucleic Acids Res. 2005;33(6):56.
243. Opitz L, Salinas-Riester G, Grade M, Jung K, Jo P, Emons G, et al. Impact of

RNA degradation on gene expression profiling. BMC medical genomics. 2010;3:36.
244. Adamopoulos IE, Mellins ED. Alternative pathways of osteoclastogenesis in inflammatory arthritis. Nature reviews Rheumatology. 2015;11(3):189-94.
245. Booij-Vrieling HE, de Vries TJ, Schoenmaker T, Tryfonidou MA, Penning LC, Hazewinkel HA, et al. Osteoclast progenitors from cats with and without tooth resorption respond differently to 1,25-dihydroxyvitamin D and interleukin-6. Res Vet Sci. 2012;92(2):311-6.
246. Orriss IR, Arnett TR. Rodent osteoclast cultures. Methods in molecular biology. 2012;816:103-17.
247. Takahashi N, Yamana H, Yoshiki S, Roodman GD, Mundy GR, Jones SJ, et al. Osteoclast-like cell formation and its regulation by osteotropic hormones in mouse bone marrow cultures. Endocrinology. 1988;122(4):1373-82.
248. Suda T, Takahashi N, Martin TJ. Modulation of osteoclast differentiation. Endocrine reviews. 1992;13(1):66-80.
249. Coxon FP, Rogers MJ, Crockett JC. Isolation and purification of rabbit osteoclasts. Methods in molecular biology. 2012;816:145-58.
250. Collin-Osdoby P, Osdoby P. Isolation and culture of primary chicken osteoclasts. Methods in molecular biology. 2012;816:119-43.
251. Kessler Y, Helfer-Hungerbuehler AK, Cattori V, Meli ML, Zellweger B, Ossent P, et al. Quantitative TaqMan real-time PCR assays for gene expression normalisation in feline tissues. BMC molecular biology. 2009;10:106.
252. Penning LC, Vrieling HE, Brinkhof B, Riemers FM, Rothuizen J, Rutteman GR, et al. A validation of 10 feline reference genes for gene expression measurements in snap-frozen tissues. Veterinary Immunology and Immunopathology. 2007;120(3–4):212-22.
253. Manolagas SC. Birth and Death of Bone Cells: Basic Regulatory Mechanisms and Implications for the Pathogenesis and Treatment of Osteoporosis*. Endocrine reviews. 2000;21(2):115-37.
254. Svec D, Tichopad A, Novosadova V, Pfaffl MW, Kubista M. How good is a PCR efficiency estimate: Recommendations for precise and robust qPCR efficiency assessments. Biomolecular Detection and Quantification. 2015;3:9-16.
255. Hellemans J, Mortier G, De Paepe A, Speleman F, Vandesompele J. qBase relative quantification framework and software for management and automated analysis of real-time quantitative PCR data. Genome biology. 2007;8(2):R19-R.
256. scientific T. Real-time PCR: Understanding Ct 2016.
257. Holland PM, Abramson RD, Watson R, Gelfand DH. Detection of specific polymerase chain reaction product by utilizing the 5'-3' exonuclease activity of Thermus aquaticus DNA polymerase. Proceedings of the National Academy of Sciences of the United States of America. 1991;88(16):7276-80.
258. Vincent C, Kogawa M, Findlay DM, Atkins GJ. The generation of osteoclasts from RAW 264.7 precursors in defined, serum-free conditions. Journal of bone and mineral metabolism. 2009;27(1):114-9.
259. Al-Mousawi AM, Kulp GA, Branski LK, Kraft R, Mecott GA, Williams FN, et al. Impact of anesthesia, analgesia, and euthanasia technique on the inflammatory cytokine profile in a rodent model of severe burn injury. Shock. 2010;34(3):261-8.

260. Halleen JM, Tiitinen SL, Ylipahkala H, Fagerlund KM, Väänänen HK. Tartrate-resistant acid phosphatase 5b (TRACP 5b) as a marker of bone resorption. Clin Lab. 2006;52(9-10):499-509.
261. Watanabe T, Kukita T, Kukita A, Wada N, Toh K, Nagata K, et al. Direct stimulation of osteoclastogenesis by MIP-1alpha: evidence obtained from studies using RAW264 cell clone highly responsive to RANKL. The Journal of endocrinology. 2004;180(1):193-201.
262. Wu H, Xu G, Li YP. Atp6v0d2 is an essential component of the osteoclast-specific proton pump that mediates extracellular acidification in bone resorption. J Bone Miner Res. 2009;24(5):871-85.
263. Christensen J, Shastri VP. Matrix-metalloproteinase-9 is cleaved and activated by cathepsin K. BMC research notes. 2015;8:322.
264. Kim JH, Kim K, Kim I, Seong S, Nam K-I, Lee SH, et al. Role of CrkII Signaling in RANKL-Induced Osteoclast Differentiation and Function. The Journal of Immunology. 2016;196(3):1123-31.
265. Lee SK, Kim H, Park J, Kim H-J, Kim KR, Son SH, et al. Artemisia annua extract prevents ovariectomy-induced bone loss by blocking receptor activator of nuclear factor kappa-B ligand-induced differentiation of osteoclasts. Scientific Reports. 2017;7(1):17332.
266. Nicolin V, Bortul R, Bareggi R, Baldini G, Martinelli B, Narducci P. Breast adenocarcinoma MCF-7 cell line induces spontaneous osteoclastogenesis via a RANK-ligand-dependent pathway. Acta Histochemica. 2008;110(5):388-96.
267. Kogawa M, Anderson PH, Findlay DM, Morris HA, Atkins GJ. The metabolism of 25-(OH)vitamin D3 by osteoclasts and their precursors regulates the differentiation of osteoclasts. The Journal of steroid biochemistry and molecular biology. 2010;121(1-2):277-80.
268. Low E, Zoellner H, Kharbanda OP, Darendeliler MA. Expression of mRNA for osteoprotegerin and receptor activator of nuclear factor kappa beta ligand (RANKL) during root resorption induced by the application of heavy orthodontic forces on rat molars. American journal of orthodontics and dentofacial orthopedics : official publication of the American Association of Orthodontists, its constituent societies, and the American Board of Orthodontics. 2005;128(4):497-503.
269. Nakashima T, Kobayashi Y, Yamasaki S, Kawakami A, Eguchi K, Sasaki H, et al. Protein expression and functional difference of membrane-bound and soluble receptor activator of NF-kappaB ligand: modulation of the expression by osteotropic factors and cytokines. Biochemical and biophysical research communications. 2000;275(3):768-75.
270. Furuya M, Kikuta J, Fujimori S, Seno S, Maeda H, Shirazaki M, et al. Direct cell-cell contact between mature osteoblasts and osteoclasts dynamically controls their functions in vivo. Nature communications. 2018;9(1):300.
271. Bloemen V, Schoenmaker T, de Vries TJ, Everts V. Direct cell-cell contact between periodontal ligament fibroblasts and osteoclast precursors synergistically increases the expression of genes related to osteoclastogenesis. Journal of cellular physiology. 2010;222(3):565-73.
272. Szczesniak KA, Ciecierska A, Ostaszewski P, Sadkowski T. Transcriptomic

profile adaptations following exposure of equine satellite cells to nutriactive phytochemical gamma-oryzanol. Genes & nutrition. 2016;11:5.
273. Chen Y, Lun ATL, Smyth GK. From reads to genes to pathways: differential expression analysis of RNA-Seq experiments using Rsubread and the edgeR quasi-likelihood pipeline. F1000Research. 2016;5:1438.
274. Tarca AL, Draghici S, Khatri P, Hassan SS, Mittal P, Kim J-s, et al. A novel signaling pathway impact analysis. Bioinformatics. 2009;25(1):75-82.
275. Ross FP. M-CSF, c-Fms, and signaling in osteoclasts and their precursors. Ann N Y Acad Sci. 2006;1068:110-6.
276. Halleen J, Hentunen TA, Hellman J, Väänänen HK. Tartrate-resistant acid phosphatase from human bone: purification and development of an immunoassay. J Bone Miner Res. 1996;11(10):1444-52.
277. Granholm S, Lundberg P, Lerner UH. Expression of the calcitonin receptor, calcitonin receptor-like receptor, and receptor activity modifying proteins during osteoclast differentiation. Journal of cellular biochemistry. 2008;104(3):920-33.
278. Wilson SR, Peters C, Saftig P, Bromme D. Cathepsin K activity-dependent regulation of osteoclast actin ring formation and bone resorption. J Biol Chem. 2009;284(4):2584-92.
279. Park JH, Lee NK, Lee SY. Current Understanding of RANK Signaling in Osteoclast Differentiation and Maturation. Molecules and Cells. 2017;40(10):706-13.
280. Despars G, Pandruvada SNM, Anginot A, Domenget C, Jurdic P, Mazzorana M. DAP12 Overexpression Induces Osteopenia and Impaired Early Hematopoiesis. PloS one. 2013;8(6):65297.
281. Sasaki H, Yamamoto H, Tominaga K, Masuda K, Kawai T, Teshima-Kondo S, et al. NADPH oxidase-derived reactive oxygen species are essential for differentiation of a mouse macrophage cell line (RAW264.7) into osteoclasts. The journal of medical investigation : JMI. 2009;56(1-2):33-41.
282. Quinn JM, Itoh K, Udagawa N, Hausler K, Yasuda H, Shima N, et al. Transforming growth factor beta affects osteoclast differentiation via direct and indirect actions. J Bone Miner Res. 2001;16(10):1787-94.
283. Burnstock G, Arnett TR, Orriss IR. Purinergic signalling in the musculoskeletal system. Purinergic Signalling. 2013;9(4):541-72.
284. Kajiya H. Calcium signaling in osteoclast differentiation and bone resorption. Advances in experimental medicine and biology. 2012;740:917-32.
285. Hwang SY, Putney JW, Jr. Calcium signaling in osteoclasts. Biochimica et biophysica acta. 2011;1813(5):979-83.
286. Wang N, Agrawal A, Jorgensen NR, Gartland A. P2X7 receptor regulates osteoclast function and bone loss in a mouse model of osteoporosis. Sci Rep. 2018;8(1):3507.
287. Hughes AE, Ralston SH, Marken J, Bell C, MacPherson H, Wallace RG, et al. Mutations in TNFRSF11A, affecting the signal peptide of RANK, cause familial expansile osteolysis. Nat Genet. 2000;24(1):45-8.
288. Roshandel D, Holliday KL, Pye SR, Boonen S, Borghs H, Vanderschueren D, et al. Genetic variation in the RANKL/RANK/OPG signaling pathway is associated with

bone turnover and bone mineral density in men. J Bone Miner Res. 2010;25(8):1830-8.
289. Viecilli RF, Katona TR, Chen J, Hartsfield JK, Roberts WE. Orthodontic mechanotransduction and the role of the P2X7 receptor. American journal of orthodontics and dentofacial orthopedics : official publication of the American Association of Orthodontists, its constituent societies, and the American Board of Orthodontics. 2009;135(6):694.1-16.
290. Grant M, Wilson J, Rock P, Chapple I. Induction of cytokines, MMP9, TIMPs, RANKL and OPG during orthodontic tooth movement. European journal of orthodontics. 2013;35(5):644-51.
291. Hansen KD, Wu Z, Irizarry RA, Leek JT. Sequencing technology does not eliminate biological variability. Nature biotechnology. 2011;29(7):572-3.
292. Song JS, Hwang DH, Kim S-O, Jeon M, Choi B-J, Jung H-S, et al. Comparative Gene Expression Analysis of the Human Periodontal Ligament in Deciduous and Permanent Teeth. PloS one. 2013;8(4):61231.
293. Kim J-H, Jeon M, Song J-S, Lee J-H, Choi B-J, Jung H-S, et al. Distinctive Genetic Activity Pattern of the Human Dental Pulp between Deciduous and Permanent Teeth. PloS one. 2014;9(7):102893.
294. DeLaurier A, Boyde A, Jackson B, Horton MA, Price JS. Identifying early osteoclastic resorptive lesions in feline teeth: a model for understanding the origin of multiple idiopathic root resorption. Journal of periodontal research. 2009;44(2):248-57.
295. Riihonen R, Supuran CT, Parkkila S, Pastorekova S, Vaananen HK, Laitala-Leinonen T. Membrane-bound carbonic anhydrases in osteoclasts. Bone. 2007;40(4):1021-31.
296. Reibring CG, El Shahawy M, Hallberg K, Kannius-Janson M, Nilsson J, Parkkila S, et al. Expression patterns and subcellular localization of carbonic anhydrases are developmentally regulated during tooth formation. PloS one. 2014;9(5):96007.
297. Leinonen J, Kivela J, Parkkila S, Parkkila AK, Rajaniemi H. Salivary carbonic anhydrase isoenzyme VI is located in the human enamel pellicle. Caries research. 1999;33(3):185-90.
298. Raju K, Tang S, Dube ID, Kamel-Reid S, Bryce DM, Breitman ML. Characterization and developmental expression of Tlx-1, the murine homolog of HOX11. Mechanisms of development. 1993;44(1):51-64.
299. Ahn Y, Sanderson BW, Klein OD, Krumlauf R. Inhibition of Wnt signaling by Wise (Sostdc1) and negative feedback from Shh controls tooth number and patterning. Development. 2010;137(19):3221-31.
300. Amri N, Djole SX, Petit S, Babajko S, Coudert AE, Castaneda B, et al. Distorted Patterns of Dentinogenesis and Eruption in Msx2 Null Mutants: Involvement of Sost/Sclerostin. Am J Pathol. 2016.
301. Ramanathan A, Srijaya TC, Sukumaran P, Zain RB, Abu Kasim NH. Homeobox genes and tooth development: Understanding the biological pathways and applications in regenerative dental science. Archives of oral biology. 2018;85:23-39.
302. Mitrea C, Taghavi Z, Bokanizad B, Hanoudi S, Tagett R, Donato M, et al. Methods and approaches in the topology-based analysis of biological pathways.

Frontiers in physiology. 2013;4:278.
303. Khatri P, Sirota M, Butte AJ. Ten years of pathway analysis: current approaches and outstanding challenges. PLoS computational biology. 2012;8(2):1002375.
304. Paic F, Igwe JC, Nori R, Kronenberg MS, Franceschetti T, Harrington P, et al. Identification of differentially expressed genes between osteoblasts and osteocytes. Bone. 2009;45(4):682-92.
305. Krysinska H, Hoogenkamp M, Ingram R, Wilson N, Tagoh H, Laslo P, et al. A two-step, PU.1-dependent mechanism for developmentally regulated chromatin remodeling and transcription of the c-fms gene. Mol Cell Biol. 2007;27(3):878-87.
306. Hofbauer LC, Khosla S, Dunstan CR, Lacey DL, Boyle WJ, Riggs BL. The roles of osteoprotegerin and osteoprotegerin ligand in the paracrine regulation of bone resorption. J Bone Miner Res. 2000;15(1):2-12.
307. Verbrugghe A, Janssens GP, Van de Velde H, Cox E, De Smet S, Vlaeminck B, et al. Failure of a dietary model to affect markers of inflammation in domestic cats. BMC veterinary research. 2014;10:104.
308. Clark KC, Fierro FA, Ko EM, Walker NJ, Arzi B, Tepper CG, et al. Human and feline adipose-derived mesenchymal stem cells have comparable phenotype, immunomodulatory functions, and transcriptome. Stem Cell Research & Therapy. 2017;8:69.
309. Subrahmanyam MV, Sangeetha M. Gingival crevicular fluid a marker of the periodontal disease activity. Indian Journal of Clinical Biochemistry. 2003;18(1):5-7.
310. Dong Z, Bonfil RD, Chinni S, Deng X, Trindade Filho JC, Bernardo M, et al. Matrix metalloproteinase activity and osteoclasts in experimental prostate cancer bone metastasis tissue. Am J Pathol. 2005;166(4):1173-86.
311. Jain A, Bahuguna R. Role of matrix metalloproteinases in dental caries, pulp and periapical inflammation: An overview. Journal of Oral Biology and Craniofacial Research. 2015;5(3):212-8.
312. Tezuka K, Nemoto K, Tezuka Y, Sato T, Ikeda Y, Kobori M, et al. Identification of matrix metalloproteinase 9 in rabbit osteoclasts. J Biol Chem. 1994;269(21):15006-9.
313. Reponen P, Sahlberg C, Munaut C, Thesleff I, Tryggvason K. High expression of 92-kD type IV collagenase (gelatinase B) in the osteoclast lineage during mouse development. The Journal of cell biology. 1994;124(6):1091-102.
314. Orriss IR, Key ML, Hajjawi MOR, Arnett TR. Extracellular ATP Released by Osteoblasts Is A Key Local Inhibitor of Bone Mineralisation. PloS one. 2013;8(7):69057.
315. Yeung D, Kharidia R, Brown SC, Gorecki DC. Enhanced expression of the P2X4 receptor in Duchenne muscular dystrophy correlates with macrophage invasion. Neurobiology of disease. 2004;15(2):212-20.
316. Zippel N, Limbach CA, Ratajski N, Urban C, Luparello C, Pansky A, et al. Purinergic receptors influence the differentiation of human mesenchymal stem cells. Stem cells and development. 2012;21(6):884-900.
317. Zhang L, Yin X, Wang J, Xu D, Wang Y, Yang J, et al. Associations between VDR Gene Polymorphisms and Osteoporosis Risk and Bone Mineral Density in

Postmenopausal Women: A systematic review and Meta-Analysis. Scientific Reports. 2018;8(1):981.
318. Franco C, Patricia HR, Timo S, Claudia B, Marcela H. Matrix Metalloproteinases as Regulators of Periodontal Inflammation. International journal of molecular sciences. 2017;18(2).
319. Engsig MT, Chen QJ, Vu TH, Pedersen AC, Therkidsen B, Lund LR, et al. Matrix metalloproteinase 9 and vascular endothelial growth factor are essential for osteoclast recruitment into developing long bones. The Journal of cell biology. 2000;151(4):879-89.
320. Chellaiah MA, Ma T. Membrane Localization of Membrane Type 1 Matrix Metalloproteinase by CD44 Regulates the Activation of Pro-Matrix Metalloproteinase 9 in Osteoclasts. BioMed Research International. 2013;2013:302392.
321. Marshall DC, Lyman SK, McCauley S, Kovalenko M, Spangler R, Liu C, et al. Selective Allosteric Inhibition of MMP9 Is Efficacious in Preclinical Models of Ulcerative Colitis and Colorectal Cancer. PloS one. 2015;10(5):e0127063.
322. Mehner C, Hockla A, Miller E, Ran S, Radisky DC, Radisky ES. Tumor cell-produced matrix metalloproteinase 9 (MMP-9) drives malignant progression and metastasis of basal-like triple negative breast cancer. Oncotarget. 2014;5(9):2736-49.
323. Aalinkeel R, Nair BB, Reynolds JL, Sykes DE, Mahajan SD, Chadha KC, et al. Overexpression of MMP-9 contributes to invasiveness of prostate cancer cell line LNCaP. Immunological investigations. 2011;40(5):447-64.
324. Andersen TL, del Carmen Ovejero M, Kirkegaard T, Lenhard T, Foged NT, Delaisse JM. A scrutiny of matrix metalloproteinases in osteoclasts: evidence for heterogeneity and for the presence of MMPs synthesized by other cells. Bone. 2004;35(5):1107-19.
325. Agrawal N, Dasaradhi PV, Mohmmed A, Malhotra P, Bhatnagar RK, Mukherjee SK. RNA interference: biology, mechanism, and applications. Microbiology and molecular biology reviews : MMBR. 2003;67(4):657-85.
326. Jiang H, Chen W, Zhu G, Zhang L, Tucker B, Hao L, et al. RNAi-mediated silencing of Atp6i and Atp6i haploinsufficiency prevents both bone loss and inflammation in a mouse model of periodontal disease. PloS one. 2013;8(4):e58599.
327. Sanceau J, Truchet S, Bauvois B. Matrix metalloproteinase-9 silencing by RNA interference triggers the migratory-adhesive switch in Ewing's sarcoma cells. J Biol Chem. 2003;278(38):36537-46.
328. Senn D, Schwalder P, Roux P, Bosshardt DD, Stoffel MH. Immunohistochemical localization of osteoclastogenic cell mediators in feline tooth resorption and healthy teeth. Journal of veterinary dentistry. 2010;27(2): 75-83.
329. Wittenburg G, Volkel C, Mai R, Lauer G. Immunohistochemical comparison of differentiation markers on paraffin and plastic embedded human bone samples. Journal of physiology and pharmacology : an official journal of the Polish Physiological Society. 2009;60 Suppl 8:43-9.
330. Beutler B, Mahoney J, Le Trang N, Pekala P, Cerami A. Purification of cachectin, a lipoprotein lipase-suppressing hormone secreted by endotoxin-induced

RAW 264.7 cells. The Journal of experimental medicine. 1985;161(5):984-95.
331. Verma RP. Hydroxamic acids as matrix metalloproteinase inhibitors. Exs. 2012;103:137-76.
332. Stacey KJ, Ross IL, Hume DA. Electroporation and DNA-dependent cell death in murine macrophages. Immunology and cell biology. 1993;71(Pt 2):75-85.
333. Crockett JC, Mellis DJ, Taylor A. Transfection of osteoclasts and osteoclast precursors. Methods in molecular biology. 2012;816:205-22.
334. Gauthier JY, Chauret N, Cromlish W, Desmarais S, Duong LT, Falgueyret JP, et al. The discovery of odanacatib (MK-0822), a selective inhibitor of cathepsin K. Bioorganic & medicinal chemistry letters. 2008;18(3):923-8.
335. Zerbini CA, McClung MR. Odanacatib in postmenopausal women with low bone mineral density: a review of current clinical evidence. Therapeutic advances in musculoskeletal disease. 2013;5(4):199-209.
336. Eisman JA, Bone HG, Hosking DJ, McClung MR, Reid IR, Rizzoli R, et al. Odanacatib in the treatment of postmenopausal women with low bone mineral density: three-year continued therapy and resolution of effect. J Bone Miner Res. 2011;26(2):242-51.
337. Wang L, Wang S, Li W. RSeQC: quality control of RNA-seq experiments. Bioinformatics. 2012;28(16):2184-5.
338. Benjamini Y, Speed TP. Summarizing and correcting the GC content bias in high-throughput sequencing. Nucleic Acids Res. 2012;40(10):72.
339. Kamat M, Puranik R, Vanaki S, Kamat S. An insight into the regulatory mechanisms of cells involved in resorption of dental hard tissues. Journal of oral and maxillofacial pathology : JOMFP. 2013;17(2):228-33.
340. Nakashima T, Takayanagi H. New regulation mechanisms of osteoclast differentiation. Annals of the New York Academy of Sciences. 2011;1240(1):13-8.
341. Crotti TN, Sharma SM, Fleming JD, Flannery MR, Ostrowski MC, Goldring SR, et al. PU.1 and NFATc1 mediate osteoclastic induction of the mouse beta3 integrin promoter. Journal of cellular physiology. 2008;215(3):636-44.
342. Tsuchiya M, Akiba Y, Takahashi I, Sasano Y, Kashiwazaki J, Tsuchiya S, et al. Comparison of expression patterns of cathepsin K and MMP-9 in odontoclasts and osteoclasts in physiological root resorption in the rat molar. Archives of histology and cytology. 2008;71(2):89-100.
343. Sims NA, Martin TJ. Coupling Signals between the Osteoclast and Osteoblast: How are Messages Transmitted between These Temporary Visitors to the Bone Surface? Frontiers in Endocrinology. 2015;6:41.
344. Hart SN, Therneau TM, Zhang Y, Poland GA, Kocher J-P. Calculating Sample Size Estimates for RNA Sequencing Data. Journal of Computational Biology. 2013;20(12):970-8.